

LOAD FREQUENCY CONTROL USING  
ADAPTIVE AND FUZZY BASED  
CONTROLLER FOR HYBRID MICRO-GRID  
SYSTEM

MAZIN MUSTAFA MAHDI

UMP

Doctor of Philosophy

UNIVERSITI MALAYSIA PAHANG

## UNIVERSITI MALAYSIA PAHANG

### DECLARATION OF THESIS AND COPYRIGHT

Author's Full Name : MAZIN MUSTAFA MAHDI  
Date of Birth : 21 SEPTEMBER 1962  
Title : LOAD FREQUENCY CONTROL USING ADAPTIVE AND FUZZY BASED CONTROLLER FOR HYBRID MICRO-GRID SYSTEM  
Academic Session : 2017/2018

I declare that this thesis is classified as:

- CONFIDENTIAL (Contains confidential information under the Official Secret Act 1997)\*  
 RESTRICTED (Contains restricted information as specified by the organization where research was done)\*  
 OPEN ACCESS I agree that my thesis to be published as online open access (Full Text)

I acknowledge that Universiti Malaysia Pahang reserves the following rights:

1. The Thesis is the Property of Universiti Malaysia Pahang
2. The Library of Universiti Malaysia Pahang has the right to make copies of the thesis for the purpose of research only.
3. The Library has the right to make copies of the thesis for academic exchange.

Certified by:

\_\_\_\_\_  
(Student's Signature)

A5997298

\_\_\_\_\_  
New IC/Passport Number

Date: June 2018

\_\_\_\_\_  
(Supervisor's Signature)

DR. Abu Zaharin Bin Ahmad

\_\_\_\_\_  
Name of Supervisor

Date: June 2018

### **SUPERVISOR'S DECLARATION**

I hereby declare that I have checked this thesis and in my opinion, this thesis is adequate in terms of scope and quality for the award of the degree of Doctor of Philosophy of Engineering.

---

(Supervisor's Signature)

Full Name : ASSOC. PROF DR. ABU ZAHARIN BIN AHMAD

Position : SENIOR LECTURER

Date : JUNE 2018



UMP

### STUDENT'S DECLARATION

I hereby declare that the work in this thesis is based on my original work except for quotations and citations which have been duly acknowledged. I also declare that it has not been previously or concurrently submitted for any other degree at Universiti Malaysia Pahang or any other institutions.

---

(Student's Signature)

Full Name : MAZIN MUSTAFA MAHDI

ID Number : PEE 14002

Date : JUNE 2018



UMP

LOAD FREQUENCY CONTROL USING ADAPTIVE AND FUZZY BASED  
CONTROLLER FOR HYBRID MICRO-GRID SYSTEM

The logo of the University of Malaysia Pahang (UMP) is a shield-shaped emblem. It features a central white vertical band with a yellow diamond at the top. The shield is divided into four quadrants: top-left is light blue, top-right is light purple, bottom-left is light blue, and bottom-right is light purple. A stylized, glowing ring in shades of blue and green encircles the top portion of the shield.

MAZIN MUSTAFA MAHDI

Thesis submitted in fulfillment of the requirements  
for the award of the degree of  
Doctor of Philosophy

UMP

Faculty of Electrical & Electronics Engineering

UNIVERSITI MALAYSIA PAHANG

JUNE 2018

## ACKNOWLEDGEMENTS

In the name of Allah, Most Gracious, and Most Merciful

First of all, I would like to thank **Allah** for his great help, continuous guidance and support. This work would have been impossible without his help and support.

My deep appreciation and heartfelt gratitude goes to my supervisor, Assoc.Prof DR. **Abu Zaharin Bin Ahmad** for his **guidance** throughout this work. His help, support, creative ideas and suggestions **made it more valuable.**

I would like to express my sincere gratitude to **University Malaysia Pahang (UMP)** for moral supports during my work and it was a wonderful place to study.

To my devoted **Mother**

.....and to the memory of my beloved **Father**

Finally, my sincere thanks to **my family** for their prayers and encouragement which helped me take the right step in life.



UMP

## ABSTRAK

A hibrid mikro grid adalah subset dan menjadi penting dalam grid kuasa moden, yang menggunakan inersia, dan bukan inersia. Disediakan Generations (DGS) untuk membekalkan kuasa kepada masyarakat di kawasan kecil daripada kawasan yang luas. Mikro grid boleh beroperasi dalam segerak dengan utiliti grid atau sebagai berasingan (islanded). Ia adalah satu kaedah yang berguna untuk mencapai pengembangan rangkaian tetapi mempunyai beberapa isu. Mod pemindahan dari grid utama tempatan untuk mod berasingan menghadapi banyak cabaran, berkaitan dengan perubahan beban yang besar tiba-tiba berubah dan kehilangan grid elektrik utama. Apabila mikro-grid terputus, dan dalam mod berasingan, kuasa aktif dan reaktif perlu dikawal oleh unit-unit DG. Laporan penyelidikan ini termasuk analisis Kawalan Frekuensi Beban (LFC) untuk mengawal hibrid mikro grid disambungkan ke grid, dan apabila beroperasi dalam mod berasingan. Manfaat kaedah kawalan adalah untuk membetulkan penyimpangan kekerapan semasa syarat-syarat operasi berasingan (islanded) sebagai DG berterusan akan menyuntik kuasa pada tahap yang dikehendaki. Strategi kawalan mikro-grid disiasat dalam kerja-kerja ini termasuk analisis sambutan fasa sisihan frekuensi dan perkongsian kuasa dalam kedua-dua operasi iaitu sambungan dengan grid dan berasingan (islanded) mod operasi mikro grid. Pengawal PI adaptif digunakan dengan menggunakan peraturan MIT berdasarkan Kawalan Penyesuaian Rujukan Model (MRAC) untuk kelancaran mikro grid dari grid utama tempatan ke mod berasingan (islanded) untuk mengelakkan penyimpangan kekerapan yang tinggi. Kemudian, pengawal Rangkaian Neural Buatan (ANN) digunakan untuk mengemas kini keluaran MRAC dan meningkatkan prestasi operasi grid mikro. Dari kajian simulasi, jelas bahawa pengawal berasaskan MRAC-ANN berkesan dapat mengurangkan ayunan (transient) dan mengurangkan masa penyelesaian. Kawalan Jadual Logik Fuzzy (FLTC) digunakan di LFC di sistem grid mikro untuk mengawal frekuensi sistem, dan memberikan prestasi yang diinginkan terhadap perubahan beban secara tiba-tiba dan gangguan kerosakan didalam mikro grid, meningkatkan perbezaan kekerapan dan keluaran kuasa output. Untuk pengesahan, semua analisis dibandingkan dengan pengawal PI konvensional dan hasilnya menunjukkan pengawal yang dicadangkan mengatasi pengawal PI konvensional dalam dengan menunjukkan keputusan yang memberangsangkan. Pengawal yang dicadangkan boleh diklasifikasikan mudah dan mudah dilaksanakan. Oleh itu, pengawal LFC yang dicadangkan ini boleh menyumbang kepada peningkatan penggunaan tenaga ke dalam persekitaran mikro-grid.

## ABSTRACT

A hybrid micro-grid is a subset and becomes vital in the modern power grid, which is using inertia and non-inertia Distributed Generations (DGs) to supply power to communities in the small-scale area rather than vast regions. A micro-grid can operate in synchronous with the grid utility or as islanding; it is a useful method of achieving network expansion but have some issues. The transfer mode from the local main grid to islanding mode faces many challenges, related to significant load changes suddenly and the loss of the main electricity grid. When the micro-grid is disconnected, and in islanded mode, the active and reactive power needs to be controlled by the DG units. This research report includes an analysis of Load Frequency Control (LFC) for control of a hybrid micro-grid connected to the grid, and when operating in islanded mode. The benefit of this method of control is to correct frequency deviations during conditions of islanded operation as the DG would continually inject power at the desired level. The micro-grid control strategies investigated in this work included an analysis of the transient response of the frequency deviation and power sharing in both grid-connected and islanded modes of micro-grid operation. The adaptive PI controller is utilized by applying a Model Reference Adaptive Control (MRAC) based MIT rule for a smooth transfer micro-grid from the local main grid to the islanded mode for avoiding high-frequency deviations. Then, an Artificial Neural Network (ANN) controller is used to update the output of MRAC and to enhance micro-grid operation performance. From the simulation studies, it is clear that MRAC-ANN based controller can effectively damp out the oscillations and reduce the settling time. The Fuzzy Logic Table Control (FLTC) is employed in LFC at islanded micro-grid system to regulate the system's frequency, and provides desirable performance against sudden load changes and fault disturbances, improving the frequency deviation and output power variation. For verification, all the analyses are compared with conventional PI controller and the results show the proposed controller outperform the conventional PI controller in promising response. The proposed controller can classify simple and easy to implement. Therefore, these proposed controllers of LFC can contribute to the expanding the energy utilization into the micro-grid environment.

The logo for UMP (Universiti Malaysia Perlis) is a large, stylized letter 'U' composed of two overlapping triangles. The left triangle is light blue and the right triangle is light green. The letters 'UMP' are written in white, bold, sans-serif font across the center of the 'U'.



# TABLE OF CONTENT

<b>DECLARATION</b>	
<b>TITLE PAGE</b>	
<b>ACKNOWLEDGEMENTS</b>	<b>ii</b>
<b>ABSTRAK</b>	<b>iii</b>
<b>ABSTRACT</b>	<b>iv</b>
<b>TABLE OF CONTENT</b>	<b>v</b>
<b>LIST OF TABLES</b>	<b>ix</b>
<b>LIST OF FIGURES</b>	<b>x</b>
<b>LIST OF SYMBOLS</b>	<b>xiv</b>
<b>LIST OF ABBREVIATIONS</b>	<b>xvi</b>
<b>CHAPTER 1 INTRODUCTION</b>	<b>1</b>
1.1 Introduction	1
1.2 Motivation of Research	4
1.3 Problem Statement	5
1.4 Objectives of Research	7
1.5 Scope of Study	7
1.6 Outline of Thesis	8
<b>CHAPTER 2 LITERATURE REVIEW</b>	<b>9</b>
2.1 Introduction	9
2.2 Distributed Generation System	10
2.3 Interfacing of Distributed Generation to the Grid	10

2.3.1	Direct Grid-Connected Distributed Generation	10
2.3.2	Indirect Grid-Connected Distributed Generation	11
2.4	Micro- grid and its Benefits	12
2.5	Micro-grid Operation Modes	13
2.5.1	Grid Connected Mode	14
2.5.2	Islanded Mode	15
2.6	The Necessity for the Synchronous Generator in Micro-grid	16
2.6.1	Turbine Governor	18
2.7	Load Frequency Control in Power System	19
2.8	Micro-grid Control	23
2.8.1	Micro-Grid Centralized Control (MGCC)	24
2.8.2	Decentralized Control	25
2.9	Load Frequency Control in Micro-grid.	26
2.9.1	Conventional Load Frequency Control in Micro-grid	27
2.9.2	Intelligent Load Frequency Control in Micro-grid	33
2.10	Control of VSI in MG	46
2.10.1	Synchronous Reference Frame Control	46
2.10.2	Stationary Reference Frame Control	47
2.11	Power Sharing Droop Method in MG	48
2.11.1	Conventional Droop Control	49
2.11.2	Modified Droop Control	51
2.12	Summary	55
<b>CHAPTER 3 METHODOLOGY</b>		<b>56</b>
3.1	Introduction	56
3.2	Strategy of Work Frame	58

3.3	Consideration of LFC in MG System	59
3.3.1	Area Control Error (ACE)	65
3.4	Micro-grid System Configuration	66
3.4.1	Model of Synchronous Generator	68
3.4.2	Turbine-Governor Control	69
3.4.3	Proportional Integral (PI) Control Scheme	71
3.4.4	Generator-Voltage Control	72
3.5	Micro-grid Loads	74
3.6	Micro-grid in Connected Mode	76
3.6.1	Model Reference Adaptive Controller (MRAC)	76
3.6.2	Artificial Neural Network (ANN)	84
3.7	Micro-grid in Island Mode	89
3.7.1	Fuzzy Inference System (FIS)	90
3.8	Modeling of PV Solar Generation	99
3.8.1	Characteristic of PV Array	100
3.8.2	Maximum Power Point Tracking (MPPT)	102
3.9	Battery Energy Storage Systems	102
3.9.1	Boost Converter	106
3.9.2	Phase Lock Loop for Inverter Synchronization	107
3.9.3	VSI Control Approaches	108
3.10	Power Sharing Droop	110
3.11	Summary	112
<b>CHAPTER 4 RESULTS AND DISCUSSION</b>		<b>113</b>
4.1	Introduction	113
4.2	Simulation Results in Grid –Connected Mode	115

4.2.1	Performance of MIT rule Controlled Based API at Load Change	116
4.2.2	Performance of API with ANN at Load Change	118
4.2.4	VSC in Grid Connected Mode	134
4.3	Island Mode Control	135
4.3.1	Performance of MG Using FLTC	136
4.3.2	Fault in Island Mode	144
4.4	Summary	147
<b>CHAPTER 5 CONCLUSION</b>		<b>148</b>
5.1	Introduction	148
5.2	Summary of Findings	148
5.3	Attainment of research objectives	149
5.4	Contribution to the Study	150
5.5	Recommendations for Future Work	151
<b>REFERENCES</b>		<b>152</b>
<b>LIST OF PUBLICATION</b>		<b>167</b>
<b>APPENDIX A</b>		<b>168</b>
<b>APPENDIX B</b>		<b>172</b>

## LIST OF TABLES

Table 2.1	Summarizes the interfacing and power flow control options of common DG	12
Table 2.2	The comparison between inertia and non- inertia DG units.	13
Table 2.3	Micro-grid control techniques	26
Table 2.4	Fuzzy inference rule for Fuzzy Logic Control	39
Table 2.5	The background and literature reviews of LFC	44
Table 2.6	Conventional Load frequency control	45
Table 2.7	Intelligent Load Frequency Control	45
Table 2.8	Line parameters for different networks	50
Table 2.9	Different techniques of droop control methods	54
Table 3.1	Applications of LFC in (SG) in MG system and the (area) in electrical power system	60
Table 3.2	Parameters of Synchronous Generator, Grid and Load	74
Table 3.3	Load variation and its percentage	75
Table 3.4	2-D Lookup Table Row x Column (Data 3x3)	97
Table 3.5	Parameters and values controller	98
Table 3.6	Parameters of PV solar system	102
Table 3.7	Parameters of Battery	103
Table 4.1	Cases study in grid-connected mode	134
Table 4.2	Cases study in island mode	146

UMP

## LIST OF FIGURES

Figure 1.1	Energy consumption from 2012 and 2040	4
Figure 1.2	Forecast of micro-grid growth in 2022	5
Figure 2.1	Schematic diagram of direct grid-connected DG	11
Figure 2.2	Interface-connected DG with DC output	11
Figure 2.3	MG system connected to grid includes three DGs and loads	14
Figure 2.4	Synchronous machine (a) circuit diagram (b) phasor diagram	18
Figure 2.5	Simplified turbine governor	19
Figure 2.6	Mechanical torque and rotational speed	21
Figure 2.7	Single-area power system	22
Figure 2.8	Centralized control Multi Input Multi Output systems	24
Figure 2.9	Decentralized regulators for Multi Input Multi Output systems	25
Figure 2.10	Load Frequency Control of a micro-grid with two-level hierarchical	27
Figure 2.11	General adaptive control scheme	31
Figure 2.12	Model Reference Adaptive Control System	32
Figure 2.13	Multi layered ANN interconnected group of nodes	35
Figure 2.14	Control styles of ANN-based micro-grid	36
Figure 2.15	Simulation results of Plant output $y$ (solid lines) and the Reference output $y_m$ (dotted lines) of the conventional MRAC system	37
Figure 2.16	Schematic representation of a FL system	38
Figure 2.17	Membership Function for the control input variables	40
Figure 2.18	Structure of the fuzzy logic controller	41
Figure 2.19	Membership functions, (a) Membership functions of $e$ , (b) Membership functions of $de$ , (c) Membership functions of $du$	41
Figure 2.20	Block diagram of lookup table fuzzy control system	42
Figure 2.21	Controller $C$ for simulation with $f1 = \sin x2$	43
Figure 2.22	Circuit diagram of the grid-connected inverter	47
Figure 2.23	Two AC voltage sources connected in parallel through line impedance	49
Figure 3.1	The block diagram for the work methodology	57
Figure 3.2	Block diagram of strategy work	59
Figure 3.3	Block diagram of speed governor	61
Figure 3.4	Block diagram of speed governor together with hydraulic valve actuator	62
Figure 3.5	Block diagram linear model corresponding power system response	64

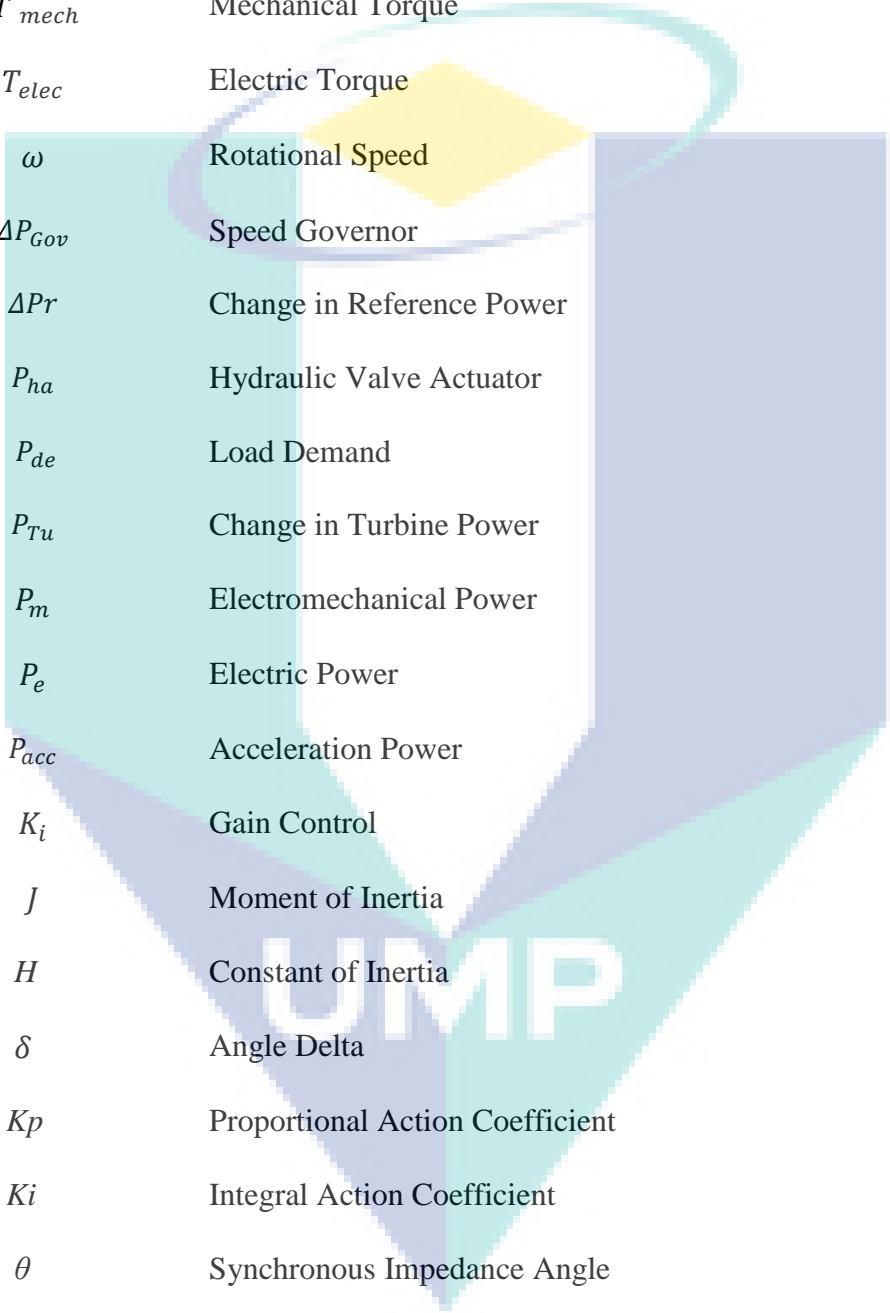
Figure 3.6	Block diagram closed loop of LFC	64
Figure 3.7	Block diagram corresponding to complete LFC	65
Figure 3.8	Reduced block diagram synchronous generator	66
Figure 3.9	The flow charts of MG transfer to island mode	67
Figure 3.10	Structure of the proposed hybrid micro-grid system	68
Figure 3.11	Steady-state frequency–power relation	70
Figure 3.12	Block diagram of PI controller	72
Figure 3.13	Block diagram for the Exciter	73
Figure 3.14	Model Reference Adaptive Control using MIT rule	79
Figure 3.15	Principle of Back-Propagation training	85
Figure 3.16	Block diagram of the NARMA-L2 controller	86
Figure 3.17	Block diagram of MRAC using MIT rule with ANN (NARMA –L2) based speed control	88
Figure 3.18	The MRAC based MIT rule and ANN algorithm flowchart	89
Figure 3.19	Architecture of FLTC block diagram	91
Figure 3.20	Block diagram of lookup table	92
Figure 3.21	(a) The grid-based mode of the interpolation nodes of the (2-D) lookup table, (b) Areas for interpolation within a (2-D) lookup table	94
Figure 3.22	Proposed FLTC to control the speed governor in island	96
Figure 3.23	Three membership functions for each input	97
Figure 3.24	Mesh plot of table data and breakpoints data (row & column breakpoints) for proposed controller	97
Figure 3.25	The surface control of speed	98
Figure 3.26	Flow chart of FLTC algorithm	99
Figure 3.27	PV cell modeled as diode circuit	100
Figure 3.28	Output – I-V and P-V-characteristics with various temperature and constant irradianations	101
Figure 3.29	Output – I-V and P-V-characteristics with various irradianations and constant temperature	101
Figure 3.30	Battery model schematic diagram	104
Figure 3.31	Characteristics discharge of lithium ion battery	105
Figure 3.32	Characteristics charge of lithium ion battery	105
Figure 3.33	Boost converter	107
Figure 3.34	Block diagram of phase locked loop	108
Figure 3.35	Schematic diagram of inverter-based microgrid	108
Figure 3.36	Schematic diagram of Voltage Regulator	109

Figure 4.1	Block diagram of load-frequency control using API with ANN for SG control in grid connected mode	115
Figure 4.2	Performance of real model tracking reference model with different value of adaptation gain in real model for API	116
Figure 4.3	Output response characteristic of real model tracking reference model in API control for adaptation gain = 25	117
Figure 4.4	Performance of real model tracking reference by API control: (a) Output response error, and load change in (b) 30%, (c) 40% and (d) 50%	118
Figure 4.5	Performance of real model tracking reference model with different value of adaptation gain in real model for API with ANN	119
Figure 4.6	Output response characteristic of real model tracking reference model in API with ANN control for adaptation gain = 25	119
Figure 4.7	Performance of real model tracking reference model by API with ANN control : (a) Output response error, and load change in (b) 30%, (c) 40% and (d) 50%	121
Figure 4.8	Comparing the performance of two methods control for different adaptation gain values	122
Figure 4.9	Active power response of SG following a step change increase in load	123
Figure 4.10	Reactive power sharing performance by SG using three different controls following a step change increase load	124
Figure 4.11	Active power share load by SG and grid	125
Figure 4.12	Output reactive power of SG and grid	125
Figure 4.13	Time frames included in the micro-grid system frequency response in conventional PI controller	126
Figure 4.14	Step response of frequency at operation and load change 30% with different control	127
Figure 4.15	Step response of frequency at steady state	127
Figure 4.16	Frequency error at transient load change 30% and grid disconnect with different controller	128
Figure 4.17	Voltage and current of phase "a" at load increase 30%.	128
Figure 4.18	Frequency error at transient load change 40% and grid disconnect with different controller	129
Figure 4.19	Voltage and current of phase "a" at load increase 40%	130
Figure 4.20	Frequency error at transient load change 50% and grid disconnect with different controller	130
Figure 4.21	Voltage and current of phase "a" at load increase 50%	131
Figure 4.22	Rotor speed variation with different control at load change 30%	131
Figure 4.23	Rotor speed at step operation with different control	132



Figure 4.24	Speed rotor deviation at grid disconnect with deferent controller	132
Figure 4.25	Speed rotor response for a 40% step change in electrical load	133
Figure 4.26	Speed rotor response for a 50% step change in electrical load	133
Figure 4.27	Output active power for PV and battery in grid connected	135
Figure 4.28	Output reactive power for PV and battery in grid connected	135
Figure 4.29	Fuzzy Logic Table Control (FLTC) for synchronous generator	136
Figure 4.30	The response start-ups active power sharing performance produced from the synchronous generator unit	137
Figure 4.31	The transient response active power sharing performance produced from the synchronous generator unit	137
Figure 4.32	Active power sharing performance of micro-grid units	138
Figure 4.33	Reactive power response of DGs following change load	138
Figure 4.34	Frequency deviation (Hz) and time response	139
Figure 4.35	Frequency time response from transient to steady- state	139
Figure 4.36	Frequency error during step load change	140
Figure 4.37	Rotor speed oscillation in island MG	140
Figure 4.38	Rotor speed response by proposed FLTC and PI control	141
Figure 4.39	Rotor speed oscillation at step load change in island mode	141
Figure 4.40	The rotor speed oscillations for the different adaptation gain (a.g) values	142
Figure 4.41	The rotor speed oscillations with values of adaptation gain (a.g)	142
Figure 4.42	Different adaptation gain (a.g) on speed deviation with FLTC controller in case of load change	143
Figure 4.43	Voltage and current of phase "a" at load increase 50% in island mode	143
Figure 4.44	Frequency oscillations during 3-phase to ground fault in island mode	144
Figure 4.45	Rotor speed controls, during symmetrical fault occurs in island micro-grid	145
Figure 4.46	(a) Phase voltages (b) Line currents during three phase ground fault on the load side	146

## LIST OF SYMBOLS

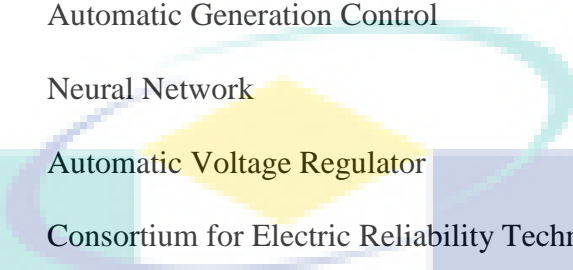


$\Delta f$	Frequency Error
$E_g$	Internal Voltage
$T_{mech}$	Mechanical Torque
$T_{elec}$	Electric Torque
$\omega$	Rotational Speed
$\Delta P_{Gov}$	Speed Governor
$\Delta P_r$	Change in Reference Power
$P_{ha}$	Hydraulic Valve Actuator
$P_{de}$	Load Demand
$P_{Tu}$	Change in Turbine Power
$P_m$	Electromechanical Power
$P_e$	Electric Power
$P_{acc}$	Acceleration Power
$K_i$	Gain Control
$J$	Moment of Inertia
$H$	Constant of Inertia
$\delta$	Angle Delta
$K_p$	Proportional Action Coefficient
$K_i$	Integral Action Coefficient
$\theta$	Synchronous Impedance Angle
$V_t$	Terminal Voltage
$V_{ref}$	Voltage Reference
$\Delta V$	Voltage Error

$X_{eq}$	Equivalent Reactance
$P$	Active Power
$Q$	Reactive Power
$F(\vartheta)$	Loss function
$\varepsilon$	Error between the Process output and the Reference model
$y$	Measured Output
$y_m$	Reference Model
$\gamma$	Gamma
$u$	Control Variable
$\vartheta_1$	Controller Parameter 1
$\vartheta_2$	Controller Parameter 2
$w_{ji}$	Weight Connection
$2-D$	Two-Dimensional Function

UMP

## LIST OF ABBREVIATIONS



AC	Alternate Current
ACE	Area Control Error
AGC	Automatic Generation Control
ANN	Neural Network
AVR	Automatic Voltage Regulator
CERTS	Consortium for Electric Reliability Technology Solutions
DC	Direct Current
DER	Distributed Energy Resources
DG	Distributed Generators
ESS	Energy Storage System
FLC	Fuzzy Logic Control
FLTC	Fuzzy Logic Table Control
IC	Incremental Conductance
IG	Induction Generator
IGBTs	Insulated Gate Bipolar Transistors
LFC	Load Frequency Control
LI	Lithium Ion
LQR	Linear Quadratic Regulators
MG	Micro-grid
MGCC	Micro-Grid Centralized Control
MIT	Massachusetts Institute of Technology
MPPT	Maximum Power Point Tracking
MRAC	Model Reference Adaptive Control

PCC	Point of Common Coupling
PI	Proportional-Integral
PLL	Phase Lock Loop
PV	Photovoltaic
RES	Renewable Energy Sources
SG	Synchronous Generator
SOC	State of Charge
STS	Static Transfer Switch
VSC	Voltage Source Converter
VSG	Virtual Synchronous Generator
WTG	Wind Turbine Generator
Z-N	Ziegler-Nichols



UMP

## CHAPTER 1

### INTRODUCTION

#### 1.1 Introduction

The power plants need to send the electricity to the customers using long transmission and distribution lines because they have been installed concentrated in one place and also out of the big cities. A lot of power is lost along the lines which creates the need for power substations to increase the voltage level at the point of transmission and reduce it at the point of consumption to minimize these losses. Also, most countries today recognize that climate change is a significant problem and are experimenting with ways to reduce greenhouse gas emissions that match their national interests (Peng et al., 2017). Furthermore, if the transmission system is subjected to proper or improper shutdown, the distribution networks will no more be an active part of the power system. However, recently there has been considered of interest in accommodating generating units to distribution networks. These units may be called as Distributed Generators (DGs), and the connection of these units may alter the operation of the network such as lessen the power losses, enhance the reliability of the system, improve the power quality and provide voltage support (Dulău et al., 2016).

Micro-grids (MGs) are a subset of the modern power structure that can operate either in grid-connected or island (i.e., autonomous) using DG to meet the total load demand and supply power to communities rather than vast regions (Patterson, 2013). The Consortium for Electric Reliability Technology Solutions (CERTS) is pioneering the concept of the CERTS micro-grid as an alternative approach for integrating small-scale Distributed Energy Resources (DER of < 500 kW) into electricity distribution systems (M. Kumar et al., 2016; Marnay & Bailey, 2004). This is an addition to IEEE Application Guide for IEEE Std 1547™, in which the IEEE Standard for Interconnecting Distributed Resources with Electric Power Systems is foundation

document for the interconnection of distributed energy resources (DER) in the electric power system or the grid.

The DGs in a hybrid micro-grid can be classified as inertial and non-inertial depending on their power flow control and dynamic behavior. First, the renewable energy sources (RESs) typically have low or non-existent inertial responses. For example; the variable speed wind turbines are usually connected to the network by power electronic converter, which effectively decouples the wind turbine inertia from mitigating system transients. Furthermore, solar photovoltaic plants do not provide any inertia response to the power system. Therefore, replacing conventional sources with RESs will reduce the inertia of the whole power system (Dreidy et al., 2017).

In a hybrid micro-grid, dynamic response of DGs is different between inertial and non-inertial DGs. The slow response is getting in inertial DGs, which is based on a rotary machine such as a synchronous generator. It is due to the response from its rotor inertia and governor control. Nonetheless, for non-inertial DGs which are using power converter interfacing produces a fast response to any changes. The synchronous generator has an effect on power system dynamic behavior, can lead to a different system frequency response to a disturbance event. Since then, the inertia sets the frequency sensitivity system to the overall system. As the inertia of the system is low, the change of system frequency associated with an imbalance of load generation will be faster. Adding synchronous generation (SG) to the power system increases the system's inertial response (Hassan Bevrani & Daneshmand, 2012). An essential part of the synchronous generator is the load frequency control (LFC). Since the primary objective of LFC or can be called automatic generation control (AGC) holds the frequency constant ( $\Delta f = 0$ ) against any load change. This controller is suitably designed to respond to the load variations and set the frequency to a constant value when working alone as an islanded system and to control the output power when operating in parallel at grid connected (Ghadiri et al., 2011). The mismatch would create a power and frequency oscillation especially in an isolated micro-grid (Majumder, Ghosh, et al., 2010).

The micro-grid should provide not only the power but also control the ac voltage amplitude and frequency. The DG control method can be classified into three categories according to the DG control method, i.e., PQ control, V/f control and droop

control (Soni & Firdaus, 2015). In Malaysia environment perspective, photovoltaic (PV) power is anticipated as a critical role in supplying electrical power in future electricity source. Since the PV is naturally intermittent, a help from energy storage is vital to increase the reliability of the power supply (Sparacino et al., 2012). The energy storage and RE sources also could improve the voltage regulation in the grid (Keshtkar et al., 2012).

Most of the LFC used PI-based controllers. Nevertheless, the gains tuning procedure and process, are the lacking of the controller to get a promising dynamic performance especially when the load varies (Taher et al., 2008). If the network is operated in fixed operating point (the disturbance does not involve any net change in power), the traditional LFC may perform in acceptable performances. The different operational philosophy of micro-grids as compared to conventional power networks brings to the need for adequate control strategies (Ambia et al., 2016).

However, the network of micro-grid system changeable due to fluctuation in power supply and loads, the improvement and efficient LFC must be introduced (John & Ramesh, 2013). The main advantage that expected from a micro-grid is that it allows treating as a controlled aggregated load within the power system. Also, for being in the vicinity of smart grid systems, the micro-grids should facilitate adaptive control approaches (Lidula & Rajapakse, 2011). However, fixed gain controllers were created at nominal operating points that will never be suited to all operating conditions (Mosaad & Salem, 2014).

In general, the term of adapting to something can be explained as behavior changes due to direct reactions to given circumstances. Based on this broad definition, an adaptive controller can be defined as the controller's ability to modify its behavior in response to any changes of the process dynamics that have an impact on the system (Coman & Boldisor, 2014). This type controller is desired to sustain the dynamic performance of the micro-grid for the whole choice of its operating issues. Nowadays, adaptive control systems are fascinating to explore due to the nature of this control approaches can cope with nonlinearity of the system. For the case of micro-grid, the following characteristics are difficult to grasp (Swarnkar et al., 2011):



1. The loads are changing abruptly.
2. Faults in the micro-grid could happen suddenly.
3. Unpredictable of external disturbances in the micro-grid.

Model reference adaptive control (MRAC) has been widely applied recently to solve control problems for a system with matched unmodeled dynamics (Dydek et al., 2010). Other than adaptive control, using the intelligence knowledge of models also can enhance the flexibility of the controller. In the many studies, it has shown the controller such as a fuzzy logic controller (FLC) has outperformed the linear controller such as PI controller. The field of neural networks (NN) also has seen phenomenal growth in the last decades. This is a good indication to use this type of controller for enhancing the performance in micro-grid.

## 1.2 Motivation of Research

The demand energy usage every year is constantly increasing that add to the challenging of generating electrical power as shown in Figure 1.1 (Bayindir et al., 2014). As a result, an explosive demand of all types of electric machines especially for power generation applications is expected in the near future (Guo, L. 2016).

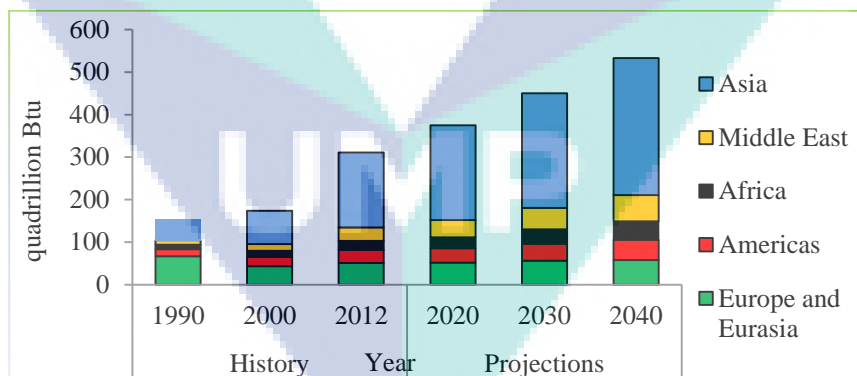


Figure 1.1 Energy consumption from 2012 and 2040

A micro-grid (MG) is defined as an independent of low or medium voltage power network consists of several distributed generators, energy storages and controllable loads (Ahn et al., 2010). Many economic benefits can be gained by applying the MG concept in all the countries (Venkataraman & Marnay, 2008). Over

3.1GW of new MG capacity is projected to be implemented worldwide. As shown in Figure 1.2, the United States is the current leader, with over 3 GW operating at 2012, and that capacity is expected to increase in next period (Asmus et al., 2009).

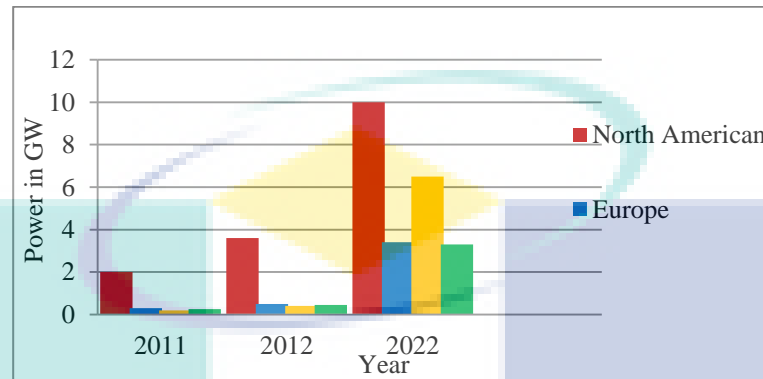


Figure 1.2 Forecast of micro-grid growth in 2022

However before selecting a hybrid micro-grid system as a power system option, it is necessary to perform the LFC analysis and observe control performances. On the other hand, the loads can change suddenly which can degrade the performance and frequency deviation. To make an efficient control approach, the LFC designs need to be considered as a decentralized robust control problem. However, there is also in previous studies for LFC in hybrid micro-grid systems using centralized control approach, but still, there is a minimal number of works involved in rotor speed control for controlling speed regulation.

### 1.3 Problem Statement

A hybrid micro-grid can operate in synchronous with the utility or as an island. It can disconnect from the grid at occurrences of faults or voltage collapses. Nonetheless, it may also intentionally detach when the power and voltage from the grid dip below specific standards (Guo, Y. & Gawlik, 2014). When micro-grid transfers from grid-connected mode to islanded mode, frequency control represents a major issue because the DG units in the micro-grid need to maintain the frequency (Hatipoglu et al., 2013; Rahman, 2015). Also, the combination of these various types of operation makes the hybrid micro-grid control a challenging task, mainly when the micro-grid operates in an autonomous mode. Therefore, the load power sharing among the micro-grid sources which maintaining the adequate system frequency and voltage is an important

control issue. In the application of SG as an inertia DG that interfaced to the hybrid micro-grid system, PI controllers have been designed to obtain adequate dynamic responses. In most of PI control methods, the control gains in these controllers are tuned with time-consuming job for utility engineers to find acceptable parameters. Furthermore, these methods are designed for one operating mode only, and that is may not be suitable in another operation condition mode, and large oscillations may occur in the system. As discussed, little or no attention between operation condition modes is presented in term of LFC which includes inertial and non-inertial sources. Moreover, the guarantee of the quality of transient from grid connected mode to islanded mode is one of the LFC problem need to be encountered. From these operation modes, the potentially undesirable power sharing among DGs degrades the performance in terms of over-power sharing or under-power sharing. As a result, the overall system's performance is not ensured.

In the distribution network, loads always fluctuate, and they are unbalanced, the main problems associated in the hybrid micro-grid (i.e., interfaced of inertia, non-inertia (DG)) and unbalanced load are as follow:

- 1) During sudden changes in loads, the power balance between supply and demand is not matched which can degrade the micro-grid transient behavior (Nisar & Thomas, 2016), may lead to frequency fluctuate, due to rotor inertia and governor speed control of rotating generators (Pota et al., 2014).
- 2) During the transition to island mode, the frequency of micro-grid is changed due to the loss of power transferred between main grid and micro-grid. Frequency deviation from the nominal value can exceed the limit if the loss of power is large enough (Nguyen, K.-L. et al., 2012). The control system is significantly influenced transient condition in micro-grid operations (Bakar et al., 2017).
- 3) Loss of grid supported and synchronization of micro-grid, in island mode lead to slow response and oscillation of the power-sharing and does not achieved the desired sharing, lead to increase the difference between the speed of response inertia and non-inertia DGs (Manaz & Lu, 2017) (Goyal et al., 2013).

## 1.4 Objectives of Research

Based on the above problems, many of the technical and controller issues need to be addressed carefully before their implementation. Thus the research aims to track the load variation and smooth the transfer from grid-connected to island mode. Further, covering any fluctuation occurring in frequency, as well as the required amount of power is provided at nominal frequency and voltage in the micro-grid during islanded mode operation. The specific objectives are as follows:

- 1) To develop the Load Frequency Control (LFC) of Synchronous Generator (SG) based Adaptive Proportional-Integral (API) controller in a hybrid micro-grid system using Model Reference Adaptive Control (MRAC).
- 2) To reduce the error signal in the MRAC and enhance tracking between grid connection to island mode operations by employing an Artificial Neural Network (ANN).
- 3) To improve the micro-grid response and synchronization during islanded mode operation by introducing a Fuzzy Logic Table Control (FLTC).

Lastly, all the performances of the proposed control methods are compared with conventional PI control method.

## 1.5 Scope of Study

When a massive change in micro-grid system operations occurs for instance when a suddenly significant load change or transfer micro-grid from grid-connected mode to island mode the degrading performances, and frequency deviation could occur. The existing or conventional PI-based controllers are not so efficient in term transient performances. Thus, to improve this, new and more efficient control methods such as MRAC, ANN and FLTC are proposed.

This work investigates the LFC in hybrid micro-grid under load variations by controlling the speed of SG to control the frequency. This study gives the detailed analysis and design of speed control using an adaptive PI controller and also concentrates on transferring of two-mode operations (i.e., grid-connected to islanded mode). The adaptive PI controller is utilized to build the control system by applying the MRAC. Associating ANN controller is used to update the output of MRAC and to

enhance control parameters at grid-connected micro-grid. The second operation employs FLTC in the isolated system to track the frequency deviation and then regulating the frequency. These proposed are developed and compared with the conventional PI controller through the simulation study using Matlab/SIMULINK.

## **1.6 Outline of Thesis**

This research comprises five chapters. Contents of each chapter are briefly described as follows:

Chapter 1: Starts with the thesis introduction present the importance of using the micro-grid system, motivation of research, the problem statement, the primary objectives, and the scope.

Chapter 2: Presents a discussion on the literature review of distributed generations, synchronous machines, and micro-grids.

Chapter 3: Describes the methodology in implementing the proposed control methods. The control strategies during different modes of operation are discussed in detail.

Chapter 4: Deals with the simulations and results of the system studied. It also includes the discussions of the results. The results of all control strategies studies are tabulated and discussed.

Chapter 5: Contains the conclusions about the work carried out. The main findings, discussions, attainment the objectives and contribute to the study are presented in this chapter. The recommendations for further investigation and improvement are also presented in this chapter.

## CHAPTER 2

### LITERATURE REVIEW

#### 2.1 Introduction

The demand for electricity continues to grow, providing for loads using local power generation is becoming competitive with central station generation. The hybrid micro-grid control and power sharing strategies are known as essential research issues. Micro-grids can be defined as autonomous small-scale power networks that contain multiple DGs and various critical loads. The first industrial micro-grid is built at the Whiting Refinery in Indiana, with 64 MW of installed power.

First, several DGs have been classified in the literature depending on their connection to the grid. The DGs in a hybrid micro-grid can be either inertial (rotating generators) or non-inertial (converter interfaced). In modern micro-grid, the combination of fossil-fueled generation (inertial) and RE sources (non-inertial) is introduced. The classification for micro-grid control is also presented by some researchers based on the concept of voltage performs and frequency regulation such as centralized and decentralized control systems. The response of the system to load changes and need for including for LFC is focused. The objective of LFC problem has been specified as to drive the speed control error back to zero for SG when operating as a DG unit in hybrid micro-grid.

Traditional LFC, such as PI/PID and LQR controllers, are not designed to be robust to uncertainties. For this reason, robust control techniques have been developed to make controllers that are less sensitive to uncertainties and disturbances in the process. Some of the authors use the artificial intelligent methods such as an artificial neural network (ANN), fuzzy logic control (FLC) to find the optimal configuration of a hybrid micro-grid which satisfies the optimal control strategy. Based on discussions of

the authors, it is promising to combine the advantages of ANN control and adaptive control methods in designing robust controller.

## **2.2 Distributed Generation System**

DGs are a crucial role in the modern electricity supply, in which the DGs could offer improved reliability and cutting the cost of long transmission infrastructure. Different benefits can be secured by merging multiple DGs units into the distribution network, such as low line losses, delayed network expansion, reduced emissions, improved power quality, reliability, and so forth (Panora et al., 2014). IEEE defines DG as “the generation of electricity by facilities that are sufficiently smaller than central generating plants to allow interconnection at nearly any point in a power system”. DGs have changed the distribution concept of electricity in medium and low voltage stage (Hatipoglu, 2013). Since the DGs are controllable, the power and voltage distribution could be controlled.

For further detail, the standard criteria and requirement interconnection of DGs in the electric power system can be referred in standard IEEE 1547.6 (Basso & DeBlasio, 2011). Meanwhile, the design and operation of DGs are documented in IEEE 1547.4 guide (Basso & DeBlasio, 2009).

## **2.3 Interfacing of Distributed Generation to the Grid**

The interface of DG units to the grid can be divided into two types (Al-Abri, 2012). i.e., direct grid-connected and indirect grid-connected of DGs.

### **2.3.1 Direct Grid-Connected Distributed Generation**

When the unit is achieved either using SG or induction generator, the prime mover operates at a fixed speed to drive these generators, as shown in Figure 2.1. SG is the most common type of electric generator used as an inertia DG unit. These are the rotating machines which convert the mechanical power applied from the turbine shaft to the electrical power. The controller is based on the concept of synchronverter (Synchronous Generator and inverter) which has been recently proposed in (Zhong & Weiss, 2011) to emulate the behavior of a synchronous generator by a virtual rotor. SG has an advantage over induction generators in that an SG's automatic voltage regulator



(AVR) can directly control power factor by supplying reactive power to the grid if needed, providing additional voltage support (Greacen, 2014). When an SG operates on infinite busbars, over-excitation will cause the generator to provide power at lagging power factor, and during under-excitation, the generator will deliver power at leading power factor. Thus, SG is a source or sink of reactive power.

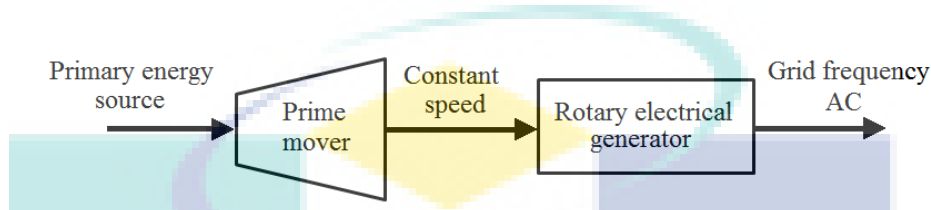


Figure 2.1 Schematic diagram of direct grid-connected DG

### 2.3.2 Indirect Grid-Connected Distributed Generation

Indirect grid interfacing DG is used when the output of the source is DC. In these types of DG units, a VSC is necessary to facilitate DG interfacing to the utility, which is used as the interface of renewable energy sources and energy storage elements to a distribution grid, as shown in Figure 2.2.

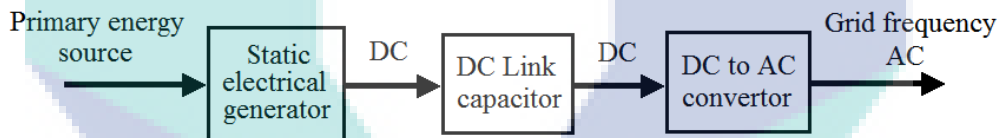


Figure 2.2 Interface-connected DG with DC output

The DC output voltage is produced in PV panel arrays and naturally intermittent. Therefore, the Maximum Power Point Tracking (MPPT) is a method to get maximum power from PV array that should be embedded in PV inverter (Benkhilil & Gherbi, 2012). Other than that, energy storage (such as battery, flywheels, and supercapacitors), also producing DC voltage that plays an important part in architecture micro-grid. Table 2.1 summarizes the interfacing and power flow control options of common DG.



Table 2.1 Summarizes the interfacing and power flow control options of common DG

<b>DG energy source type</b>	<b>Typical interface</b>	<b>Power flow control</b>
SG , IG, Small hydro	Direct	AVR and Governor ( $+P, \pm Q$ )
Micro-turbine	Converter (AC–DC–AC)	Speed of turbine and DC link $V$ controls( $+P, \pm Q$ )
Photovoltaic (PV)	Converter (DC–DC–AC)	MPPT and DC link $V$ controls( $+P, \pm Q$ )
Battery	Converter (DC–DC–AC)	SoC and output $V/f$ control ( $\pm P, \pm Q$ )

Source: Lidula & Rajapakse (2011)

## 2.4 Micro- grid and its Benefits

Future power grids must be attainable, flexible, reliable and economical according to the smart grid initiative around the world. Micro-grids are becoming an important concept to integrate DG and distributed energy storage systems (Micallef et al., 2012). The traditional definition of MG is succinctly defined by (Kazmi et al., 2017) as the following: “The micro-grid concept assumes a cluster of loads and micro-sources operating as a single controllable system that provides both power and heat to its local area”. The application of DGs has been increasing rapidly in the past decades. Compared to the conventional centralized power generation DG units provide more advantages such as less CO<sub>2</sub> dissipation, higher efficiency of energy utilization, flexible installation location and reducing pollution(Han et al., 2016). Distributed energy resources (DER) refer to both DG and energy storage technologies (Akorede et al., 2010). Most DGs operate at a power factor of 1 or close to it (Paraskevadaki et al., 2009). The below is explanation covers the essential features of micro-grid (Federau et al., 2016).

1. Composed of the standard grid components: generation, load and storage.
2. Closed power network, locally.
3. Operates as a controlled unit.
4. Can be disconnected from grid physically.
5. Two operational modes (connection and island).

The application of distributed power energy resources as DG can cause problems such as local voltage rise, the possibility of exceeding the thermal limits of

specific lines and a transformer, isolated and costly, which is the micro-grid, can solve these problems. In the hybrid micro-grid, the DG unit can be non-inertia DG (RE based sources) interfaced through voltage-source-converter (VSC) or inertia DG such as a synchronous generator. The response time for each DG to any change in load power demand will be different. The producing energy could be delivered to the local loads within the micro-grid area or exported to the main grid (utility) (Majumder, Ghosh, et al., 2010). Photovoltaic (PV) generations are expected to play an essential role as one of a clean electrical power that can meet the requirement in future electricity demands (Liyanage et al., 2011). Synchronous power generators are commonly used to provide power to distant and isolated regions where grid expansion is expensive due to economic and technical constraints. Micro-grid operation control is necessary, the purpose of control for the micro-grid system is to generate correct control signal regarding to the generators for producing electric power to achieve the stability of the system. In addition to smooth transfer from grid-connected mode to island mode, the response of the system should be fast, and it must be able to minimize frequency fluctuation and many other considerations. Some differences between inertia and non-inertia DGs are tabulated in Table 2.2.

Table 2.2 The comparison between inertia and non- inertia DG units.

<b>Inertia DG unit</b>	<b>Non-inertia DG unit</b>
Conventional	Non-Conventional
Connected directly to the grid	Interfaced through power electronic
Slow response to disturbance	Fast response to disturbance
Provide reactive power	Limit reactive power capability
SG, IG	Photovoltaic , ESS

## 2.5 Micro-grid Operation Modes

As shown in Figure 2.3, the micro-grid is composed of various DGs and loads, which are inertia distributed generator (synchronous generator), inertialess distributed generator (renewable), energy storage devices (battery), static transfer switch (STS), different types of micro-grid loads. The point of common coupling (PCC) is the distributed generation interconnection aspect of the micro-grid to the utility grid (Patrao et al., 2015). These DG units must be able to operate in two modes within the micro-grid operations. The output power depends on the synchronous generator as almost every type of inertial source is somehow related to a speed governor system. So,

building a power system without any synchronous machine (small hydro, thermal, fixed speed wind turbine, Diesel, etc.) DG is critical in term of reliability. The philosophy of micro-grid operations is that it typically operates in grid-connected mode. If the grid utility fails or is scheduled for maintenance, it can be isolated smoothly from the PCC utility and continue to operate as islanded mode (Bayindir et al., 2014).

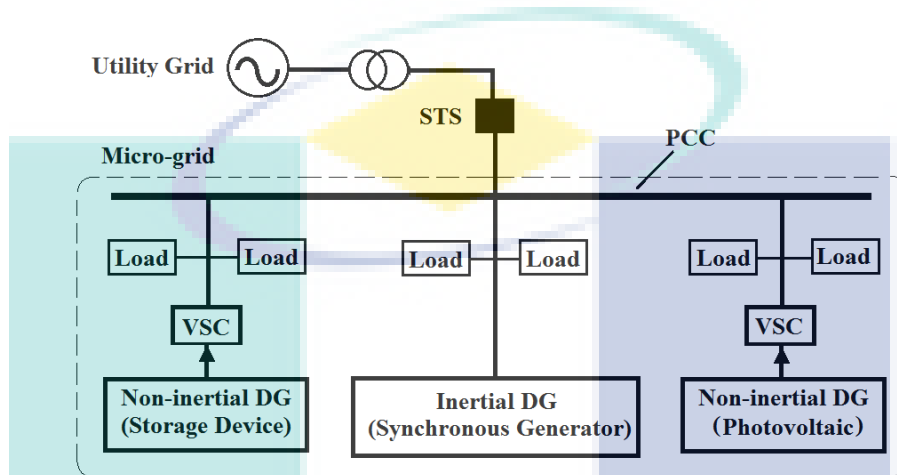


Figure 2.3 MG system connected to grid includes three DGs and loads

Source: Nguyen, K.-L. et al., (2012)

### 2.5.1 Grid Connected Mode

One of the main advantages of grid-tied micro-grid is the quality of service, reliability, and security. Besides that is to supply real and reactive powers under high power quality injection constraints. A micro-grid should appear as a single controllable load that responds to changes in the distribution system. In grid-connected mode operation, the MG is connected to the main grid at the Point of Common Coupling (PCC) to deliver power to the load (Nguyen, K.-L. et al., 2012). The SG runs at speed known as synchronous speed which is in synchronism with the frequency of the connected area (Adhikari, 2013). Any voltage or frequency fluctuation in the utility side has a direct impact on the load, voltage and power oscillation in the MG side. The influence of the grid connected to the synchronous generator and converter DG units, during the voltage drops is summarized in (Renders et al., 2008). The effect of the DG connected to the grid by the converter is reported to be negligible since most converters operate at one power factor and the current injected into the grid is limited to the inverter's nominal current.

Detailed models of the components and controls of the micro-turbine power plant are presented in (Grillo et al., 2010). The modeled includes various control loops; one of them is a speed controller (droop control) for primary frequency control. The speed controller is a PI controller. Modelling of the control scheme in the electrical subsystem is another issue of this work from the perspective of providing efficient power production from DGs.

In (Freitas et al., 2006; Londero et al., 2009), voltage sags are worsened with the increase of the DG penetration level. The isolation between the grid and MG not only ensures safe operation of the MG load, but it also prevents direct impact of MG load change or change in DG output voltage on the utility side. In case a disturbance occurs on the main grid the entire or a part of the MG can separate from the network to minimize disturbance to the local loads. These can be industrial or sensitive loads which require a high level of power quality and reliability.

### **2.5.2 Islanded Mode**

In the islanded mode, DG units are required to supply “regulated power” under controllable voltage and frequency while maintaining accurate power sharing among different DG units (Horowitz et al., 2010; Mohamed & El-Saadany, 2008). Islanding happens when the DG (or group of DGs) continually activates a portion of the micro-grid system separated from the main utility system (Sarabia, 2011). In this mode, the purpose of control is specific that the required amount of power is provided in nominal voltage and frequency. Further to ensure that the generations in the micro-grid do not lose synchronism (Bhaskara, 2012). During islanded mode, the utility grid is not existing; Therefore, if there is no unit DG support the fundamental frequency and control voltage, frequency and voltage will be changed freely in the micro-grid (Ashabani & Mohamed, 2012). In (Delghavi & Yazdani, 2009) a control design for DG's island type operation is presented. This adopts the feedforward method, but only one MS is employed. The impact of rotating machine based DGs on the frequency stability is examined by (Manaz & Lu, 2017) in this reference; the total load is supplied by the solar PV operated under MPPT and a diesel generator. According to the net load variation, the controller measures the Change Rate. The controller frequency records the  $P_m$  at that time as the reference value ( $P_{m\_ref}$ ). When the difference between  $P_m$  and  $P_{m\_ref}$  is smaller than the specified threshold  $\Delta$ , the ramp command is gradually

reduced to zero. This work lacks an energy storage system unit when that solar PV output changes. The islanded operation is possible only when there is sufficient local generation to meet load demands, if not a few non-critical loads to be shed after the islanding (Khorramabadi & Bakhshai, 2015).

## **2.6 The Necessity for the Synchronous Generator in Micro-grid**

In particular, for large load changes, synchronous generators based Distributed Energy Resources (DER) can lead to significant transient voltage and frequency (Ajit A Renjit et al., 2014). When operating a micro-grid system, continuous demand change must be accompanied by appropriate changes in a generation to preserve the balance between production and consumption.

Mini size synchronous generator as a DG it mostly has a short time to start – up and can provide power in a micro-grid concept. Synchronous machine based DG is usually used in combination with heat and power application. A system that combines heat and power can reduce the energy cost with very high energy efficiency. Therefore, it is very beneficial to include asynchronous machine-based DG in the micro-grid (Bhaskara, 2012). In an environment of micro-grid, the synchronous generator will be needed to operate in various scenarios or modes. A distributed natural gas power supply is typically connected to a micro-grid through a synchronous generator (Mondai et al., 2014). The benefit is that it allows the electric network to operate in an actual smart grid. Therefore depending on the operating mode of micro-grid control systems for synchronous generator control strategies must change to meet the needs mode of operation.

In the micro-grid system, the control system of the synchronous machines needs to ensure certainly that the synchronous generates real and reactive power within the ratings of the machine at nominal voltage and frequency as required by the system to which it is connected. An algorithm of the stability type suitable for analyzing the inverted dominant LV micro-grid is presented in (Soultanis et al., 2007). The approach to sustainability is adapted in such a way that it can be applied to systems inertialess.

This work did not offer any approach for micro-grid containing DG based on synchronous machines and inverter together. The actual power from the generators can be controlled mechanical power input, and reactive power can be controlled by

excitation control (Quamruzzaman & Rahman, 2008). For increase inertia in the grid is to mimic the behavior of the actual synchronous generator by appropriately controlling the power electronic inverter with the energy storage unit. This basic concept is investigated as a virtual synchronous generator (VSG) in (Beck & Hesse, 2007). A flexible virtual synchronous generator control (FVSG) with adaptive inertia is proposed in (Meng et al., 2016) and introduced to VSG control by thoroughly considering the relation between frequency fluctuation rate and system inertia. Compared to the actual synchronous generator, the VSG has no real rotor system. And this means the cancellation of rotor activity which in turn provides the required frequency in the general operation of power system.

For control synchronous generator it is confirmed that generates active and reactive powers within the machine's rating at the nominal voltage and frequency required by the system it is connected to it (Bhaskara, 2012). The frequency behavior is relatively usual because the phenomenon starts and ends in a stable process: a range of  $50 \text{ Hz} \pm 100 \text{ mHz}$ . The shape of the frequency deviations follows the load development. As the load growth, the frequency deviation begins with an increase. When the evolution of the load decreases, the frequency deviation starts to drop. The structure of frequency control in the synchronous generator could alleviate frequency deviations, and generate unit deliver active power reserves. In system areas having automatic frequency restoration control, this control enables frequency restoring reserve proportional to the variance (Entso-E, 2011).

Figure 2.4 shows the model of a synchronous generator and its phasor diagram, which could be represented by a constant internal voltage  $E_g$  behind the axis transient reactance  $X$  in the circuit diagram. SG is represented by a constant internal voltage  $E^\circ$  behind its direct axis transient reactance  $X^\circ$ .



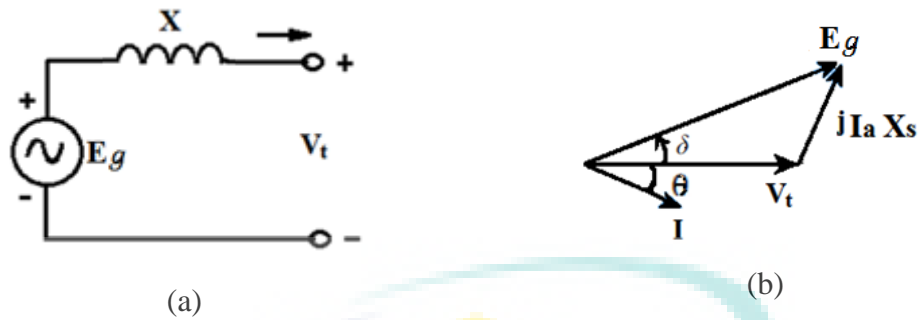


Figure 2.4 Synchronous machine (a) circuit diagram (b) phasor diagram

By controlling the mechanical power input, the real power can deliver from the generator, while reactive power can be controlled by controlling the excitation. The changes of the opening of a valve which fuel enter the turbine will change the input mechanical power of the synchronous generator. Thus, the active power generated through the valve could be defined as;

$$P = \frac{E_g \cdot V_t}{X} \sin \delta \quad 2.1$$

If an excitation that applied to synchronous generator is kept constant, the  $E_g$  will remain constant. Then, with the increasing of input mechanical power, the rotor speed will also increase. Thus,  $\delta$  will increase if  $V_t$  and  $X$  are remain constant. As a result, the generator will deliver more real power as follows;

$$P = V_t * I \cos \theta \quad 2.2$$

### 2.6.1 Turbine Governor

From Figure 2.5 the turbine governor contains two main parts of PI controller and droop characteristics. The governor can be set with various parameters as follows, existing operational situation, startup, normal, disturbance, etc. The turbine governor controller has two inputs; the deviation of the mains frequency [Hz] from the rated value of 50 Hz, as well as the set power value [MW] (Kaisinger, 2011).

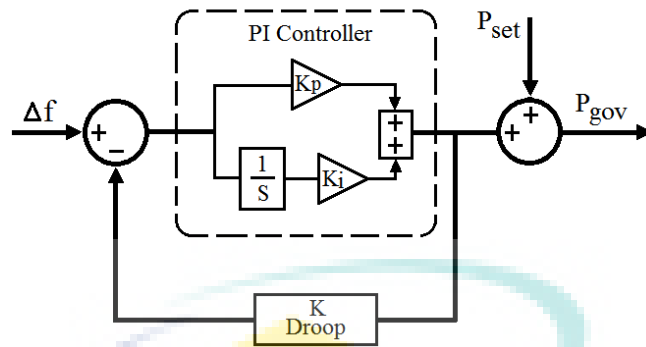


Figure 2.5 Simplified turbine governor

Source: Kaisinger (2011)

The speed-governing system is used to adjust the frequency. Governors change the turbine valve/gate to bring the frequency back to the nominal or scheduled value. For power and load sharing among generators connected to the system, speed regulation or droop characteristics must be provided (Galassini et al., 2016). The speed governor is an essential component of a synchronous generator that regulates the flow of water through the turbine by controlling the gate position, based on the feedback error signal generated by analyzing speed and load fluctuations. This ensures not only the girdle of frequency stability but also the balance of the active power considering load fluctuations (Ali, W. et al., 2017). The governor controls the changes of fuel supply to the turbine in response to a difference in generator speed, thereby controlling the generated power and regulating the changes in frequency. Speed regulation or droop is provided to ensure the proper load sharing.

## 2.7 Load Frequency Control in Power System

Load frequency control (LFC) involves the problem of matching the power generation and loads, which is essential in power system operation. In fact, when the load's changes, the power supply must be capable of reacting appropriately for maintaining the grid stability (Pandey et al., 2013). The primary objective of LFC is held the frequency constant ( $\Delta f = 0$ ) against any load change (Prakash, S. et al., 2009; Usman & Divakar, 2012), and the tie-line must keeping the power flow to the distribution areas. From (Zhang et al., 2009), the PI controllers are widely adapted to the LFC for over the decades.



The abrupt changes of loads lead to frequency mismatches and power interchanges. The zero frequency deviation is difficult to obtain for huge loads change even it has a speed governor in generators. Hence, the LFC is essential to overcome the mismatches issue, which could be divided as follows (Rebours et al., 2007; Xu, 2014):

- (1) Primary control is a local automatic control that adjusts the active power generation of the generators and the consumption of controllable loads to restore the balance between the load and the generation to eliminate frequency variations. Primary control is indispensable for the stability of power systems and is performed by the speed governors of the dedicated power generation units.
- (2) Secondary control is a centralized automatic control that adjusts the active power production of the generators to restore the frequency and the interchanges with other systems to their target values. In other words, if primary control cannot stop frequency excursions, secondary control will bring the frequency back to its target value.
- (3) Tertiary control is to manual changes in the dispatch and commitment of generators. Tertiary control is used to restore the primary and secondary frequency control reserves, to manage congestions in the transmission network, and to bring the frequency and the interchanges back to their target value when the secondary control is unable to perform this last task.

Today the synchronous generator is modeled in both axes with quantities of transient and sub-transient (Hasni et al., 2008). The purpose of LFC is to maintain system frequency and tie-line power interchanges close to specified values (Ganapathy & Velusami, 2009). The generation units, driven by their turbines are responsible for maintaining the frequency in the system. The frequency of the system voltage (50Hz) is directly proportional to the speed of the traditional generation unit typically (Droop Speed Control) (Reza, 2006). Frequency directly related to the speed of rotation, i.e. (constant frequency = constant rotation). If input mechanical energy identical and equal with electrical energy output lead to positive mechanical torque similar to negative of electric torque as shown in Figure 2.6, then speed remains constant. The electrical load

changes are uncontrolled and subject to disturbance, mechanical energy input must be controlled to match this disturbance.

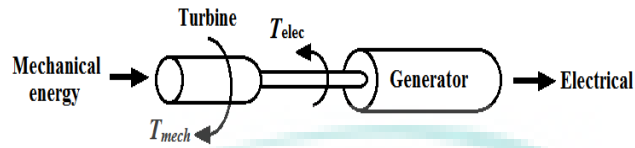


Figure 2.6 Mechanical torque and rotational speed

From Figure 2.6,  $T_{mech}$  is the mechanical torque by turbine,  $T_{elec}$  electric torque by generator, the rotational acceleration is  $\alpha$ , when:

$$I\alpha = T_{net} \quad 2.3$$

$$M = \omega I \quad 2.4$$

$$P_{net} = \omega T_{net} = \omega(I\alpha) = M\alpha \quad 2.5$$

Where  $\omega$  rotational speed,  $\alpha$  rotational acceleration,  $T_{net}$  net accelerating torque in machine.  $I$  is a moment of inertia for the machine,  $M$  angular momentum for the machine,  $P_{net}$  net accelerating power.

$$\Delta P_{mech} - \Delta P_{elec} = \omega_0 I \frac{d}{dt}(\Delta\omega) \quad 2.6$$

$$= M \frac{d}{dt}(\Delta\omega) \quad 2.7$$

All of the conventional control schemes of LFC have inherent problems that increase the frequency feedback gain and results in the instability of the LFC loop, which restricts the control range of frequency droop. To improve this, the conventional PI control scheme can be adopted, which are the main drawback of this result is that the selection of its gain is mainly based on a trial and error method and the system operators' experience (Khodabakhshian & Golbon, 2005). It is also well known that the speed governor of turbine needs to be equipped by a transient droop compensator. This ensures that the system will be stable when the load changes and, as a result the

frequency alters. However, this makes the system response to be comparatively sluggish (Kundur et al., 1994).

In the case of one generator provides power to one service area. This system has the linear model shown in Figure 2.7; It is obtained by linearizing the plant around the operating point (Tan, 2011).

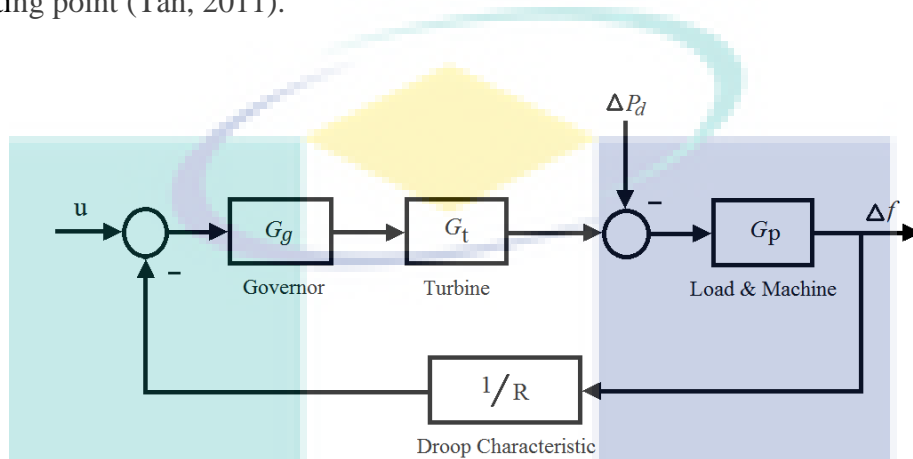


Figure 2.7 Single-area power system

The model of the system can be expressed as:

$$\Delta f = G(s)u + G_d(s)\Delta P_d \quad 2.8$$

Where

$$G(s) = G_p G_t G_g / (1 + G_p G_t G_g / R) \quad 2.9$$

$$G_d(s) = G_p / (1 + G_p G_t G_g / R) \quad 2.10$$

$G_g$  is the governor dynamics  $= (1/T_G s + 1)$

$G_t$  is the turbine dynamics  $= (1/T_T s + 1)$

$G_p$  is the power system dynamics  $= (K_p/T_p s + 1)$

$1/R$  is the droop characteristics.

Therefore Load frequency control is the problem of disturbance rejection; it utilizes feedback  $u = -K(s)\Delta f$  to stabilize  $G(s)$  when the load disturbance occurs  $\Delta P_d$ , at the same time reduce the impact of  $\Delta P_d$  on  $\Delta f$ .

In synchronous generator rotor speed, under steady state conditions, is proportional to the frequency of the armature current. The following equation governs this;

$$\Delta f = \frac{p}{50} n_{sys} \quad 2.11$$

Where  $n_{sys}$  denotes the synchronous speed of the generator in revolutions per minute [rpm],  $p$  the number of pole pairs of the magnetic field circuit, and  $f$  the frequency of the generated voltage (Hz).

## 2.8 Micro-grid Control

The fundamental problem with a micro-grid is the control of the number of micro-sources (i.e., distributed generation (DG)). Furthermore, recent research has confirmed a technical challenges of efficient micro-grid control (Majumder, 2013; Su et al., 2011). Therefore, development of future micro-grids requires control systems to ensure the system's operation. Some of the basic issues that need to be addressed are:

1. Attach or detach new micro sources. This would affect the power flow of micro-grid system.
2. Optimizing the micro-grid operation either grid-connected or isolated modes.
3. Effect of immediately isolate from the utility grid. This could degrade the micro-grid frequency and voltage.
4. Power control in micro-grid (active and reactive power).
5. Correction of distortions imbalances such as voltage sag and faults.
6. Dynamic of loads (demand variations).

With the growth of distributed generation and its operation in tandem with utility power supply, the interconnection of distributed generators (DGs) to the utility grid has raised concern about system control and power sharing among the DGs. Control of the DG system is important and system regulation such as frequency deviation and voltage drop becomes very crucial during the decentralized power sharing through control methods.

There are many control methods described in the literature, which help to address the challenges from implementing micro-grid. These control methods are based on the concept of voltage perform and frequency regulation (Planas et al., 2013).

### 2.8.1 Micro-Grid Centralized Control (MGCC)

The centralized control system can realize intelligence from a specific central location that depends on the network system type, and it can be a transition, a server, or a controller can be seen in Figure 2.8. It is easy to operate a centrally controlled network and enhances control to operators and conserves the entire system, while requires a single controller to deal with all measurement data (Justo et al., 2013).

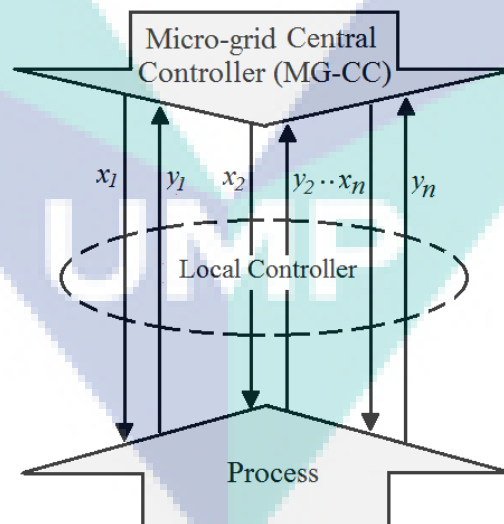


Figure 2.8 Centralized control Multi Input Multi Output systems

Referring to Figure 2.8,  $x$  is control input, and  $y$  is output. A distributed control is proposed that every DG has its own local secondary control that can produce appropriate control signal for the primary control level by using the measurements of

other DGs in each sample time. The communication latency is considered when (sending / receiving) information (to / from) other DG units and the results are compared with the conventional MGCC. This unique controller point can cause some communication problems and can lead to several disturbances, so is not highly reliable and that may damage all the system (Shafiee et al., 2014). With the addition of distributed generators in the power distribution system, centralized control of the real and reactive power dispatch is neither cost-effective nor practical (Fuad, 2017).

### 2.8.2 Decentralized Control

As a second basic concept, decentralized controls systems define build multiple and independent control algorithms to perform the same control functions for different sub-processes without continuous overall perceptions. A decentralized control approach intends to maximize the autonomy of DER. For example, it may require an operation or not from a distribution point where such a decision increases the communication speed of the entire system.

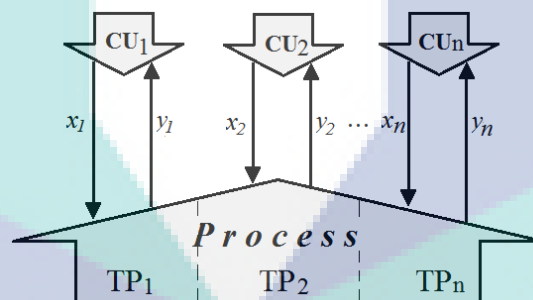


Figure 2.9 Decentralized regulators for Multi Input Multi Output systems

As illustrated in Figure 2.9, the decentralized controller allows a system in which all devices can independently control themselves, unlike the "master" controller. Where CU is control unit/algorithm, TP subprocess, x is control input, and y is output. In (Zamora & Srivastava, 2010), the investigation is a very simple scheme of a micro-grid with three DGs. In this article, there is no mention and was not analyzed DG resource structure, controller of each micro source. Decentralized control is the best selection in cases of various requirements that are directed to the micro-grid on the sides of generation and consumption, where a variety of sources and loads require monitoring and tuning in real time (Vasquez Quintero, 2009). Table 2.3 indicates

various approaches are possible with two operational modes of micro-grid (Bayindir et al., 2014).

Table 2.3 Micro-grid control techniques

Micro-grid Central Controller (MGCC)		DG Controllers (DGCs)	
Grid-Connected	Islanded	Grid-Connected	Islanded
*Monitoring is based on data collection inherited from LV networks, DG, and loads.	*Controls the power flow of DG (P,Q), and stabilizes V and f, prevents interruptions by improving strategies and using management with ESS support.	*Monitors and controls each DG unit in order to manage the load demand in both grid-tied and islanded modes, and controls the transitions through modes with the help of MGCC.	*Checks all DG units independently in order to assure that the generated voltage has been transferred to the load in islanded mode, and tracks the utility grid to operate in synchronized mode due to micro-grid control features.
*Provides many control methods: prediction, security, power flow, and requirements management.	*Initializes local black start to maintain reliability of power supply and sustainability of service.		
*Maintains synchronized operation with grid and keep power exchange at or before the contract points.	*Interconnects the micro-grid to grid-tied mode when the utility grid is stabilized after a probable fault.		

## 2.9 Load Frequency Control in Micro-grid.

Unlike high voltage interconnected power systems, MG is typically used to form the best low voltage distribution systems. It is a combined energy system, including interconnected loads, DG and storage units (Liu, S. et al., 2013; Liu. S. et al., 2014). LFC is an essential part of the SG. This controller can be designed correctly to handle load fluctuations and to fix the frequency at a constant value. Furthermore, when working in parallel with the main system, the output power is controlled. In MG system operations, the load is changing continuously and randomly, leads to an imbalance between the actual and the scheduled generation quantities. It will not be common to find fully controllable SGs in MG, which are typically responsible for voltage and frequency control in conventional power systems (Lopes et al., 2006) this issue is becoming more significant, due to the increasing number of MGs. Most DG technologies that can be installed in MG are not suitable for direct connection to the electrical network due to the characteristics of the energy produced (Pogaku et al., 2007) (Blaabjerg et al., 2006). The power electronic inverter based interfaces used in the majority of DG units forming the islanded MG lacks the physical inertia typically

available in the SG rotating masses. This lack of physical inertia introduces a high level of susceptibility to the choice of system parameters, the system load ability and to system disturbances arising in the MG including system transition between the grid-connected and islanded modes of operation (Farag et al., 2013). In (Liu, S. 2014) the author classified load frequency control in micro-grid to the two-level hierarchical structures shown in Figure 2.10.

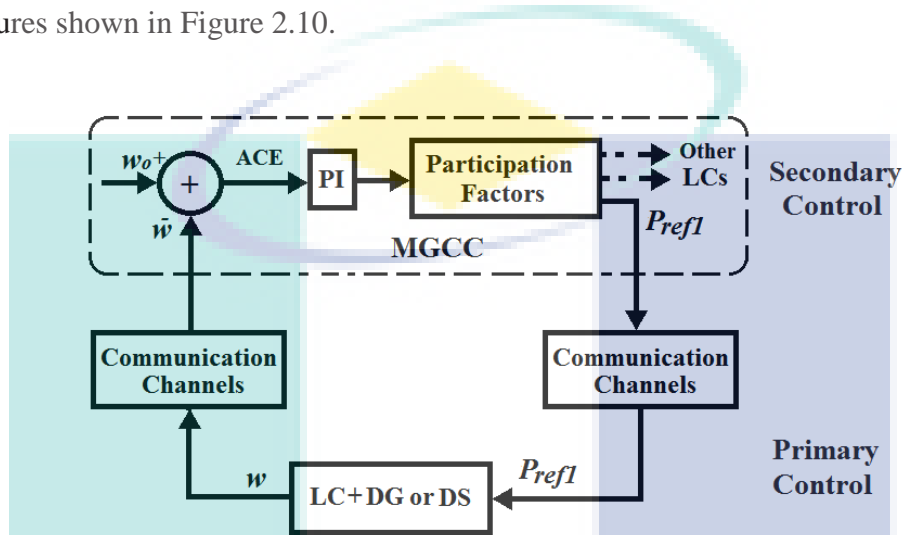


Figure 2.10 Load Frequency Control of a micro-grid with two-level hierarchical

Primary control, the local controller LC commonly refers to the control of inverter because the DG is connected to the prime mover via VSI including a fixed power controller with droop controller. By the support of a second frequency controller, the micro-grids frequency can be restored to its nominal frequency.

Secondary control, it is run only in island micro-grid mode where a micro-grid centralized controller (MGCC) is present at the low voltage direction of a substation in a micro-grid. To restore the frequency to the nominal value constant by the utility, MGCC produces additional real power values for the LC DG and distributed storage DS and sends them to relevant LCs with a low bandwidth communication channels.

### 2.9.1 Conventional Load Frequency Control in Micro-grid

In general, the MGs should be able to operate autonomously but also interact with the main grid. In the islanded mode, to cope with the variations, and to respond to load change, and performing active power/frequency regulation, and reactive power/voltage regulation, the MGs need to use proper control loops (Bevrani, H. et al., 2012). Some previous studies presented different techniques of providing power



regulation and LFC for micro-grids. The power system model for LFC has also been proposed incorporating wind turbine generator (WTG).

### 2.9.1.1 Proportional, Integral and Derivative Control (PID)

Typically, the commercial production of the generator is the electronic speed governor and is modeled as the traditional PID control block which adjusts the engine speed equal to the reference speed generator set-point. During load change, it regulates the amount of fuel injection in the engine cylinders depending on the error value of the engine speed (Ajit Anbiah Renjit, 2016).

In MG operation of wind-diesel-photovoltaic and BESS hybrid power system, the intermittency in wind speed, and solar radiation cause a significant fluctuation in system power and frequency. A coordinated control approach based on the minimal-order observer for the LFC problem is presented in (Datta et al., 2011). In the reference (Ullah et al., 2008) variable speed wind turbines have a speed controller, which has the task to keep the optimal tip speed ratio  $X$  over different wind speeds, by adapting the steady state generator speed to its reference value. A variable speed wind turbine is supplied on the wind, which is not controllable. Therefore wind turbines cannot participate in the load frequency control.

In (Gözde et al., 2008), the LFC is designed using PI controller, but the tuned gain of integral (I) contributes to the difficulty of getting a promising dynamic performance in various scenarios. The SG consists of controller (which is to be tuned) governor, turbine, and generator (Wood & Wollenberg, 2012), a governor, or speed limiter, is used to regulate and measure the speed of a machine, and this reflected in frequency regulation. The output commands of speed governor are  $\Delta P_g$ . The speed governor has two inputs: change in the reference power setting,  $\Delta P_{ref}$  and change in the speed of the generator,  $\Delta f$ . It is to be noted that a positive  $\Delta P_{ref}$  will result in positive  $\Delta P_g$ .

However, there is a steady-state frequency error  $\Delta f$  when the change in the turbine-governor reference setting  $\Delta f$  is zero. The change in reference power setting  $\Delta P_{ref}$  of each turbine-governor operating under LFC is proportional to the integral of the area control error (Glover et al., 2012; Shah & Kotwal, 2012).

For a hydro turbine, (Ruzhekov et al., 2011) has proposed adaptive gain scheduling technique for turbine power control. The investigation of hydro turbine power variations is carried out and compared with PI controller. The author has used the dependent parameter model and power as a variable reference. The pole placement approach is adapted to get an adaptive state space that applied to plant model.

In (Ahn & Choi, 2012) trying to restore the micro-grid frequency to a nominal value, and ensuring proper power sharing among multiple DGs, rating and dynamic characteristics of various energy sources which considering in this study. The author uses the power vs. frequency droop control, also suggests two secondary LFC, the first one is using a central controller which sets the power reference signal of each DG and the second one inserted as integral controller to the existing droop controller.

Majority of isolated micro-grids, especially in remote communities, depend on synchronous machines with diesel engines (Farrokhabadi et al., 2017). In (Ota et al., 2007) a BSS is used with PV, diesel generator and wind power generation for LFC of a power system. The LFC was performed in two different ways. First, using an estimation of power demand and second using proportional control. The purpose is to track the frequency deviation with minimum error. However, it is not an appropriate working when the load is varied. This method is typically used when the absent of energy storage. It is also, since the load changes are not often occurred, contributes to the shortcomings of the load demand estimation method.

### **2.9.1.2 Linear Quadratic Regulator (LQR)**

Classical optimal control theory has evolved over decades to formulate the well-known Linear Quadratic Regulators which minimizes the excursion in state trajectories of a system while requiring minimum controller effort. LQR is an optimal controller. Optimal means are providing least possible error to its input; i.e., one or more of the outputs of the plant combined with minimizing the control output. This control mechanism is based on the model of the plant taken into consideration or control. The controller is said to be optimal if the model replicates plant accurately. The LQR is a state feedback controller where the states of a system may have some physical meaning, or may not have at all. Accordingly, there may be trouble in finding out the states to use for feedback. For this, another function called an observer is required, which estimates

the values of the state. But the complexity of the system increases due to the involvement of observer. This is based on state space model (Nagrath, 2006). In (Wang & Crow, 2011), linear optimal controls based on the linear quadratic regular (LQR) control are proposed. LQR is also a pole placement method. In this method, the poles of the system are placed indirectly by minimizing a given performance index (J), by optimizing the given performance index J, the feedback gain matrix K can be obtained.

### **2.9.1.3 Model Reference Adaptive Control (MRAC)**

Adaptive Control techniques allow controlling systems where specific system parameters are not known or change over time e. g., due to the changing the operating environment (Stellet, 2011). Model reference adaptive control (MRAC) is derived from the model following problem or model reference control (MRC) problem. In MRC, a good understanding of the plant and the performance requirements are allowed to meet the designer to come up with a model referred to as the reference model that describes the desired I/O properties of the closed-loop plant. The objective of MRC is to find the feedback control law that changes the structure and dynamics of the plant so that its I/O properties are the same as those of the reference model (Ioannou & Sun, 2012; Swarnkar et al., 2010). The primary MRAC system consists of four essential elements (Swarnkar et al., 2011) as follow:

- 1- Plant to be controlled.
- 2- Reference model to generate desired closed loop output response.
- 3- Controller that is time-varying and whose coefficients are adjusted by an adaptive mechanism.
- 4- Adaptive mechanism that uses 'error' (the difference between the plant and the desired model output) to produce controller coefficient regardless of the actual process parameters.

Adaptation in MRAC takes the form of adjustment of some or all of the controller coefficients so as to force the response of the resulting closed-loop control system to that of the reference model. Consider the general adaptive control setup

shown in Figure 2.11 the controller receives specific references or set points to follow and some input and output measurements (Gallestey et al., 2015).

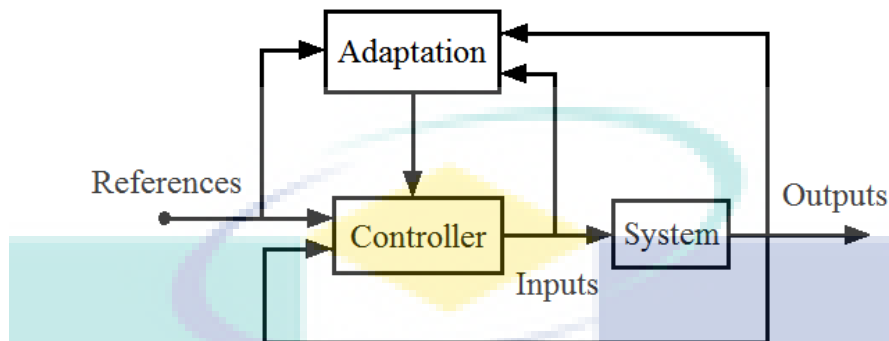


Figure 2.11 General adaptive control scheme

MRAC is well known that the system parameters will change over time, this leads to the degradation in the performance of a fixed parameter controller. Fixed gain controllers can become even unstable with these parametric uncertainties. This problem can be avoided by using adaptive control design techniques. An adaptive controller has an advantage over a fixed gain controller by using a reference model that describes the desired response characteristic for the system, and then applying adjustable parameters and mechanisms for adjusting the parameters in the controller to drive the system's response to behave like that of the reference model (Nguyen, T. D. 2016).

a) MIT Rule in MRAC

MIT rule was first developed and used in Massachusetts Institute of Technology for designing the autopilot systems for aircraft, is used to apply the model reference adaptive control approach to any practical system. The reference (Jain & Nigam, 2013), deals with the MRAC PID control using MIT rule to control a second order system and achieves satisfactory performance the output speed response of the DC motor. The cost function is defined regarding the error between the actual behavior and ideal behavior of the plant as shown in Figure 2.12. Defining the cost variable:

$$J(\theta) = \frac{e^2}{2} \tag{2.12}$$

This is merely the difference between the plant output and the reference model output:

$$e(t) = y(t) - y_m(t) \quad 2.13$$

Parameter  $\theta$  is adjusted in such a fashion so that the cost function can be minimized to zero. For this reason, the change in the parameter  $\theta$  is kept in the direction of the negative gradient of  $J$ , that is

$$\frac{d\theta}{dt} = -\gamma \frac{\partial J}{\partial \theta} \quad 2.14$$

In (Yadav et al., 2013), by providing smooth control to the excited DC motor, the model reference adaptive PID control (MRAPIDC) have been implemented. The goal is to converge the ideal value so that the parameter matches the response of the reference model. The output of the system is compared with the response from the reference model. In (Sengupta & Dey, 2017), also dealing with speed control of DC motor using MRAC that use the MIT rule with the normalization algorithm to cope with the fluctuation of the reference signal. It is shown that the adaptive system becomes oscillatory if the value of the adaptive gain or the amplitude of the reference signal is sufficiently large.

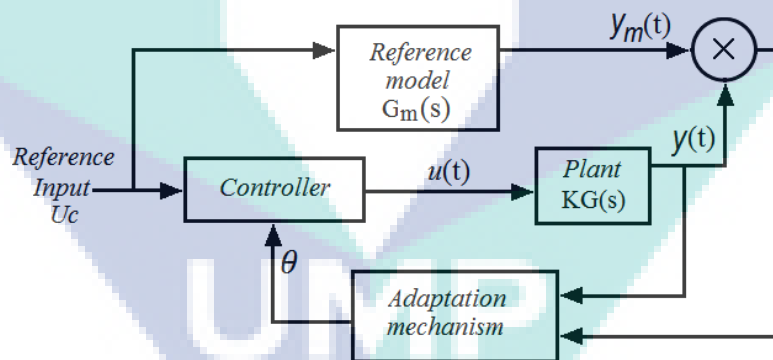


Figure 2.12 Model Reference Adaptive Control System

Source: Jain & Nigam (2013)

a) Lyapunov's Theory in MRAC

The Lyapunov stability theory can be used to design adaptive control laws that guarantee the stability of the closed-loop system. The Russian mathematician Lyapunov made the fundamental contribution to stability theory for the nonlinear system at the end of the nineteenth century. Lyapunov investigated the nonlinear differential equation; this approach is based on finding suitable candidates for Lyapunov functions

(Al Hokayem & Gallestey, 2011). For an update, the law is the “Lyapunov rule” which is given as:

$$\frac{d}{dt}\theta = -\gamma e r \quad 2.15$$

Where  $r$  is the reference input signal, in order to derive this formula, the following Lyapunov function is defined:

$$V = \frac{1}{2}\gamma e^2 + \frac{1}{2}b(\theta - b_m/b)^2 \quad 2.16$$

In (Pankaj et al., 2011) Compares the MIT rule and Lyapunov rule for developing the adaptation mechanism by different time response specifications, the characteristics show that there is very less difference in responses for both the models. So the physical realization of the system under consideration is comparatively more feasible with Lyapunov theory. But the mathematical modeling of system is more straightforward for MIT rule.

In (Mohammed, 2017), Conventional Power System Stabilizers structure is considered based on the mathematical model of generator control system with PSS; the system damping is increased depending on the PSS. The author introduced a method for PSS design based on model reference adaptive control. Adaptive control applied to design of power system stabilizer by MIT Rule and Lyapunov method. In both methods, the range of adaptation gain is chosen from 0.4 to 5 for the system under consideration.

### 2.9.2 Intelligent Load Frequency Control in Micro-grid

Traditional LFC may not be suitable for a hybrid micro-grid control due to the integration of renewable energy sources and changes in structure and size of the power system. In the dominant control scheme, the structural complexity and reconfiguration of the plant may be required. To avoid this problem, intelligent control scheme using soft computing technology such as particle swarm optimization (PSO) algorithms, genetic algorithm (GA), artificial neural network (ANN), fuzzy logic, etc. (Pandey et

al., 2013). In last decade, Artificial Neural Network Controllers (ANNCs) and Fuzzy Logic Controllers (FLCs) being used as power system stabilizers, have been developed. Unlike other classical control methods, ANNCs and FLCs are model-free controllers; i.e., they do not require an exact mathematical model of the controlled system. Moreover, speed and robustness are the most significant properties in comparison to the other classical schemes. But these controllers present some disadvantages. There are not practical, systematic procedures for the Fuzzy PSS (FPSS) design, so the rules and the membership functions of the controller are tuned subjectively, making the design laborious and a time-consuming task.

### 2.9.2.1 Artificial Neural Network (ANN)

The field of Neural Networks (NN) and its application to control systems has seen phenomenal growth in the last decades. Neural networks NN control method has been used in current controllers because of its high robustness (Prakash, R. & Anita, 2011). Like the biological systems, networks modify themselves as a result of experience to produce a more desirable behavior pattern. Adjusting the weights is commonly called “training,” and the network is said to “learn”. A single neuron can perform a particular simple pattern detection function; the power of neural computation comes from connecting neurons into networks.

Figure 2.13 shown an artificial neural network is an interconnected group of nodes, nigh to the vast network of neuron in a brain. Here, each circular node represents an artificial neuron and an arrow represents a connection from the output of one neuron to the input of another.



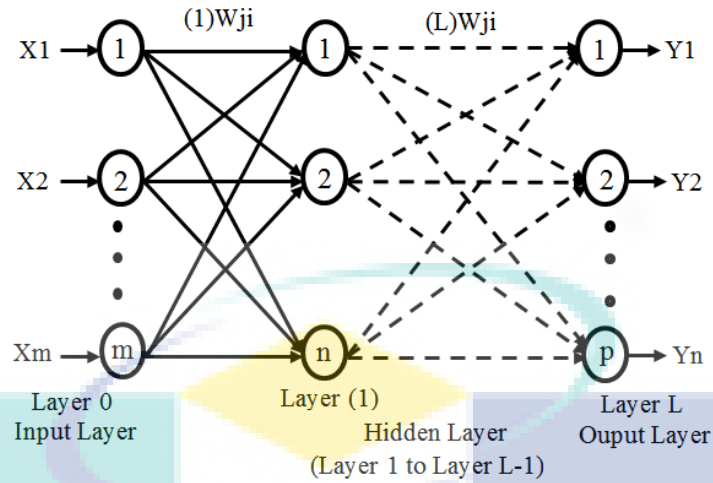


Figure 2.13 Multi layered ANN interconnected group of nodes

There are different types of neural network architectures available, such as Single Layer Feed Forward Network (SLFF), Multi-Layer Feed Forward Network (MLFF), and Cascade Correlation architecture (CC). Network with an input layer, one or more hidden layers, and an output layer are called as feed-forward networks. In feed-forward networks the signal moves only in one direction. Network with only one hidden layer is known as SLFF, while a network with a multiple numbers of hidden layers is called as MLFF. In CC architecture, a neuron receives system inputs and all the outputs of the preceding layers (Selvakumar et al., 2016).

From the control configuration viewpoint, the most recommended ANN-based micro-grid control design can be divided into three general control styles conceptually represented in Figure 2.14 (Hassan Bevrani & Ise, 2017):

- (a) Use the ANN system directly as a controller and provide the control command in the major feedback loop.
- (b) Using ANN to adjust the parameters of existing fixed structure controller, e.g. (PI).
- (c) Using ANN system as an additional controller in parallel with the existing conventional simple controller such as PI, in order improves the closed loop performance.



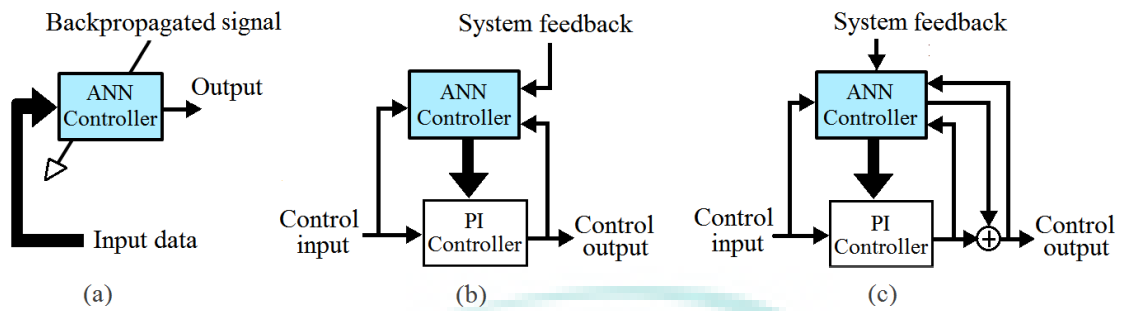


Figure 2.14 Control styles of ANN-based micro-grid

Power system consists of a governor, a turbine, and a generator with feedback of regulation constant. The system also includes step load change input to the generator. Much has been written on intelligent control using neural networks (NNs). Neural network-based saturation compensation signal is inserted into the actuator control signal, effectively preventing it from being saturated have used in (Gao & Selmic, 2006). The proposed NN saturation compensation scheme presents a form of intelligent anti-windup saturation where NN adjusts its output to prevent saturation of the control signal. Neural network based controller is used in (Hassan Bevrani et al., 2006) and has good result for LFC. Because of the uncertainties on the parameter of the power system and because of the change in the load demand, adaptive control referred to be used for LFC. To achieve the sensitivity of power systems model, neural network emulator (NN-emulator) used for identifying the power system that the proposed in (Sabahi et al., 2007) the control is compared with conventional neural network (CNN) controller.

MRAC has been widely applied recently to solve control problems for a system with matched unmodeled dynamics (Dydek et al., 2010). When uncertainty MRAC is present, it is difficult to achieve a fast transient performance and at the same time avoid undesired frequency oscillations. If NN is used to represent uncertainty, this process necessarily results. Different methods of MARC-based NN have been recently developed, although these developments help improve the robustness of the adaptive control laws, their tracking accuracy can only be shown to be bounded, and the bound depends on the magnitude of disturbances. For instance, in (Cao & Hovakimyan, 2007; Hindman et al., 2007), a new MRAC neural networks controller named L1 adaptive controller is proposed, and the transient performance of input and output signal of the system.

This adaptive control has a lowpass filter in the feedback loop. In (Muse & Calise, 2010), an adaptive control method that allows fast adaptation for systems with slow reference models is given. In this method, to enable quick adjustment, the neural network is trained with a high bandwidth state emulator. (Adriana Vargas-Martínez et al., 2013) Presents of two different adaptive control designs for improving the performance of a hybrid diesel-wind power system, the first one uses MRAC with PID controller adjusted by GA to control the frequency, the second one is same of first one, but the author added ANN with MRAC for controlling the voltage amplitude. This work is in an islanded micro-grid configuration only.

In (Prakash, R. & Anita, 2011) utilizing online loop multilayer back propagation structure of ANN, it is incorporate into the conventional MRAC framework in parallel. At the same time respond to the plant by tuning of ANN multilayer back propagation online. The controller is designed to achieve plant production converges to reference model output based on the plant which is linear ,as shown in Figure 2.15 Plant output  $y$  and the reference output  $y_m$  of the conventional MRAC system.

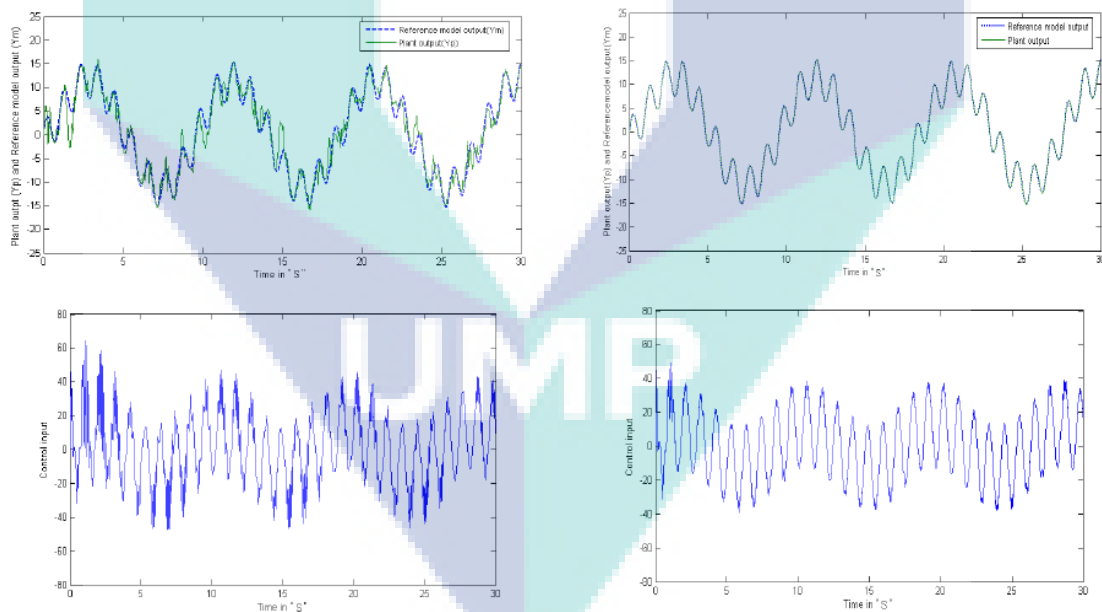


Figure 2.15 Simulation results of Plant output  $y$  (solid lines) and the Reference output  $y_m$  (dotted lines) of the conventional MRAC system

Source: Prakash, R. & Anita (2011)

Two-hybrid fault-tolerant control schemes were applied in (Vargas-Martínez et al., 2015) to adjust the frequency and voltage amplitude of the island micro-grid. A PID

controller tuned by GA to control the speed of the diesel engine and a traditional MRAC system to control the voltage amplitude of the synchronous generator in the first scheme. Also, a hybrid controller with MRAC coupled with ANN and a PID controller tuned with GA are designed for SG used in the second scheme. This scheme uses the ANN and the PID as feed-forward controllers for achieving tracking and regulation control of the island micro-grid.

### 2.9.2.2 Fuzzy Logic Control (FLC)

Control of the fuzzy logic system is considered as a primary branch of artificial intelligence and expert systems distinguished by features that make them robust in control applications. It also provides promising performance, with a less mathematical model of the system (Madbouly et al., 2010). The capability of a fuzzy logic system to include an artificially intelligent language that represents human thought for numerical computations that can be performed by a computer. Accordingly, it is important to submit elements of fuzzy logic system control that is shown in Figure 2.16.

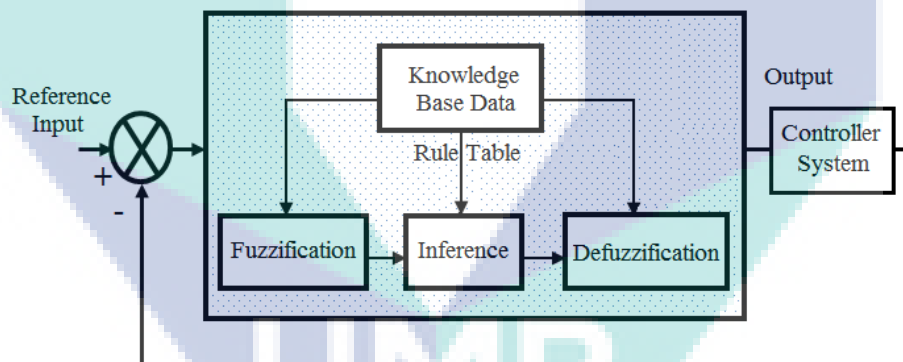


Figure 2.16 Schematic representation of a FL system

To implement the technique of fuzzy logic to an actual application requires the following steps;

1. Fuzzification – convert the crisp data into fuzzy data.
2. Fuzzy Inference Process – is the tuning process of the if-then rule.
3. Defuzzification – convert the crisp data to real signal that can be used the various method of computation.

Although FLC can process a reasonable number of inputs, increasing the number of inputs and outputs increases the complexity of the system. Therefore, a distributed processor is probably easier to implement. The output of the fuzzy process can be the logical union of two or more fuzzy membership functions defined on the universe of the discourse of the output variable. In case of considering the frequency is speed rotor; the variable error is equal to the real power system frequency deviation  $\Delta f$ . The frequency deviation  $\Delta f$ , is the difference between the nominal or scheduled power system frequency ( $f_N$ ) and the real power system frequency ( $f$ ). Taking the scaling gains into account, the global function of the FLC output signal can be written as (Prasanth & Kumar, 2005).

$$\Delta P_C = F[n_e e(k), n_{ce} ce(k)] \quad 2.17$$

Where  $n_e$  and  $n_{ce}$  are the error and the change of error scaling gains, respectively, and  $F$  is a fuzzy nonlinear function. FLC is dependent to its inputs scaling gains,  $n_u$  is output control gain. A label set corresponding to linguistic variables of the input control signals,  $e(k)$  and  $ce(k)$  as in Table 2.4 and Figure 2.17:

$L(e, ce) = \{NB, NM, ZE, PM, PB\}$ , Where, NB = Negative Big, NM = Negative Medium, ZE = Zero, PM = Positive Medium, PB = Positive Big.

Table 2.4 Fuzzy inference rule for Fuzzy Logic Control

Input	e(k)					
ce(k)	NB	NB	NM	ZE	PM	PB
	NB	NB	NB	NM	NM	ZE
	NM	NB	NB	NM	ZE	ZE
	ZE	NM	NM	ZE	PM	PM
	PM	ZE	PM	PM	PB	PB
	PB	ZE	ZE	PM	PB	PB

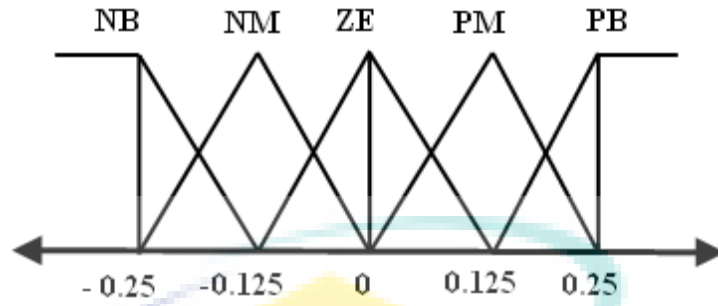


Figure 2.17 Membership Function for the control input variables

In the MGs, by keeping the frequency in the allowable limit, each unit generation has also been controlled. This fact requires the control of power generation according to load variations. In some of the papers (Marzband et al., 2011) classic PID controllers have been used. The main disadvantage of such controllers is the constant integral term. In another word, it is not possible to change the value of this term according to the grid conditions (Marzband, 2013). But, by using fuzzy controllers including fuzzy fractional order controller, the integral term can be changed in a predetermined range to enhance the MG performance. The design of a fuzzy logic controller a precise mathematical description of the system is not necessary; as such an accurate description is replaced by common sense knowledge of the system's behavior. This experience is reflected in a series of rules, which the controller uses to derive its output signal from its input signals.

The FLC, which is proposed to replace the PI controller, used to reduce errors in a traditional PI speed controller. When the structure of the FLC controller, shown in Figure 2.18 is examined, the controller has two input elements, specifically the speed error ( $e$ ) and the change of the speed error ( $de$ ) (Dursun & Boz, 2015). At the same time, change in the reference phase current  $i_q^*$  was output  $\Delta i_q^*$ .  $e$  and  $de$  were then measured as in Equations 2.18 and 2.19 for each sampling time.

$$e(k) = w^*(k) - w_r(k) \quad 2.18$$

$$d_e(k) = e(k) - e(k - 1) \quad 2.19$$

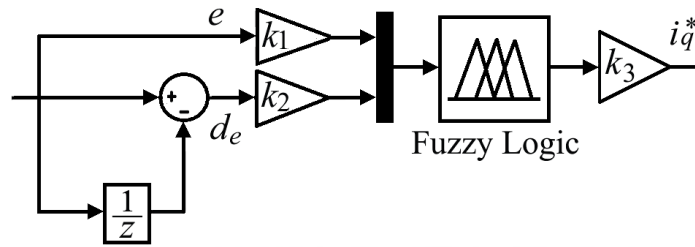


Figure 2.18 Structure of the fuzzy logic controller

Source: Dursun & Boz (2015)

These two inputs were multiplied by the two scale factors  $k_1$  and  $k_2$ , respectively. The controller output is multiplied by the third scale factor  $k_3$ . The input and output pattern of fuzzy membership functions, the inputs was  $-1.5$  and  $1.5$ , and outputs of the FLC were chosen between  $-3$  and  $3$  with triangular membership functions, as shown in Figure 2.19.

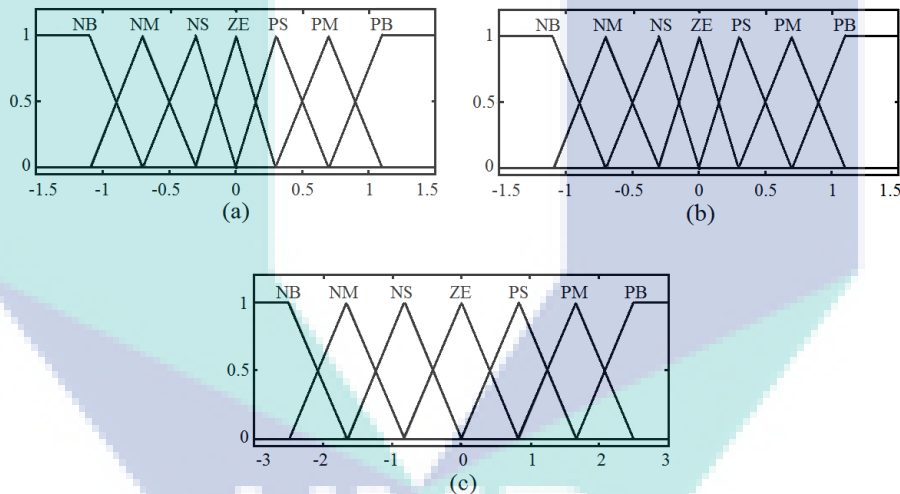


Figure 2.19 Membership functions, (a) Membership functions of  $e$ , (b) Membership functions of  $de$ , (c) Membership functions of  $du$

Fuzzy Gain Scheduled P-I (FGSPI) was proposed in reference (Jeddi et al., 2012), the control is proposed to get a better response when the load disturbance. Combining of neural network and fuzzy logic control algorithms is a new approach in power system and turbine control applications. It is called ANFIS (Adaptive Neural-Fuzzy Inference System). (Chaloshtori et al., 2011) proposed this algorithm to turbine governor control system. The fuzzy part has two inputs and one output which are rotor speed changes and speed changes of rotor speed as inputs, signal voltage as an output. It has 49 rules and seven states. The NN controller is designed using fuzzy membership functions. They are presented like neural network body structure which has five layers.

After training and teaching, membership functions are re-adjusted. NN part tunes the membership functions of the fuzzy controller so that fuzzy part can adapt to changing conditions. Compared to the fuzzy logic control system, ANFIS control algorithm shows better performance in both settling time and overshoot. During islanded operation, the frequency and voltage of an MG may change rapidly due to power unbalance between supply and demand. A fuzzy PID frequency controller was proposed in (Kim, J.-Y. et al., 2011) for the ESS, is provided a better controller performance than the conventional PI controller. The gains of two controllers were tuned by the PSO algorithm to compare the performance. The frequency deviations in islanded operation are reduced by the effective control action of the proposed fuzzy PID controller. Fuzzy Logic Control is utilized in (Dhanalakshmi & Palaniswami, 2011), but it is difficult to develop a good (simulation) model for Fuzzy Logic control, which can facilitate fine-tuning the controller.

### 2.9.2.3 Fuzzy Logic Table Control (FLTC)

The output of control obtained from the input, output membership functions and fuzzy rules is still fuzziness, and this process is called fuzzy inference and then to defuzzification process adapting to real signal. The defuzzification process is meant to convert the fuzzy output back to the crisp or classical output to the control objective.

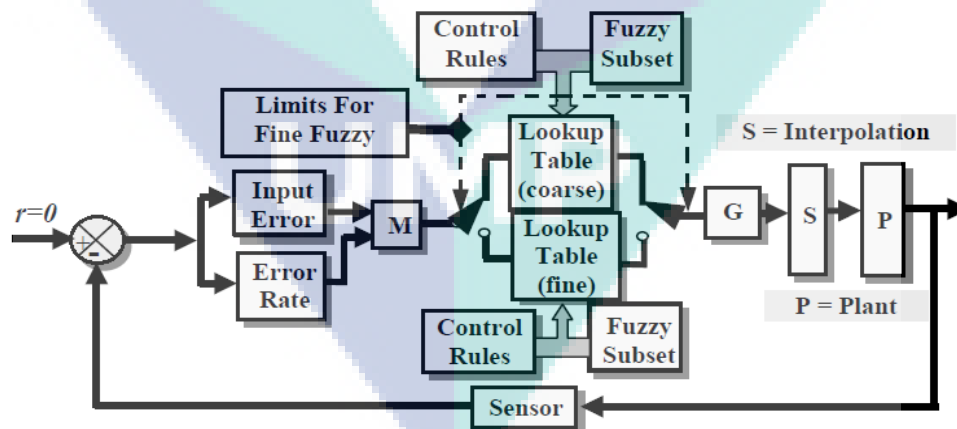


Figure 2.20 Block diagram of lookup table fuzzy control system

Source: Bai & Wang (2006)

As shown in Figure 2.20, which is a typical fuzzy closed-loop control system, the inputs are error and error rate, which are combined by block M to input to the fuzzy inference system. The lookup table is derived based on the membership function of



inputs, the output, and the fuzzy control rules. A control gain factor  $G$  is used to tune the output of the lookup table to obtain different output values (Bai & Wang, 2006). Multiple lookup tables fuzzy control system is used which increases the hypothesis of complexity and cost. (Eciolaza & Sugeno, 2012) proposed the system approach represents the implementation of a global online design of lookup table. Vertex Placement Principle (VPP) is applied to design a controller (C) simultaneously as shown in Figure 2.21, for an initially unknown objective plant (P) based on the desired plant (DP) model. The proposed theory that if a plant is unknown, designs of lookup table based on the desired plant by estimating it online.

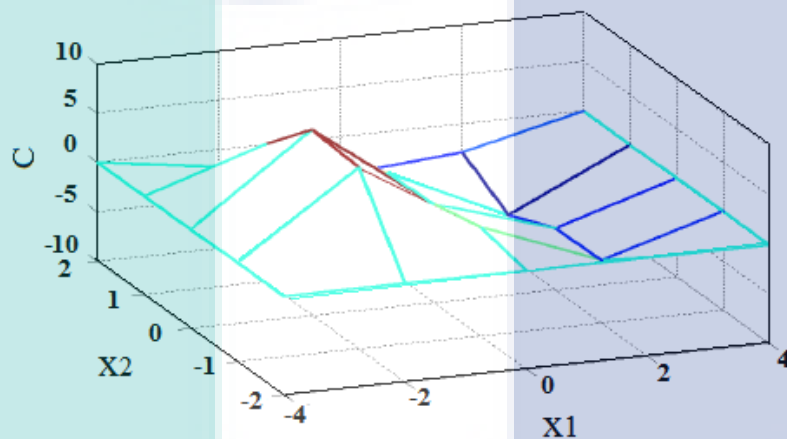


Figure 2.21 Controller  $C$  for simulation with  $f1 = \sin x2$

Based on the previous studies, many of the technical and controller issues are not addressed accurately before their implementation. The background and literature review of LFC methods are presented in this chapter and are summarized in in Table 2.5.



Table 2.5 The background and literature reviews of LFC

LFC Method	Author	Remarks	Gap
PID:	Ota et al., 2007	The LFC was performed to track the frequency deviation with minimum error	It is not an appropriate working when the load is varied.
	Gözde et al., 2008	The LFC is designed using PI to get a good dynamic performance in various scenarios.	The tuned gain of integral (I) was obstacle for getting a good dynamic performance.
LQR	Wang & Crow, 2011	The poles of the system are placed indirectly by minimizing a given performance index (J),	The disadvantage of this method is its tracking accuracy during load changes.
MRAC:	Sengupta & Dey, 2017	For speed control of DC motor and fluctuation of the reference signal using MRAC based MIT rule	System becomes oscillatory if the adaptive gain or the amplitude of the reference signal is sufficiently large.
ANN:	Vargas-Martínez et al., 2013	Two different controls, first one uses MRAC with PID controller adjusted by GA to control the frequency, the second one is added ANN with MRAC for controlling the voltage amplitude.	Difficulty in implementation and more complicated in grid connected mode, due to change in operating point when transition from grid-connected to islanded mode.
FLC:	Dhanalakshmi & Palaniswami, 2011	Multi stage fuzzy logic control application for load frequency control for large frequency fluctuation problem	Difficult to develop a good (simulation) model for Fuzzy Logic control, which can facilitate fine-tuning the controller.

LFC strategies that a micro-grid have been presented in literature and compared in Table 2.6 and 2.7 for conventional and intelligent LFC respectively (Bouزيد et al., 2015).

UMP

Table 2.6 Conventional Load frequency control

Conventional LFC in MG	MG mode	Advantage	Disadvantage
PID	Grid-Connected	*Simple control structures	*Cannot response variations fast and not perform the required constant speed in all loading conditions. *For unbalanced systems, it does not ensure good performance
	Islanded		
LQR	Grid-Connected	*Information about the system is not lost and to obtain better voltage regulation and load sharing simultaneously *It guaranteeing signal boundary and asymptotic convergence of tracking error to zero.	*State-feedback control schemes do not inherently include any means against external noise. *The complexity of the system increases.
	Islanded		
MRAC	Grid-Connected		*MRAC scheme is that it takes some time to adapt and some oscillations will come after a certain period.
	Islanded		

Table 2.7 Intelligent Load Frequency Control

Intelligent LFC in MG	MG mode	Advantage	Disadvantage
ANN	Grid-Connected	*Trained in offline or on-line approaches and used in recent controllers because of its high robustness.	*The off-line method lacks a suitable performance
	Islanded		
FLC	Grid-Connected	*Insensitive to parametric variations and operation points. *Sophisticated technique, easy to design and implement a large-scale nonlinear system.	*Slow control method.
	Islanded		

The contribution of the load frequency control to the formation of the grid frequency at power sharing is studied and each method is useful if it is chosen for an appropriate application in both grid-connected and islanded mode. We have found that

with the advancement of synchronous generator as DG, the researchers developed various control strategy so that the signal error reduced as possible, secure the stability and power quality. The synchronization is a significant issue for disconnection of DGs from the main grid in a hybrid micro-grid. This issue is still need to take into account for guarantee and smooth the transfer from grid-connected to island mode, as well as the required amount of power is provided at nominal frequency and voltage in the micro-grid during islanded mode operation.

## **2.10 Control of VSI in MG**

Distributed sources are usually connected to the load or the main grid through an interface power electronic inverter to control their output voltage and power. They can work in either autonomous mode or grid-connected mode. The control strategy applied to the stand-alone and grid-connected inverter usually consists of two cascaded loops, i.e., a fast internal current loop, which regulates the grid active and reactive current, and an external voltage loop, which controls DC link voltage. The current loop is responsible for power quality issues and current protection; thus harmonic compensation and dynamics are the important properties of the current controller (Blaabjerg et al., 2006). The DC link voltage controller is designed for balancing the power flow in the system. Usually, the design of this controller aims for system stability having slow dynamics. Some authors propose grid-side control based on the fact that the dc-link voltage loop can be cascaded with an inner power loop instead of a current loop, so the current is not controlled directly (Kadri et al., 2011). The DC-AC inverters usually operate on Pulse Width Modulation (PWM), which is characterized by the generation of constant amplitude pulse by modulating the pulse duration by modulating the duty cycle (Zope et al., 2012). Some PV inverters can absorb or inject reactive power as needed, provided that the rated values of current and terminal voltage are not exceeded (Kim, J. et al., 2011). There are two ways to implement current and voltage control for VSI as in below.

### **2.10.1 Synchronous Reference Frame Control**

Synchronous reference control is also known as control uses reference frame transformation  $abc \rightarrow dq$  to transform the grid current and voltage waveforms into a reference frame that rotates synchronously with the grid voltage instantaneous angular

frequency. After such transformation, the control variables become dc variables, thus control and filtering can be achieved relatively simple. The control structure is usually associated with a proportional-integral (PI) strategy since they have a satisfactory performance when regulating dc variables. The controlled current must be in phase with the grid voltage, so the phase angle used by the  $abc \rightarrow dq$  transformation module has to be extracted from the grid or reference voltage model (Hadjidemetriou et al., 2013).

Figure 2.22 shows the inverter's power stage including the voltage control loop scheme. The "Voltage Reference Generator" block computes the voltage references in  $dq$  by converting the inputs ( $V_{ref}$  and  $\omega_{ref}$ ) to a three-phase balanced signal than to  $dqo$  signals (El Boubakri, 2013).

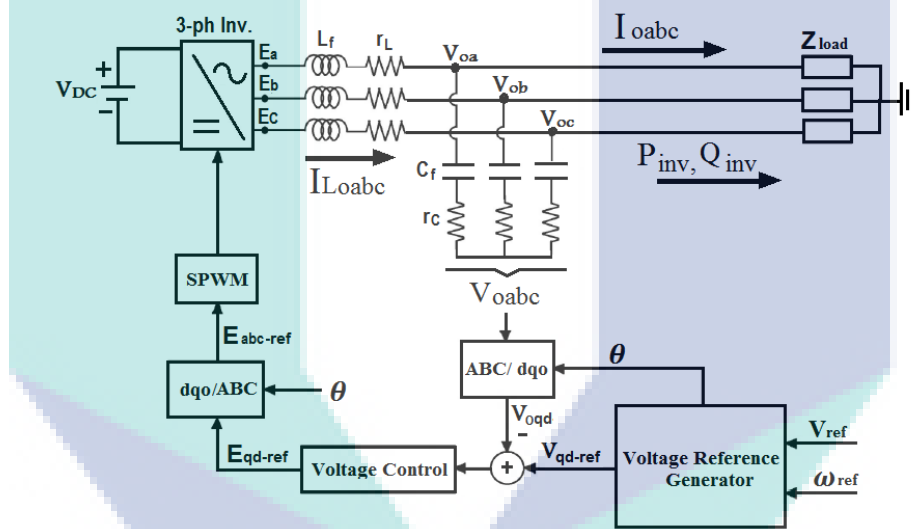


Figure 2.22 Circuit diagram of the grid-connected inverter

### 2.10.2 Stationary Reference Frame Control

Another possible control implementation can be implemented using the stationary reference frame (Amirnasir & Reza, 2010). In this control structure, the grid currents are transformed to stationary reference frame using the  $abc \rightarrow \alpha\beta$  transformation. Here the control variables are sinusoidal and because of known drawback of PI controller in failing to remove the steady-state error when controlling sinusoidal waveforms, other controller types are required. One of the most popular and wide spread controller is the proportional resonant (PR) controller for current regulation of grid-tied systems (Shen et al., 2009). The main advantage of this controller is that it achieves a very high gain around the resonant frequency, thus being able ideally to

eliminate the steady-state error between the controlled signal and its reference (Dash et al., 2011). The infinite gain that is possible in theory for a PR controller is not possible in practice. There are other modifications of this kind of control like model predictive resonant controller described in (Yoo & Wang, 2011). The PR controller does not work well for variable frequency operation such as in machine drive systems or weak-grid utility systems.

### **2.11 Power Sharing Droop Method in MG**

Any DG controlling in the micro-grid system and data collecting insert a synchronous generator as well, that should be considered in the micro-grid analysis, which is neglected in the recently published research works. There are various control techniques listed below that, help manage the component level of a distribution system (Guerrero, J. 2011):

- a) Master and slave control: master fixes the voltage and frequency values while the slaves control the current sources.
- b) Current and power flow control: this method controls the current and power distribution by using control signals.
- c) Droop control: this method is improved to combine with previous methods since the converters behave as a non-ideal voltage source.

To ensure a smooth transformation and minimizing frequency fluctuation of MG, the active and reactive powers of the DG units should be shared simultaneously. The active and reactive power sharing could be achieved by using two independent parameters, i.e., voltage and frequency (Vandoorn et al., 2010; Zhao-Xia & Hong-Wei, 2012). The most important advantage of using the droop control is to maintain system stability while multiple DG units are operating in the system. The droop control is controlled commonly applied to generators for primary frequency control (and occasionally voltage control) to allow parallel generator operation (e.g., load sharing). The advantage of the droop method, it does not require the communication signals amongst units in parallel; thereby increasing the reliability of the system and reducing the cost significantly. It is also imitating the steady-state characteristics of the synchronous generator (SG) in islanded MG (Barklund et al., 2008; Liu, J. et al.) (Mohamed, 2008). Therefore, the droop method appears to be the standard control

strategy in future MG systems. Droop control can be categorized as conventional and modified droop control that by regulating the MG parameters.

### 2.11.1 Conventional Droop Control

Traditionally, the major sources of electricity in micro-grids are synchronous generator sets, or genets, which supplies electricity to the different loads using a local distribution system. Droop control technology is commonly used in a rotating (synchronous machine based) interface of power supply. A droop in the voltage magnitude with the reactive power is used to ensure reactive power sharing. Therefore, the droop method appears to be the standard control strategy in future micro-grid systems (Mohamed, 2008).

The role of droop control in power sharing is that it control the real power on the basis of frequency droop control and it control the reactive power on the basis of voltage control (Dou et al., 2011; Steenis, 2013). The conventional droop control is Real power–frequency (P–F) droop control and Reactive power–voltage magnitude (Q–V) droop control. As shown in Figure 2.23, the values of real power and reactive power flowing between two AC voltage sources connected in parallel via line impedance are given by (Guerrero, J. M. et al., 2007):

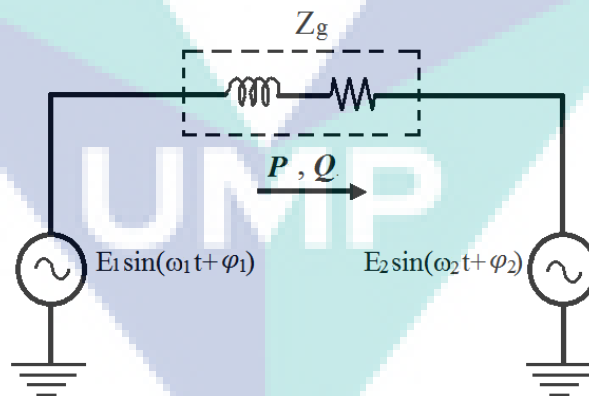


Figure 2.23 Two AC voltage sources connected in parallel through line impedance

Assuming that the line impedance is highly inductive (Where,  $\theta_g \approx \pi/2$  rad in high-voltage). The values of the active and reactive powers become;

$$P = \frac{E_1 E_2}{X_g} \sin(\varphi_1 - \varphi_2) \quad 2.20$$

$$Q = \frac{E_1 E_2}{X_g} \cos(\varphi_1 - \varphi_2) - \frac{E_2^2}{Z_g} \quad 2.21$$

Where,  $X_g$  is the inductive part of the line impedance  $Z_g$ .  $E_1$  and  $E_2$  are the RMS value of the AC voltage sources, and  $\varphi_1$  and  $\varphi_2$  are their phases respectively. In the above mentioned equations, Resistance ( $R$ ) is neglected for an overhead transmission lines as it is much lower than inductance ( $L$ ). Also the power angle  $\delta$  is lesser, therefore,  $\sin \delta \approx \delta$ ,  $\cos \delta \approx 1$  (Where,  $\delta = \varphi_1 - \varphi_2$ ). In low-voltage (LV) networks or in MGs, line impedances are mainly resistive where  $R \gg X$  (Eid et al., 2016; Hou et al., 2016). The table 2.8 shows the type of MG and valuable of  $R, X$  and ratio of  $R/X$ .

Table 2.8 Line parameters for different networks

Type of MG	$R(\Omega/km)$	$X(\Omega/km)$	$R/X$
LV	0.642	0.083	7.7
MV	0.161	0.190	0.85
HV	0.060	0.191	0.31

Source: Eid et al., (2016)

The decoupling of the real and reactive power is achieved in (De Brabandere et al., 2007) for a high  $R/X$  line with frequency droop control. It is shown that a modification of the droop equation can accommodate the effect of line impedance. However, the choice of droop gains for rating based sharing of power has not been addressed in (De Brabandere et al., 2007). An enhanced droop control featuring a transient droop performance is proposed in (Guerrero, J. M. et al., 2004). In other words, the higher is the capacity of the DG, the higher is its share in supplying the loads. It has been discussed in (Diaz et al., 2010) that such a load sharing strategy is not justified economically.

To realize decoupled power control and improve the system stability, some different variations of the traditional droop control are proposed, Virtual impedance is the most practical one for decoupled active and reactive power control (De & Ramanarayanan, 2010). The most important benefit from utilizing virtual output impedance is that the magnitude and phase angle of the output impedance can be controllable variables. The limitation of virtual impedance is that it is too dependent on



the voltage loop bandwidth and it may increase the reactive power control and sharing error in MG due to the increased impedance voltage drops.

Reference (Mehrizi-Sani & Iravani, 2010) introduces the potential function based control as secondary controller of a MG. It considered three levels of control for the system, primary, secondary and tertiary. The potential function has been exploited in the secondary control part which is slower than the primary controller and needs communication between MG components and DGs. For the control of MG in grid connected mode, in (Balaguer et al., 2008) (Balaguer et al., 2011) the DGs are operating in constant current mode to feed a constant power to the grid and the loads. During the islanding mode, the controller mode changes to constant voltage mode and the load shedding is applied for power balance between the source and the load. A voltage and frequency range was chosen for islanding detection. Synchronous reference frame control needs accurate angle and frequency identification and more computational power. The conventional droop method also has several drawbacks including a slow transient response, a trade-off between power-sharing accuracy and voltage deviation, unbalanced harmonic current sharing, and a high dependency on the inverter output impedance (Sao & Lehn, 2008).

The conventional droop method cannot achieve efficient power sharing in the case of a system with complex impedance condition due to the coupled active and reactive power characteristic of the system (De Brabandere et al., 2007), which causes circulating current. The transient and steady-state behaviors of the droop method also highly depend on the system mismatches which can affect the inverter output impedance accuracy and the line impedance of the wires.

### **2.11.2 Modified Droop Control**

The modified droop control arises by changing the parameters of the conventional droop control as per their system requirement. The modified droop control can be classified as:

#### **2.11.2.1 P-V and Q-F Droop Control**

The idea of proper power sharing in an inverter coupled with MG by means of P-V & Q-F droop control was given by (Sao & Lehn, 2008) (Zhong, 2013). In their



views, the active power was shared properly in hybrid MG by using the interlinked converters. It is a challenge of interlinking dc grid with ac grid through converters. This is not an easy thing in island operation. In (Zhong, 2013) auxiliary control used to achieve rated values of deviating voltage and frequency. This tends to delay in measurement as well as a communication channel which causes slow response. In references (Majumder et al., 2009) active power/voltage magnitude and reactive power/frequency is used. The only advantage of this method is direct voltage control in islanded mode, but the connection of the MG to the network will cause counteracting with the valid normal droop control of synchronous generators and no active power dispatch will be possible; also, voltage deviation will remain in the grid.

#### **2.11.2.2 V-F Droop Control**

For power sharing in island operation through programmed virtual impedance by V-F droop control was put forth by (He et al., 2012). It was primarily aimed at the proportional real and reactive power sharing to the rated power of DG unit. Power control technique was introduced to index load sharing deviation in island MGs. In order to send harmonic voltage signals at PCC to the local DG controller from central controllers, a low bandwidth communication scheme was proposed, it also concerned about accurate reactive power sharing. Reference (Lee et al., 2013) detailed study illustrates about the load sharing controller stability analysis by using V-F control for the DG, but it is not suitable for complex feeder impedance condition. Also the small-signal stability was briefly analyzed with combinational droop as well as average power scheme for load sharing of manifold DGs.

#### **2.11.2.3 Adaptive Control Transient Droop**

An adaptive voltage droop control is presented in (He & Li, 2012) to share the reactive power accurately, where the active power disturbance is adopted to identify the error of reactive power sharing and it is eliminated by using a slow integral term. Unfortunately, the signal injection method deteriorates the power quality and affects the system stability. Scheduling the transient droop gains, the proposed control in (Hassanzahraee & Bakhshai, 2012) to improve the transient performance of MG based on the static droop characteristics. Also is provided the active damping of the low-frequency power sharing modes at different loading conditions. Based on these previous

researches, if the control gains are not chosen appropriately, the system response may be poor and even cause instability.

#### **2.11.2.4 SoC (State of Charge) Based Droop Control**

The energy storage unit with higher SoC generates more active power than the lower SoC. In (Lu et al., 2012) for dynamic power sharing on the basis of SoC (State-of-Charge). The main aim of this proposal is to eradicate the problem of sharing power in the distributed energy storage system. By the SoC-based droop control, the frequency deviates from its nominal value. PV generation and batteries are coordinated to feed utility grid or plug-in hybrid electric vehicle loads (Gurkaynak & Khaligh, 2009; Shimada et al., 2008). In these papers, different power conditions and battery capacity limits are taken into account, but the islanding operation is not considered.

#### **2.11.2.5 Angle Droop Control**

A droop real power/angle control instead of frequency can be used to avoid limiting frequency regulation due to the allowable range of frequency droop gain. In (Moussa et al., 2015) propose angle droop control. It is aimed at guaranteeing appropriate load sharing for stable grid parameters and load fluctuations in a wide range of operating conditions with little fluctuation frequency and less voltage amplitude variation in the system. Furthermore, the controller can synchronize inverters that operate in parallel without adding external communication signals. However, in the view of (Majumder, Chaudhuri, et al., 2010), appropriate power-sharing was accomplished using high angle droop gains instead of frequency in MG, especially under weak system conditions. But the use of high angle droop gain hurts overall stability. As mentioned, the droop control methods were studied to ensure the power-sharing accuracy, and to enhance the dynamic performance of the hybrid micro-grid system. The droop control methods are summarized in Table 2.9.

Table 2.9 Different techniques of droop control methods

Power Sharing	Author	Remarks	Gap
Conventional (P-F) (Q-V) droop control	De Brabandere et al., 2007	The control method for the parallel operation of MC. Frequency and voltage control, across virtual impedance with real and/or imaginary parts.	The choice of droop gains for rating based sharing of power has not been addressed.
Modified Droop Control P-V and Q-F	Balaguer et al., 2011	The DGs are operating in constant current mode to feed a constant power to the grid and the loads.	During the islanding mode, the controller mode changes to constant voltage mode and the load shedding is applied.
Modified Droop Control V-F	Zhong, 2013	To achieve accurate proportional load sharing, the auxiliary control was used to reach rated values of deviating voltage and frequency.	This tends to delay in measurement as well as a communication channel which causes slow response.
Adaptive Control Transient Droop	Lee et al., 2013	Illustrates the load sharing controller stability analysis by using V-F control to improve reactive power sharing for the DG.	Not suitable for complex feeder impedance condition. Also the small signal stability was briefly analyzed with combinational droop as well as average power scheme for load sharing of manifold DGs.
SoC (State of Charge) Based Droop Control	He & Li, 2012	For share the reactive power accurately, where the active power disturbance.	Using a slow integral term to eliminate the error of reactive power sharing, the signal injection method deteriorates the power quality and affects the system stability.
Angle Droop Control	Lu et al., 2012	To eradicate the problem of sharing power in the distributed energy storage system in an AC micro-grid.	The frequency deviates from its nominal value.
	Majumder, Chaudhuri, et al., 2010	Under weak system conditions, power sharing was proposed by means of high angle droop gains instead of frequency in MG.	But the use of high angle droop gain has an adverse effect on overall stability.

## 2.12 Summary

Based on the literature, the definition of DG, in general, they are small-scale generation units located near loads. The interface of DG units to the grid can be divided into two types direct-connected and indirect grid interfacing. Micro-grids can be defined as autonomous small-scale power networks that contain multiple DGs and various critical loads. One of the most important parts of a micro-grid is the control system for LFC. The hybrid micro-grid can run in a grid-connected operation mode or islanded operation mode. The process of mode transition between the two modes needs to be smooth to ensure the micro-grid stability.

A different control system approaches for a micro-grid are presented which can guide or partially influence centralized and decentralized system components within their separate control and regulate processes. Generally, control categories and their characteristics are presented, classified and explicitly explained. The SG is commonly used as a DG unit can be connected directly to the grid. An essential part of SG is LFC. In SG, the frequency of the output is directly related to the rotational speed of the rotor at a given speed. The SG based DG installed at the micro-grid, to control parameters, the governor can be modeled by PID controller that adjusts the engine speed and matches the generator speed reference set point. With increased size and changes in the structure of the power system due to the integration of renewable energy sources (PV), the traditional LFC (PID) may not be feasible. In the robust control scheme, the structural complexity and reshaping of the plant may be required. To circumvent this problem, the intelligent control scheme with the use of soft computing techniques such as an artificial neural network (ANN), fuzzy logic control (FLC). As a result, the proposed literature control technique, none of them has done a detailed study perform of the SG control grid connection mode of reaching zero error when it's connected to the stiff grid. Thus depending on the micro-grid operation mode, and the control system, the synchronous machine has to change its control strategy to meet the needs operating mode.

## CHAPTER 3

### METHODOLOGY

#### 3.1 Introduction

In this chapter, a load frequency control (LFC) analysis for using a synchronous generator (SG) as a DG unit in a hybrid micro-grid system from grid-connected mode to island mode has been carried out. The adaptive PI-based controller (API) has been applied for LFC in the implementation of the micro-grid controller, by two steps. For a first step in grid-connected using two different adaptive control schemes for improving the performance of hybrid micro-grid during the transition from grid-connected mode to island mode. It uses a model reference adaptive controller (MRAC) with MIT rule for smoothing this transition. The other scheme employs an MRAC with a neural network (NN) for minimizing any fluctuation occurring in power sharing and frequency deviation during sudden changes in the load and tracking between grid connection and island mode. The second step in island mode, applied Fuzzy Logic Table Control (FLTC), to obtain the required response and to maintain the synchronization of generations. This is to ensure that the desired power is supplied at the nominal frequency of the micro-grid during island mode operation. Finally, the compares results of the proposed methods with PI conventional method are carried out to verify the performance of MG. Noting that the time domain simulation is performed using MATLAB/Simulink simulation environment. The block diagram for the work methodology is represented in Figure 3.1.

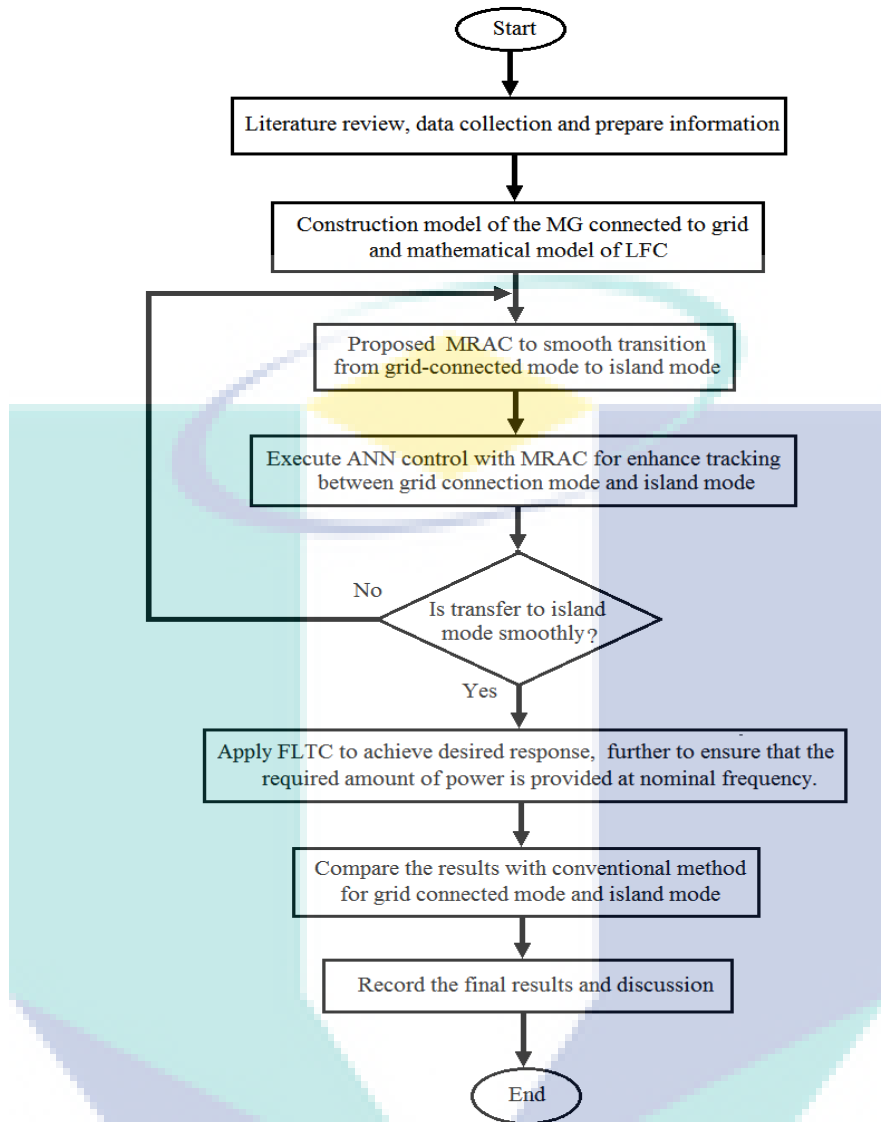
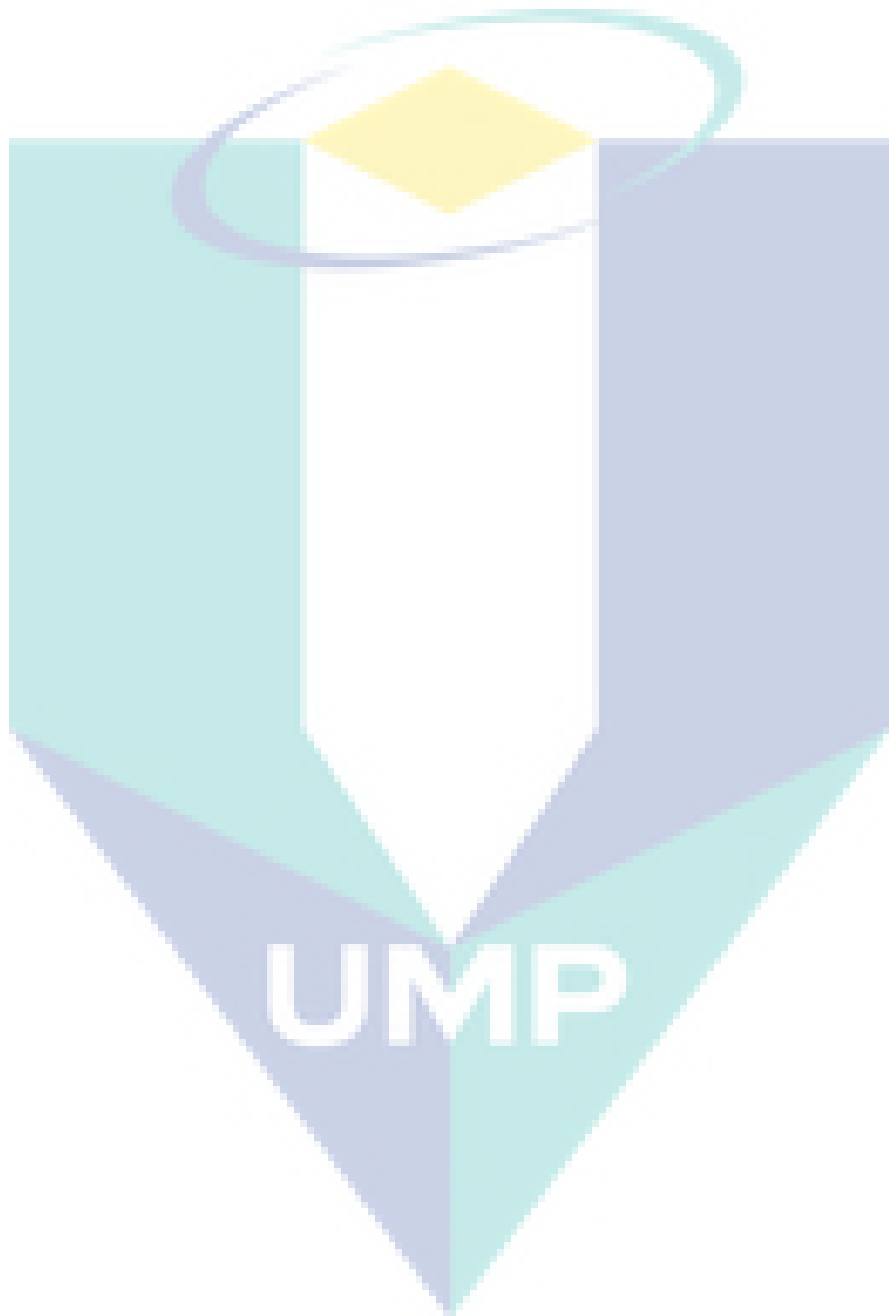


Figure 3.1 The block diagram for the work methodology

From Figure 3.1, after construction of the hybrid micro-grid based mathematical model of Load Frequency Control (LFC) connected to utility, Model reference adaptive controller (MRAC) with MIT rule is proposed for tracking error and deal with the problem of suddenly changing load based on PI. As a control is tracked sequences, Artificial Neural Network (ANN) is used to enhance and smooth transition from grid connection to island mode operations. After the island detected, it can be applied a Fuzzy Logic Table Control (FLTC) to improve the hybrid micro-grid response and synchronization during island mode. Also to ensure the required power is provided at nominal frequency and voltage. The results of the proposed methods compare with conventional PI controller.

### 3.2 Strategy of Work Frame

In MG operation modes, which consists of multiple DG units (i.e., inertial and converter interfaced DGs), the problem appears when the load changes suddenly or loss power grid (supported). As a rule, need to transfer MG to island mode, because the power balance between supply and demand does not match, lead to fluctuating the frequency due to the low inertia of the MG. In the LFC, primary control is a local automatic control that adjusts the active power generation of the SG and the consumption of controllable loads to restore the balance between the load and the generation to eliminate frequency variations. Primary control is indispensable for the stability of power systems and is performed by the speed governors of the dedicated power generation units. Again, the problem occurs when the island mode setting, due to loss of grid supported and synchronization, leading to slow response and oscillation of the active power sharing. To smooth transfer MG from grid-connected to island mode, Model Reference Adaptive Control (MRAC) based MIT rule is proposed. Then, the Neural Network (NN) has been proposed to modify the output signal of MRAC for minimizing the error that occurs during power sharing and support the tracking between grid connection mode and island mode operations. Also, the issue of the desired amount of power is provided with nominal frequency through islanded operation mode is solving by applying of Fuzzy Logic Table Control (FLTC). Figure 3.2 shows the strategy of work. This research investigates the inclusion of synchronous machine based DGs to enhance transient stability and smooth transition between islanded and grid-connected modes of operation.





consist of DGs while holding the frequency constant. LFC also is a control loop that regulates output in the range of megawatt and frequency of the generator. Nowadays power systems are connected to neighboring areas, in which the connection is made possible by tie-lines, while in MG by PCC point. Hence LFC also needs to control the tie-line power exchange error. It is can be said that information regarding local area can be obtained in the tie-line power fluctuations. Therefore the tie-line power is observed, and the resulting tie-line power is given back into both areas for a two area system. In this study, has been considered the similarities applications of LFC in (SG) by MG system and the (area) in the electric power system, as in Table 3.1.

Table 3.1 Applications of LFC in (SG) in MG system and the (area) in electrical power system

<b>SG in MG system</b>	<b>Area in power system</b>
Multi DG-units system	Multi- areas system
Interconnection by PCC point	Interconnection by tie-lines
Supplied power to various loads	Supplied power to various loads
Size is limited , usually install in LV,MV	Unlimited size , install in LV,MV and HV

The control mechanism needed to maintain the system frequency. The basic role of LFC in this work is:

- a. To maintain the desired output power of a generator matching with the changing load.
- b. To assist in controlling the frequency of interconnection of MG to the grid.
- c. To keep the net interchange power between two mode MG operations.

The mathematical modelling of the system is the first step to carry out for analysing and designing a control system. Models of fundamental components utilized in the power systems can be represented in the form of a block diagram. Frequency control is achieved primarily through a speed governor mechanism assisted by LFC to precisely control. The speed of the shaft is measured and compared with the reference value, and the feedback signal is used to increase or decrease the power generated by controlling the inlet valve.

The desired output is determined of individual generating units by controlling system generation. If the electrical load of the generator suddenly increases, the

electrical power exceeds the mechanical power input. This power shortage is provided by kinetic energy stored in the rotating system. Reduction in kinetic energy causes lower in turbine speed, which results in decrease generator frequency. The speed change is sensed by the turbine governor, which adjusts the turbine input valve to change the mechanical power output to bring the speed to a new steady state condition.

The LFC loop will maintain control during slow and large changes in load and frequency imbalances occur. In this research, the LFC is applied to a single generator supplying power to a local load service area. For stable operation, the governor is designed so that the speed can drop as the load increases. The speed governor output is  $\Delta P_{Gov}$ . The speed governor has two inputs, i.e., change in the reference power setting,  $\Delta P_r$  and change in the speed of the generator  $\Delta f$   $R$ : speed governors regulation. The positive  $\Delta P_r$  will produce positive  $\Delta P_{Gov}$ . Thus

$$\Delta P_{Gov} = \Delta P_r - \frac{1}{R} \Delta f \quad 3.1$$

Taking Laplace transform of Equation (3.1), can get (Ekka, 2014):

$$\Delta P_{Gov}(s) = \Delta P_r(s) - \frac{1}{R} \Delta f(s) \quad 3.2$$

The above Equation (3.2) is represented by block diagram shown in Figure 3.3.

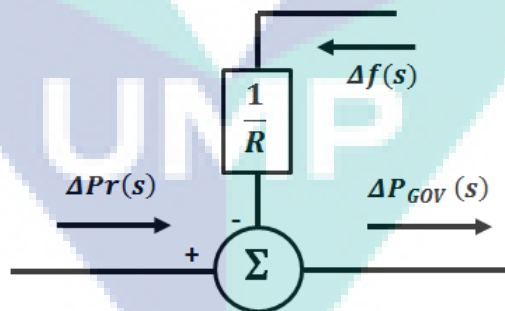


Figure 3.3 Block diagram of speed governor

The command  $\Delta P_{Gov}$  is transformed to the steam valve position command  $\Delta P_{ha}$  via the hydraulic drive. This depends on the position of main piston, which in turn depends on the quantity of fuel flow in the piston. Thus

$$\Delta P_{ha}(s) = 1/1 + sT_H \Delta P_{Gov}(s) \quad 3.3$$

Where  $T_H$  is the hydraulic time constant given by  $T_H = \frac{1}{K_H}$ , the constant  $K_H$  depends on fluid pressure. In terms of the hydraulic valve actuator's transfer function  $G_H(s)$ , can be written as:

$$G_H(s) = \Delta P_{ha}(s) / \Delta P_{Gov}(s) = 1 / 1 + sT_H \quad 3.4$$

The speed governor together with the hydraulic valve actuator is shown in Figure 3.4.

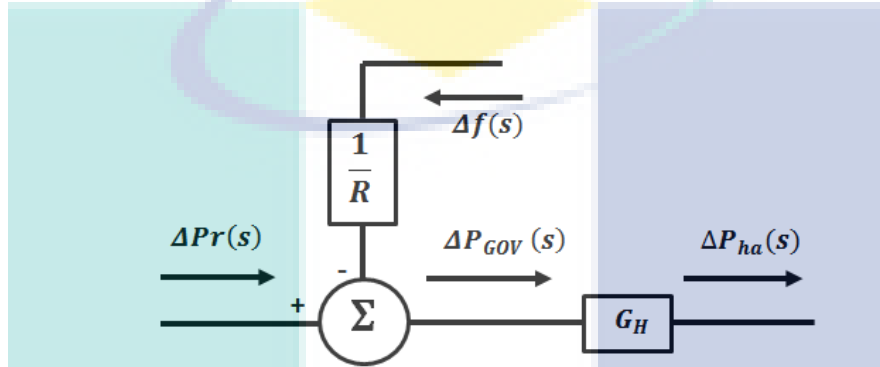


Figure 3.4 Block diagram of speed governor together with hydraulic valve actuator

In normal steady state, the turbine power  $\Delta P_{Tu}$  keeps balance with the electromechanical power  $P_m$  resulting in zero acceleration power  $\Delta P_{acc}$  and a constant speed and frequency. During transient state, the turbine power is  $\Delta P_{Tu}$  and the corresponding generator power is  $\Delta P_G$ . The accelerating power in turbine generator unit is:

$$\Delta P_{acc}(s) = \Delta P_{Tu}(s) - \Delta P_G(s) \quad 3.5$$

The generator always adjusts its output so as to meet the demand  $\Delta P_{de}$ . These adjustments are essentially instantaneous, certainly in comparison with the slow changes in turbine power  $\Delta P_{Tu}$ . So it can be set (Murty, 2011):

$$\Delta P_{Tu}(s) = G_{Tu} \Delta P_{ha}(s) = 1 / 1 + sT_{Tu} \Delta P_{ha}(s) \quad 3.6$$

$$\Delta P_G(s) = \Delta P_{de}(s) \quad 3.7$$

Where  $T_{Tu}$  is the time constant for the turbine. As the next steady state is achieved, the increase in turbine power will not be the same to  $\Delta P_G$ .

Thus there will be an imbalance of power in the area that is equal  $(P_{Tu} - \Delta P_G)$  i.e.  $\Delta P_{Tu} - \Delta P_{de}$ . Note at the steady state  $\Delta P_{Tu}$  is equal to  $\Delta P_G$ . i.e.  $\Delta P_{Tu0} = \Delta P_{G0}$

As a result, the speed and frequency change, frequency dependency of load, the load damping factor (Celep, 2012):

$$D = \partial P_{de} / \partial f \quad 3.8$$

Thus

$$\begin{aligned} \Delta P_{Tu}(s) - \Delta P_{de}(s) &= \frac{2H}{f^*} s (\Delta f)(s) + D \Delta f(s) & 3.9 \\ &= \left[ \frac{2H}{f^*} s + D \right] \Delta f(s) \end{aligned}$$

$$\text{i.e. } \Delta f(s) = \frac{1}{\frac{2H}{f^*} s + D} [\Delta P_{Tu}(s) - \Delta P_{de}(s)]$$

Where  $H$  is inertia constant, thus

$$\begin{aligned} \Delta f(s) &= [\Delta P_{Tu}(s) - \Delta P_{de}(s)] (K_P / 1 + s T_P) & 3.10 \\ &= G_P(s) [\Delta P_{Tu}(s) - \Delta P_{de}(s)] \end{aligned}$$

Where  $K_P = \frac{1}{D}$  and  $T_P = \frac{2H}{f^* D}$

$$G_P(s) = K_P / 1 + s T_P \quad 3.11$$

The block diagram developed is updated as shown in Figure 3.5 is open loop. This corresponds to the linear model of primary LFC loop excluding the power system response.

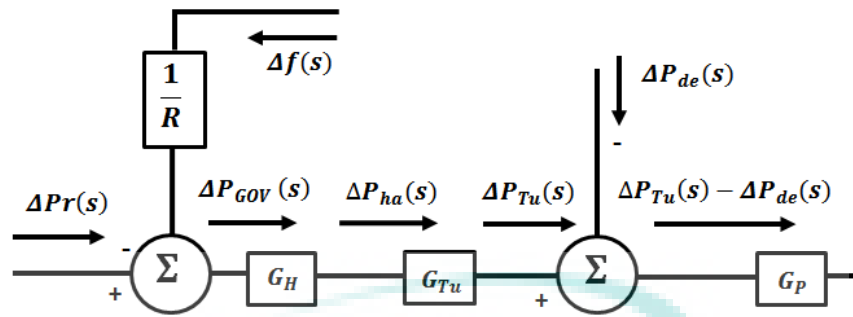


Figure 3.5 Block diagram linear model corresponding power system response

The operating system runs in its normal state with complete power balance; the frequency is at nominal value (50 Hz). By connecting additional load, load demand increases by  $\Delta P_{de}$  which refer to as new load, the generation immediately increases by  $\Delta P_G$  to meet the new load. As a result, the speed and frequency change.

The primary LFC close loop in Figure 3.6 has two inputs  $\Delta P_r$  and  $\Delta P_{de}$  and one output  $\Delta f$ , for constant reference input .i.e.  $\Delta P_r = 0$  (Usman & Divakar, 2012). The speed governing installed in each generation system, for a given speed changer setting, there is considerable frequency drop for increased system load. System frequency specification is rather strict and therefore, a lot of change in frequency cannot be tolerated. In power system, it is expected that the steady state frequency change must be equal to zero. In order to keep the frequency at the scheduled value, the speed changer setting must be regulated automatically by observing the frequency changes; therefore, the integral controller is involved. The signal that feeds into the integrator is indicated as Area Control Error (ACE).

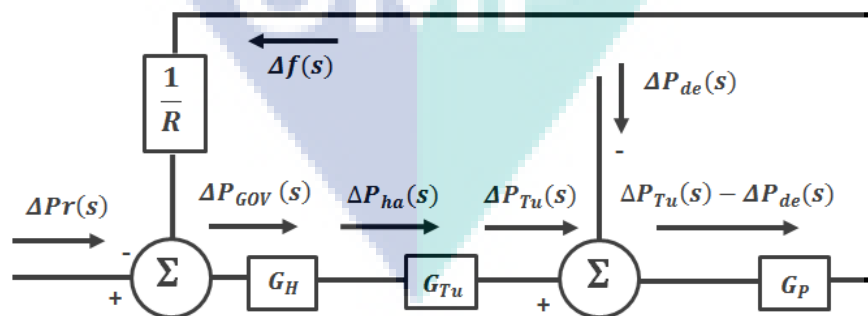


Figure 3.6 Block diagram closed loop of LFC

### 3.3.1 Area Control Error (ACE)

ACE represents a mismatch between area generation and load (Venkatachalam, 2013). Referring to the turbine-governor control eliminates rotor accelerations and decelerations following load changes during normal operation. However, there is a steady-state frequency error  $\Delta f$  when the change in turbine-governor reference setting  $\Delta P_r$  is zero. One of the objectives of LFC is to return  $\Delta f$  to zero. The change in reference power setting  $\Delta P_r$  of each turbine-governor operating under LFC is proportional to the integral of the area control error.

In case  $ACE = \Delta f$ , thus

$$\Delta P_r = -K_i \int ACE dt = -K_i \int \Delta f dt \quad 3.12$$

Taking Laplace transformation

$$\Delta P_r(s) = -\frac{K_i}{s} \Delta f(s) \quad 3.13$$

The gain constant  $K_i$  controls the rate of integration and thus the speed of response of the loop. For this signal  $\Delta f(s)$  is fed to an integrator whose output controls the speed changer, as shown in Figure 3.7 (Datta et al., 2011).

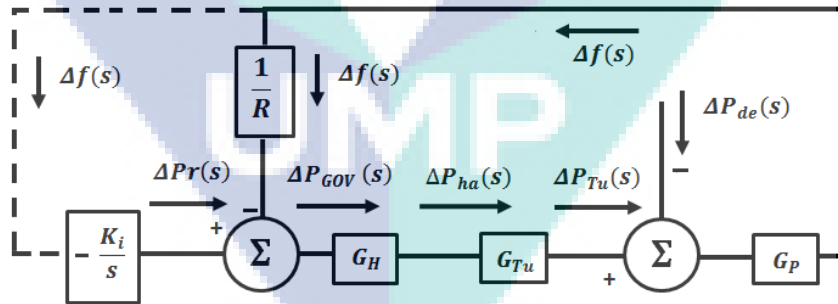


Figure 3.7 Block diagram corresponding to complete LFC

As long as that an error remains, the integrator output will rise, causing the speed changer to move. When the frequency error has been minimized to zero, the integrator output ceases, and the speed changer fixed value. The integral controller will give rise to zero steady-state frequency error following a step load change because of the reason stated above. Referring to a single control area block diagram with the

integral controller shown in Figure 3.7, input to  $G_{HTu}$  is;  $-\frac{K_i}{s}\Delta f(s) - \frac{1}{R}\Delta f(s)$  i.e.  $-\left[\frac{K_i}{s} + \frac{1}{R}\right]\Delta f(s)$ . The block diagram in Figure 3.7 can be reduced as shown in Figure 3.8 (Andersson, 2012).

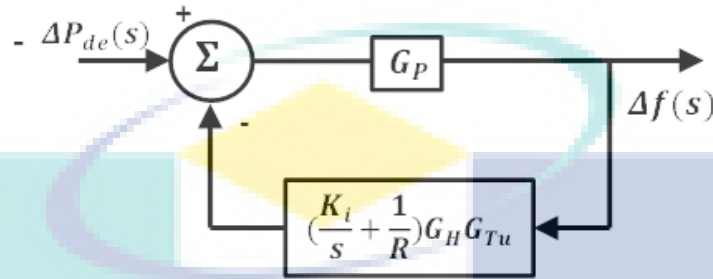


Figure 3.8 Reduced block diagram synchronous generator

By setting  $K_i$  as zero, can get the expression for  $\Delta f(s)$ . Corresponding to uncontrolled case the exact frequency error is:

$$\Delta f(s) = \frac{G_P}{1 + \frac{1}{R} G_H G_{Tu} G_P} \Delta P_{de}(s) \quad 3.14$$

### 3.4 Micro-grid System Configuration

The major objective of control for MG system is to generate a correct control signal to achieve the stability of the system. In addition to smooth transfer from grid-connected mode to island mode, the response of the system should be fast, and it must be able to minimize frequency fluctuation. A micro-grid can operate in synchronous with the utility or as an island. It can disconnect from the grid at any occurrences (i.e., faults, voltage collapses), but may also intentionally disconnect when the quality of power from the grid dip below certain standards providing higher power quality to these loads through island mode (Lasseter, 2011).

When a sudden change in load or fault occurs on the distribution network, the MG is scheduled to operate in an islanded mode, which is the MG switches to this transition mode. The static transfer switch (STS) plays a crucial role in the interface between the MG and the utility grid system. This device needs to be controlled by a logic that verifies some constraints at the terminals of the switch before allowing for synchronization. Synchronization conditions are detected by ascertaining two

constraints, i.e., first is the voltage across the switch has to be very small (ideally zero), and the second is the resulting current after the switch closed must be inbound from the utility system towards the MG. Figure 3.9 shows the flowchart of MG transfer from grid-connected mode to island mode operation (Li et al., 2015).

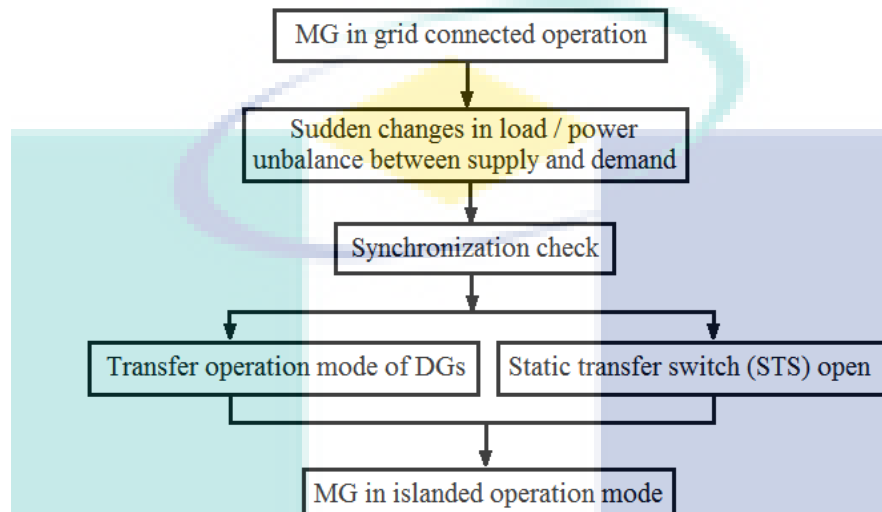


Figure 3.9 The flow charts of MG transfer to island mode

The hybrid micro-grid system under consideration comprises of one synchronous generator, one PV array, one battery storage unit and loads connected to the utility through the isolation switch at PCC point. Due to decentralized controller, each component is completed separately. Then, the models are combined to form a complete model of a hybrid micro-grid system as shown in Figure 3.10 (Taheri Ledari, 2017). The proposed control strategy, are developed using MATLAB/ Simulink environment.



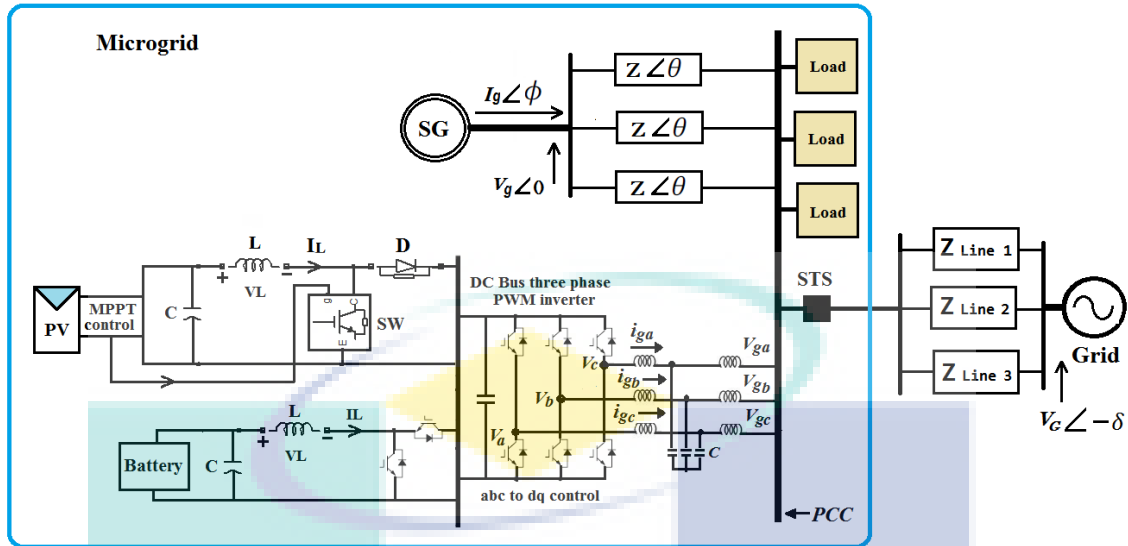


Figure 3.10 Structure of the proposed hybrid micro-grid system

To implement the proposed control methods, a simulation model (see Figure 3.10) of the proposed hybrid micro-grid system connected to grid by static transfer switch (STS) is developed in Matlab /Simulink software. This includes modelling of controllers, PV array, three-phase inverter, DC-DC power electronics converters, Lithium Ion (LI) battery, load and SG.

### 3.4.1 Model of Synchronous Generator

The model of synchronous generator in this study is based on the following assumptions:

1. It is operating under balanced three-phase positive sequence conditions.
2. The losses and saturation are neglected.

The synchronous generator based DG installed at the hybrid micro-grid has a salient pole rotor with a field excitation system. It is modeled using the standard block available in the MATLAB/Simulink and SimPowerSystems toolbox library. It has two control inputs,  $\omega$  and  $V_e$ , coming from the governor and exciter, respectively. The generator parameters are programmed in this simulation block. The PI conventional controller which regulates the speed engines,  $\omega$  to equal generator speed reference,  $\omega_{ref}$ . During load change, it adjusts the amount of fuel injected into the engine cylinders depending on the engine speed error value. The error in engine speed counted

as difference between actual speed and desired reference speed is used as input to the governor. The governors output is the desired fuel quantity to be shifted for generate the required torque.

The swing equation represents the imbalance between the power and the rotating speed in a SG. The electrical frequency of the induced voltage depends on the speed of rotation of the generator. The equations of motion of the rotor machine provided by:

$$J(d^2\theta/dt^2) = T_m - T_e = T_a \quad 3.15$$

Where  $J$  is the total moment of inertia of the rotor mass in  $kgm^2$ ,  $T_m$  is the mechanical torque, supplied by the prime mover in N-m,  $T_e$  is the electrical torque, output of the alternator in N-m,  $T_a$  accelerating torque and  $\theta$  is the angular position of the rotor in rad. In steady-state  $T_m$  equals  $T_e$ , the accelerating torque  $T_a$  is zero, resulting in a constant rotor speed. When  $T_m$  is greater than  $T_e$ ,  $T_a$  is positive therefore, resulting in increasing rotor speed. Similarly, when  $T_m$  is less than  $T_e$ , the rotor speed is decreasing. The simplified SG, mechanical system described by:

$$\Delta \omega(t) = 1/2H \int_0^t (T_m - T_e)dt - Kd\Delta\omega(t) \quad 3.16$$

$$\omega(t) = \Delta\omega(t) + \omega_0 \quad 3.17$$

Where  $\Delta \omega$  is speed variation,  $H$  constant of inertia,  $Kd$  damping factor,  $\omega(t)$  mechanical speed of the rotor, and  $\omega_0$  speed of operation.

### 3.4.2 Turbine-Governor Control

Depending on the valve position, the turbine (prime mover) changes its output power to establish the real power balance. The governors of all the machines sense the frequency and the mechanical power outputs will be adjusted automatically to match the combined generation with the newly combined load. This action is called primary regulation. But frequency remains at a new value and set points must be adjusted, just

as in single machine case for frequency restoration. This job is done by Load Frequency Controller (LFC) (John & Ramesh, 2013). Governor is the unit that is used in power system to sense the frequency bias caused by the load change and cancel it by varying the input of the turbines. Turbine-generator units operating in an SG contain stored kinetic energy due to their rotating masses. If the MG load suddenly increases, stored kinetic energy is released to supply the load increase initially. Since it is not possible to store a large amount of electric power, it is necessary to maintain a balance between the power demand of the generated power and the load. In the event of fluctuations in the load, the mechanical power provided by the turbine (which can be modeled by transfer function) does not correspond to the power generated by the generator; leading to an error integrated into the rotor speed deviation ( $\Delta\omega$ ).

Figure 3.11 (Glover et al., 2012) illustrates a steady state frequency power relation for a turbine-governor control. Note that when  $\Delta P_r$  is fixed,  $\Delta P_{Tu}$  is directly proportional to the drop in frequency. As in the figure below, when an electrical load change occurs, the turbine-generator rotor accelerates or decelerates, and frequency undergoes a transient disturbance. Under normal operating conditions, the rotor acceleration eventually becomes zero, and the frequency reaches a new steady-state.

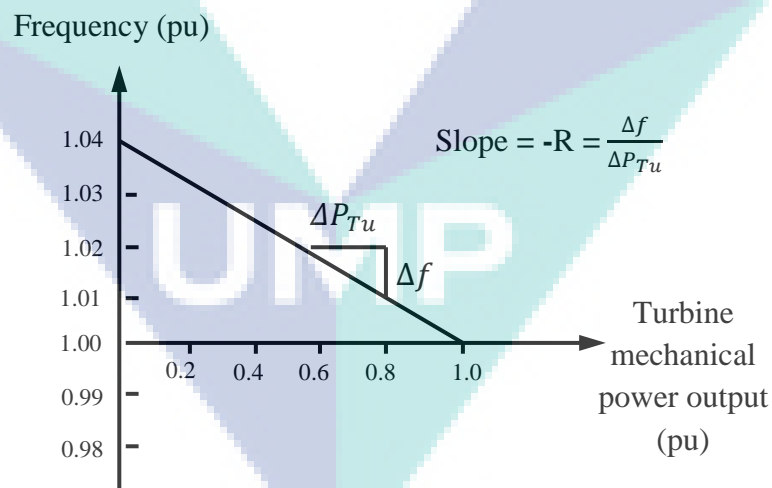


Figure 3.11 Steady-state frequency–power relation

The SG in the MG model is connected to a grid at PCC; grid can be represented by an “infinite bus”. An infinite bus is an ideal voltage source that maintains constant voltage magnitude, constant phase, and constant frequency.

### 3.4.3 Proportional Integral (PI) Control Scheme

The selection procedure of controller parameters such that to attain desired performance demands is known as tuning of the controller. The need to tune controller is for fast response and to have good stability. Ziegler-Nichols (Z-N) first proposed procedure of the controller and it is most popular tuning methodology (Kumar, R. et al., 2015). What leads to the development of other tuning methods after Z-N method is that it involves trial and error procedure which is not desirable. The conventional method of controller tuning is a trial and error based method. This makes it difficult to be implemented in all kind of problems. Because this requires continuous tuning of parameters values and observing the response which consumes a lot of time and requires effort, which is a tedious method.

The mechanical and electrical torques has been converted to powers by multiplying by the nominal frequency. The input signal is being connected to the output of the hydraulic turbine and governor. The frequency of the internal voltage sources depends on the mechanical speed of the machine, and speed governor adjusts the mechanical power based on the measurement of frequency. The mechanical power supplied to the machine. The power reference  $\Delta P_r$  is provided by a proportional-integral (PI) controller acting on the frequency error, to change the power reference of synchronous machine. The proportional part of this controller is commonly known as “primary frequency control” or “droop control”. In general, the conventional PI controller is preferred for speed control in outer loop due to its simplicity in execution and satisfying performance during steady state. However, its response depends on the gain values of proportional ( $K_p$ ) and integral ( $K_i$ ) which are responsible for the sensitivity of error speed in steady state. In the PI-controller, they require high gain values for speeding up and for fast load disturbances rejection. Therefore sudden change in load condition or speed change will result in overshoot, oscillation in speed or frequency and settling time. Figure 3.12 shows the block diagram for a conventional PI controller.  $K_p$  is the proportional action coefficient,  $K_i$  is the integral action coefficient. Transfer function can be easily changed by adjusting the parameters  $K_p$  and  $K_i$ .

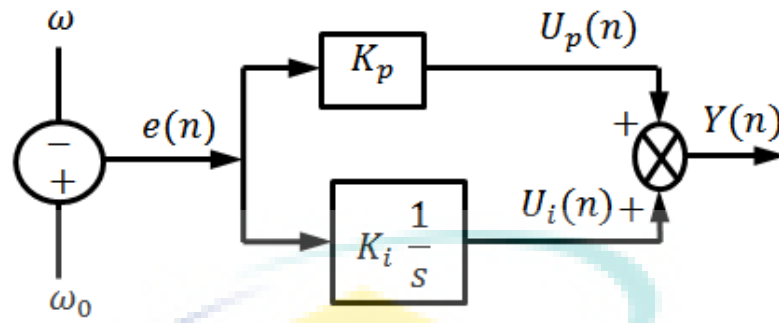


Figure 3.12 Block diagram of PI controller

$$U_p(n) = K_p e(n) \quad 3.18$$

$$U_i(n) = U_i(n - 1) + K_i \cdot e(n - 1) \quad 3.19$$

$$Y(n) = U_p(n) + U_i = U_i(n - 1) + K_p \cdot e(n) + K_i \cdot e(n - 1) \quad 3.20$$

Where  $U_p(n)$  is the control signal of proportional coefficient  $K_p$  and  $U_i(n)$  is the control signal of integral coefficient  $K_i$ ,  $Y_n(n)$  is the output control volume in the  $n$ -sampling time,  $e(n)$  is the input deviation in the  $n$ -sampling time,  $e(n - 1)$  is the input deviation in the  $(n - 1)$ -sampling time (Kiruthika, 2014).

For this work the transfer function of PI controller is written in the “Parallel form”:

$$G(s) = K_p + K_i \frac{1}{s} = K_p \left( 1 + \frac{1}{T_i} \right) \quad 3.21$$

Where  $K_p$  is the proportional gain,  $K_i$  is the integral gain and  $T_i$  is the integral time constant.

#### 3.4.4 Generator-Voltage Control

The generator field is supplied by a static exciter and automatic voltage regulator (AVR). The output voltage of SG is remained constant using an excitation system. In fact, the main task of the excitation system is to supply required excitation

current of synchronous machine within the allowable range of generator and adjust it automatically to accommodate the terminal voltage ( $V_t$ ) of the machine at a constant value. In Figure 3.13 (Mahzarnia et al., 2013) the model below provide an AVR system compensated with a first-order transfer function, which is represents the delay associated with measuring the terminal voltage  $V_t$ .

$$V_t = \frac{1}{1 + sT_r} \tag{3.22}$$

Where  $s$  is the Laplace operator and  $T_r$  is the measurement time constant.

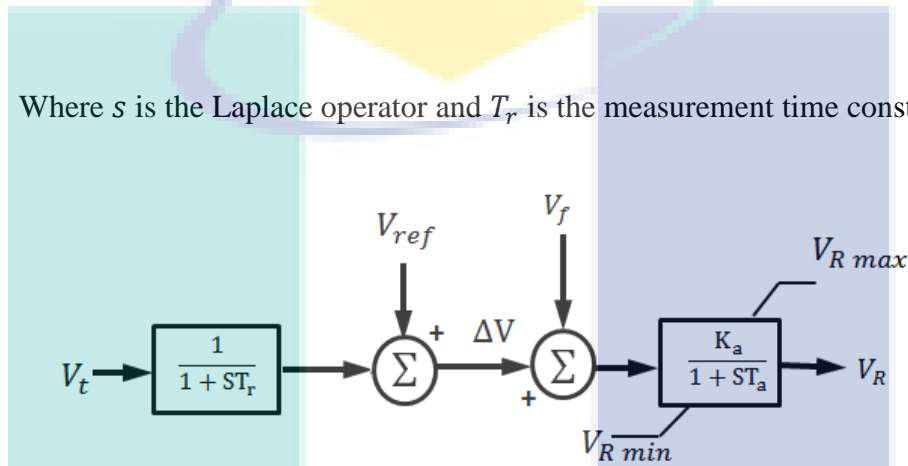


Figure 3.13 Block diagram for the Exciter

The measured generator terminal voltage  $V_t$  is compared with a voltage reference  $V_{ref}$  to obtain a voltage error,  $\Delta V$ , which in turn is applied to the voltage regulator. The voltage regulator  $V_R$  is modeled as an amplifier with gain  $K_a$  and a time constant  $T_a$  as below:

$$V_R = \frac{K_a}{1 + sT_a} \tag{3.23}$$

For simulation parameters in grid-connected mode are given in Table 3.2.

Table 3.2 Parameters of Synchronous Generator, Grid and Load

<b>Parameters of Synchronous Generator , Grid and Load</b>	
<b>Parameters Synchronous Generator</b>	
Nominal power	300KW
line-to-line Vn(rms)	430 V
Frequency	50Hz
Inertia constant, H	0.4 s
Internal impedance	R=0.157pu ,X= 0.1pu
<b>Parameters of Grid</b>	
Phase-to-phase rms voltage	13800(V)
Frequency	50Hz
Source resistance (Ohms)	0.001
Source inductance (H)	0.000001
<b>Parameters of three phase transformer</b>	
Winding 1 [ V1 Ph-Ph(Vrms) , R1(Ohm) , L1(H) ]	[13800 27.648 0.220022]
Winding 2 [ V2 Ph-Ph(Vrms) , R2(Ohm) , L2(H) ]	[400 0.75 14.5e-8 ]
Magnetization resistance Rm	0.3824e5 (Ohm)
Magnetization inductance Lm	266 (H)
Nominal frequency	50Hz
<b>Parameters of Load</b>	
RL load	80 kW,15kVAr
AC Induction Motor	16hp

### 3.5 Micro-grid Loads

An MG system has various kinds of load, and it plays a vital role in its operation, stability, and control. An electrical load can be categorized as a static or motor/electronic load. The MG can supply various kinds of loads (such as household or industrial) which are assumed to be sensitive or critical, and demand high-level reliability. This sort of operation requires several considerations such as priority to critical loads, power quality improvement supplied to specific loads, and enhancement of reliability for pre-specified load categories. Additionally, local generation prevents unexpected disturbances with fast and accurate protection systems (de Boer & Raadschelders, 2007; Lidula & Rajapakse, 2011; Planas et al., 2013).

The load classification is important to define the predicted operating strategy in an MG arrangement under the following considerations (Eto et al., 2009):

- i. The load/source operation strategy required to meet the net active and reactive power in grid- tied mode and stabilization of the voltage and frequency in island mode.

- ii. Reduction of maximum load to enhance the distributed resource (DR) ratings.

For a general load composed of RLC elements under sinusoidal-steady-state excitation, the load current is of the form:

$$i(t) = I_{max} \cos(\omega t + \beta) \quad A \quad 3.24$$

The instantaneous power absorbed by the load is then

$$\begin{aligned}
 P(t) &= v(t)i(t) = V_{max}I_{max} \cos(\omega t + \delta)\cos(\omega t + \beta) \\
 &= \frac{1}{2} V_{max}I_{max} \{ \cos(\delta - \beta) + \cos[2(\omega t + \delta) - (\delta - \beta)] \} \\
 &= VI \cos(\delta - \beta) + VI \cos(\delta - \beta) \cos[2(\omega t + \delta)] + VI \sin(\delta - \beta) \sin[2(\omega t + \delta)] \\
 P(t) &= VI \cos(\delta - \beta) \{ 1 + \cos[2(\omega t + \delta)] \} + VI \sin(\delta - \beta) \sin[2(\omega t + \delta)] \quad 3.25 \\
 &\text{Letting } I \cos(\delta - \beta) = I_R \text{ and } I \sin(\delta - \beta) = I_X \text{ gives} \\
 P(t) &= \underbrace{VI_R \{ 1 + \cos[2(\omega t + \delta)] \}}_{P_R(t)} + \underbrace{VI_X \sin[2(\omega t + \delta)]}_{P_X(t)}
 \end{aligned}$$

As indicated by Equation 3.25, the instantaneous power absorbed by the load has two components: One can be associated with the power  $P_R(t)$  absorbed by the resistive component of the load, and the other can be associated with the power  $P_X(t)$  absorbed by the reactive (inductive or capacitive) component of the load. The first component  $P_R(t)$  in Equation 3.25, where  $I_R = I \cos(\delta - \beta)$  is the component of the load current in phase with the load voltage. The phase angle  $(\delta - \beta)$  represents the angle between the voltage and current. The second component  $P_X(t)$  in Equation 3.25, where  $I_X = I \sin(\delta - \beta)$  is the component of load current  $90^\circ$  out of phase with the voltage. The values of micro-grid simulation system for load variation and its percentage, in grid connected mode are given in Table 3.3 below.

Table 3.3 Load variation and its percentage

Increase load	Percentage%
24kW+j4.5kVAr	30%
32kW+j6kVAr	40%
40kW+j7.5kVAr	50%



### **3.6 Micro-grid in Connected Mode**

A micro-grid can operate in synchronous with the grid utility. An important part of a synchronous generator is LFC. This controller is appropriately designed to respond to load variations and to fix the frequency at a constant value when working alone as an islanding mode. Also, when connected the synchronous generator to the grid, it is capable of providing active and reactive power. The frequency is held stiff with main grid frequency, nonetheless, when a micro-grid transfer from grid-connected mode to islanded mode, the DG units in the micro-grid still need to maintain the frequency.

#### **3.6.1 Model Reference Adaptive Controller (MRAC)**

The first purpose of this research is to propose a control method that can guarantee a fast and required response is available in grid-connected operation mode. The proposed technique uses MRAC structure to ensure the dynamic performance of the SG under load changes. In other words, to avoid harmful effects, such as slower response, overshoot, settling time and transient state to the system performance when load amounts change. Therefore, the MRAC guarantees corresponding output tracking, has inherent ability to adapt disturbances and errors, has a direct physical explanation and a simple implementation (Vargas-Martínez et al., 2015). Using of adaptive control the entire dynamic characteristic of the hybrid micro-grid system is improved. Here the controller parameters are adjusted to give a desired performance throughout the working of the micro-grid connected to grid. Therefore, the advanced control strategies Adaptive Proportional-Integral (API) controllers are applied to overcome deficiencies of the conventional PI controllers.

The adaptive control process is one that continuously and automatically measures the dynamic behavior of a plant, compares it with the desired output and uses the difference to vary adjustable system parameters or to generate an actuating signal in such a way. Adaptation law searches for the parameters such that the response of the plant which should be same as the reference model. It is designed to guarantee the stability of the control system as well as conversance of tracking error to zero.

### 3.6.1.1 Adaptation Mechanism

It is used to adjust the parameters in the control law. Adaptation law searches for the parameters such that the response of the plant which should be same as the reference model. It is designed to guarantee the stability of the control system as well as convergence of tracking error to zero, as a  $\Delta f = 0$ . From past study, the PI controller can be used to control the designed micro-grid control in different operation mode. That is due to, the parameters of the PI controller need to be tuned on-line automatically. Different ways can be used to adjust the PI parameters, pointing for combining the features of the MRAC and PI controller, the MRAC PI controller based on MIT rule is adopted in this work.

Some or all of the plant parameters may not be exactly known, and the adaptation mechanism tries to identify the individual parameters. It then passes this information to the controller, which in turn adapts its behavior based on the updated system information. When considering the scalar linear system (Gallestey et al., 2015), such as:

$$\dot{x} = ax + bu \quad 3.26$$

Where ( $a$ ) and ( $b$ ) are the two unknown system parameters or change over time e. g. due to changing operating environment. The goal is to stabilize the system to the origin, i.e., to have  $x(t) \rightarrow 0$  as  $t \rightarrow \infty$ . If the perfect knowledge of  $a$  and  $b$ , the task of stabilization is trivial. However, there are more different scenarios of uncertainties in the parameters:

1.  $a < 0$  unknown and  $b \neq 0$  unknown  $\Rightarrow$  it is sufficient to have  $u(t) \equiv 0$ .
2.  $a$  unknown with  $0 < a \leq \bar{a}$  and  $\bar{a}$  is a known constant,  $b = 1 \Rightarrow$  this is the robust case and  $u = -(\bar{a} + 1)x$  stabilizes the system.
3.  $a > 0$  unknown and  $b > 0$  unknown, i.e., It is the known sign of  $b \Rightarrow$  this is the case that shall further investigate.
4.  $a > 0$  unknown and  $b$  unknown  $\Rightarrow$  difficult case which requires the construction of universal controllers that 'discover' the sign of  $b$ .

### 3.6.1.2 The MIT Rule

The plant which is taken to deal with controlling is the first order system. So the physical realization for the micro-grid system under consideration is comparatively more feasible and less complicated with mathematical modeling for MIT rule, loss function is defined (Jain & Nigam, 2015):

$$F(\vartheta) = \frac{\mathcal{E}^2}{2} \quad 3.27$$

The difference between the actual response of the plant ( $y$ ) and the reference model response ( $y_m$ ) produces the tracking errors:

$$\mathcal{E} = y - y_m \quad 3.28$$

Where  $\mathcal{E}$  is the output error and is the difference between the output of the reference model and the actual model, whereby theta  $\vartheta$  is the adjustable parameter known as the control parameter. This error must be minimized through an adaptation mechanism applying the MIT rule. In this rule, the parameter  $\vartheta$  could be adjusted so as the losses function is minimized. Therefore, it can be further by changing the parameter in the direction the negative gradient of  $F$ , as follows:

$$\frac{d\vartheta}{dt} = -\gamma \frac{\partial F}{\partial \vartheta} = -\gamma \mathcal{E} \frac{\partial \mathcal{E}}{\partial \vartheta} \quad 3.29$$

This Equation 3.29 is called the MIT rule. Where the component of partial derivative term  $\partial \mathcal{E} / \partial \vartheta$  is denoted as sensitivity derivative of the system. This has shown on how the error is dependent from the adjustable parameter  $\vartheta$ , and  $\gamma$  is a positive quantity which indicates the adaption gain of the controller. Alternatively, the loss function ( $F$ ) can be chosen as;

$$\frac{d\vartheta}{dt} = -\gamma \frac{\partial \mathcal{E}}{\partial \vartheta} \text{Sign } \mathcal{E} \quad 3.30$$

Where (Sign) is the signum function then, MIT rule can be modified as follows;

$$\text{Sign } \mathcal{E} = 1 \text{ for } \mathcal{E} > 0$$

$$= 0 \text{ for } \mathcal{E} = 0$$

$$= -1 \text{ for } \mathcal{E} < 0$$

Figure 3.14 shows that the real model with transfer function  $kG(s)$ , where  $k$  is an unknown parameter and  $G(s)$  is a first order known transfer function. The aim in this section is to design a controller so that the real model can track the reference model using transfer function  $k_0 G_m(s)$ , where  $k_0$  is a known parameter.

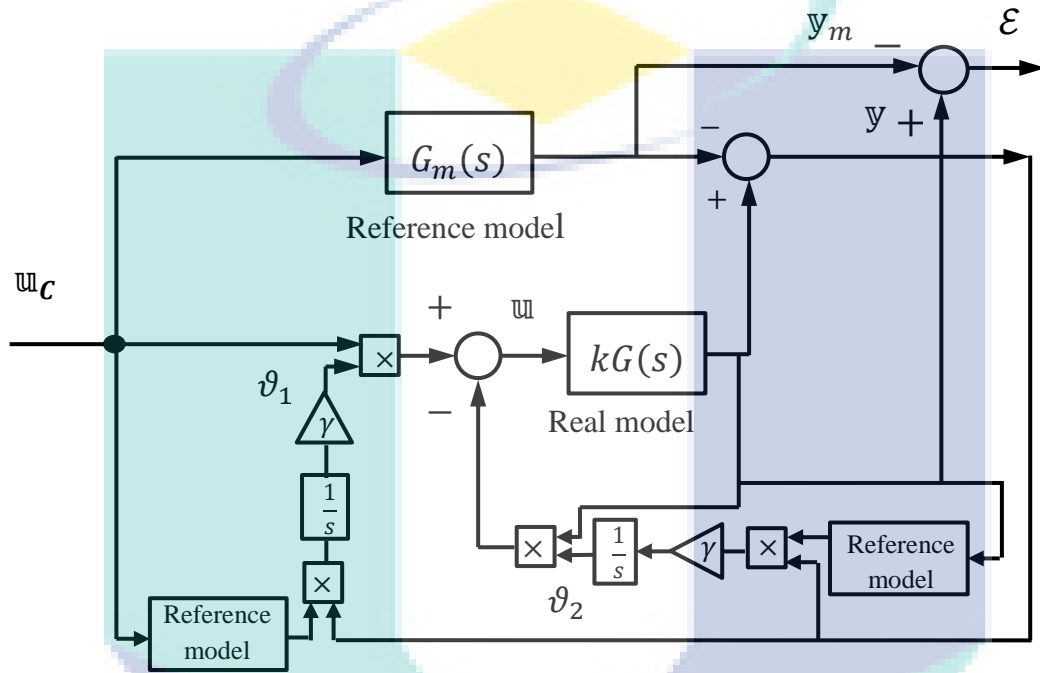


Figure 3.14 Model Reference Adaptive Control using MIT rule

The feed forward controller:

$$u = \vartheta u_c \tag{3.31}$$

Where  $u$  is the control signal and  $u_c$  the command signal.

From Equation 3.28 the error can give

$$\mathcal{E} = y - y_m = kG(s)u(s) - k_0 G_m(s)u_c(s) \tag{3.32}$$

Substituting Equation 3.31 into Equation 3.32:

$$\mathcal{E} = kG(p)\vartheta u_c - k_0 G_m(p)u_c \tag{3.33}$$

Where:

$$p = \frac{d}{dt}$$

$$\frac{\partial \mathcal{E}}{\partial \vartheta} = \frac{\partial}{\partial \vartheta} kG(p)\vartheta \mathfrak{u}_c - k \circ G_m(p)\mathfrak{u}_c = kG(p) \mathfrak{u}_c \quad 3.34$$

From Equation 3.33:  $y_m = k \circ G_m(p)\mathfrak{u}_c$

Then

$$G_m(p)\mathfrak{u}_c = \frac{y_m}{k \circ} \quad 3.35$$

$$\therefore \frac{\partial \mathcal{E}}{\partial \vartheta} = k \frac{y_m}{k \circ} = \frac{k}{k \circ} y_m \quad 3.36$$

The MIT rule thus gives:

$$\frac{d\vartheta}{dt} = -\gamma \circ \mathcal{E} \frac{k}{k \circ} y_m = -\gamma \circ \frac{k}{k \circ} y_m \mathcal{E} \quad 3.37$$

From Equation 3.30 and 3.37 gives the adaptive laws of MRAC as:

$$\frac{d\vartheta}{dt} = -\gamma \circ y_m \mathcal{E} \quad 3.38$$

Now let

$$\gamma \circ \frac{k}{k \circ} = \gamma$$

$$\therefore \frac{d\vartheta}{dt} = -\gamma y_m \mathcal{E} \quad 3.39$$

By using MIT rule the system is modified in this work and applied to first order system as follows:

$$\frac{dy}{dt} = -ay + b\mathfrak{u} \quad 3.40$$

Where  $\mathfrak{u}$  is control variable and  $y$  is measured output (Pawar & Parvat, 2015). Consider the model described as a reference model by:

$$\frac{dy_m}{dt} = -a_m y_m + b_m u_c \quad 3.41$$

Let the controller be given by:

$$u(t) = \vartheta_1 u_c(t) - \vartheta_2 y(t) \quad 3.42$$

The controller parameters are chosen to be:

$$\vartheta_1 = \frac{b_m}{b} \quad 3.43$$

$$\text{And } \vartheta_2 = \frac{a_m - a}{b} \quad 3.44$$

Then perfect model following is achieved (i.e. the input-output relationship of the system and model are same). Now the error of the system can be found from Equation 3.28.

From Equation 3.40:

$$\frac{dy}{dt} = -ay + bu \Rightarrow py = -ay + bu \Rightarrow (p + a)y = bu \quad 3.45$$

Now substituting  $u = \vartheta_1 u_c - \vartheta_2 y$ , we get:

$$(p + a)y = b(\vartheta_1 u_c - \vartheta_2 y) \quad 3.46$$

$$= b\vartheta_1 u_c - b\vartheta_2 y \Rightarrow (p + a + b\vartheta_2)y = b\vartheta_1 u_c \Rightarrow y = \frac{b\vartheta_1 u_c}{p + a + b\vartheta_2}$$

It should be noted here that the process output  $y$  is a function of the parameter vector  $\vartheta$ , while, the model output  $y_m$  is independent of  $\vartheta$ .

$$\therefore \frac{\partial \mathcal{E}}{\partial \vartheta} = \frac{\partial y}{\partial \vartheta} - \frac{\partial y_m}{\partial \vartheta} = \frac{\partial y}{\partial \vartheta}$$

$$\therefore \frac{\partial y_m}{\partial \vartheta} = 0 \quad 3.47$$

$$\therefore \frac{\partial \mathcal{E}}{\partial \vartheta_1} = \frac{\partial y}{\partial \vartheta_1} = \frac{\partial}{\partial \vartheta_1} \left( \frac{b\vartheta_1 \mathbb{U}_C}{p+a+b\vartheta_2} \right) = \frac{b}{p+a+b\vartheta_2} \mathbb{U}_C$$

And

$$\frac{\partial \mathcal{E}}{\partial \vartheta_2} = \frac{\partial y}{\partial \vartheta_2} = \frac{\partial}{\partial \vartheta_2} \left( \frac{b\vartheta_1 \mathbb{U}_C}{p+a+b\vartheta_2} \right) = -\frac{b^2 \vartheta_1}{(p+a+b\vartheta_2)^2} \mathbb{U}_C$$

$$\text{But } \frac{b\vartheta_1 \mathbb{U}_C}{p+a+b\vartheta_2} = y$$

$$\therefore \frac{\partial \mathcal{E}}{\partial \vartheta_2} = -\frac{b}{p+a+b\vartheta_2} y \quad 3.48$$

Now for perfect model following

$$\vartheta_2 = \frac{a_m - a}{b} \Rightarrow (p+a+b\vartheta_2) = p+a+b\left(\frac{a_m - a}{b}\right) = p+a+a_m - a$$

$$\therefore (p+a+b\vartheta_2) = p+a_m$$

Substituting in  $\frac{\partial \mathcal{E}}{\partial \vartheta_1}$  and  $\frac{\partial \mathcal{E}}{\partial \vartheta_2}$ , we get:

$$\frac{\partial \mathcal{E}}{\partial \vartheta_1} = \frac{b}{p+a+b\vartheta_2} \mathbb{U}_C = \frac{b}{p+a_m} \mathbb{U}_C \quad 3.49$$

And

$$\frac{\partial \mathcal{E}}{\partial \vartheta_2} = -\frac{b}{p+a+b\vartheta_2} y = -\frac{b}{p+a_m} y \quad 3.50$$

The parameter adjustment is thus given by:

$$\begin{aligned} \frac{d\vartheta_1}{dt} &= -\gamma^\circ \mathcal{E} \frac{\partial \mathcal{E}}{\partial \vartheta_1} = -\gamma^\circ \mathcal{E} \frac{b}{p+a_m} \mathbb{U}_C \mathcal{E} = -\gamma^\circ \mathcal{E} \frac{b a_m}{a_m(p+a_m)} \mathbb{U}_C \mathcal{E} \quad 3.51 \\ &= -\frac{\gamma^\circ b}{a_m} \frac{a_m}{(p+a_m)} \mathbb{U}_C \mathcal{E} \end{aligned}$$

Now let:

$$\frac{\gamma^\circ \ell}{a_m} = \gamma$$

$$\therefore \frac{d\vartheta_1}{dt} = -\gamma \left[ \frac{a_m}{(p + a_m)} \mathbb{W}_C \right] \mathcal{E} \quad 3.52$$

Similarly

$$\begin{aligned} \frac{d\vartheta_2}{dt} &= -\gamma^\circ \mathcal{E} \frac{\partial \mathcal{E}}{\partial \vartheta_2} = -\gamma^\circ \mathcal{E} \left( -\frac{\ell}{p + a_m} \mathbb{y} \right) = \gamma^\circ \mathcal{E} \left( \frac{\ell}{p + a_m} \mathbb{y} \right) \\ &= \frac{\gamma^\circ \ell}{a_m} \frac{a_m}{(p + a_m)} \mathbb{y} \mathcal{E} \end{aligned} \quad 3.53$$

Now let  $\frac{\gamma^\circ \ell}{a_m} = \gamma$

$$\therefore \frac{d\vartheta_2}{dt} = \gamma \left[ \frac{a_m}{(p + a_m)} \mathbb{y} \right] \mathcal{E} \quad 3.54$$

In this case  $\gamma$  is adaptive gain, Equation 3.52 and Equation 3.54 representing how the parameters should be varied for first order system so that the error will be zero. The different output of the reference model  $\mathbb{y}_m$  and the process output  $\mathbb{y}$  is a tracking error of deviation output signal to desired path. This is an outer loop that needs to adjust the controller parameters, in which the error is target to minimize or zero. To determine the mechanism adjustment for a stable system is an issue to be solved so that the zero error could be achieved. Thus, this adjustment mechanism of parameters is called the MIT rule that adapted to MRAC.

Under changing loads of the turbine system, the model reference adaptive controller is designed by using the Equations (3.28), (3.37) and (3.38). Consider a first-order system with the transfer function of actual mode output is;

$$\mathbb{y} = kG(s) = G_H(s) = 1/0.045s + 1 \quad 3.55$$

$$\text{The reference model is taken } \mathbb{y}_m = k \circ G_m(s) = 1/0.021s + 1 \quad 3.56$$

Where  $k$  is an unknown parameter and  $G(s)$  is a first order transfer function.  $k \circ$  is a given constant = 0.025. From Equation (3.28) gives:



$$\mathcal{E} = kG(s) - k_0G_m(s)$$

3.57

### 3.6.2 Artificial Neural Network (ANN)

The field of Neural Networks (NN) and its application to control systems has seen phenomenal growth over the last decades. Some advantages of artificial neural networks are the ability to handle parallel processing, learning, and generalizing about fault/noise (Shokoochi et al., 2014). Model Reference Adaptive Control (MRAC) has been widely applied recently to solve control problems for a system with matched unmodeled dynamics (Dydek et al., 2010). Furthermore, ANN could deal with nonlinear systems and was selected as an additional controller as it can train to follow an ideal trajectory (load change trajectory). In this chapter, it is proposed to integrate a neural network in MRAC to cope with the problem. The input control is provided by the aggregate of the output of traditional MRAC and the output of NN. The NN is applied for covering any fluctuation occurring in the micro-grid system that is not taken into consideration in the conventional MRAC, and tracking between grid connection mode and island mode. The proposed NN-based MRAC can significantly improve the micro-grid behavior and compel the system to follow the reference model, and reduce the output error between the model and plant.

#### 3.6.2.1 Learning Styles of ANN

Learning is based on the error in the controller output. Batch training, in which weights and biases are only updated after all the inputs and targets are presented, can be applied to both static and dynamic networks.

The error in case of  $\Delta\omega$  is control error, the input to the NN controller is the change in load and fault (given by speed governor). The output updates the two control parameters  $K_p$  and  $K_i$ . The connection weight,  $w$  is updated according to the relational expression using the back-propagation algorithm. The net input of the  $j$ -th hidden unit is:

$$n_j^1 = \sum_{i=1}^1 w_{ji} u_i + b_j^1 \quad 3.58$$

Where  $w_{ji}$  is the weighting on the connection from the  $i$ th input unit,  $b_j^1$  represent the bias for the hidden layer neurons. The output of the neurons in the hidden layer is:

$$v_j = f_1(n_j^1), f_1(x) = x \quad 3.59$$

And the net input to the neurons in the output layer can be written as:

$$n_k^2 = \sum_{j=1}^1 w_{kj} v_j + b_k^2, k = 1 \quad 3.60$$

Where  $w_{kj}$  is the weighting on the connection from the  $j$ th input unit,  $b_k^2$  represent the bias for the second layer neurons. The output of the second layer is the network outputs of interest and these outputs are labeled as  $y_k$ : as depicted in Figure 3.15.

$$y_k = f_2(n_k^2), f_2(x) = x \quad 3.61$$

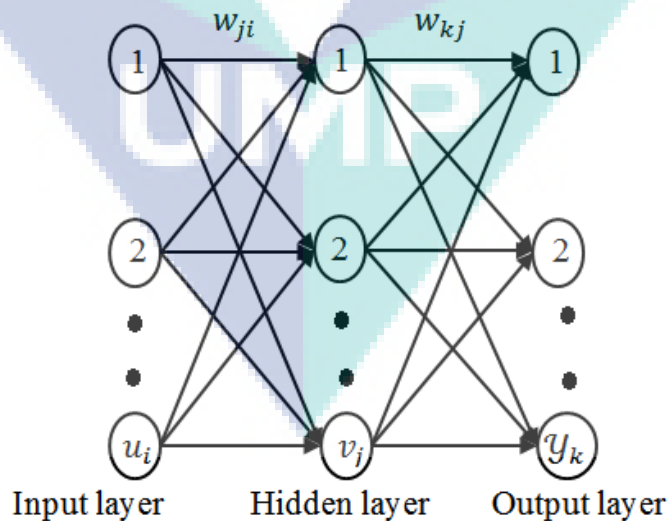


Figure 3.15 Principle of Back-Propagation training

### 3.6.2.2 NARMA –L2

Typically there are two steps involved when using neural networks for control first step is system identification and the second is control design. System identification stage can develop a neural network model of the plant that is selected to control. Whereas, to train the controller, neural network plant model is applied in the control design stage. NARMA-L2 control is a controller from the rearrangement of the plant mode; the controller is a neural network that is trained to control a plant so that it follows a reference model. One standard model that has been used to represent general discrete-time nonlinear systems is the NARMA-L2 model (Nguyen, N. et al., 2016). The neural network plant model is used to assist the controller training. NARMA-L2 controller requires the least computation architecture. The controller is a rearrangement of the neural network plant model, which is trained offline, in batch form as shown in Figure 3.16.

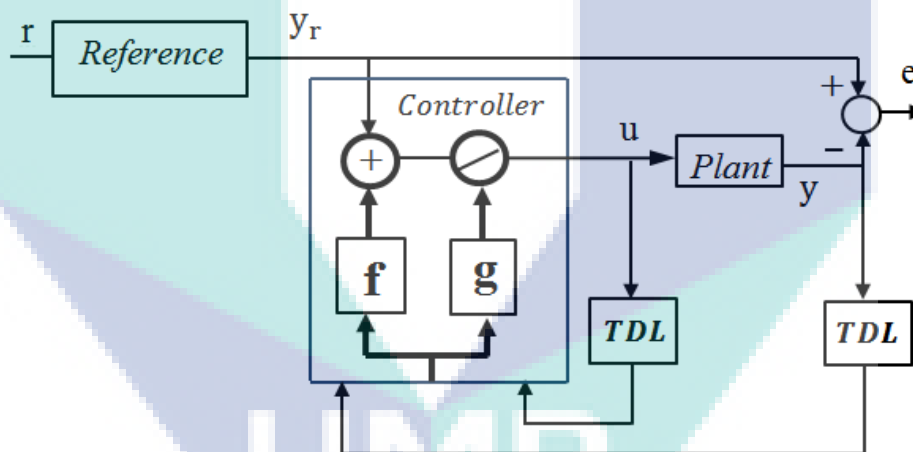


Figure 3.16 Block diagram of the NARMA-L2 controller

In this work, the NARMA –L2 architecture is applied with the aid of the Neural Network Toolbox of MATLAB software. The identification can be summarized by the following steps:

Step -1- Using feedback linearization (or NARMA-L2 control) is to identify the system that will be controlled. Neural network is trained to represent the forward dynamics of the system:

$$y(t + c) = N[y(t), y(t - 1), \dots, y(t - n + 1), u(t), u(t - 1), \dots, u(t - n + 1)] \quad 3.62$$

Where  $u(t)$  is the system input,  $y(t)$  is the system output,  $t, c, n$  are integral number and  $N$  is the function of the output system after identification.

Step -2- To make the output system to follow some reference trajectory by developing a nonlinear controller of the following form:

$$y(t + c) = yr(t + c) \quad 3.63$$

$$u(t) = G[y(t), y(t - 1), \dots, y(t - n + 1), yr(t + c), u(t - 1), \dots, u(t - m + 1)] \quad 3.64$$

The problem with using this controller is the fact that training a neural network to minimize mean square error needs to use dynamic backpropagation, which is quite slow. One solution to this problem is to use approximate models to represent the system. The controller used in this section is based on the NARMA-L2 approximate model:

$$y^{\wedge}(t + c) = f[y(t), y(t - 1), \dots, y(t - n + 1), u(t - 1), \dots, u(t - m + 1)] + g[y(t), y(t - 1), \dots, y(t - n + 1), u(t - 1), \dots, u(t - m + 1)]u(t) \quad 3.65$$

The advantage of this form is that controlled input make the system output follows the reference Equation 3.20. The resulting controller is:

$$u(t) = (yr(t + 1) - f[y(t), y(t - 1), \dots, y(t - n + 1), u(t - n + 1)]) / g[y(t), \dots, y(t - n + 1), u(t - n + 1)] \quad 3.66$$

Using this equation directly can cause realization problems because the control input based on the output at the same time should be determined before that, i.e.:

$$y(t + c) = f[y(t), y(t - 1), \dots, y(t - n + 1), u(t - 1), \dots, u(t - n + 1)] + g[y(t), \dots, y(t - n + 1), u(t), \dots, u(t - n + 1)]u(t + 1) \quad 3.67$$

MRAC is used to design the adaptive controller that works based on the principle of adjusting the control parameters so that the output of the actual plant tracks the output of a reference model. Based on the MRAC using MIT rule controller, the network structure is modified in this work. The proposed network has been trained by using backpropagation algorithm. Learning algorithms cause the adjustment in the weights so that the controlled system gives the desired response. The controller is designed using a parallel combination of MRAC system and ANN controller. The block diagram of the proposed neural network-based MRAC is shown in Figure 3.17, which applies for adjusting the PI parameters such that the error between the reference model output and process output is reduced.

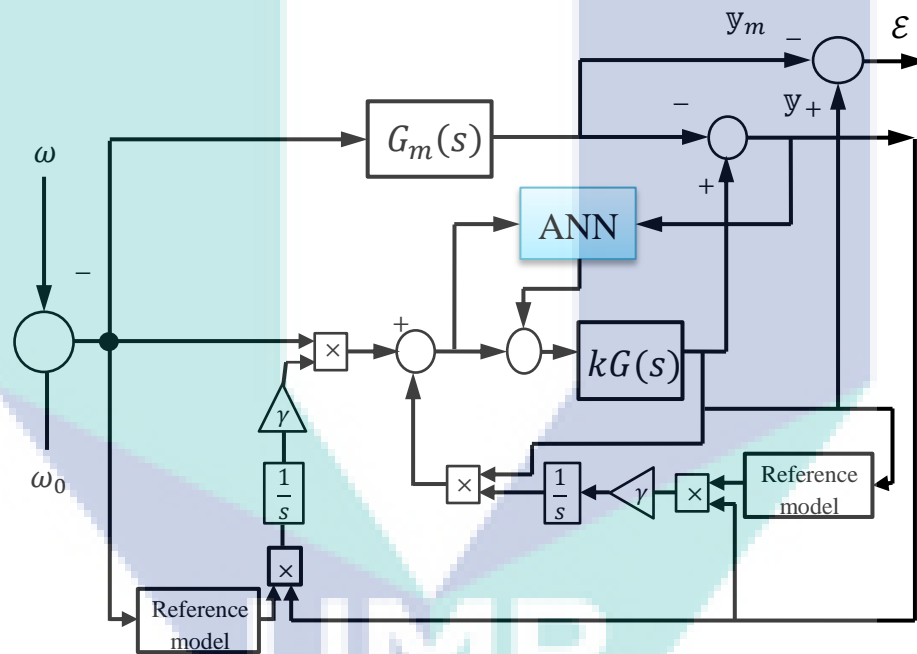


Figure 3.17 Block diagram of MRAC using MIT rule with ANN (NARMA -L2) based speed control

Learning is done to reduce the function given by Equations 3.27 and 3.28 respectively. The error ( $\epsilon$ ) is used to update the weights as follows Equations 3.52 and 3.54. In the forward process, when using the input vector, the values of the hidden layer output and the result of the output layer are provided from MRAC, and then the error value obtained from the process is used to update the weights. During continues of the learning process can reach the required minimum error.

The NN takes the values output of the previous plant, control signal and set point signal as inputs, and tuned according to a disturbance applied and the required changes in the PI controller parameters. During training, the values of reference speed and the rate change of input speed are considered as input data, and the optimal gains are regarded as output data. Figure 3.18 illustrates a flowchart of the algorithm used in this work.

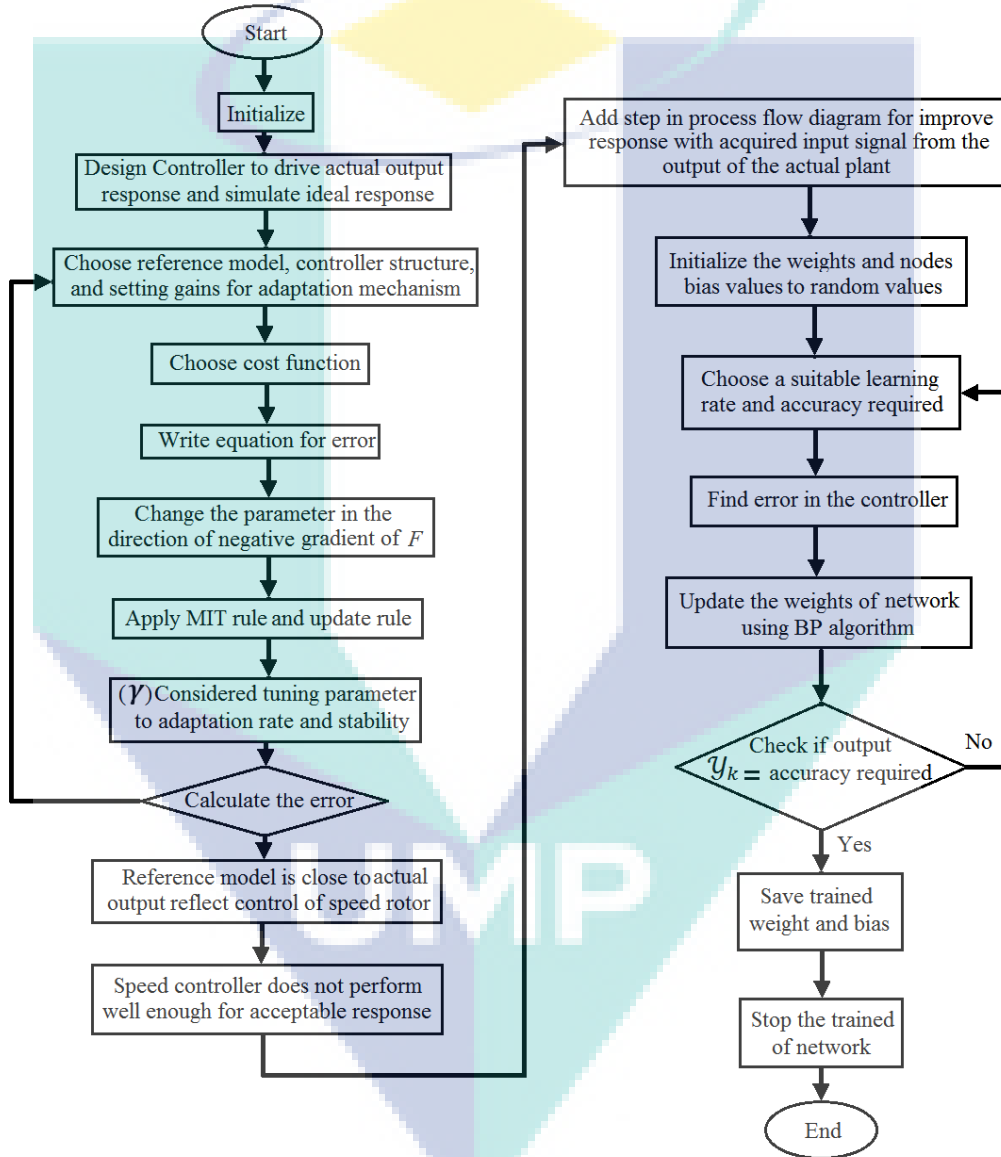


Figure 3.18 The MRAC based MIT rule and ANN algorithm flowchart

### 3.7 Micro-grid in Island Mode

After disconnection from the main grid, the islanded system initially faces with power generation mismatch that then will lead to an over generated or under the

generated situation. A generation less than remained demand leads to low frequency and voltage status in the islanded system; whereas generation overload level can be directed to stabilized frequency and voltage amplitude.

Since the micro-grid is in islanded operating mode, the system inertia is decreased, and the LFC capacity is not sufficient to quickly damp the frequency oscillation. After activating the synchronous generator into LFC, the system inertia could be increased, thus improving the grid frequency stability. To get a desirable LFC, the fuzzy logic table control (FLTC) is proposed to increase a fast response of the SG. When a micro-grid operates in an islanded mode, local frequency control is always one of the leading issues. The main advantage expected from a micro-grid is that it should allow treating as a controlled aggregated load within the power system. Increasing in size and complexity of MG as well as emerging SG and their effects on the dynamic behavior of power system, caused conventional LFC systems (Proportional-Integral (PI) controllers) is incapable of providing good dynamical performance over a wide range of operating condition. All of conventional control schemes of LFC have inherent problems that increase the frequency feedback gain and results in the instability of the LFC loop, which restricts the control range of frequency droop.

### **3.7.1 Fuzzy Inference System (FIS)**

In this work, FIS consists of three stages. As shown in Figure 3.19, the first, fuzzification converts crisp value input to a linguistic variable using the breakpoint data sets retained in the knowledge base. In the second stage, the inference engine is assigned the task of evaluating the input's degree of the breakpoint to the fuzzy output sets using the table data. Finally, the defuzzifier stage transforms the fuzzy output into a crisp value. The inference stage utilizes the data set input values to activate the inference table data and generate the fuzzy output value.

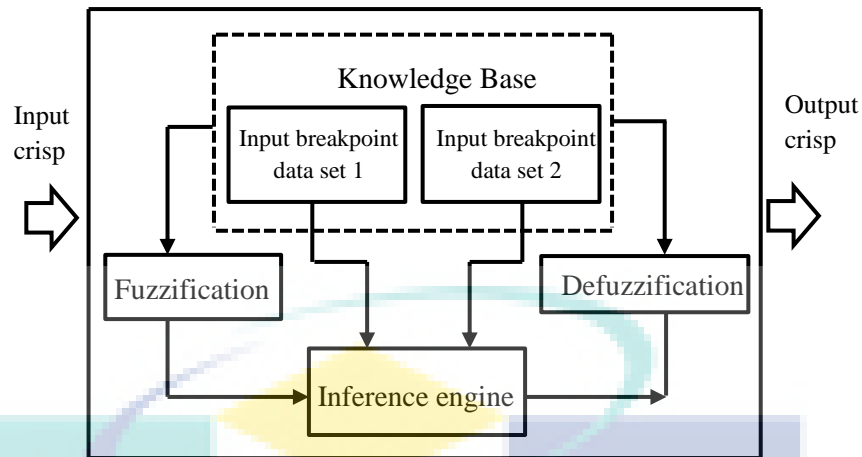


Figure 3.19 Architecture of FLTC block diagram

### 3.7.1.1 The Lookup Table (2-D)

A grid-based lookup table in Figure 3.20 is the most common type of nonlinear static model. In particular, modern combustion engine control, an enormous number of one- and two-dimensional lookup tables are used (Hausberg et al., 2014). The lookup table is derived based on the breakpoint data of inputs, the output, and the table data. A control output gain is used as a filter to tune the output of the lookup table to obtain different output values. Most researchers are widely utilized two blocks lookup table input in actual applications of lookup table fuzzy and two outputs, and that is very complicated. The advantage of this work is that the fuzzy output is based on the estimation of one lookup table with two input and one output parameters, so the control is high accuracy and easy application especially in power system containing some of the different DGs.

To design a 2-D lookup table, the first step in constructing this is to define the inputs and outputs of the system. The input signal is same as output to keep track of error. The gain is tuned by choosing the appropriate of required values in the table. In this case, the 2-D lookup table is proposed, which is suitable for use PI controller. The scope of this section is limited explicitly to the 2-D lookup table used to control the rotor speed of the generator in island operation mode.

The lookup table can be applied in different ways. For example, to store the state of sample support parameters or controller parameters such as gain, depending on the operation. The 2-D lookup table computes an approximation to a function of  $z =$



$f(\mathbf{x}, \mathbf{y})$  for a given  $\mathbf{x}, \mathbf{y}, \mathbf{z}$  data points. The row and column indexes could be defined as 1-by- $m$  of  $\mathbf{x}$  data point and 1-by- $n$  of  $\mathbf{y}$  data point of vectors. While, the table data is defined as  $m$ -by- $n$  matrix of  $\mathbf{z}$  data point. It can be illustrated as the first input port mapped to the first table of dimension  $\mathbf{x}$ , and the second input port mapped to the second table of dimension  $\mathbf{y}$ . As shown in Figure 3.20, the first input identifies the first dimension (row) breakpoints and the second input identifies the second dimension (column) breakpoints.

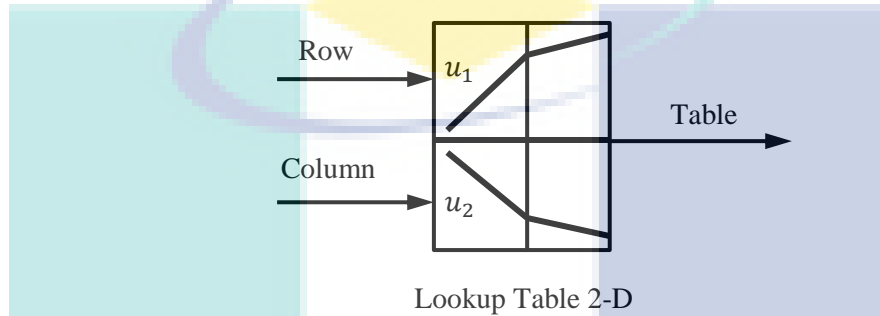


Figure 3.20 Block diagram of lookup table

Lookup table uses many methods for the input values to generate output values. In this FLTC, the Interpolation-Extrapolation method is employed. If the value corresponds to the input, the output is the identity element to the output vector. If the input does not match row and column parameter values, the lookup table performs linear internal update between the appropriate row and column values. If one or both lookup table inputs are lower than the first or higher than the last row or column values, the lookup table extrapolates using the first two or the previous two points. This method implements linear interpolation but does not extrapolate outside the endpoints of  $\mathbf{x}$  and  $\mathbf{y}$ . On the other hand, the lookup table uses the end values method. The Input Nearest method detects the elements in  $\mathbf{x}$  and  $\mathbf{y}$  nearest to the current inputs that corresponding to  $\mathbf{z}$  as the output.

### 3.7.1.2 Data Sets and Table Data

Lookup tables can be regarded as the first order in the network. They comprise of a set of data or interpolation nodes placed on a multi-dimensional point of the network with each node consisting of two elements. The numerical data point heights are an estimation of the approximate nonlinear function in its data point position. All nodes are stored, for example, in the memory of the control unit. To generate the model,

all data point positions are usually pre-consistent. The sizes of breakpoint data sets and table data, some concerns should be taken into consideration:

- I. The limitations of the memory system constraint for the overall size of a lookup table.
- II. Lookup tables must use consistent dimensions so that the overall size of the table data reflects the size of each breakpoint data set.

The dimensions of the lookup table are created by dynamically updating the dormant lookup table which can be used to model time-varying systems with two inputs. Each breakpoint data set is an index of input values for a particular dimension of the lookup table. The array of table data serves as a sampled representation of a function evaluated at the breakpoint values.

In the following equation the consideration of two-dimensional lookup table of the size  $M \times N$  is shown in Figure 3.21 (a). It consists of interpolation nodes located on the grid lines  $S_{1,1}, \dots, S_{1,M}$  and  $S_{2,1}, \dots, S_{2,N}$ . The output of model  $\hat{\mathbb{Z}}(u_1, u_2)$  for certain inputs  $(u_1, u_2)$  is determined by taking into account the nearest points to bottom left, bottom right, top left, and top right of the model input as shown in Figure 3.21 (b). The heights of the interpolation nodes  $Q_{k,t}, Q_{k+1,t}, Q_{k,t+1},$  and  $Q_{k+1,t+1}$  are weighted with the corresponding opposite area (Müller & Isermann, 2004):

$$\hat{\mathbb{Z}} = Q_{k,t} \cdot \frac{AR_{k+1,t+1}}{AR} + Q_{k+1,t} \cdot \frac{AR_{k,t+1}}{AR} + Q_{k,t+1} \cdot \frac{AR_{k+1,t}}{AR} + Q_{k+1,t+1} \cdot \frac{AR_{k,t}}{AR} \quad 3.68$$

With the areas

$$AR_{k+1,t+1} = (S_{1,k+1} - u_1)(S_{2,t+1} - u_2) \quad 3.69$$

$$AR_{k,t+1} = (u_1 - S_{1,k})(S_{2,t+1} - u_2) \quad 3.70$$

$$AR_{k+1,t} = (S_{1,k+1} - u_1)(u_2 - S_{2,t}) \quad 3.71$$

$$AR_{k,t} = (u_1 - S_{1,k})(u_2 - S_{2,t}) \quad 3.72$$

The total area,  $AR$  is calculated as

$$AR = (S_{1,k+1} - S_{1,K})(S_{2,t+1} - S_{2,t}) \quad 3.73$$

The control surfaces can be approached through lookup tables to simplify the generated code and improve performance speed. FLTC can be applied by a set of the lookup table, one lookup table for both inputs defined in the FIS. In this section, the task is to design and replace PI controller for the plant. The plant is a two-input one-output system in discrete time, and the aim of controlling rotor speed is to make each breakpoint work with high efficiency and safety, at the same time to achieve good performance, which is based on breakpoints data (row & column breakpoints).

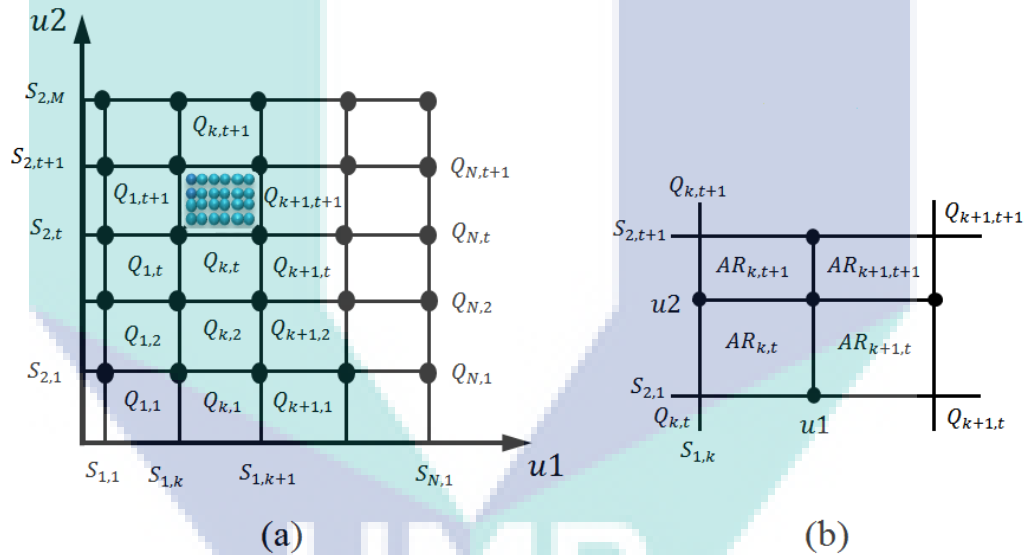


Figure 3.21 (a) The grid-based mode of the interpolation nodes of the (2-D) lookup table, (b) Areas for interpolation within a (2-D) lookup table

### 3.7.1.3 Inputs and Outputs of System

With the aim to design a 2-D lookup table, a data collection and the development analysis has to be built. The first procedure in developing this is to identify the inputs and outputs of the system. The original inputs are speed error ( $e$ ) and its derivative, which represents the change of speed error ( $\Delta e$ ) in (pu). Both ( $e$ ) and ( $\Delta e$ ) inputs are determined to meet the system response and to reduce the error effect, which is the essential problem of the island mode. These inputs where the speed controller settled is required in order to sustain the proper speed of synchronous generator ( $\omega$ )

while saving the required power to the rest of the micro-grid. The output of the original system was speed rotor in per unit (pu). This is the oversight that set the control desired speed of the synchronous generator to maintain the appropriate frequency. The desired speed signal in this condition was determined by inputting the signal error of speed into the existing controller of the 2-D lookup table which then determined the appropriate synchronous generator speed (pu). This speed is the feedback signal during the *adaptation gain (a.g)*. In this controller, the two inputs of breakpoint sets (set1 and set2) for the table data are the speed control error signal ( $e$ ) and the change of speed error ( $\Delta e$ ). These two inputs show the cell in the table data that will be updated following the new measurements.

#### 3.7.1.4 Proposed Mechanism

This research proposes a new Fuzzy Logic Table Control (FLTC). The proposed controller is initialized using the lookup table rule that grasps the features of adaptive control and fuzzy-logic techniques. In this operations mode (island mode), a FLTC controller was proposed to replace the PI controller used to minimize error in the traditional PI speed controller. From Figure 3.22, the speed control error signal ( $e$ ) and its derivative error, which represents the change of speed error ( $\Delta e$ ) inputs are fed to the FLTC, though input gains  $Ke$ ,  $Kde$ , respectively. While the control an output is the mechanical rotor speed of turbine to match to the synchronous generator rotor speed. The strategy considers FLTC to improve the overall performance of hybrid micro-grid in islanding mode according to the nature of disturbances (load step change and fault). Using this technique the control algorithm becomes shorter and runs faster than traditional PI controller.

The FLTC controller block has two inputs ( $e$  and  $\Delta e$ ) and one output. Therefore, it is ease to replace the PI system using a 2-D lookup table. To generate a 2-D lookup table from FIS, loop through the input, and the corresponding output values using Interpolation-Extrapolation method. The speed error and change of speed error could be defined as follows:

$$e(k) = \omega_{des}(k) - \omega_m(k) \quad 3.74$$

$$\Delta e(k) = e(k) - e(k - 1) \quad 3.75$$

Where  $\omega_{des} = \omega_0$  is the desired speed and  $\omega_m = \omega$  is the measured speed. The gains  $K_e$ ,  $K_{de}$  and adaptation gain are used to normalize the SG response and to adjust the controller's sensitivity.

The modification can be made for faster estimation that is resulting in calculating speed gains when simulating the model. As shown in Figure 3.22, which is a proposed FLTC closed-loop control system, the inputs are an error. The proposed FLTC has the tracking error signal as two inputs  $K_e$ ,  $K_{de}$  and single output  $K_{a.g}$  adaptation gain. The lookup table is derived based on the table data; an adaptation gain is used to tune the output of the lookup table to obtain different output values.

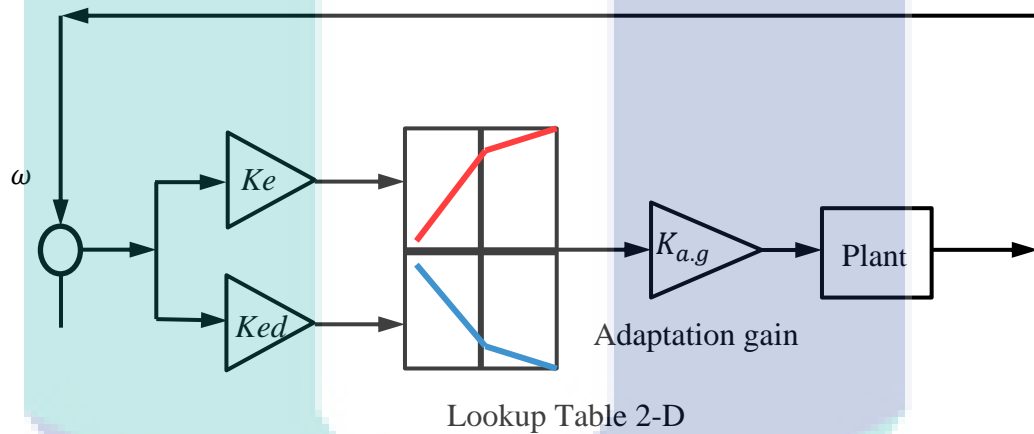


Figure 3.22 Proposed FLTC to control the speed governor in island

A feedback signal is obtained from the output of the system. The reference point is representing speed signal ( $\omega_{des}$ ) of SG. The style of FLTC is:

$$IF \ x \text{ is } A \text{ AND } y \text{ is } B \text{ THEN } z \text{ is } f(x, y) \quad 3.76$$

Where  $x$ ,  $y$  and  $z$  are linguistic variables,  $A$  and  $B$  are breakpoint data sets on universe of discourses  $\mathbb{X}$  and  $\mathbb{Y}$  and  $f(x, y)$  is a mathematical function. For this proposed controller the configuration of a 2-D lookup table (Data 3x3) is shown in Table 3.4, and Figure 3.23.

Table 3.4 2-D Lookup Table Row x Column (Data 3x3)

Breakpoint	Column	(1)	(2)	(3)
Row	-----	-1	0	1
(1)	-1	-2	0	2
(2)	0	-10	0	12
(3)	1	-12	0	14

In the current FLTC, the speed error, ( $e$ ), and its derivative, ( $\Delta e$ ), of the synchronous machine are chosen as the inputs. The input gains are named  $Ke$ ,  $Kde$ .

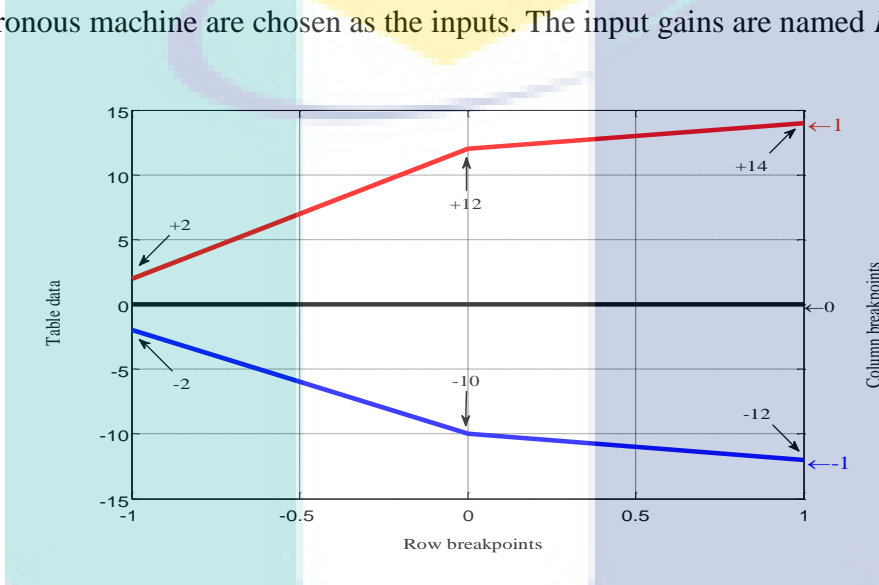


Figure 3.23 Three membership functions for each input

The values use the input to generate the output values using the method of selecting the lookup table parameters. The above input and output values define the 2-D lookup table that is graphically shown in Figure 3.24.

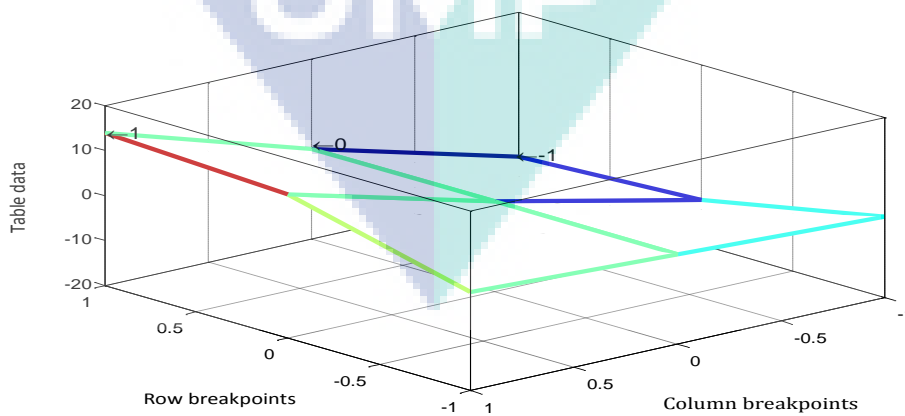


Figure 3.24 Mesh plot of table data and breakpoints data (row & column breakpoints) for proposed controller

Figure 3.25 viewer is a three-dimensional plot of the control surface which will predict the outcome of any output variable depending on the values of two input variables. In this figure, it is shown the various values of speed error ( $e$ ) and change of speed error ( $\Delta e$ ) signal of the synchronous generator that FLTC applied to predict the output, which is the speed in pu.

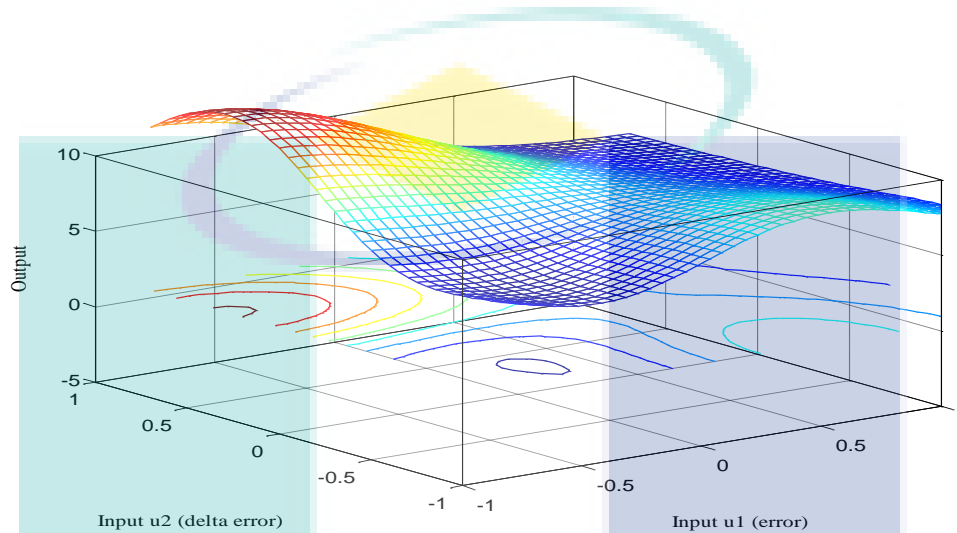


Figure 3.25 The surface control of speed

The parameters and values, for simulation system controller, in islanded mode are shown in Table 3.5.

Table 3.5 Parameters and values controller

Parameter	Value
$K_e$	1
$K_{ed}$	4
$K_{a.g}$	5

The whole design of proposed FLTC algorithm can be expressed with flow chart in Figure 3.26.

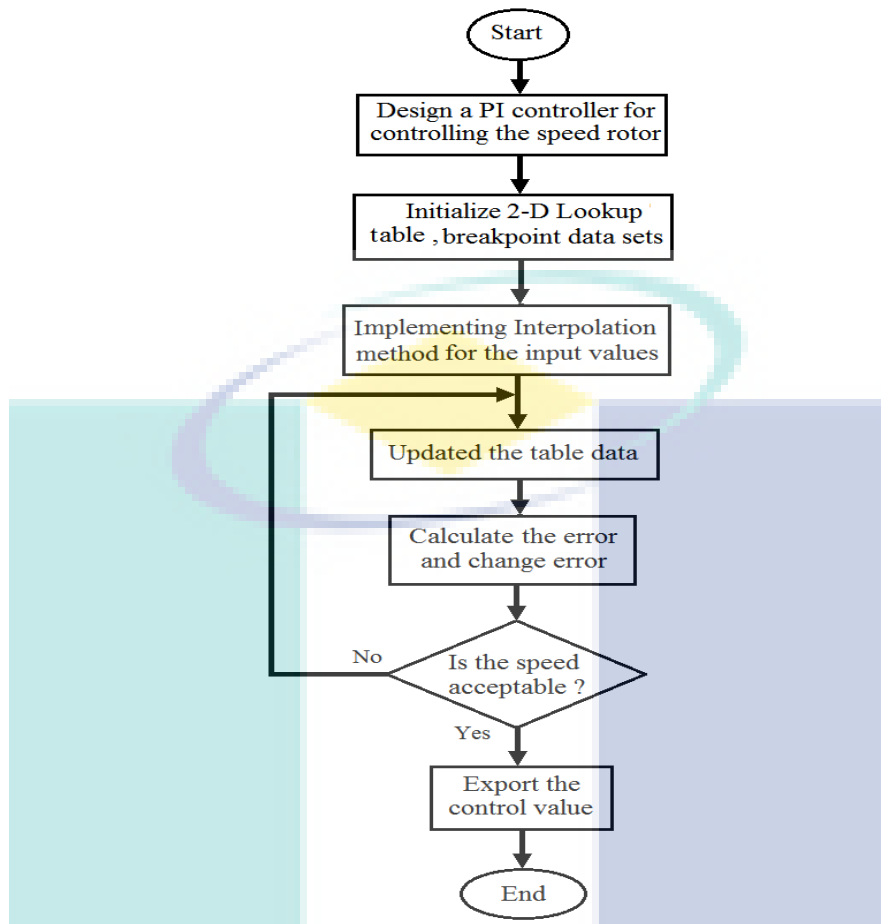


Figure 3.26 Flow chart of FLTC algorithm

### 3.8 Modeling of PV Solar Generation

The design of power converter and control approach is significantly influenced by the solar module characteristics. In this work, a step-by-step for the simulation of photovoltaic modules, that the PV array is optimized the power produced using the maximum power point method for given temperature and irradiance conditions is presented. The inputs of the model are ambient temperature and solar irradiance while its output is maximum array power (Mahela & Ola, 2013). The construction of the PV system is the solar cell, which is a (p-n) semiconductor junction that directly converts solar radiation into direct current with photovoltaic effect, shown in Figure 3.27.



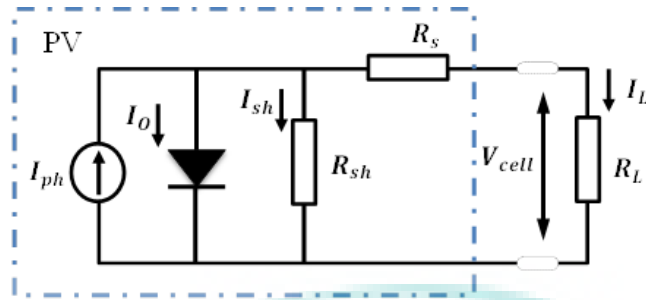


Figure 3.27 PV cell modeled as diode circuit

The current load  $I_L$  is the photocurrent of the cell.  $R_{sh}$  and  $R_s$  are intrinsic shunt and series resistance of the cell, respectively. Usually the value of  $R_{sh}$  is very large and that of  $R_s$  is very small, PV arrays are built with aggregate an of parallel and series PV cells which are usually represented by simplified Equations as shown below:

$$I_{ph} = [I_{scr} + K_i(T - 298)] * \frac{\lambda}{1000} \quad 3.77$$

Saturation current reverses ( $I_{rs}$ ):

$$I_{rs} = I_{scr} / [\exp(qV_{oc}/N_s kAT) - 1] \quad 3.78$$

Saturation current  $I_o$  varies with the cell temperature, which is given by:

$$I_o = I_{rs} [(T / T_r)]^3 \exp[q * E_{g0}/Bk \{1/T_r - 1/T\}] \quad 3.79$$

The output current of PV module is:

$$I_{PV} = N_p * I_{ph} - N_p * I_o [\exp\{q * (V_{pv} + I_{PV} R_s)/N_s AkT\} - 1] \quad 3.80$$

Where  $V_{pv} = V_{oc}$ ,  $N_p = 1$  and  $N_s = 36$

### 3.8.1 Characteristic of PV Array

Unlike SG, PV panels do not have rotating parts and thus have no inertia. A Photovoltaic (PV) system's power output is not constant and fluctuates depending on weather conditions. This potentially causes a problem when the solar irradiance incident upon a PV plant changes suddenly.

From Figure 3.28 it can be seen that the ambient temperature increases, the power output of photovoltaic cells decline with the other conditions remain unchanged.

In Figure 3.29, other things being constant, the emerging power from photovoltaic cells increased when the intensity of the light strengthens. In particular light energy, there is a unique maximum output power for photovoltaic cells, called maximum power point. The above analysis shows that the power output of photovoltaic cells, with uncertainty, and changes in light intensity and ambient temperature. Based on this, PV arrays must maximize the adaption of control tracking maximum power, regarding environmental conditions (Ellis et al., 2012).

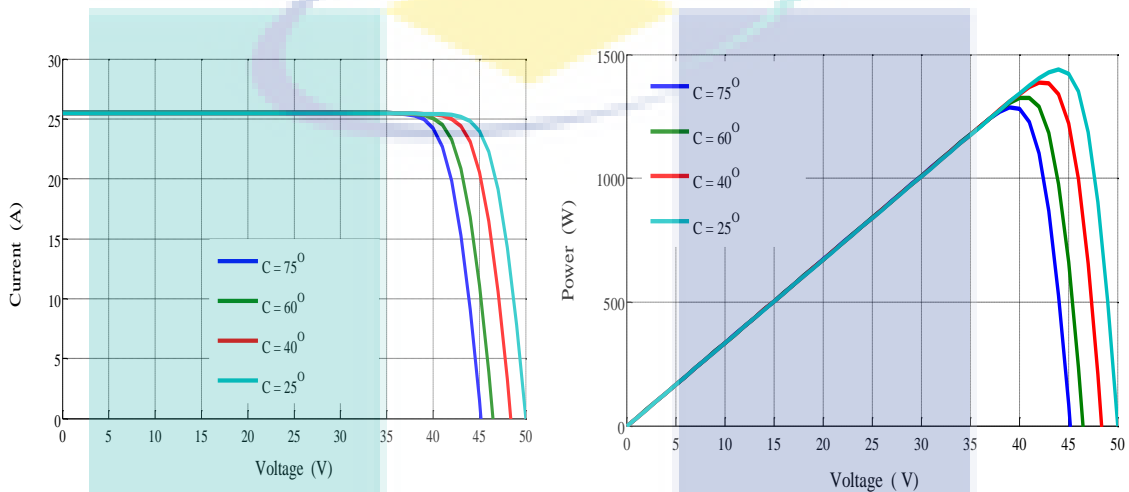


Figure 3.28 Output – I-V and P-V-characteristics with various temperature and constant irradianations

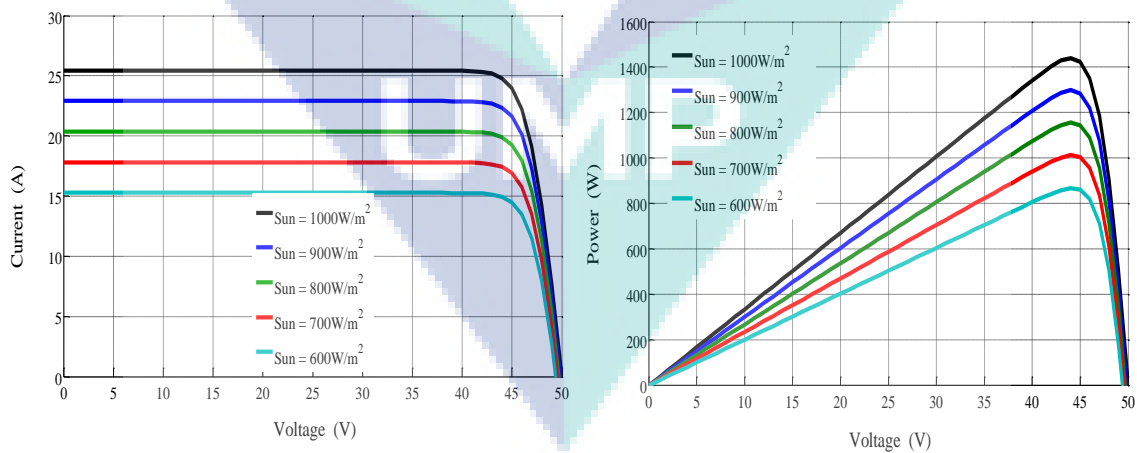


Figure 3.29 Output – I-V and P-V-characteristics with various irradianations and constant temperature

### 3.8.2 Maximum Power Point Tracking (MPPT)

Maximum Power Point Tracking (MPPT) is an electronic system that controls the Photovoltaic (PV) modules in a way that allows the module to generate all the power they can produce. A photovoltaic cell has a single point of operating at which the values of the current (I) and voltage (V) cells result in maximum power output. It is a challenge to control the PV array maximum power consistent on this point that many algorithms have been developed. In source side, boost converter connected to the solar panel to increase the output voltage. By varying the duty cycle of the boost converter, respectively, the source impedance matches the impedance of the load. Therefore, the existing Incremental Conductance (IC) method is employed in this work, which is has been widely used in PV inverter nowadays. Table 3.6 shows the parameters of PV solar the system applied in this research.

Table 3.6 Parameters of PV solar system

<b>Parameters of PV solar</b>	
Open circuit voltage ( VOC)	66 V
Short circuit current ( ISC)	25.44 A
Rated Power	530.5W
Voltage at Maximum power (V <sub>mp</sub> )	54.2 V
Current at Maximum power ( I <sub>mp</sub> )	23.25 A
Total number of cells in parallel (N <sub>p</sub> )	6
Total number of cells in series (N <sub>s</sub> )	36
Module operating temperature (TaK)	30 to 70C
Module reference temperature (TrK)	25C
Insolation/ Irradiation – (G / 1000)	1 kW/ m <sup>2</sup> = 1
Carrier frequency	2kHz
Maximum dc input voltage	331V

### 3.9 Battery Energy Storage Systems

Energy storage, in general, can be used to reduce the load on a grid temporarily by absorbing energy in times and discharging in times of high consumption (load change). At the same time, energy storage based on Lithium-Ion technology can switch fast from charging to discharging and vice versa by providing a high dynamic in power output (Schollhorn, 2012). The power of the battery is dissipating through a resistor, and simultaneously it is charged by a DC voltage source as shown in Figure 3.30 (Elbaz & Feliachi, 2012). The values of State of Charge (SOC) vary with change the value of

DC voltage source as a nominal voltage. If the DC voltage is higher than the nominal voltage of the battery, the SOC is kept the same, .i.e. (one). If the DC voltage is less than the nominal voltage of the battery, then SOC will decrease. The battery DC-DC converter should control the DC link voltage. Together battery and PV connected to the DC bus via a DC/DC converter respectively, and then interconnected to the AC grid via DC/AC inverter. Battery energy storage can charge and discharge to help balance the power between PV generation and loads demand. When the generation exceeds the demand, PV array will charge the battery to store the extra power; meanwhile, when the generation is less than the demand, the battery will discharge the stored power to supply loads. Each of PV system, battery energy storage system and the inverter has its independent control. Table 3.7 shows the parameters of battery used in this work.

Table 3.7 Parameters of Battery

<b>Parameters of Battery</b>	
No. of battery units	1
Nominal Voltage	256V
Capacity	6.2 Ah
Maximum Capacity	7 Ah
Discharge current	20A

Lithium Ion (LI) battery technology is amongst the famous battery storage technologies. Its applications are vast starting from hybrid electric vehicles, portable electronics, and grid storage applications. They are also environmentally friendly compared to other battery technologies such as the Nickel-Metal-Hydride. Hence, the battery unit in this work is selected to be Lithium Ion (LI).

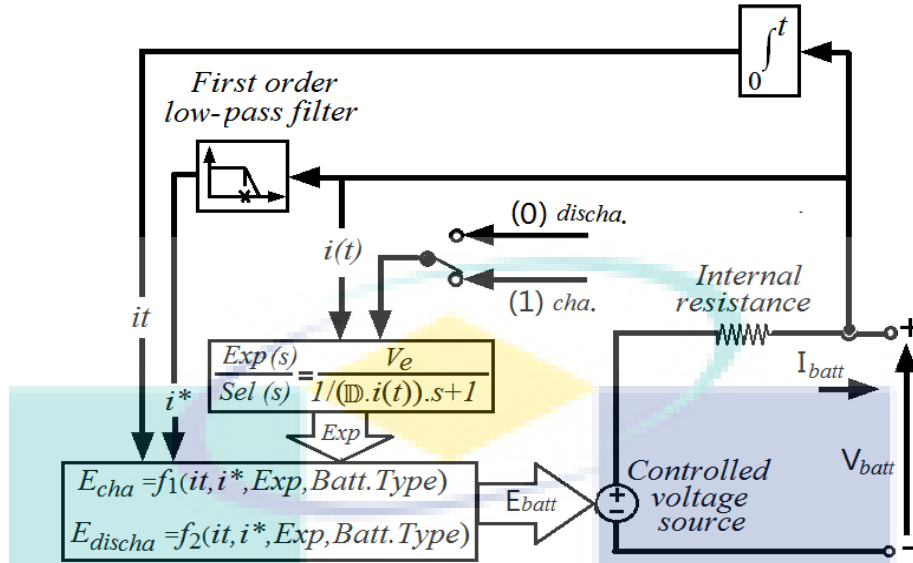


Figure 3.30 Battery model schematic diagram

The equivalent circuit of the battery is shown below: Lithium-Ion model, discharge model ( $i^* > 0$ ):

$$f_1(it, i^*, i) = E_0 - K \cdot \frac{\mathbb{B}}{\mathbb{B} - it} \cdot i^* - K \cdot \frac{\mathbb{B}}{\mathbb{B} - it} \cdot it + V_e \cdot \exp(-\mathbb{D} \cdot it) \quad 3.81$$

Charge model ( $i^* < 0$ ):

$$f_2(it, i^*, i) = E_0 - K \cdot \frac{\mathbb{B}}{it + 0.1 \cdot \mathbb{B}} \cdot i^* - K \cdot \frac{\mathbb{B}}{\mathbb{B} - it} \cdot it + V_e \cdot \exp(-\mathbb{D} \cdot it) \quad 3.82$$

$E_{batt}$  = Nonlinear voltage (V),  $E_0$  = Constant voltage (V),  $Exp(s)$  = Exponential zone dynamics (V).

$Sel(s)$  = Represents the battery mode, = 0 during battery discharge, = 1 during battery charging.  $K$  = Polarization constant (Ah-1) or Polarization resistance (Ohms),  $i^*$  = Low frequency current dynamics (A),  $i$  = Battery current (A),  $it$  = Extracted capacity (Ah),  $\mathbb{B}$  = Maximum capacity of battery (Ah),  $V_e$  = Exponential voltage (V),  $\mathbb{D}$  = Exponential capacity (Ah)-1.

From Figure 3.30, the battery is modeled as a controlled voltage source, and a resistance connected in series with the voltage source. The value of the controlled voltage source is dependent on the mode of operation (charge or discharge). Equations 3.81 and 3.82 represent the discharge and the charge voltages as nonlinear functions in

the above parameters. The parameters of the equivalent circuit can be modified to represent a particular battery type, based on its discharge characteristics. A typical discharge curve is composed of three sections, as shown in the Figure 3.31 and Figure 3.32.

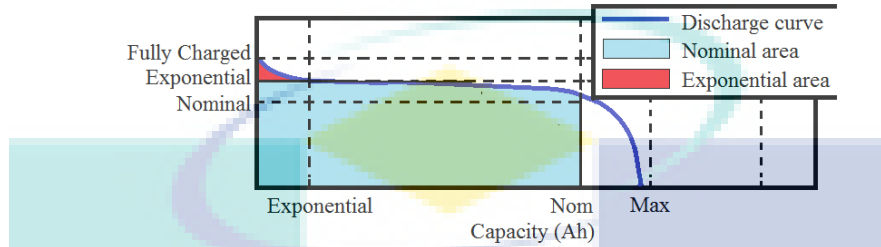


Figure 3.31 Characteristics discharge of lithium ion battery

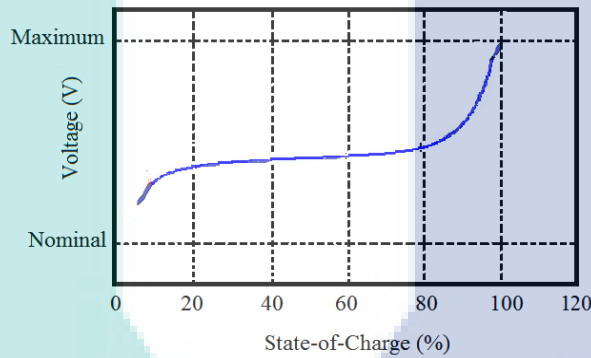


Figure 3.32 Characteristics charge of lithium ion battery

Nominal Voltage (V): The nominal voltage ( $V_{nom}$ ) of the battery (*volts*). The nominal voltage represents the end of the linear zone of the discharge characteristics.

Initial State-Of-Charge (%): The initial State-Of-Charge (SOC) of the battery. 100% indicates a fully charged battery and 0% indicates an empty battery. The SOC is calculated as:

$$SOC = 100 \left( 1 - \frac{1}{\mathbb{B}} \int_0^t i(t) dt \right) \quad 3.83$$

Maximum Capacity (Ah): The maximum theoretical capacity ( $\mathbb{B}_m$ ), when a discontinuity occurs in the battery voltage.

Fully charged Voltage (V): The fully charged voltage ( $V_{full}$ ), for given discharge current, note that the fully charged voltage is not the no-load voltage.

Nominal Discharge Current (A): The nominal discharge current, for which the discharge curve has been measured.

Internal Resistance: The internal resistance of the battery (*ohms*). When a preset model is used, a generic value is loaded, corresponding to 1% of the nominal power (nominal voltage \* rated capacity of the battery). The resistance is supposed to be constant during the charge and the discharge cycles and does not vary with the amplitude of the current. Capacity (Ah) at nominal voltage: The capacity ( $\mathbb{B}_{nom}$ ) extracted from the battery until the voltage drops under the nominal voltage. This value should be between  $\mathbb{B}_{exp}$  and  $\mathbb{B}_{max}$ .

Exponential zone [Voltage (V), Capacity (Ah)]: The voltage ( $V_{exp}$ ) and the capacity ( $\mathbb{B}_{exp}$ ) corresponding to the end of the exponential zone. The voltage should be between  $V_{nom}$  and  $V_{full}$ . The capacity should be between 0 and  $\mathbb{B}_{nom}$ . The grid-connected battery system is not much different from the PV system. The controls implemented in the battery system must maintain the voltage of the DC-DC converter at a desired level, and respond to a power signal to inject or absorb certain amount of power in order to provide regulation service.

### 3.9.1 Boost Converter

A boost converter comprises an inductor, switch, diode, and capacitor, as shown in Figure 3.33. Two modes can be divided scheme of the boost converter (Alsadi & Alsayid, 2012). First mode starts when the switch, SW is turned on at  $t = T_{on}$ . The input current that rises flowing through the inductor L and switches SW. In this mode, the energy is stored in the inductor. The second mode begins when the switch is off at  $t = T_{off}$ . Current flowing through the switch should now flow through inductor L, diode D, capacitor C and load R. Inductor current falls until it is switched on again in the next cycle. Energy accumulated in the inductor is transferred to the load. Thus the output voltage is higher than the input voltage, as in the Equation 3.84.

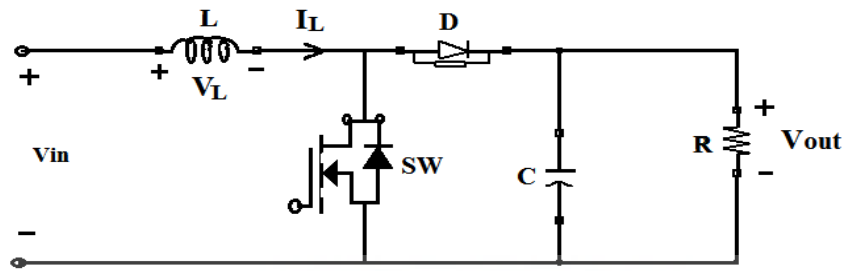


Figure 3.33 Boost converter

$$V_{out} = \frac{1}{(1 - D)} * V_{in}$$

3.84

Where  $V_{out}$  is the output voltage,  $D$  is the duty cycle, and  $V_{in}$  is the input voltage, which in this case would be voltage from a solar panel.

### 3.9.2 Phase Lock Loop for Inverter Synchronization

A Phase Lock Loop (PLL) system is used for various signal applications such as power electronic applications. A basic phase lock loop configuration is depicted in Figure 3.34, the phase voltages  $V_{gA}, V_{gB}, V_{gC}$  are obtained from sampled phase voltages. These stationary reference frame voltages are then transformed to  $V_d, V_q$  (in a frame of reference synchronized to the utility frequency) using  $\alpha\beta$  and  $dq$  transformation. The transformation  $\alpha\beta$  (Clarke transformation) allows to represent three phase system  $V_{gA}, V_{gB}, V_{gC}$  as two phase  $V_\alpha$  and  $V_\beta$ . The control in  $\alpha\beta$  frame has the feature of reducing the number of required control loops from three to two. However, the reference and feedback signals are in general sinusoidal functions of time.



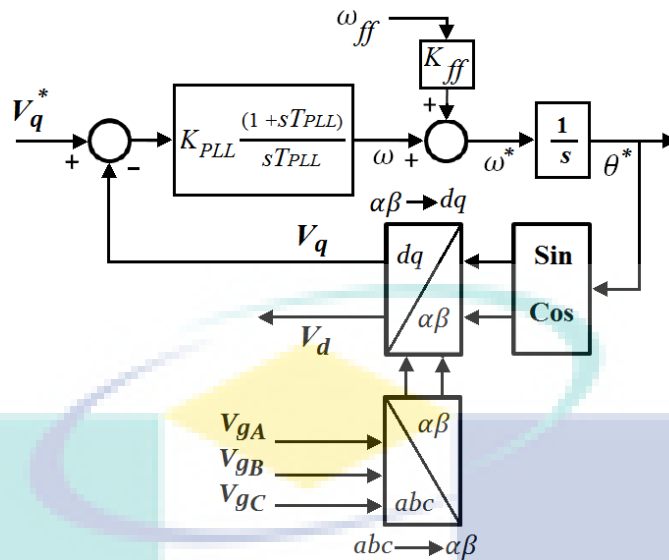


Figure 3.34 Block diagram of phase locked loop

Therefore, to achieve satisfactory performance and small steady-state errors in magnitude and phase, the compensator design is not a straightforward task. In  $dq$  frame (Park transformation) the signals assume DC waveform under steady-state conditions. This, in turn, permits the utilization of compensators with simpler structures and lower dynamic orders. Figure 3.35 shows the inverter's power stage including the voltage control loop scheme. The "Voltage Reference Generator" block computes the voltage references in  $dq$  by converting the inputs ( $V_{ref}$  and  $\omega_{ref}$ ) to a three-phase balanced signal than to  $dqo$  signals.

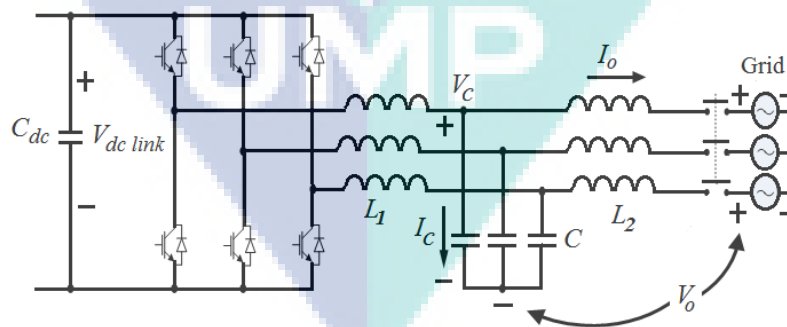


Figure 3.35 Schematic diagram of inverter-based microgrid

### 3.9.3 VSI Control Approaches

A PV panel generating DC and voltage require a power electronics interface for its connection to the grid. The inverter is an electrical power converter that changes

direct current (DC) to alternating current (AC). Inverters are commonly used to supply AC power from DC sources such as solar panels or batteries. In a Voltage Source Inverter (VSI) system the active power and reactive power can be controlled based on voltage-mode control. The primary role of the voltage controller is to regulate the inverter's output voltage when perturbations occur due to load and voltage reference variations. A PI-type controller has been chosen to get zero steady-state error and to provide a good, fast transient response with a good damping. The load voltage is regulated by a PI voltage regulator using transformation  $abc$  to  $dq0$  and  $dq0$  to  $abc$  on a set of three-phase signals as shown in Figure 3.36.

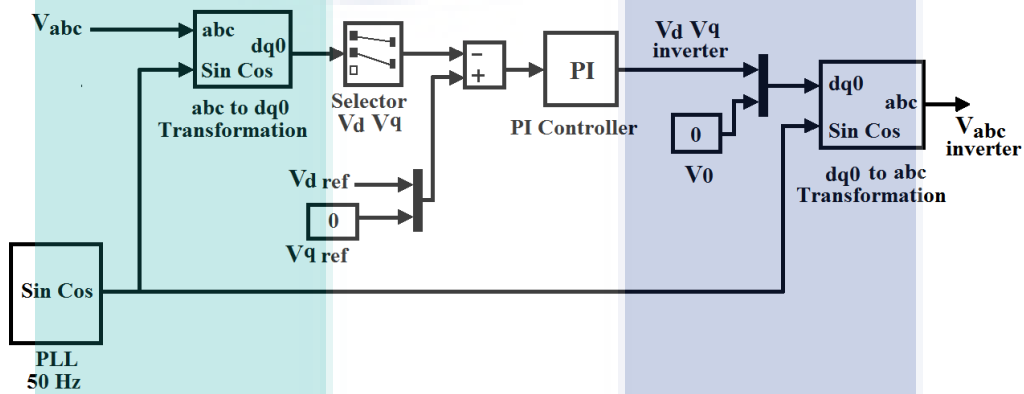


Figure 3.36 Schematic diagram of Voltage Regulator

It computes the direct axis  $V_d$ , quadratic axis  $V_q$ , and zero sequence  $V_0$  quantities in a two axis rotating reference frame according to the following transformation:

$$V_d = \frac{2}{3} (V_a \sin(\omega t) + V_b \sin(\omega t - 2\pi/3) + V_c \sin(\omega t + 2\pi/3)) \quad 3.85$$

$$V_q = \frac{2}{3} (V_a \cos(\omega t) + V_b \cos(\omega t - 2\pi/3) + V_c \cos(\omega t + 2\pi/3)) \quad 3.86$$

$$V_0 = \frac{1}{3} (V_a + V_b + V_c) \quad 3.87$$

$$V_a = [V_d * \sin(\omega t) + V_q * \cos(\omega t) + V_0] \quad 3.88$$

$$V_b = [V_d * \sin(\omega t - 2\pi/3) + V_q * \cos(\omega t - 2\pi/3) + V_0]$$

$$V_c = [V_d * \sin(\omega t + 2\pi/3) + V_q * \cos(\omega t + 2\pi/3) + V_0]$$

### 3.10 Power Sharing Droop

In a complex power system, when multiple DGs are attached to the MG, the power-sharing among them be made correctly with the help of a control strategy called droop control. Droop control also enables the system to disconnect smoothly and reconnect routinely to the complex power system. The role of droop control in power sharing is that it controls the real power by frequency droop control and it controls the reactive power by voltage control. The voltage and frequency can be manipulated by regulating the real and reactive power of the system.

When DGs operate in a hybrid micro-grid environment, there is a need for coordinated operation among the DGs, the utility grid and the loads. The control strategy adopted for the DGs connected to the network is droop control. Droop control ensures that the load needed to be served is shared by all the generators in the network in proportion to their generating capability. Another advantage of droop control where is adopted in this research, capability of simulation of synchronous generator behaviour to contribute power sharing towards stable operation.

#### 3.10.1 Power Sharing in Hybrid Micro-grid

The droop control strategy is typically utilized in rotating (synchronous unit based) interfaces of power sources. The P vs. f droop loop allows parallel interconnected generators to operate in an effective technique sharing variations in the load/demand in a pre-determined way without any allocate communication requires. Furthermore, the Q vs. V droop loop is used to reduce the circulation currents that would occur if the impedance between the generators and a common local load were not the exact same. As shown in Figure 3.10; the SG is connected to grid with the importance of grid impedance. The output power per phase is:

$$P = VI \cdot \cos\phi = \frac{E \cdot V_t}{jX'_d} \cos(\delta - \theta) - \frac{V_t^2}{jX'_d} \cos\theta \quad 3.89$$

In general,  $R \ll X'_d$ ,  $\therefore \theta \cong 90^\circ$  and  $jX'_d \cong X'_d$ . Hence the total output power is

$$P = \frac{3E'V_t}{X'_d} \sin\delta \quad 3.90$$

The real power delivered by the SG to the grid is:

$$P_e = \frac{E' * V_{bus}}{X_{eq}} \sin \delta \quad 3.91$$

From the synchronous generator, that active power has an enormous influence on the power angle, where the torque applied by the primary mover to the machine shaft. However, the reactive power has a large influence on the voltage difference by the voltage across the field winding of the synchronous generator. From the Swing Equation (3.15), that frequency is relative to the power angle, so by controlling active power, therefore frequency can be controlled.

$$Q = \frac{E' * V_{bus}}{X_{eq}} \cos \delta - V_{bus}^2/X_{eq} \quad 3.92$$

During load change both  $E'$  and  $V_{bus}$  are considered constant in the Equation 3.91. Thus  $P_e$  is a sinusoidal function of the machine power angle  $\delta$ . The real and reactive powers injected to the micro-grid with each unit can be mentioned as below (Guerrero, J. M. et al., 2007):

$$P = \left[ \frac{EV}{Z} \cos(\phi_1 - \phi_2) - \frac{V^2}{Z} \right] \cos(\theta) + \frac{EV}{Z} \sin(\phi_1 - \phi_2) \sin(\theta) \quad 3.93$$

$$Q = \left[ \frac{EV}{Z} \cos(\phi_1 - \phi_2) - \frac{V^2}{Z} \right] \sin(\theta) - \frac{EV}{Z} \sin(\phi_1 - \phi_2) \cos(\theta) \quad 3.94$$

Where  $V \angle 0$  = generation voltage taken as the reference phase,  $E$  is the amplitude of the unit output voltage,  $Z$  is the line impedance where  $|Z| = \sqrt{R^2 + X^2}$ ,  $\theta$  is the phase of the output impedance,  $\phi$  is the power angle.

### 3.11 Summary

One of the most critical parts of a micro-grid is the control system approach. The micro-grid can run in a grid-connected operation or islanded operation mode. The process of mode transition between the two modes needs to be smooth to ensure the micro-grid stability. This chapter discussed the proposed LFC using SG. The problem of the PI controller is high oscillation in output response. Employed MRAC controller with MIT rule solves this issue. However, MG still has a smooth transition problem, which is addressed by an NN technique together with tracking algorithm of MRAC.

Losing support of network grid power generation from micro-grid will cause high-frequency fluctuation where the conventional LFC capability is not sufficient to compensate the unbalance of generation and load demand. Worse yet the inertia of the system decreases when the MG is in island operation mode, which would decline system damping and cause instability of the system. In this section, an FLTC is proposed in islanded operation mode. The parameters 2-D lookup table of FLTC are updated through a breakpoint data mechanism and adaptation gain (a.g) using Interpolation-Extrapolation method, thus enabling to provide the desired power sharing and frequency control. The control algorithm is implemented in SG to guarantee the dynamic response of the MG among the distributed generators which would work the same way as the control of synchronous generators. The developments of the other components (PV array, DC-DC converter, and inverter) are also presented for showing the implementation of designing the hybrid micro-grid system.

## CHAPTER 4

### RESULTS AND DISCUSSION

#### 4.1 Introduction

This chapter is dedicated to present and discuss the results obtained. Several disturbances for verifying the proposed methods are carried out. The convincing results are obtained than PI controller that has shown the effectiveness of the proposed controllers. It is known that disturbances in the micro-grid system significantly influence the convergence rates of controller parameters. The main disturbance for speed rotor system is the varying load torque on the motor shaft, and it can be shown that convergence rates depend on disturbance and its dynamics. The transfer function which is taken to analyse is the first order system. So the physical realization for the hybrid micro-grid system under consideration is comparatively feasible and less complicated with mathematical modeling of MIT rule. The different output of the reference model  $y_m$  and the process output  $y$  is a tracking error of deviation output signal to desired path. This is an outer loop that needs to adjust the controller parameters, in which the error is targeted to minimize (Vargas-Martínez et al., 2015).

The MRAC implements a closed-loop controller which involves the parameters that should be optimized in order to modify the system response to achieve the desired final value. The adaptation mechanism adjusts the controller parameters to match the process output with the reference model output. The reference model specifies the desired (reference) output response that the system is expected to follow. Although there are different algorithms for designing MRAC, the MRAC in this research is designed using MIT rule method. The mathematical procedure of this method starts with the error equation ( $\mathcal{E}$ ). For a first-order dynamic system, the implemented MRAC scheme has two adaptation parameters: adaptive feedforward gain  $\vartheta_1$  and gain  $\vartheta_2$ . These parameters will be updated to follow the reference model. One of the main

limitations of an MRAC structure is its relatively weaker disturbances (load step change and fault) accommodation capability compared to an MRAC system in combination with other structures, (Vargas-Martínez, A. & Garza-Castañón, 2011). The integrates an MRAC with an ANN as a feedforward controller in order to control the rotor shaft speed of the SG in the hybrid micro-grid system to obtain a robust LFC structure. On the other hand, an ANN was selected as an additional controller because it has the capability of dealing with nonlinear system and it can be trained to follow the ideal trajectory.

This section of chapter presents the simulation results for the hybrid micro-grid behavior including SG as a DG unit in grid connected operation mode. The speed rotor control design based on PI controller adapt (API) by MRAC using MIT rule method. The performance of the SG is accessed via the LFC modal analysis stated in chapter three and validated using time domain simulations. Then, an Artificial Neural Network (ANN) controller is used to update the output of MRAC (API with ANN) and to enhance the hybrid micro-grid operation performance. The effectiveness of the resulting speed control to damp the frequency oscillation is tested under various big load changes suddenly by  $\Delta P_{ed}$ . The results are validated through simulations of the system's response for three different load changes. The comparison is carried out between the equipped API with ANN and API. The load-frequency control using API with ANN for SG control is shown in Figure 4.1.

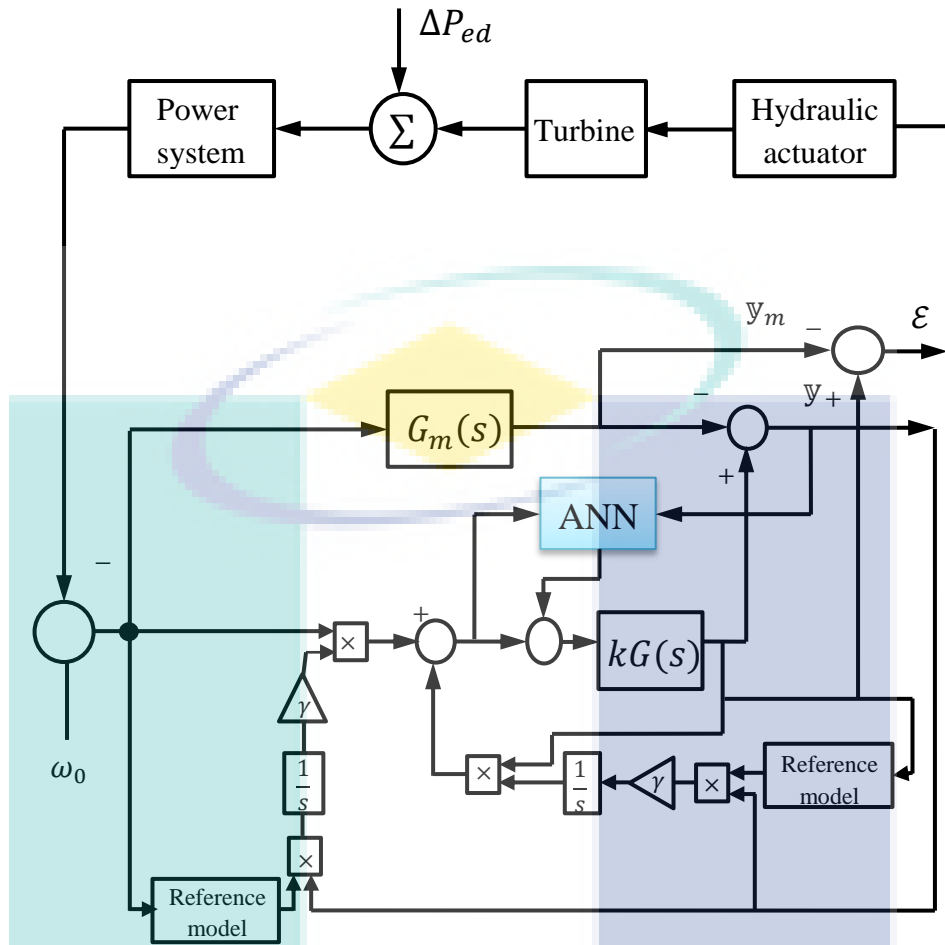


Figure 4.1 Block diagram of load-frequency control using API with ANN for SG control in grid connected mode

#### 4.2 Simulation Results in Grid –Connected Mode

In this study, Model Reference Adaptive Control (MRAC) with Massachusetts Institute of Technology (MIT) rules is proposed for a smooth transfer from grid-connected mode to island mode. In this method the control parameters are depending on the control of SG mainly. While PV, battery and an external grid and must be adapted to changing conditions. The demonstration of the capability of the SG to provide a good regulation of active power and frequency to meet the requirement of the loads is presented. The PV system is always working at the maximum power point, and the battery converter tries to control DC link voltage and limit maximum charge or discharge currents of the battery.

According to the IEEE STD 1547-2003, the island must be detected in less than 2 seconds, and the DG resource needs to be disconnected immediately from the



distribution network (Rostami et al., 2017). So, all results are facilitating in simulation and comparing the performance has been illustrated within 2 seconds.

#### 4.2.1 Performance of MIT rule Controlled Based API at Load Change

The objective is to control the speed of the SG under changing the load. The design procedure uses the transfer function obtained from Chapter 3. The generator turbine system has a governor, a turbine, and a load portion. The API based MIT rule controller is designed based on the algorithm mentioned in Chapter 3. The advantage of the API controller compared to a regular PI controller is that the controller automatically adjusts the gains under changing conditions of the controlled system. Adaptation gain can be chosen by the designer depending of the system; in this research adaptation gain is positive. The tests are done to shown the behavior of the API control loop on the SG when operating in grid-connected operation mode transition to islanded mode operation. A step load change is applied to API controller and API with ANN.

Figure 4.2 show the real model errors tracking reference model. It means that by API, the output of the plant follows the desired output, which is the main purpose of the control operation and can achieve better dynamic performance during sudden load change. In this design the range of adaptation gain is chosen from 5 to 25 for the system under consideration. It has been seen that the response is fast with increases value of adaptation gain. The effect of adaptation gain on output error ( $y - y_m$ ), the amount of error is continuously decreasing with the increment in adaptation gain.

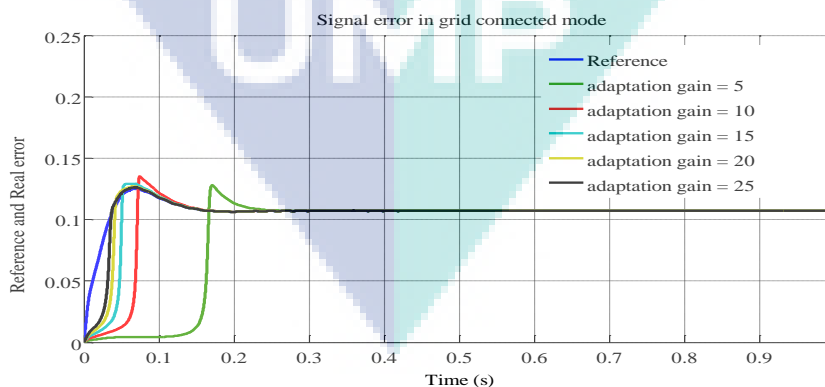


Figure 4.2 Performance of real model tracking reference model with different value of adaptation gain in real model for API

By API, response characteristic of real model tracking reference model at adaptation gain = 25 for load increases 30%, 40% and 50% respectively at time  $t=1s$  are shown in Figure 4.3. In application of API based MIT rule, the transient performance in terms of the tracking error and control signal, the overshoot ratio for variation of signal error are (13.013%, 13.664% and 13.968%) and the settling time are (1.25s, 1.27s and 1.29s).

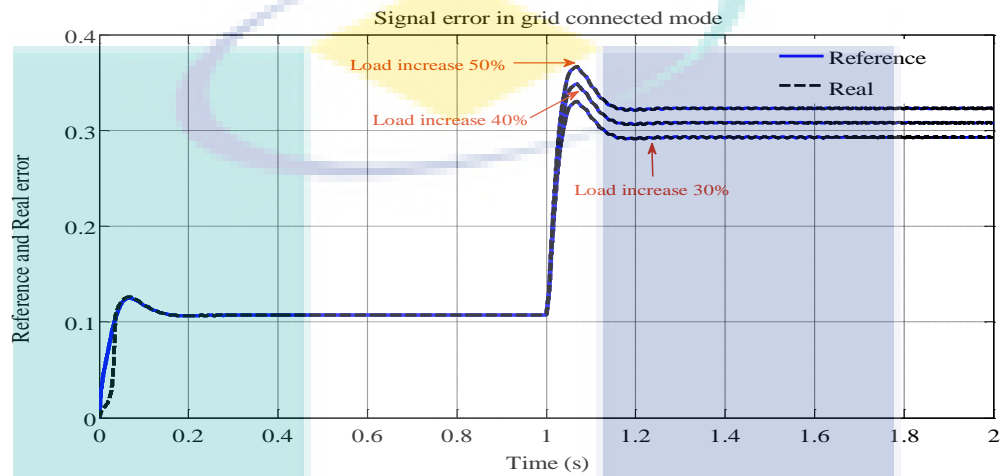


Figure 4.3 Output response characteristic of real model tracking reference model in API control for adaptation gain = 25

Figure 4.4 shows the response of API in a hybrid micro-grid system based MIT rule for adaptation gain =25. The response characteristic in (a) is same of response characteristic in Figure 4.2. It is clear that there is an oscillation during load change at time =1s (b) 30%, (c) 40% and (d) 50% respectively and that the system response is considered poorly controlled for these cases. The tracking of real model to reference model is decreased during sudden load change and separate grid utility from system. Before load increases (from  $t=0s$ ) the real model tracking of model reference the variation of error is 0.107 as shown in Figure 4.4 (a). A large oscillations occur at the output signal after load change 30% at  $t=1.65s$ , the variation of error signal reach to 0.293 as shown in Figure 4.4 (b). From Figure 4.4 (c) after load change 40% at  $t=1.56s$ , the variation of error amount to 0.308. For  $t=1.48s$  in Figure 4.4 (d) after load change 50%, the variation of error arrived to 0.323. The system performance is going to high oscillatory and the system response is unstable due to the low speed response of SG.

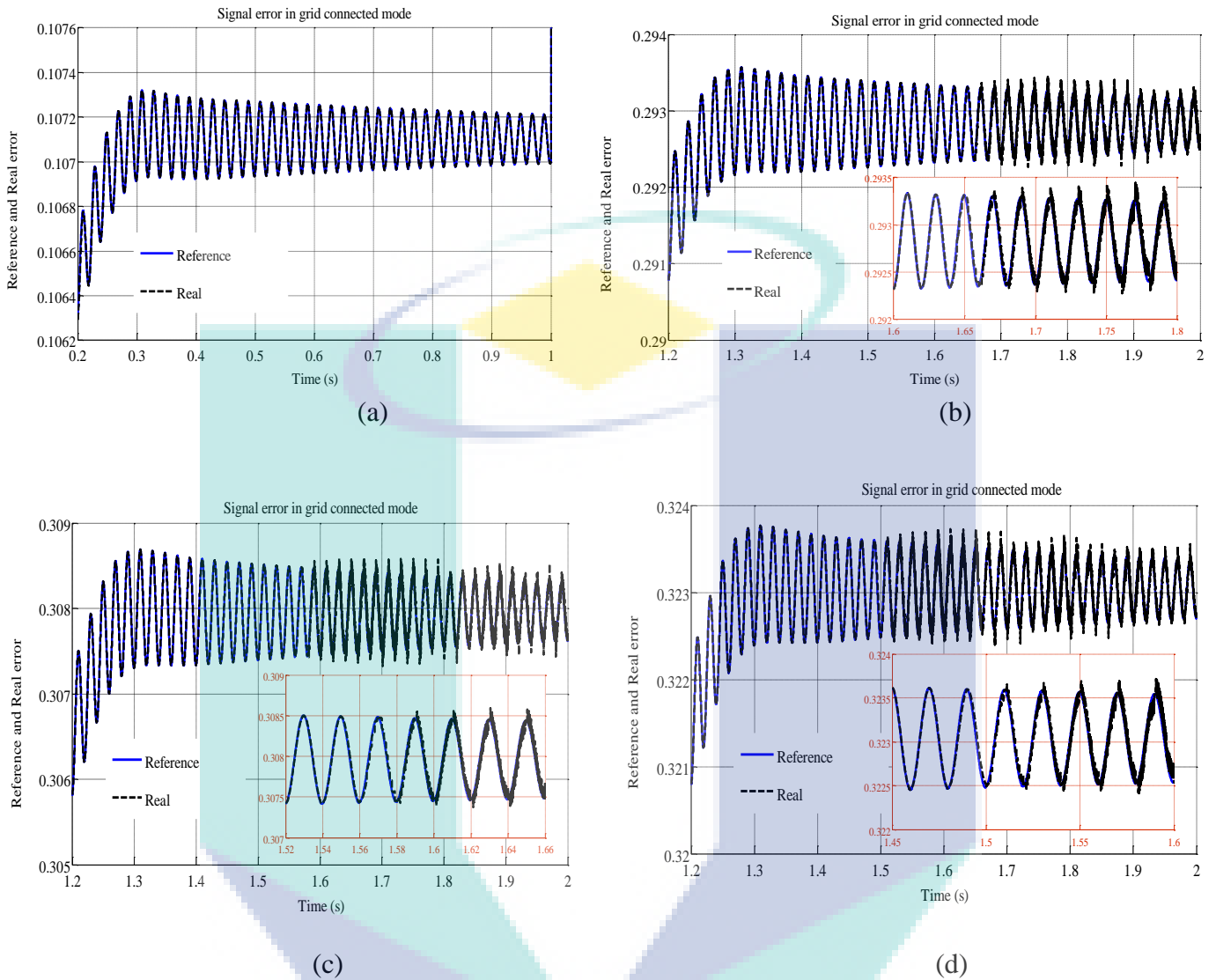


Figure 4.4 Performance of real model tracking reference by API control: (a) Output response error, and load change in (b) 30%, (c) 40% and (d) 50%

#### 4.2.2 Performance of API with ANN at Load Change

Unlike the API controller that was proposed previously, this controller shows after the initial transients oscillations, which is still not fully smooth. As tested in this research, the results showed that the API with ANN provides good damping over a wide operating range and improves the performance of the micro-grid system. Every system gives its best for the limited range of the adaptation gain. From Figure 4.5, the range of adaptation gain is chosen from 5 to 25. In both cases of API and API with ANN, it is observed that if adaptation gain increases, the time response of the system also improved for the chosen range of adaption gain. Furthermore, the system is stable

in the upper range. For this value of adaptation gain, the overshoot is less when compared with other values of adaptation gain with minimum settling time response. So, with suitable value of adaptation gain API and API with ANN, the output can be made close to reference model. It can be concluded that the performance using ANN is better than the API without ANN.

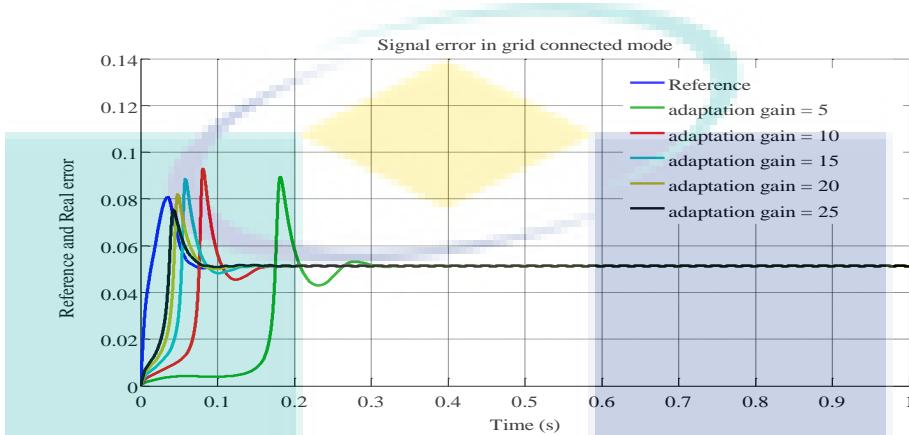


Figure 4.5 Performance of real model tracking reference model with different value of adaptation gain in real model for API with ANN

API with ANN is shown in Figure 4.6. The real model followed the reference model and responded satisfactorily. By implemented of API with ANN , the transient performance is improved appropriately compared with API for the tracking error and control signal, the overshoot ratio for variation of signal error are (7.913%, 8.219% and 8.441%) and the settling time are (0.125s, 0.126s and 1.28s).

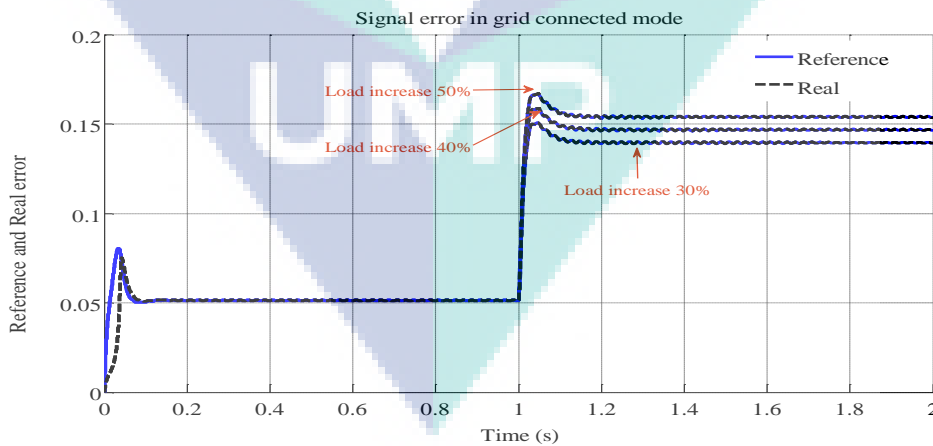


Figure 4.6 Output response characteristic of real model tracking reference model in API with ANN control for adaptation gain = 25

Figure 4.7 compares the signal error and load set change for the proposed method, following step load increase in control system. A combination of API and

ANN has been used as shown that the proposed API with ANN can be stabilizing the system and achieve good tracking performance. The proposed controllers track the load changes and meet the robust performance without oscillations occur compared to the same simulation case of API controller in Figure 4.4. Consider the design of API with ANN fictitious controlled output in the SG control framework adds enough flexibility to set the desired level of performance. The system follows closely the reference model output the response characteristic in Figure 4.7 (a) is same of response characteristic in Figure 4.6. In Figure 4.7 (b) at time  $t=1s$  load change 30%, the error reduced near zero, for adaptation gain is set to  $\gamma=25$ . In application of API with ANN, the load can be changed up to Figure 4.7 (c) 40% and Figure 4.7 (d) 50%, the output error is improved compared to API control approach. Before load increases (from  $t=0s$ ) the real model tracking of model reference the variation of error is reduced to 0.051 as shown in Figure Figure 4.7 (a). Without oscillations occur at the output signal after load change 30% at  $t=1s$ , the variation of error signal decrease to 0.139 and for 40% load increase the variation of error arrived to 0.147, while in case of 50% load change the variation of error reach to 0.154 as shown in Figure 4.7 (b),(c) and (d) respectively. Moreover the error is reduced by API with ANN control, indicates an improvement in transient in SG in comparison of previous API controller.

The logo for UMP (Universitas Muhammadiyah Palembang) is a large, stylized letter 'U' composed of several overlapping triangles in shades of teal and light blue. The letters 'UMP' are printed in a bold, white, sans-serif font across the center of the 'U' shape.

UMP

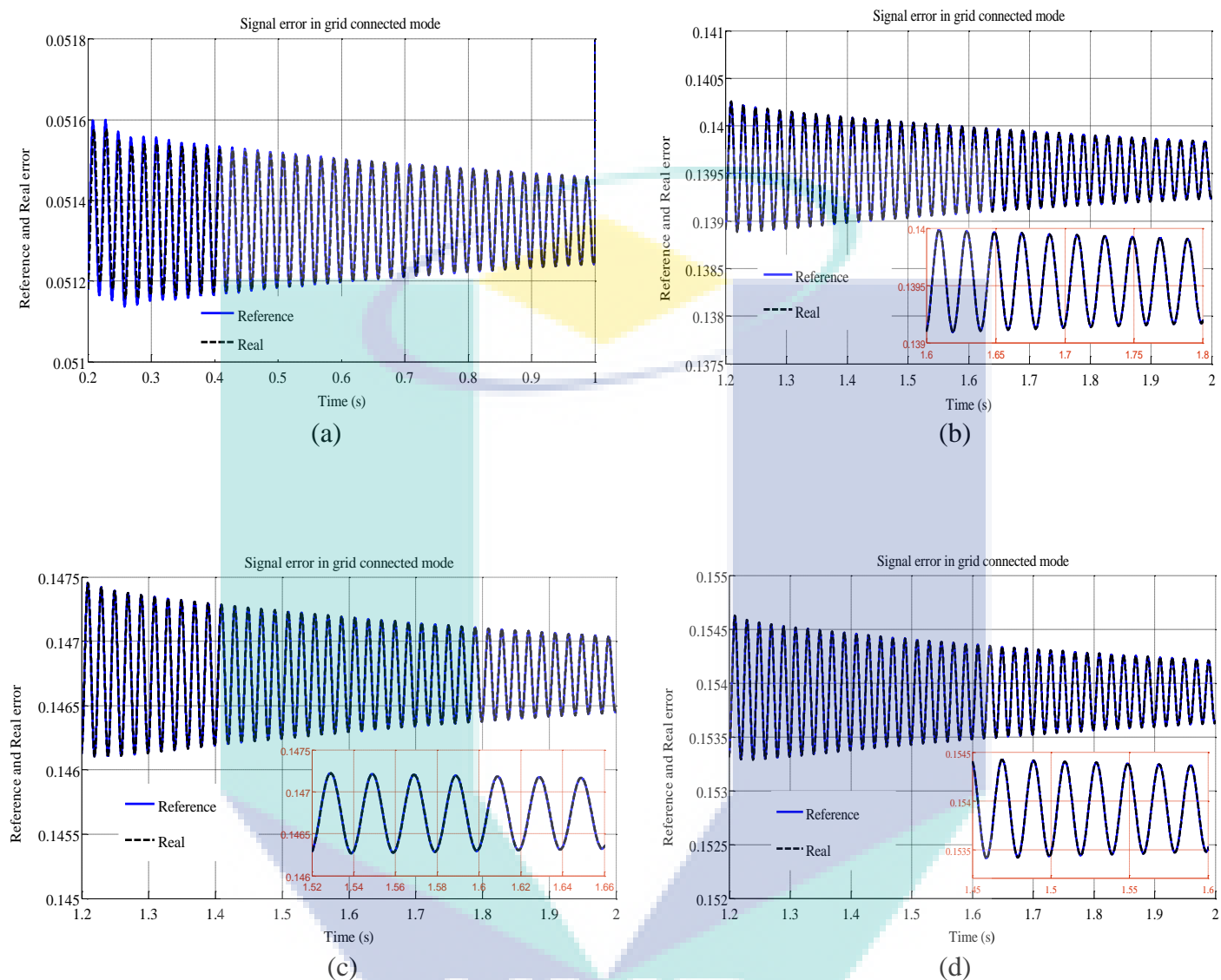


Figure 4.7 Performance of real model tracking reference model by API with ANN control : (a) Output response error, and load change in (b) 30%, (c) 40% and (d) 50%

The proposed API with ANN control improves the SG dynamic by eliminating the oscillations. One can conclude that by improving the response of real model and making it as close as possible to the reference model, the whole system dynamics is improved reducing the overshoot and the oscillations. Note that the system become is stable when the API with ANN control loop is implemented for different values load step occurs.

From Figures 4.2 and 4.5, Figure 4.8 shows the performance of two methods control for peak variation of error with different time response and overshoot signal specifications. It can be observed that the reference model is difference between these two methods due to the input control is provided by the combination of the output of traditional MRAC and the output of NN. By update the weights of ANN which takes the values output of the previous plant and tuned according to close loop during continues of the learning process. This lead to change reference model in synchronization with disturbance occur. Thus the second objective of this research can be achieved and enhance the tracking between grid connection to island mode in hybrid micro-grid system. The range of adaptation gain is chosen from 5 to 25 for both API and API with ANN controllers. So, for a suitable value of adaptation gain in API with ANN can make the plant output as close to the reference model. It can be seen that proposed method API and API with ANN both exhibit tracking its reference model.

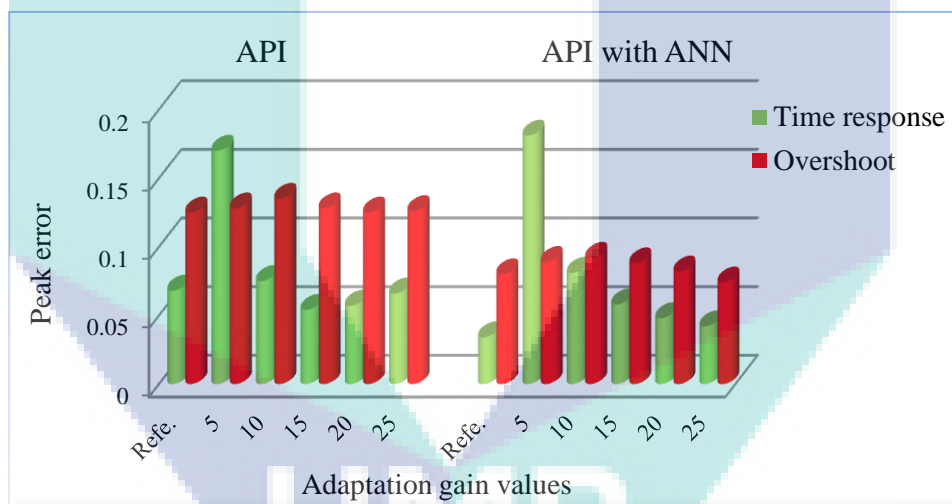


Figure 4.8 Comparing the performance of two methods control for different adaptation gain values

#### 4.2.3 Performance of SG at Load Change

When connected to the main grid the active and reactive power that is generated is balanced with the consumed power by the loads of both Micro-grid and main grid with line losses. When the Micro-grid is disconnected and in islanded mode, the active and reactive power needs to be controlled by the DG units. This is conducted through voltage and frequency control of one or more of the DGs which regulate the power sharing within the Micro-grid, to avoid circulating current among DG units (Wilson,



2015). In this research, the power sharing among parallel DGs as described in section 3.10.1. This allows the SG to dampen the fast effects of changing loads, increasing the stability of the system. In grid-connected, load changes are frequent and significant concerning the rated capacity of the system. Load changes are an unpredictable inevitability. Therefore, stable responses to positive load change in grid-connected mode are instrumental to a reliable micro-grid. Almost immediately after transient, change the load distributed over all sources proportional to the impedance of the coupling between the change of load and each source. This causes drastic changes in output from a primarily fixed power source that needs to be appropriately counteracted to maintain its safe operation. However, by maintaining constant power locally, the entirety of additional load is shifted to the other sources in the micro-grid. The load will be changed in grid-connected configuration, and the SG source will maintain its power output as no other source limits are encountered.

The performance of the SG in hybrid micro-grid system using the robust API with ANN controllers in comparison of designed PI and API controllers are tested for the various load disturbances. In the case of load sharing has been illustrated in Figure 4.9 and Figure 4.10, respectively. The figures exhibit that the active and reactive power injected by proposed controller has a good transient response and performance, which is obtained due to speed control feature.

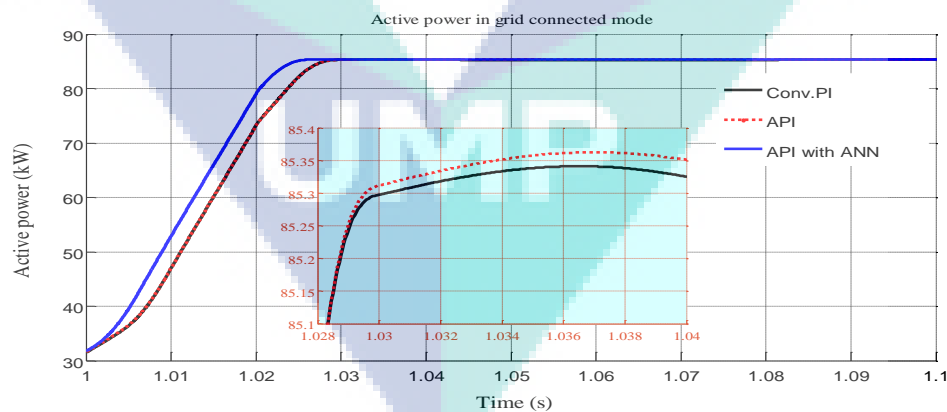


Figure 4.9 Active power response of SG following a step change increase in load

In order to demonstrate the effectiveness of the proposed control strategy, some simulations were carried out. Figure 4.10 shows the transient reactive power by SG. The transient response after application of proposed controllers has improved



significantly, and a proper reactive power sharing has been achieved with load increased 30%.

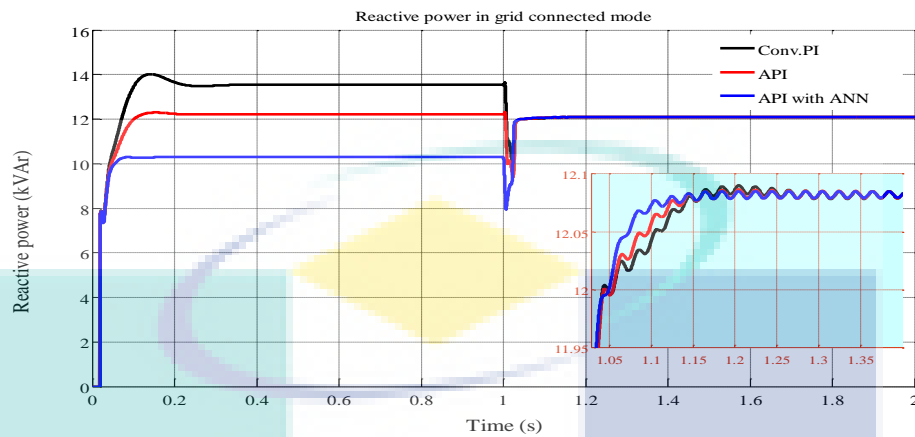


Figure 4.10 Reactive power sharing performance by SG using three different controls following a step change increase load

From the SG view point, torque applied by the prime mover to the shaft of the machine. The torque applied controls the speed of the shaft affecting the frequency of the power generated by the machine, and hence, the active power generated by the SG (Bhaskara, 2012).

Refer to Figure 4.11 and Figure 4.12, SG and the main grid supply active and reactive power respectively, after the synchronization for micro-grid is disconnected from the main grid at  $t=1s$ , the power of main grid dropping to zero. It is evident that SG starts supplying the real power after the synchronization. To test the effect of load change with the proposed method, the load increased about 30%, lead to close STS and grid disconnect. The system's smooth synchronization can be achieved in grid-connected mode operation. After the grid utility is isolated, the SG active power increased. Apparently the control system responded to the frequency error signal and increased the power from the generator unit to the approximately amount that is generated by the utility. It shows the constant active load power changes from the lower to the higher real power, most of the extra power supplied to meet the demand is from the SG. It shows the output of active power has no evident fluctuation during this disconnection. Subsequently, another test of load variation is performed (40%, 50%) to confirm the previous analysis. It is noted that the results of this additional cases for active and reactive powers have been plotted in one figure for brevity.

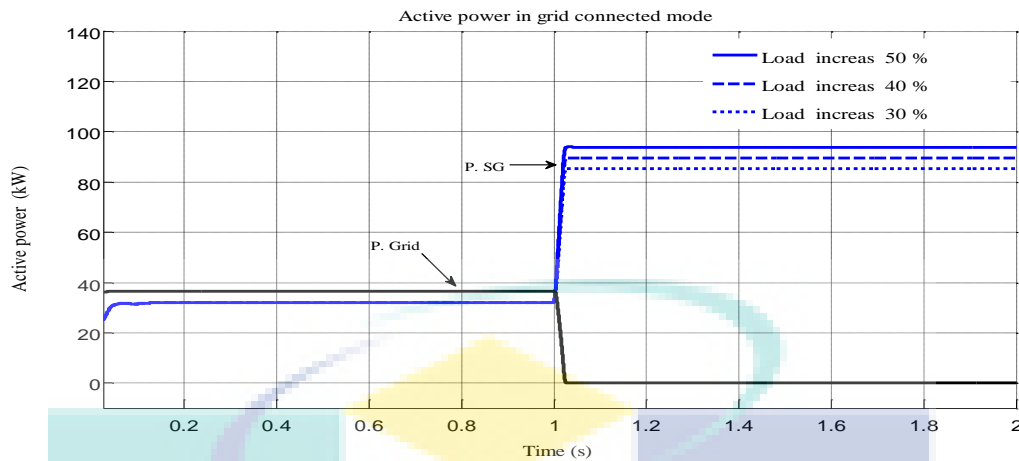


Figure 4.11 Active power share load by SG and grid

When the micro-grid transitions from grid connected mode to islanded mode, MC changes from constant power mode to droop mode. Depending on how much power was commanded from the DGs in the system, the field voltage controls the terminal voltage, and hence, the reactive power generated by the machine (Bhaskara, 2012). As shown in Figure 4.12, the reactive power output response of SG shows the event at  $t=1s$  where the grid is disconnected because of sudden changes in load. It is evident that the SG supply reactive power is required during grid-connected mode as a compensation to the disconnect event, most reactive power was produced from SG for use of the hybrid micro-grid.

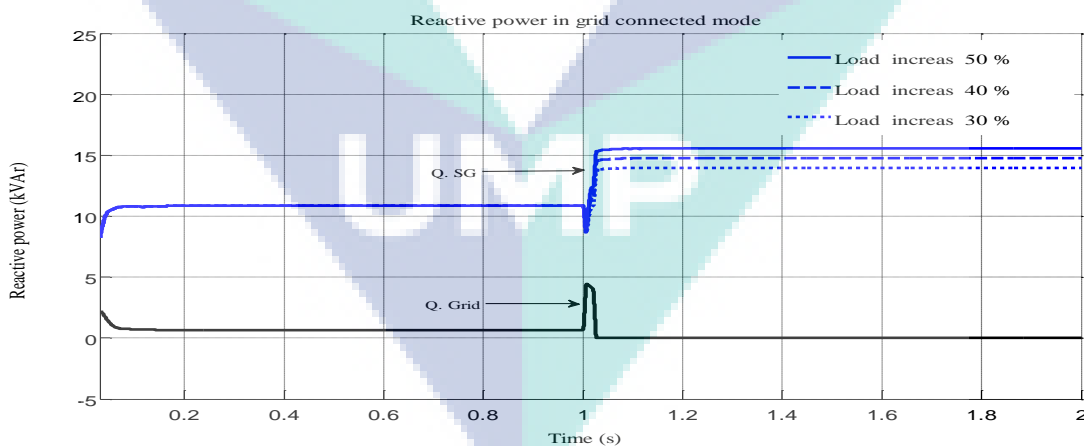


Figure 4.12 Output reactive power of SG and grid

For the conventional controller, at normal operating, the system frequency is almost 50Hz. However, if an event that causes generation-demand imbalance occurs, frequency begins to drop with frequency rates, depending on the amount of inertia and unbalanced power of the system as given by the Swing Equation (3.15). In other words

before the load change, the engine torque and torque load are equal (i.e.,  $T_m$  equals  $T_e$ , the accelerating torque  $T_a = 0$ , neglecting losses). However, after applying a step load change to the generator, the net torque becomes negative (i.e.,  $T_m - T_e = < 0$ ), resulting in a decrease in the speed (frequency) of generators.

Before starting the controller and for the inertial response, the SG releases the kinetic energy stored in the rotating mass which continues for (1.07s in this work). After that, when the frequency deviation exceeds a certain value, the primary frequency controller will be activated immediately. This controller returns the frequency to save the value within (1.09s in this work) using the governor of the generator. Figure 4.13 shows the simulation of the conventional PI controller.

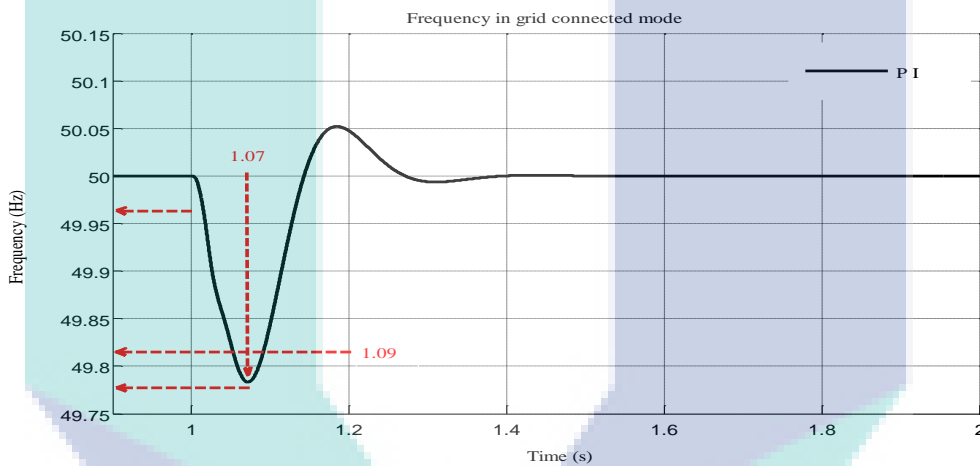


Figure 4.13 Time frames included in the micro-grid system frequency response in conventional PI controller

From sections 3.4.1 and 3.4.2, frequency– power relation for a turbine governor controls a SG which is connected to a load. The shaft torque has to be used to control the synchronous machine such that the machine serves the load at nominal frequency. According to the LFC, Equations (3.15), (3.16) and (3.17) can be used to calculate the commanded shaft speed. They also represent the base speed of the machine. The variation of speed with the active power generated by the machine can be represented by a straight line according to Equation (3.1). Note that at no load, the machine operates at rated speed. Once the machine starts to serve load the speed starts decreasing. Figure 4.14 shows frequency response with load application from no load to full load where the dead time is 0.02s. At time  $t = 1s$ , the step load change by increasing 30%, the figure shows the fluctuation of frequency in different control

methods PI, API and API with ANN controller. The effectiveness of third control approach is outperforming others. It is evident that frequency deviation and time response in the third case is better than the other two cases.

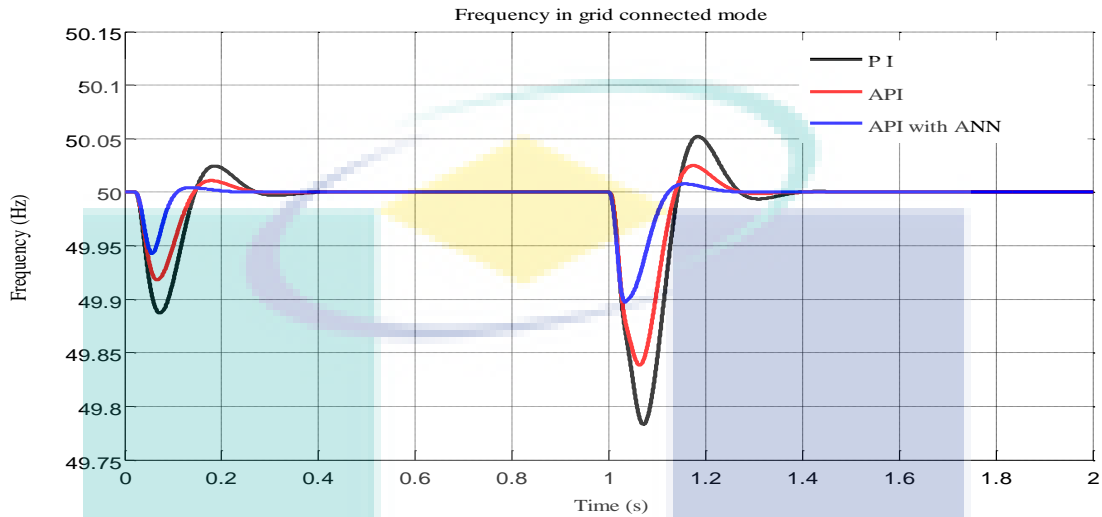


Figure 4.14 Step response of frequency at operation and load change 30% with different control

Figure 4.15 illustrates that the error of frequency at operating the micro-grid system. It can be seen that the deviation is far better for the proposed (API with ANN) controller method, which is the respond quickly improve the frequency response. The adjustment can be made steadily in relatively short period.

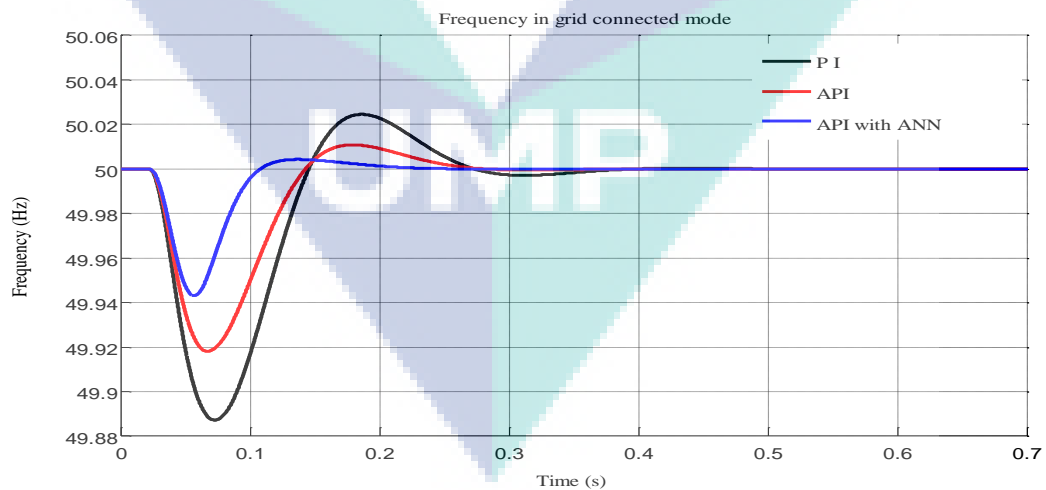


Figure 4.15 Step response of frequency at steady state

During grid connected mode the objective is to develop the LFC of SG. Figure 4.16 demonstrates the disturbance property of the closed loop system. This figure shows the frequency deviation at SG in control micro-grid, following a step disturbance of

load increase 30%. In the case of conventional PI controllers, the frequency drops about 0.22 Hz, and the overshoot reached about 0.05 Hz at time  $t = 1$  second. In the case of API, the frequency decreases about 0.16 Hz, and the overshoot reached about 0.02 Hz. The controller designed based on ANN which could efficiently regulate frequency and minimize the error, in this case the frequency drops about 0.1 Hz only, and the overshoot is 0.01.

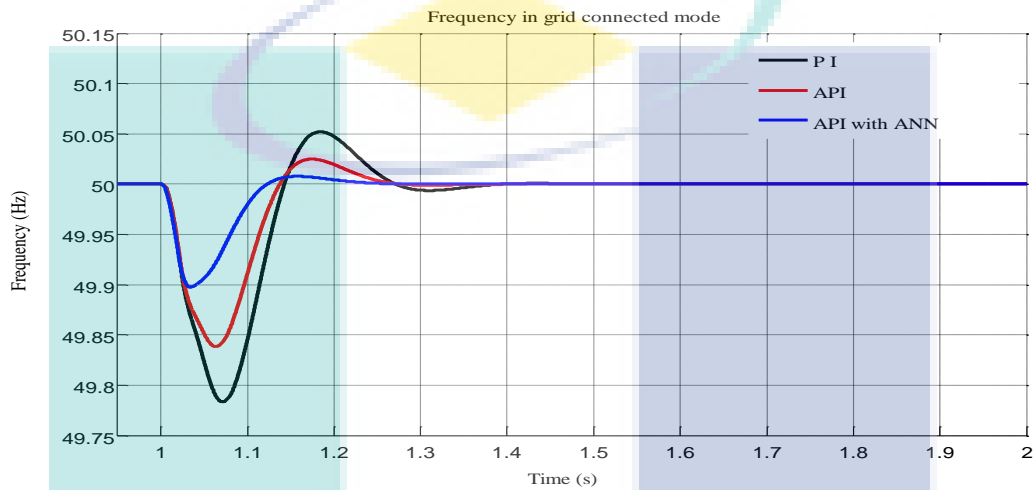


Figure 4.16 Frequency error at transient load change 30% and grid disconnect with different controller

During grid connected mode and islanded mode it can be noticed that all DGs are operating at the same voltage. Figure 4.17 shows voltage and current of phase “a” at the load side, during increased load 30% at  $t = 1$  second, the change in the current at first cycle.

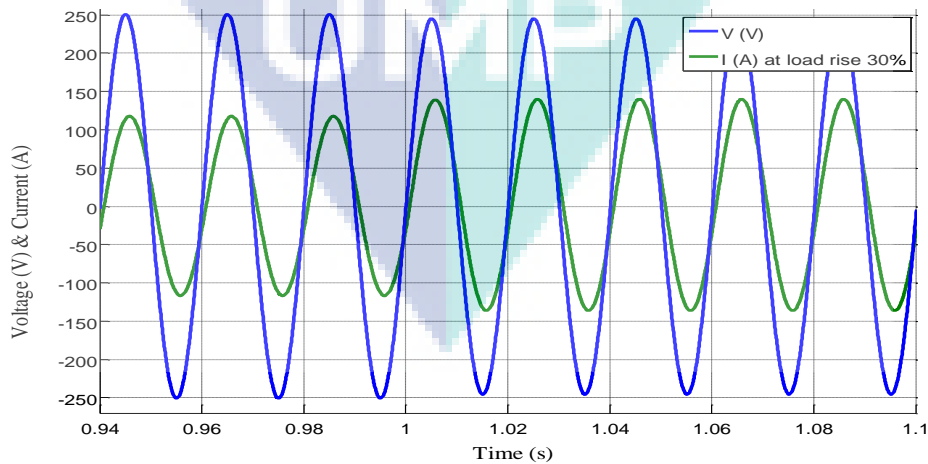


Figure 4.17 Voltage and current of phase "a" at load increase 30%.

In most reported robust LFC approaches, only one single norm is used to capture design specifications (Hassan Bevrani, 2004). For current research, the control against different load change more naturally can be addressed by MRAC and ANN approach and it is more useful for holding closed-loop stability and formulation of control constraints. It is shown that using the combination of API with ANN allows better performance for a control design problem. In Figure 4.18, the result shows that this proposed approach of (API with ANN) during load change 40%, has a significant improvement in controlling the frequency of micro-grid. Frequency response is achieved for the transition from grid-connected mode to an autonomous mode of system operation with less than overshoot and fast settling time.

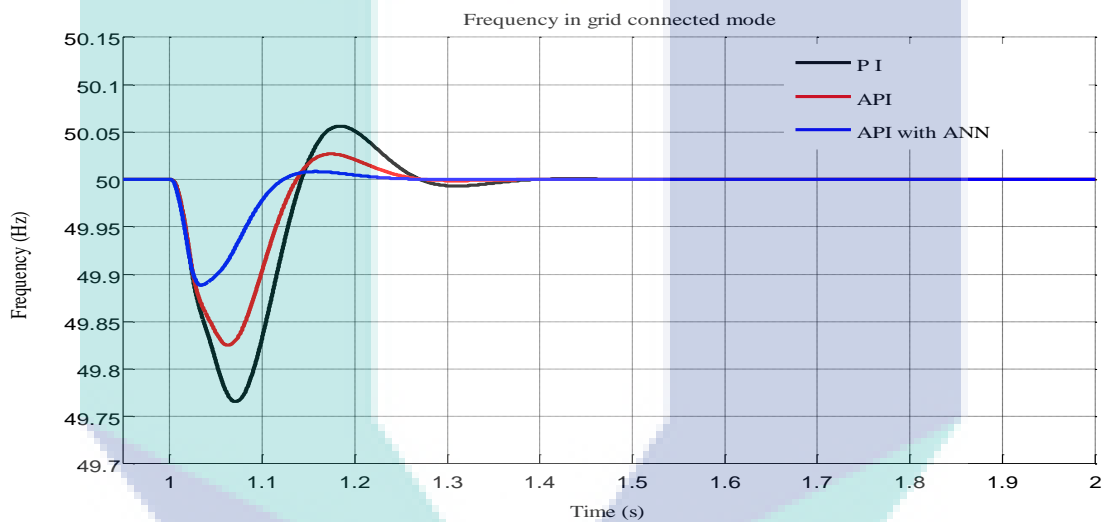


Figure 4.18 Frequency error at transient load change 40% and grid disconnect with different controller

Figure 4.19 shows the voltage and current of phase "a" over the transient period. The current sharing in desired ratio when load increase 40% at  $t=1s$  and balanced voltages even after change in the load indicate a stable operation.

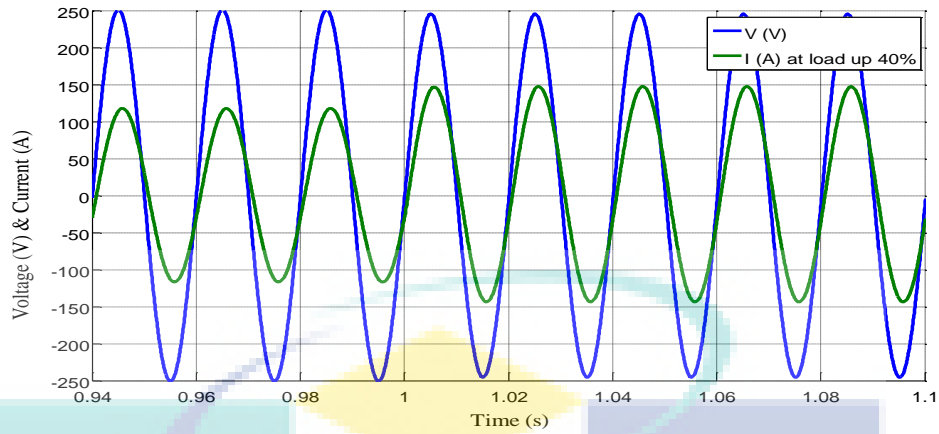


Figure 4.19 Voltage and current of phase "a" at load increase 40%

The performance of API with ANN proves the efficiency of the control strategy to enhance system stability while keeping the frequency at nominal value. It can be noticed that the API with ANN method performs adequately, reducing the deviation of frequency significantly at load change 50%, which is shown in Figure 4.20. This figure presents the frequency deviation and corresponding control action signal effectively, following a large step disturbance where represents three controllers methods. In the proposed API with ANN for LFC present a flexible enough to set a desired level of performance to cover the practical constraint on a control action signal. It is easily carried out by tuning the considered weighting functions as in section 3.6.2.1 and Equation (3.1).

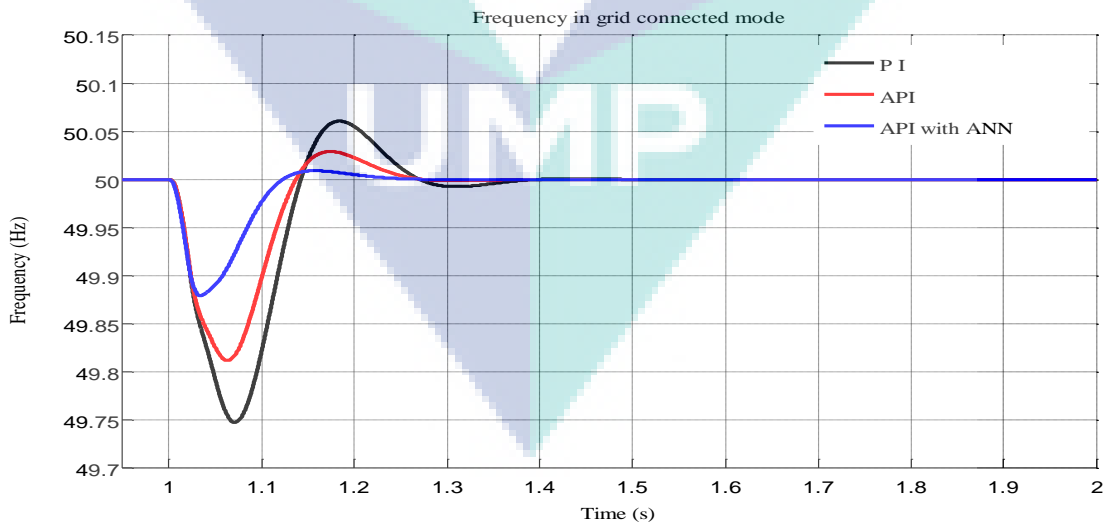


Figure 4.20 Frequency error at transient load change 50% and grid disconnect with different controller

Figure 4.21 show the voltage and current of phase "a" at the load side in the micro-grid under the transient period of the load increase 50%.

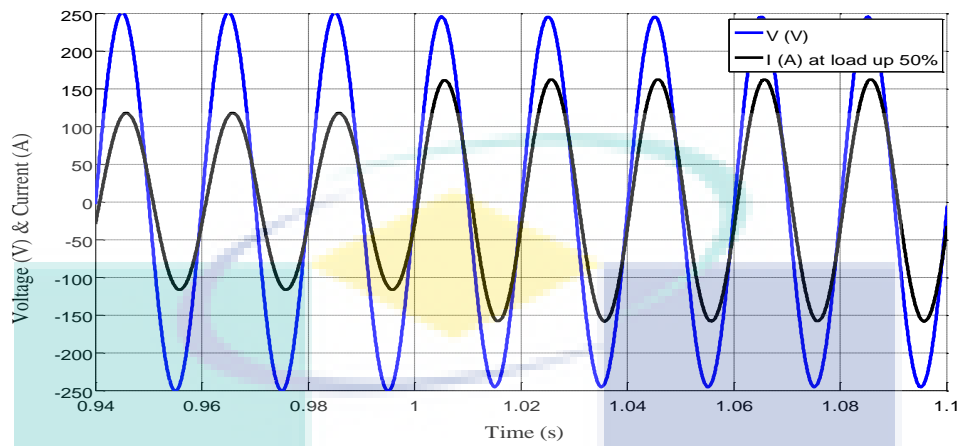


Figure 4.21 Voltage and current of phase "a" at load increase 50%

The speed rotor of synchronous generator is shown in Figure 4.22, illustrating the diverse control used and variance in the response of speed rotor dynamic from the initial operation and disconnection of grid from micro-grid system obtained using API with ANN. By load change 30%, it can be observed that it is completely smooth the transfer from grid-connected to island mode without overshoot or fluctuation in response time. The control system is improved significantly with ANN-based NARMA L2 controller.

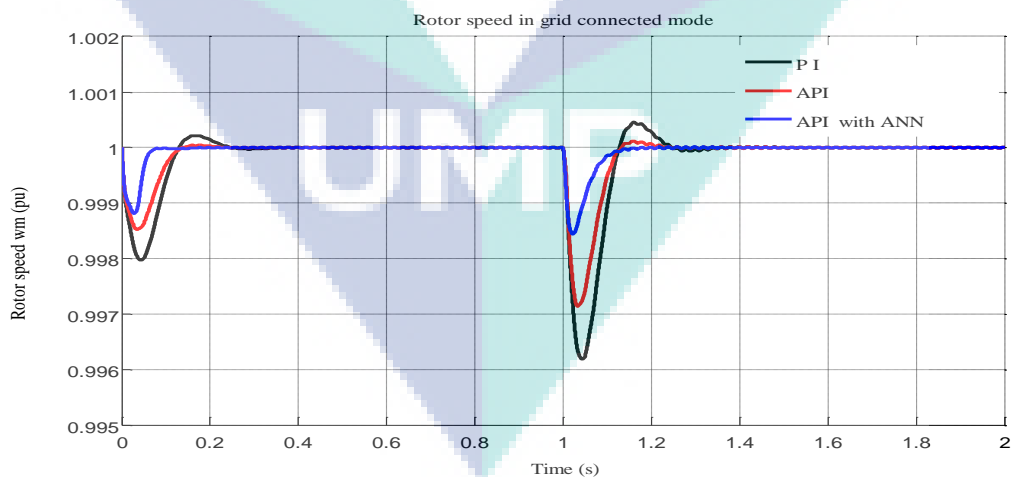


Figure 4.22 Rotor speed variation with different control at load change 30%

Rotor speed operation, comprising a conventional PI, API controller and API with ANN is shown in Figure 4.23.



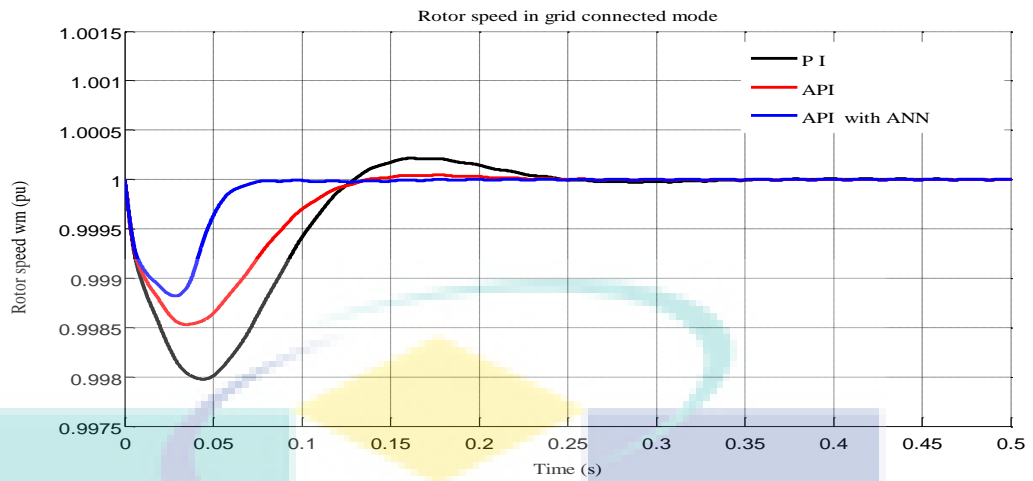


Figure 4.23 Rotor speed at step operation with different control

From the simulation results during load change 30%, it is found that in case of API and API with ANN achieve satisfactory performance of output speed response. The transient performance of SG at steady-state for step speed rotor in terms of overshoot and settling time are improved, as seen in Figure 4.24.

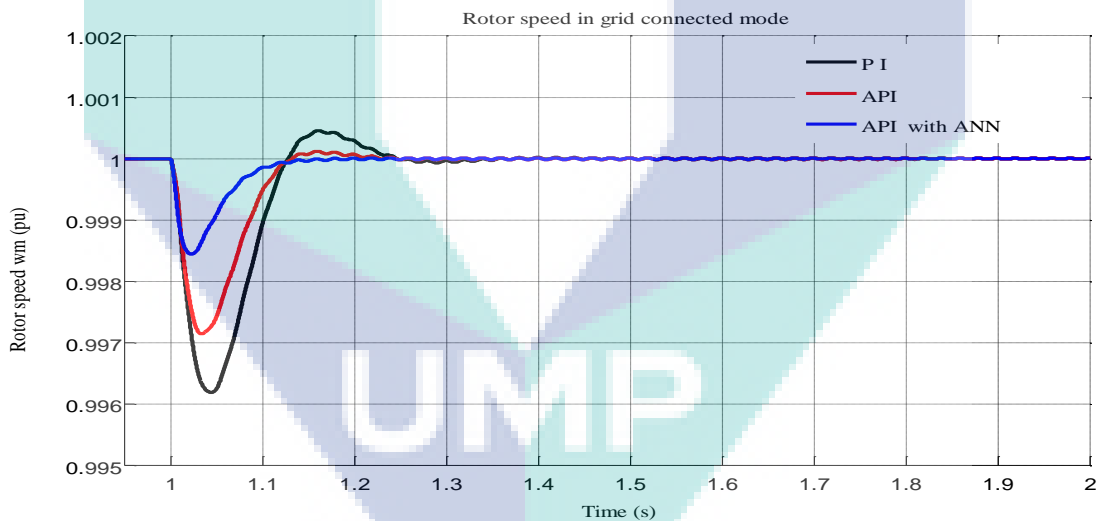


Figure 4.24 Speed rotor deviation at grid disconnect with deferent controller

Besides the above load step, the previous controls are subjected to the load application 40% and 50% of changes. The response of speed rotor after applied API with ANN controller is closed to a stable in a shorter time compared with two other controllers as indicated in Figure 4.25 and Figure 4.26.

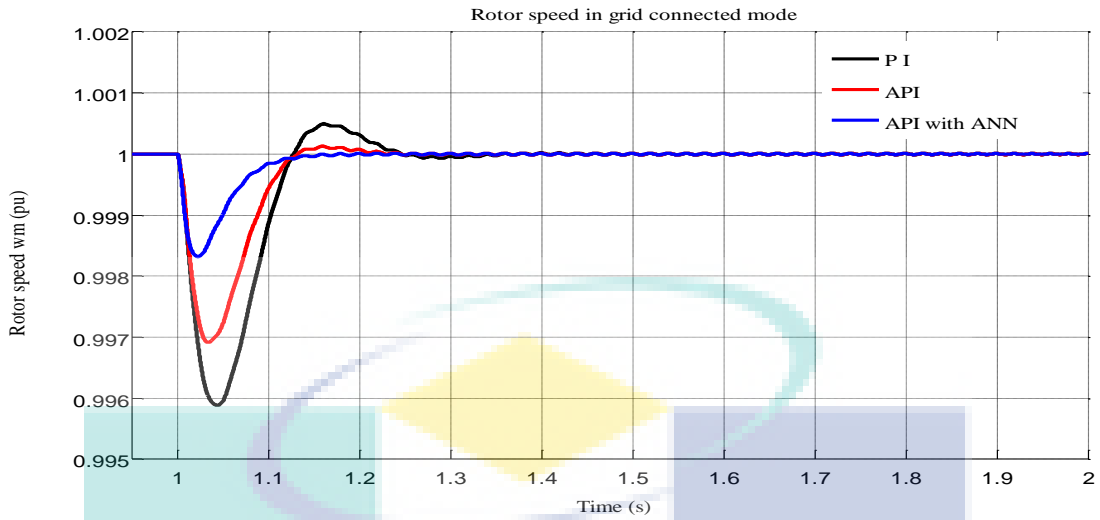


Figure 4.25 Speed rotor response for a 40% step change in electrical load

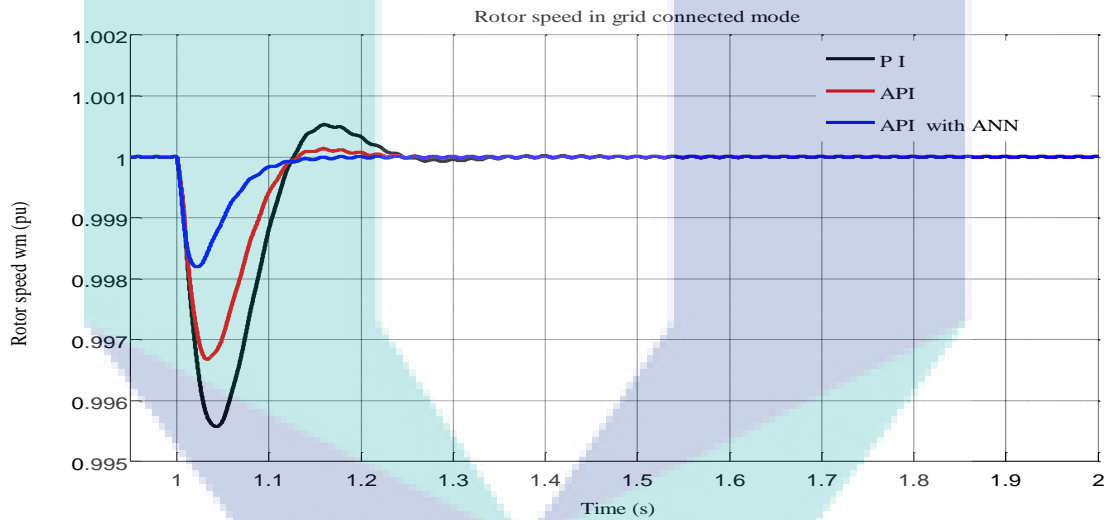


Figure 4.26 Speed rotor response for a 50% step change in electrical load

To verify the effectiveness of the control method in this mode of hybrid micro-grid operation (from grid-connected transfer to islanded mode), three comparative controllers are presented, which are (i) Conventional PI control, (ii) API control (proposed in this research), (iii) API with ANN (improved proposed in this research). The tests and their outcome dependence on frequency in load change at  $t=1s$  including Settling Time (ST), Rise Time (RT), Overshoot (OS) and Undershoot (US). The tests summarized are written in Table 4.1.

In these simulations mode the purpose is to show that proposed method reach a steady-state active power and the frequency response with fast, and reducing the

undamped behavior of frequency response. The adaptive nature of the proposed controller ensures active damping of frequency oscillations at different load changes; subsequently, stable and robust power-sharing performance is obtained in the micro-grid system. The results are reserving the hybrid micro-grid stability and reliability.

Table 4.1 Cases study in grid-connected mode

Methodology	Case Study	Meaning of Error	Rate of error%
Switching micro-grid operation from grid-connected mode to islanded mode is an important part for extension in the application side of the methodology	PI	Various Load changes	Illustrate the limitations of the method in unbalanced power sharing and deviated frequency ST in sec. = 1.403 RT in sec. = 0.054 OS % = 0.24 US % = 1
	API	Various Load changes	Eliminate the limitations in conventional PI by activating the MRAC using MIT rule while based PI controller ST in sec. = 1.282 RT in sec. = 0.046 OS % = 0.12 US % = 0.76
	API with ANN	Various Load changes	Prove the robustness of the method by stabilizing the system whenever there is a load power change by ramping power up and switching off the grid connection ST in sec. = 1.221 RT in sec. = 0.042 OS % = 0.04 US % = 0.48

#### 4.2.4 VSC in Grid Connected Mode

In this section, the parallel operation of a three-phase voltage source inverter with a SG has been implemented. Droop control method makes DG sources work like traditional SG which are easy to control and dispatch. The boost converter is connected to a three-phase inverter which uses a PLL to detect the frequency and stay in phase with the micro-grid.

Energy storage, in general, can be used to reduce the load on a grid temporarily by absorbing energy at times of high generation and discharging in times of high consumption (load change). Output active power of the converter is always at maximum power point operation of the PV source. Therefore, the parallel inverters stall with the SG must be controlled similarly to ensure good transients and good power sharing. The droop control technique controls the frequency and voltage of the inverter. Note that the inverter including LCL filter designed in this work is used in the micro-grid system. Figure 4.27 and Figure 4.28 show the transient active and reactive power

response for an inverter using droop control for three cases of step load increase. The controller is chosen proportional to simulate the behavior of grid and a SG. The output power capacity of a given inverter is set according to its rated power.

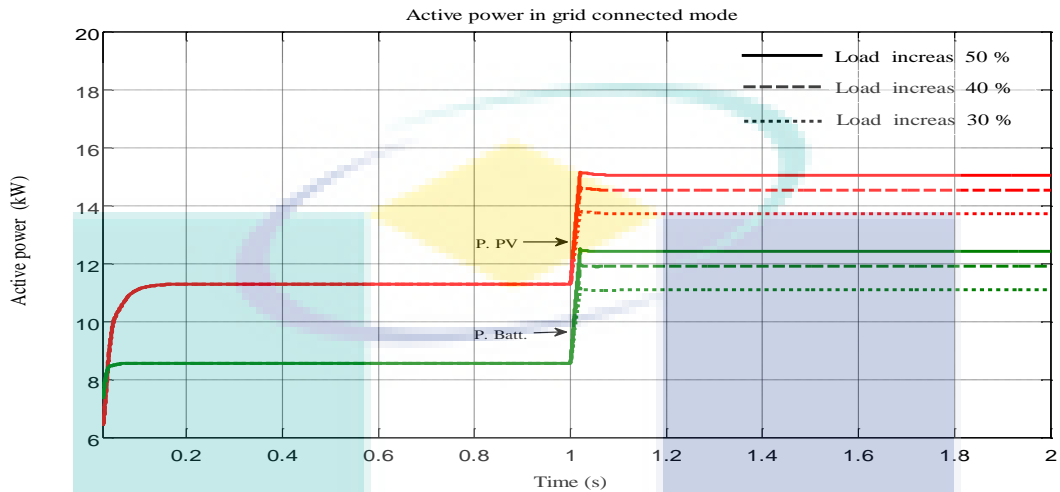


Figure 4.27 Output active power for PV and battery in grid connected

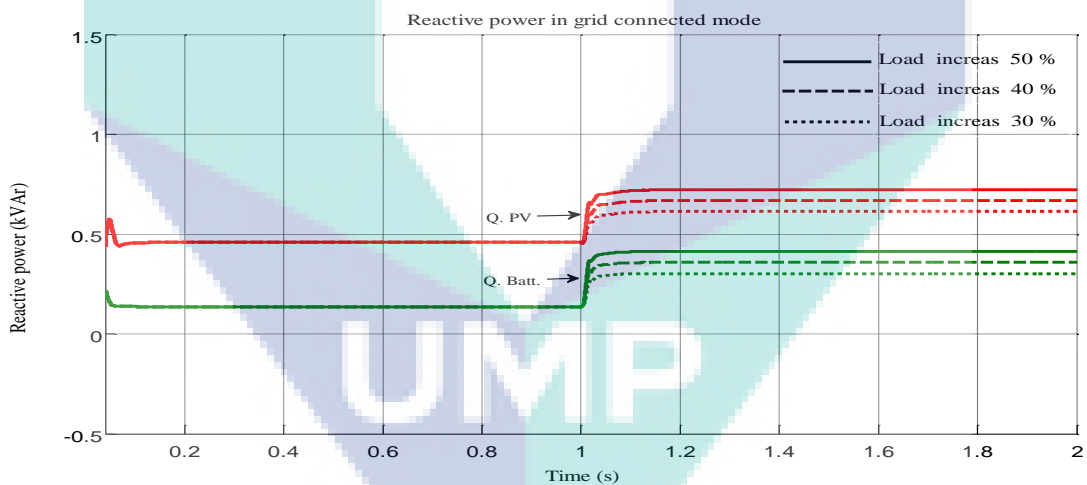


Figure 4.28 Output reactive power for PV and battery in grid connected

### 4.3 Island Mode Control

Micro-grids, especially the isolated from primary grids, will require new and robust LFC mechanisms to ensure stable operation under all operating circumstances. The system of the SG needs to ensure that the synchronous machine generates real and reactive power within the ratings of the machine at nominal voltage and frequency as demanded by the system to which it is connected. To create the islanded micro-grid

during the simulations, the switch (STS) is OFF as shown in Figure 3.10; therefore an islanded of three DGs micro-grid with loads can be implemented. The droop characteristics are same. Therefore equal power sharing between DGs is expected. The total RL load present in the system is 80kW, 15kVAr, and 16hp induction motor load. Simulations of an islanded micro-grid with three DGs under two different controls (i.e., conventional PI, proposed FLTC) have verified the effectiveness of the proposed FLTC method.

#### 4.3.1 Performance of MG Using FLTC

To get a desirable LFC in islanded hybrid micro-grid, the controller using FLTC is proposed. The control signal, which is the error signal of the frequency in the islanded micro-grid (i.e., the actual speed subtracted from the desired speed) and its derivative, is used as input for FLTC. The output of lookup table is the changes in frequency which will be integrated continuously, as shown in Figure 4.29. The feedback signal, which is the speed, will be sent again to FLTC. So, the closed-loop control works continuously to achieve the desired speed and keep it stable.

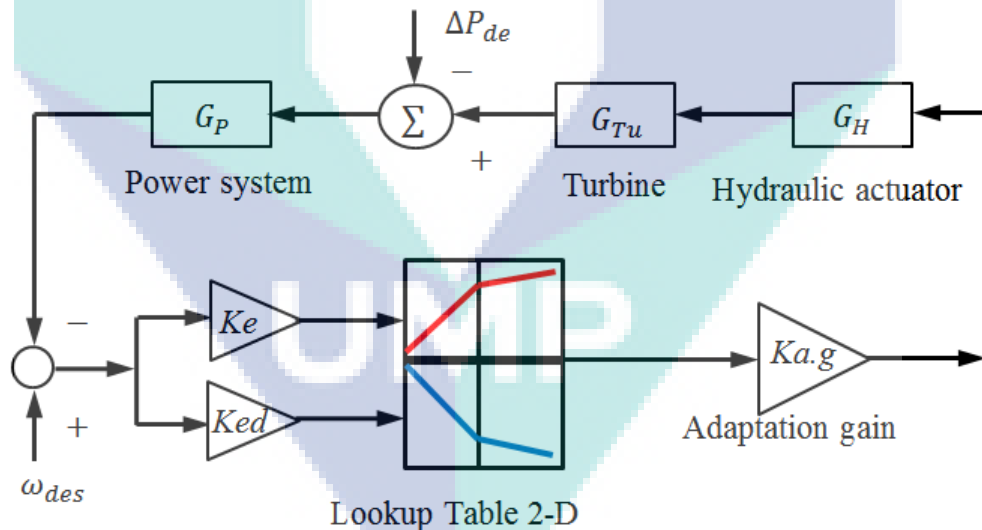


Figure 4.29 Fuzzy Logic Table Control (FLTC) for synchronous generator

The performance of conventional PI controller is examined and compared to the proposed controller. Two analyses of disturbances have been adopted, first is the impact of RL load (80-120 kW, 15- 22 kVAr) in a step change of electrical load. Meanwhile, the micro-grid is subjected to fault (three phase line to ground fault), is the second problem to be examined for a period of 1 to 1.1s when connected with the normal load.

Simulation results focus on the performance of the FLTC. The simulation implemented and tested using MATLAB/ Simulink and the details of results are presented.

To verify the feasibility of the proposed controller the active power sharing performance produced from the synchronous generator unit is shown in Figure 4.30.

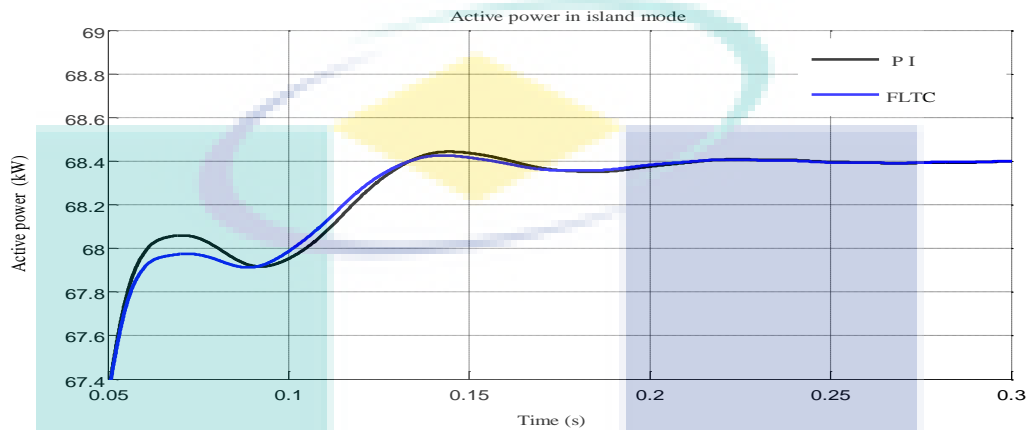


Figure 4.30 The response start-ups active power sharing performance produced from the synchronous generator unit

The low damping power-sharing leads to poor transient response and oscillating performance in the injection power with conventional PI. Due to the transient response of the proposed FLTC, the transient response real power can be significantly suppressed, as shown in Figure 4.31.

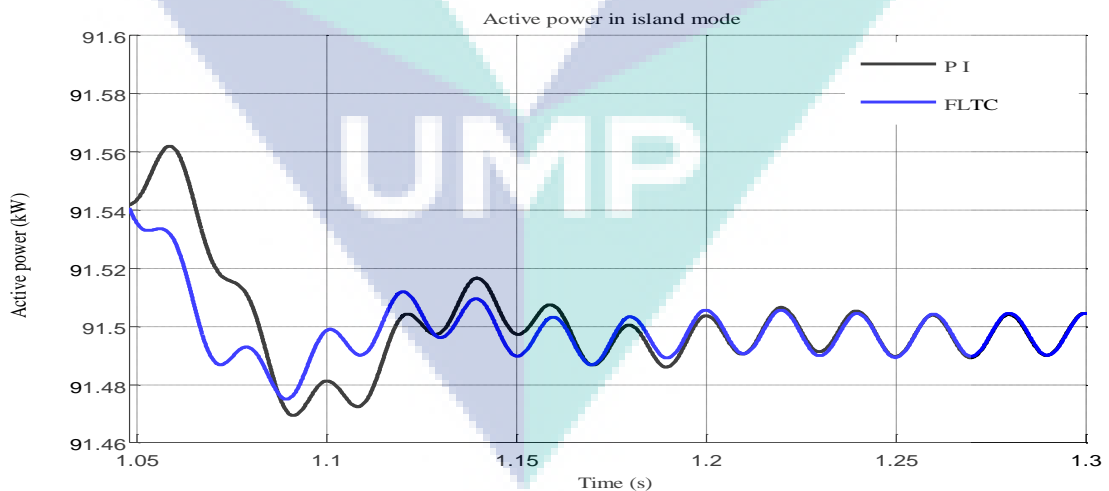


Figure 4.31 The transient response active power sharing performance produced from the synchronous generator unit

Figure 4.32, illustrating when the load is increased at  $t = 1$ s, a step change in power demand is occurs and the micro-grid tracks the transient changes. All DGs in the

proposed micro-grid system is equipped with their rated power. It can be observed that the synchronization of active power is properly distributed when the load changes.

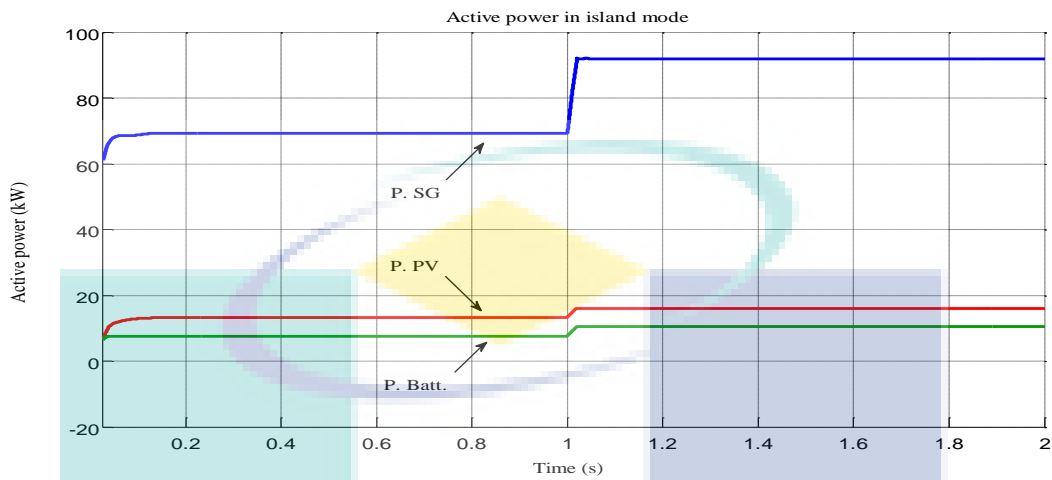


Figure 4.32 Active power sharing performance of micro-grid units

After the step reactive power load increase to 22kVAr, the FLTC shows a smooth transient to the new state with very less error or fluctuation. Figure 4.33 shows the reactive power behavior of each DG under proposed approach over the transient period.

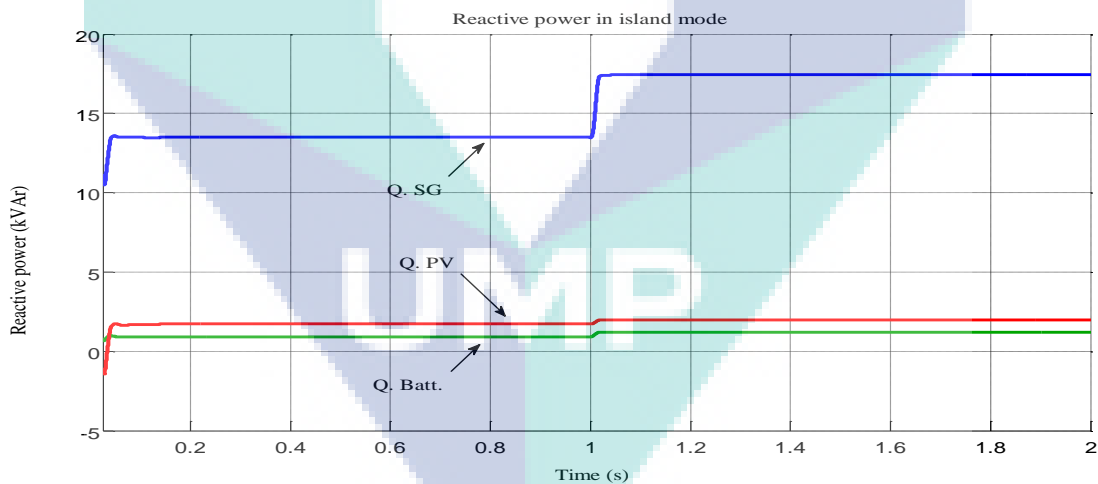


Figure 4.33 Reactive power response of DGs following change load

A frequency error of micro-grid after the operation and during step load change is shown in Figure 4.34. The enhancements of the transient responses obviously appear in this figure which illustrates the frequency deviation responses of PI controller and the proposed FLTC.

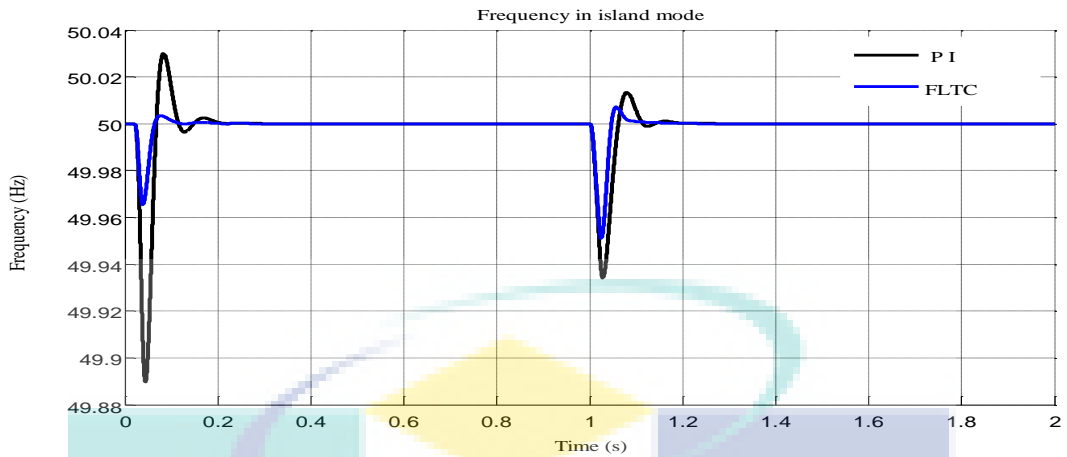


Figure 4.34 Frequency deviation (Hz) and time response

Then, in Figure 4.35, the proposed FLTC showed a promising improvement of the frequency deviation over a step response. From which the FLTC, has the best transient response than PI controller.

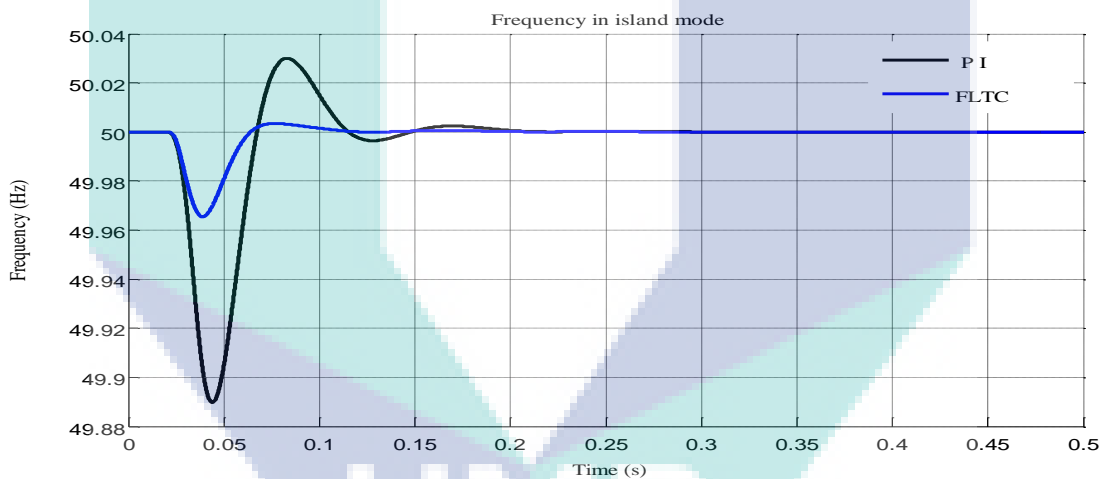


Figure 4.35 Frequency time response from transient to steady- state

An explicit comparison response of load change with these two types of controllers, the enhancements of the transient responses of frequency for proposed controller is shown in Figure 4.36.



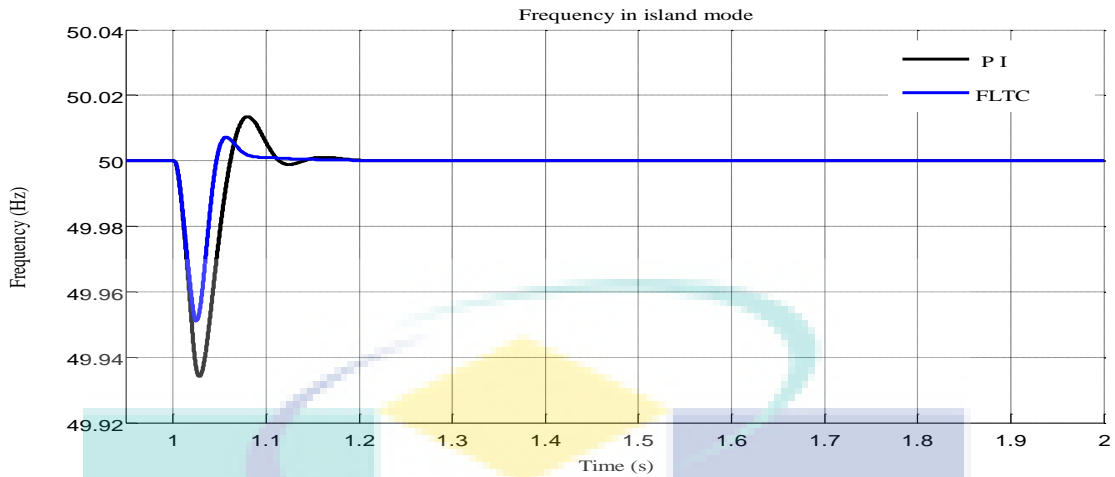


Figure 4.36 Frequency error during step load change

Figure 4.37 compares the time responses of same speed rotor controlled by PI and FLTC for the same disturbance. The characteristics show that there is big difference in responses for both controllers, though the oscillation is reduced to low extent in FLTC. The result has shown a promising improvement for the proposed FLTC compared with PI controller.

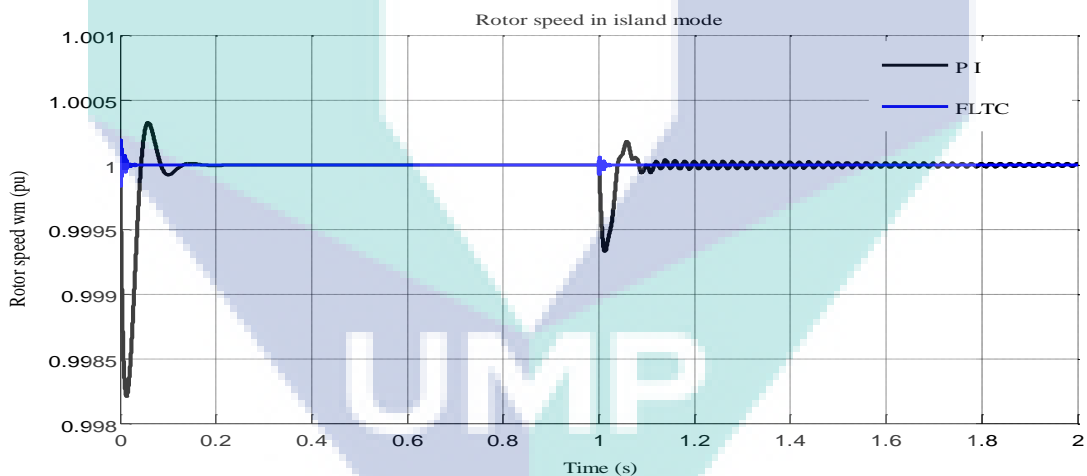


Figure 4.37 Rotor speed oscillation in island MG

When unit-step from no load to full load is applied at  $t=0s$  to both PI and FLTC controller, the response is shown in Figure 4.38 under PI controller make the system unstable. The rotor speed response was achieved the settled in 0.15 seconds. FLTC performs faster than the PI controlled system and responds satisfactorily with reached settled in  $t=0.015s$ .

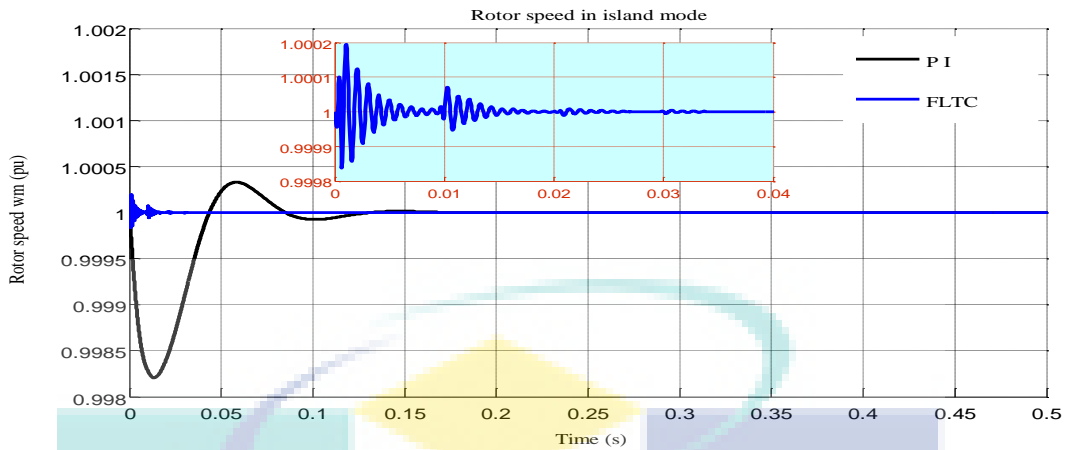


Figure 4.38 Rotor speed response by proposed FLTC and PI control

It is also showed the significantly smooth and robust controller with FLTC after load changes, whereas the proposed controller considerable stable at steady state when compared with PI controller as illustrated in in Figure 4.39. The rotor speed response is tracking the desired value in 1.015 seconds for the settling time and still. With the PI controller the performance of the system is very poor and also having high value of undershoots and overshoots with longer settling time 1.15 seconds. Figure 4.39 depicts an enlarged signal of rotor speed deviation for PI and FLTC controllers in case of step load changes at  $t = 1$  second.

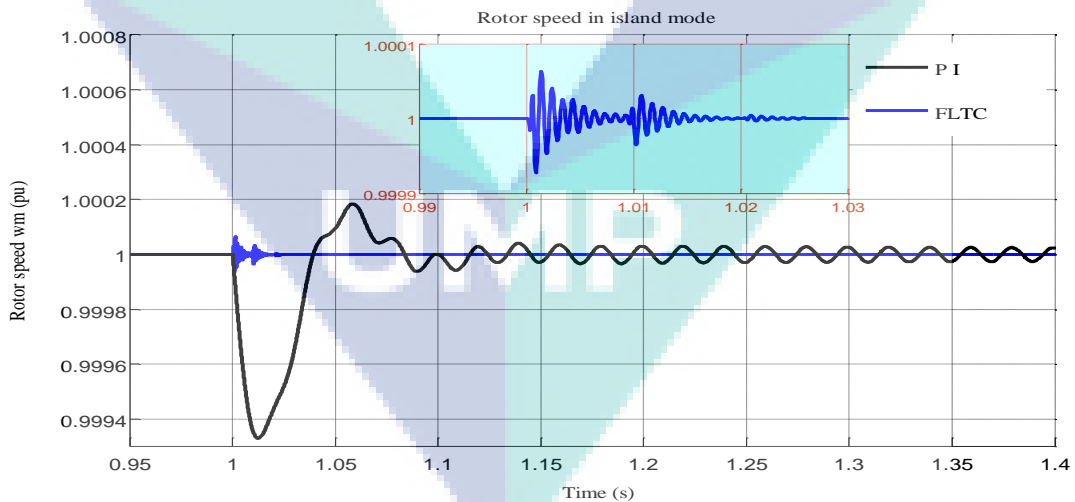


Figure 4.39 Rotor speed oscillation at step load change in island mode

A FLTC was proposed to replace the PI controller used for error minimization in the conventional PI speed controller. The choice of the values of the adaptation gains greatly affects the performance of the FLTC. The different responses was carried out by changes in the adaptation gain (5, 10, 15 and 20) as depicted in Figure 4.40 were tested

for confirming the superiority of the FLTC response speed in the unit-step is applied. The adaptation gains are responsible to improve the transient performance of the speed response in terms of overshoot, settling time, rise time and steady-state for step speed response (Ali, A. T. & Tayeb, 2012). It is evident from the results that the low adaptation gain (5), the actual speed  $\omega$  has no oscillation, decreasing adaptation gains the output speed response improved towards matching the desired value of reference speed  $\omega_0$ .

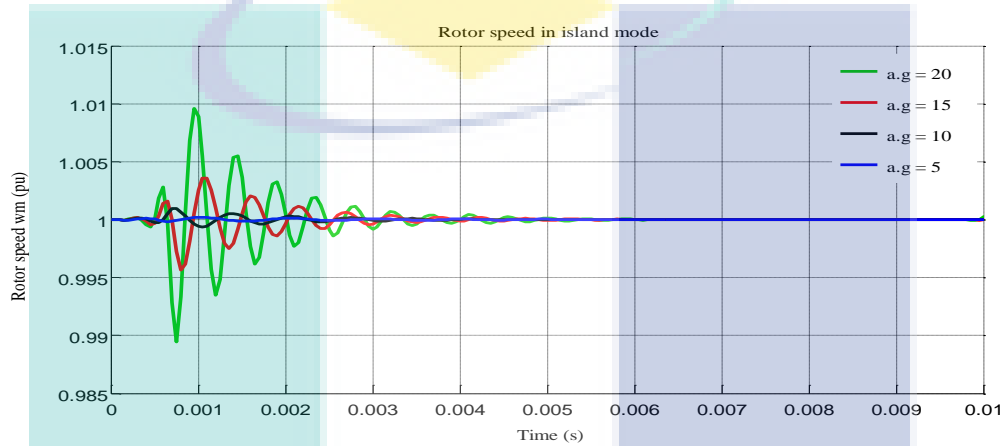


Figure 4.40 The rotor speed oscillations for the different adaptation gain (a.g) values

Then, Figure 4.41 shows the comparative performance of time responses deviation of speed rotor at each values adaptation gain that had been used in FLTC.

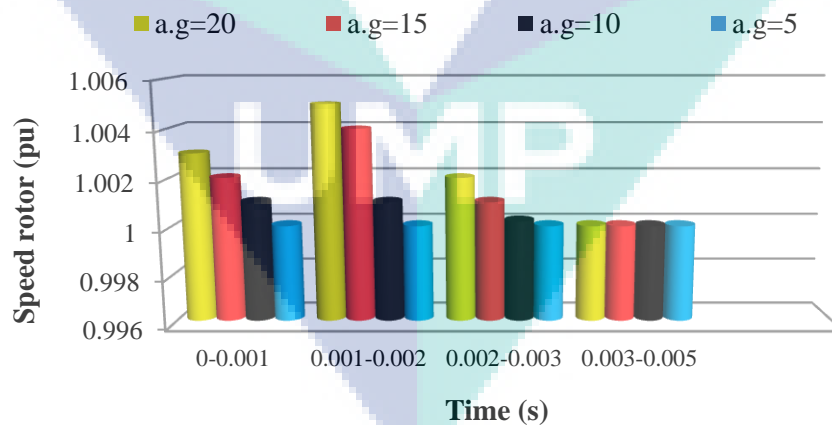


Figure 4.41 The rotor speed oscillations with values of adaptation gain (a.g)

At load change, FLTC reduces the overshoot, undershoot and settling time to lowest value and also improves the system performance by decreasing the adaptation gain. However, the gain tuning is quite simple compared with tuning PI gains. System

performance is good and stable in chosen  $a.g = 5$ . Before the chosen of FLTC, the system performance is very poor and become unstable. So for only suitable value of adaptation gain can be used to track the error closer to the disturbance. Figure 4.42 shows effect of different adaptation gain on speed deviation with FLTC controller in case of load change at  $t=1s$ .

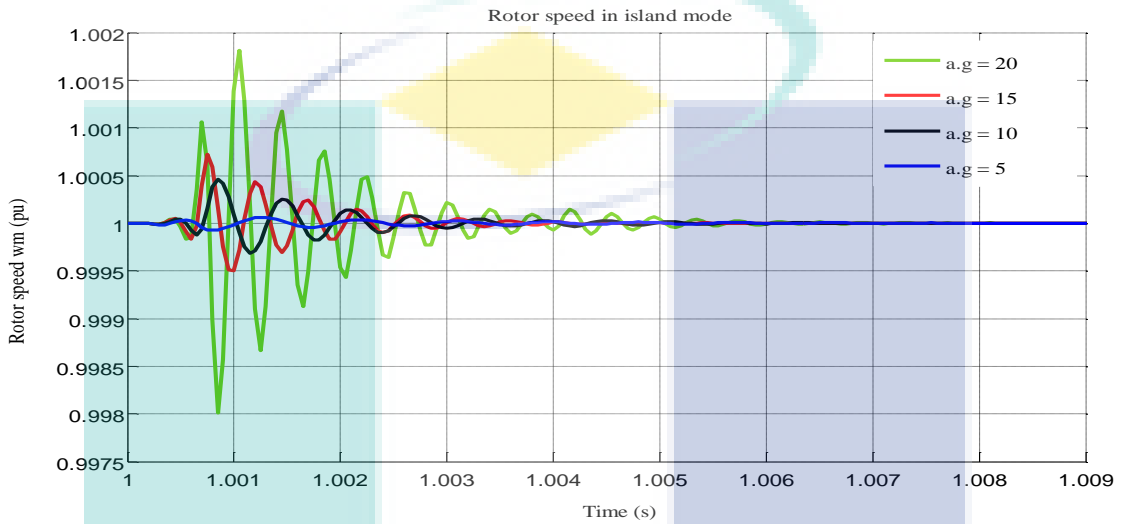


Figure 4.42 Different adaptation gain (a.g) on speed deviation with FLTC controller in case of load change

Figure 4.43 shows the voltage and current on the load side. Although the voltage is synchronized smoothly, the current increase at first cycle due to the load increased by 50% at  $t = 1$  second.

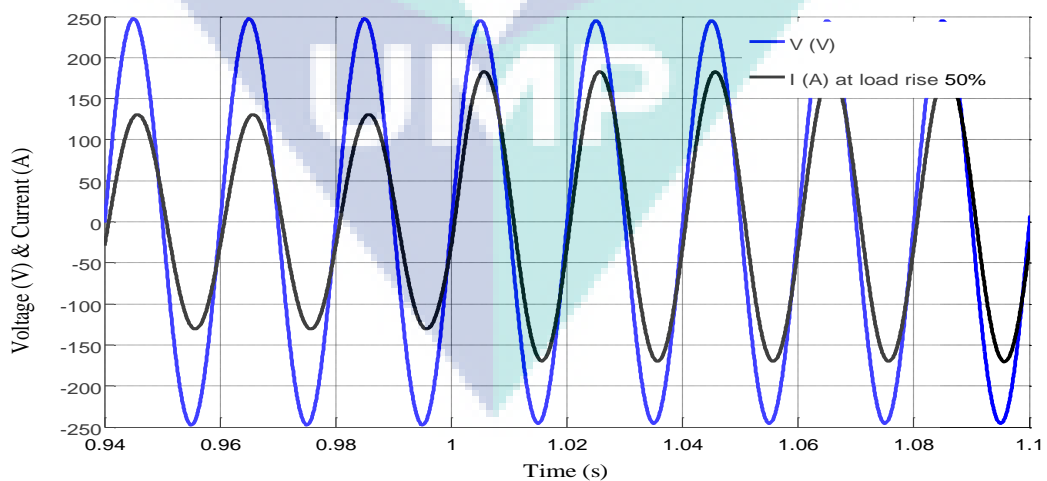


Figure 4.43 Voltage and current of phase "a" at load increase 50% in island mode

### 4.3.2 Fault in Island Mode

The effectiveness of the proposed FLTC is extended to 3-phase to ground fault analysis in islanded hybrid micro-grid, which is the SG is assessed the frequency deviation when exposed to a fault. At first, the induction motor and RL loads are connected to the hybrid micro-grid as shown in Figure 3.10. Then, a three phase to ground fault is created for a period of 1s to 1.1s, in which the fault is occurred at the distribution line on the load side.

The simulation results have shown that the proposed FLTC controller improves the LFC capability, which can be seen in frequency fault case. It can be observed that the proposed controller is able to accommodate the frequency fault, leading to minor changes in the frequency of the islanded micro-grid. After the fault, the behavior of PI controller is significantly affected causing unwanted frequency oscillations. While the proposed controller of FLTC allowed the frequency tracking the nominal value. The fault analysis in islanded the micro-grid is shown in Figure 4.44.

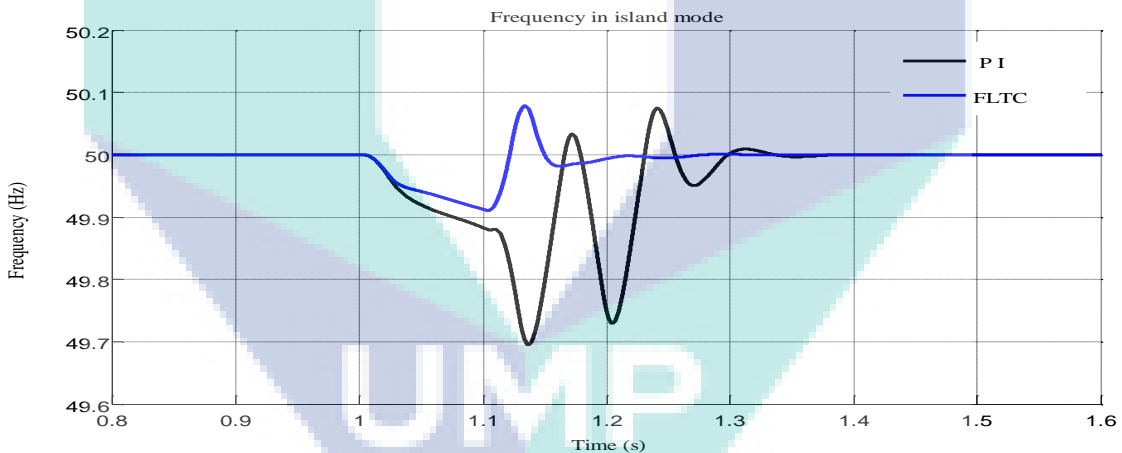


Figure 4.44 Frequency oscillations during 3-phase to ground fault in island mode

From Figure 4.45, it can be observed that when the micro-grid fault occurs, the oscillation also happened in the rotor speed for about 123 milliseconds. While high oscillation occurred for PI controller and taking longer period to stabilise the rotor speed. Due to a high fault tolerance of the proposed FLTC, an efficient and promising control has been shown and could increase the stability of the micro-grid when fault occurs.

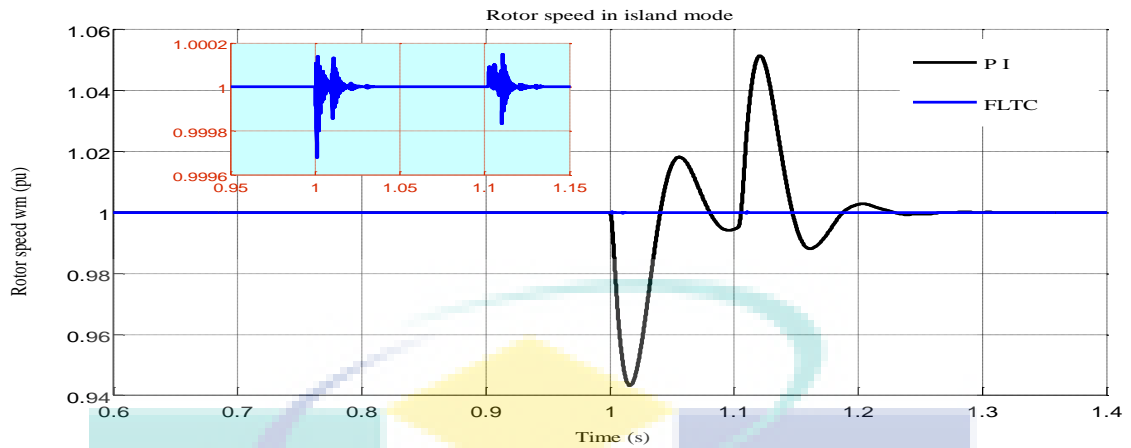
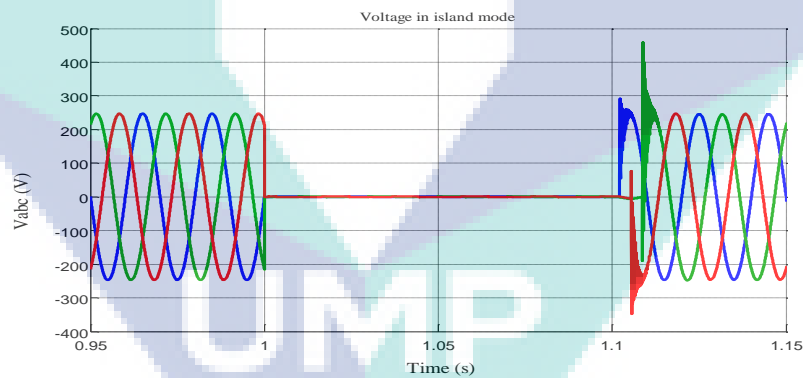


Figure 4.45 Rotor speed controls, during symmetrical fault occurs in island micro-grid

Lastly, Figures 4.46 (a) and (b) show the three phase voltages and currents in the islanded micro-grid during the three-phase ground fault on the load side and clearing time using FLTC, respectively. It is capable of re-exciting after fault clearing and reaches steady state within shorter the fault clearing time at 1.1 second. The fault current value is high due to the large contribution of the SG and distribution system to the total fault current for the three-phase fault on the load side.



(a)

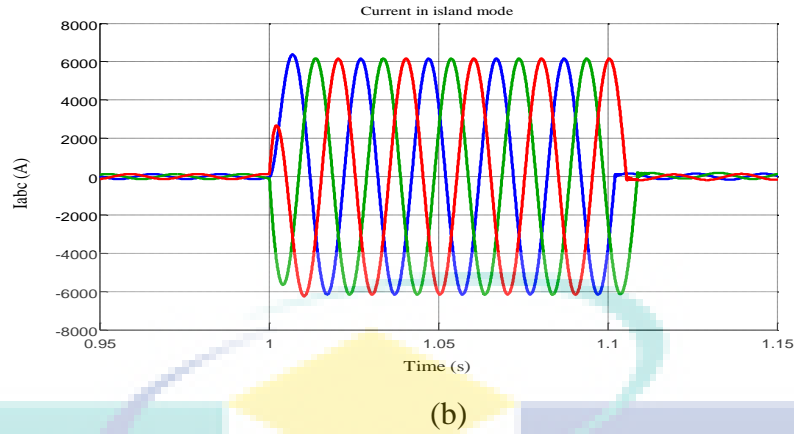


Figure 4.46 (a) Phase voltages (b) Line currents during three phase ground fault on the load side

This section presented the findings of the proposed FLTC controller for maintaining the frequency deviation in the islanded micro-grid from step and load changes, and hence line fault. The adaptation gain parameters are selected appropriately from simulation as the control gain of the proposed controllers. It is also, the FLTC algorithm could identifies the desired power sharing with keep the voltage stability. Simulations for two cases, which are load changes and 3 phase fault in islanded micro-grid, verified the effectiveness of the proposed control algorithm. In this load changes analysis, four performances criteria are preferred for comparison, i.e., Settling Times (ST), Rise Time (RT), Overshoots% (OS), and Undershoot% (US) of the frequency deviation. The test of each case and its meaning are summarized in Table 4.2. It is has showed that FLTC achieves good performances and the dynamic response of hybrid micro-grid when compared to the conventional PI controller.

Table 4.2 Cases study in island mode

Methodology	Case study	Meaning	Rate of error%
Making sure that required amount of power is provided at nominal frequency and voltage in the micro-grid during islanded mode operation.	PI	Load changes and fault disturbance influence the slow response and oscillation of the frequency, power sharing and does not achieve desired synchronization.	ST in sec. =1.157
			RT in sec. =0.023
			OS % = 0.028
			US % =0.14
	FLTC	Improve the system stability and robustness is guaranteed by activating the proposed control.	ST in sec. =1.11
			RT in sec. =0.015
			OS % = 0.021
			US % =0.1

#### 4.4 Summary

Simulation results show that the new integrated control strategy can keep the frequency of micro-grid in islanded mode and grid mode, and realize a rapid transition between the two modes. The proposed control structures are able to restore the frequency to nominal value in fast compared to PI controller. A control system is essential to cancel the effects of the step load changes and to keep the frequency at the standard values. The micro-grid is supplied by three distributed generation (DG) units, i.e., a synchronous machine, PV solar and a battery based DG unit. The benefits of using these controls proposed system maintaining the stability during both operations. In addition, it is also keeping micro-grid at robust operation in both modes during loads changes. The LFC mechanism also entailed two control systems for each of the two operations mode of micro-grid. These are designed to control the generator speeds, i.e. to maintain the frequency at the desired values. The new application controller has better performance than traditional PI controller by using MRAC based MIT rule and ANN in grid connected mode which gives the desired response to the reference signal. For islanded micro-grid, a FLTC controller is proposed to improve and enhance the operation during the load changes and fault condition. This meets the corresponding load requirements during the islanding operation. With this proposed controller, using droop control, the active and reactive power are could be proper distributed.

The logo for UMP (Universiti Malaysia Perlis) is a large, stylized letter 'V' shape. The left side of the 'V' is light blue, and the right side is light green. The letters 'UMP' are written in white, bold, sans-serif font across the center of the 'V'.



## CHAPTER 5

### CONCLUSION

#### 5.1 Introduction

This research thesis suggested advanced and control strategies based on robust adaptive control. The controller has been designed for hybrid micro-grid including synchronous generator, PV, battery and loads. The controller objectives were tracked the load variation and smooth the transfer from grid-connected to island mode. Furthermore, it covers any fluctuations that occur in frequency during power sharing. An essential part of an SG is LFC. This controller is appropriately designed to respond to load variations and to fix frequency at a constant value when operated in islanding mode and to control output power when operating in parallel with the main. In this research, a new approach based on LFC response about to the governor is introduced.

#### 5.2 Summary of Findings

A new model reference adaptive control design method using neural networks that guarantees transient performance is proposed in this work. A modified state observer structure is designed to enable desired transient performance fast and at the same time avoid high-frequency oscillations during uncertainty learning. The controller consists of sub-networks, based on the inputs and outputs of the plant adaptive MRAC based MIT rule (API) with ANN that identifies the power plant regarding its speed governors and provides the necessary control action to damp the deviation of the frequency in the micro-grid system.

An adaptive controller can improve the transient behavior of a network by allowing the parameters of the controller to adjust as the operating conditions change. A modified state observer structure is designed to enable desired transient performance fast with adaptive gains and at the same time avoid high-frequency deviations. The API

with ANN controller is used for robust power-sharing associated with better dynamics response, and hence enhancing the tracking of grid connection mode and island mode operations. The effectiveness of the API with ANN controller is then compared with that of API and PI controller. From the simulation studies, it is clear that API with ANN based controller can efficiently damp out the oscillations and reduce the settling time.

The design FLTC is implemented to rotary machine based as a DG in islanded micro-grid system operation. The FLTC algorithm is derived for robust computation; as the lookup table is generated offline to fast computational of speed control of the synchronous generator. For this plant, the variation is given on natural frequency of first order plant. In summary, FLTC controller based on the lookup table is capable to control frequency and power whose support is lost due to disconnection of the grid. Thus, proposed control strategy has better performance than the traditional method. The simulation results demonstrated that the proposed FLTC provides desirable performance against sudden load change that improves the frequency deviation and output power variation. It is evident from the results that the proposed controller gives better responses regarding overshoot and fast response. The FLTC exhibited high performance in tracking the speed reference. At the same time, the dynamic behavior of the synchronous generator with FLTC performs more stable than the PI controller during symmetrical fault occurs at the distribution lines. The proposed controller is very simple and easy to implement. Therefore the proposed controller can contribute to expanding energy utilization into isolated micro-grid. MATLAB simulation results support the validity of proposed control scheme.

The simulation results show that the input signal to the governor has various characteristics in different disturbances and loss of the primary condition. No additional equipment is needed, there will be no impact on the main system, and no further cost is required. There are many benefits of using the governor signal monitoring approach to detect island conditions.

### **5.3 Attainment of research objectives**

The overriding objective of this research is to develop control techniques of the synchronous generator as an inertial distributed generation in the hybrid micro-grid to

track the load variation and smooth the transfer from grid-connected to island mode. The required amount of power is also provided in nominal frequency and voltage.

Ultimately, three specific research objectives have been established and achieved. It has explored the phenomena of slow response and oscillation of frequency during sudden changes in loads, from the perspective of load frequency control. To achieve the objectives of the research, a mixed method approach has been considered. Firstly, by proposed MRAC based on PI (API) control technique to adapt the disturbances and track the load variation that the corresponding tracking of a reference model to control the rotor shaft speed of SG. It is found suitable for use in the hybrid micro-grid system throughout the operation of micro-grid connected to the grid.

In the second phase of the research, to guarantee the smooth transfer from grid-connected to island mode by reducing the error and enhance tracking using ANN. The controller is designed using a parallel combination of MRAC system and ANN controller (API with ANN). During training, the values of reference speed and the rate of change of input speed are considered as input data; the learning process can reach the required minimum error.

Regarding scope hybrid micro-grid system, the research has looked at islanded mode operation control. There is another perspective which may provide further insights into the islanded mode controller such as frequency deviation from the nominal value which would give more depth to improve the synchronization of micro-grid after a loss the supported and synchronization of grid utility. Using FLTC which might assist to avoid any further oscillation of the power-sharing and at the same time, it is provided the required amount of power at nominal frequency and voltage.

#### **5.4 Contribution to the Study**

According to the objectives of this thesis, the specific contributions of this work are:

1. The first contribution is in micro-grid connected to the utility grid operation mode, which is present an approach using modified MRAC based MIT rule which prevents high-frequency oscillation and smoothest the transient behavior of the micro-grid system in grid-connected mode. The proposed control

algorithms successfully reduce the initial transient time of the controller compared to traditional PI control.

2. The second contribution is proposed ANN controller based on modified MRAC algorithms, which is improving the system performance and enhancing the tracking of grid connection mode and island mode operations. The initial overshoot associated with PI control is completely removed.
3. In island operation mode, an FLTC method for the LFC is proposed as the third contribution in this work. For confirming that the desired amount of power is provided at nominal frequency and voltage, an FLTC is developed for avoiding recursive mathematical computation and could be implemented easily.

### **5.5 Recommendations for Future Work**

There is still a lot of work to be done in the future. Some of these issues are:

- (i) Electric governors can be used for diesel engine applications. The proportional, integral, and derivative (PID) controller executes the electric governor to control engine speed. Diesel engines are examined in distributed power generation systems, and the non-linear engine torque map is obtained from frequent tests, that the proposed model control in grid-connected can be used to adjust PID controllers systemically.
- (ii) Consideration of losses in the analysis of grid-connected and islanded systems comparing the losses implement the proposed load-frequency controllers.

## REFERENCES

- Adhikari, S. (2013). Control of Solar Photovoltaic (PhV) Power Generation In Grid-connected and Islanded Microgrids.
- Ahn, S.-J., & Choi, J.-H. (2012). Power sharing and frequency control of an autonomous microgrid considering the dynamic characteristics of distributed generations. *Journal of International Council on Electrical Engineering*, 2(1), 39-44.
- Ahn, S.-J., Park, J.-W., Chung, I.-Y., Moon, S.-I., Kang, S.-H., & Nam, S.-R. (2010). Power-sharing method of multiple distributed generators considering control modes and configurations of a microgrid. *Power Delivery, IEEE Transactions on*, 25(3), 2007-2016.
- Akorede, M. F., Hizam, H., & Pouresmaeil, E. (2010). Distributed energy resources and benefits to the environment. *Renewable and Sustainable Energy Reviews*, 14(2), 724-734.
- Al-Abri, R. (2012). Voltage Stability Analysis with High Distributed Generation (DG) Penetration.
- Al Hokayem, P., & Gallestey, E. (2011). Adaptive Control. *Lecture Notes Nonlinear Systems and Control, Automatic Control Laboratory, ETH Zurich*.
- Ali, A. T., & Tayeb, E. B. M. (2012). Adaptive PID Controller for Dc Motor Speed Control.
- Ali, W., Farooq, H., Abbas, W., Usama, M., & Bashir, A. (2017). PID VS PI control of speed governor for synchronous generator based grid connected micro hydro power plant. *JOURNAL OF FACULTY OF ENGINEERING & TECHNOLOGY*, 24(1), 53-62.
- Alsadi, S., & Alsayid, B. (2012). Maximum power point tracking simulation for photovoltaic systems using perturb and observe algorithm. *International Journal of Engineering and Innovative Technology (IJEIT)*, 2(6), 80-85.
- Ambia, M. N., Al-Durra, A., Caruana, C., & Muyeen, S. (2016). Islanding operation of hybrid microgrids with high integration of wind driven cage induction generators. *Sustainable Energy Technologies and Assessments*, 13, 68-75.
- Amirnaser, Y., & Reza, I. (2010). Voltage-sourced converters in power systems. *New Jersey: John Wiley&Sons*.
- Andersson, G. (2012). Dynamics and control of electric power systems. *Lecture notes*, 227-0528.
- Ashabani, S. M., & Mohamed, Y. A.-R. I. (2012). A flexible control strategy for grid-connected and islanded microgrids with enhanced stability using nonlinear microgrid stabilizer. *IEEE transactions on smart grid*, 3(3), 1291-1301.
- Asmus, P., Cornelius, A., & Wheelock, C. (2009). Microgrids–islanded power grids and distributed generation for community, commercial, and institutional applications. *Pike research*.

- Bai, Y., & Wang, D. (2006). Fundamentals of Fuzzy Logic Control—Fuzzy Sets, Fuzzy Rules and Defuzzifications *Advanced Fuzzy Logic Technologies in Industrial Applications* (pp. 17-36): Springer.
- Bakar, N. N. A., Hassan, M. Y., Sulaima, M. F., Na'im Mohd Nasir, M., & Khamis, A. (2017). Microgrid and load shedding scheme during islanded mode: A review. *Renewable and Sustainable Energy Reviews*, 71, 161-169.
- Balaguer, I. J., Lei, Q., Yang, S., Supatti, U., & Peng, F. Z. (2011). Control for grid-connected and intentional islanding operations of distributed power generation. *IEEE Transactions on industrial electronics*, 58(1), 147-157.
- Balaguer, I. J., Supatti, U., Lei, Q., Choi, N.-S., & Peng, F. Z. (2008). *Intelligent control for intentional islanding operation of microgrids*. Paper presented at the 2008 IEEE International Conference on Sustainable Energy Technologies.
- Barklund, E., Pogaku, N., Prodanovic, M., Hernandez-Aramburo, C., & Green, T. C. (2008). Energy management in autonomous microgrid using stability-constrained droop control of inverters. *IEEE Transactions on power electronics*, 23(5), 2346-2352.
- Basso, T., & DeBlasio, R. (2009). *Advancing smart grid interoperability and implementing NIST's interoperability roadmap*. Paper presented at the Proc. NREL/CP-550-47000, Grid-Interop Conf.
- Basso, T., & DeBlasio, R. (2011). IEEE smart grid series of standards IEEE 2030 (interoperability) and IEEE 1547 (interconnection) status. *Grid-Interop*, 5-8.
- Bayindir, R., Hossain, E., Kabalci, E., & Perez, R. (2014). A comprehensive study on microgrid technology. *International Journal of Renewable Energy Research*, 4(4), 1094-1107.
- Beck, H.-P., & Hesse, R. (2007). *Virtual synchronous machine*. Paper presented at the Electrical Power Quality and Utilisation, 2007. EPQU 2007. 9th International Conference on.
- Benkhilil, E., & Gherbi, A. (2012). Modeling and simulation of grid-connected photovoltaic generation system. *Deuxième séminaire international sur les énergies*, 15-17.
- Bevrani, H. (2004). Decentralized robust load-frequency control synthesis in restructured power systems.
- Bevrani, H., & Daneshmand, P. R. (2012). Fuzzy logic-based load-frequency control concerning high penetration of wind turbines. *IEEE systems journal*, 6(1), 173-180.
- Bevrani, H., Habibi, F., Babahajyani, P., Watanabe, M., & Mitani, Y. (2012). Intelligent frequency control in an ac microgrid: online PSO-based fuzzy tuning approach. *IEEE transactions on smart grid*, 3(4), 1935-1944.
- Bevrani, H., Hiyama, T., Mitani, Y., Tsuji, K., & Teshnehlab, M. (2006). Load-frequency regulation under a bilateral LFC scheme using flexible neural networks. *Engineering Intelligent Systems*, 14(2), 109-117.
- Bevrani, H., & Ise, T. (2017). *Microgrid Dynamics and Control*: John Wiley & Sons.
- Bhaskara, S. N. (2012). Control and operation of multiple distributed generators in a microgrid.



- Blaabjerg, F., Teodorescu, R., Liserre, M., & Timbus, A. V. (2006). Overview of control and grid synchronization for distributed power generation systems. *IEEE Transactions on industrial electronics*, 53(5), 1398-1409.
- Bouزيد, A. M., Guerrero, J. M., Cheriti, A., Bouhamida, M., Sicard, P., & Benghanem, M. (2015). A survey on control of electric power distributed generation systems for microgrid applications. *Renewable and Sustainable Energy Reviews*, 44, 751-766.
- Cao, C., & Hovakimyan, N. (2007). Novel neural network adaptive control architecture with guaranteed transient performance. *IEEE Transactions on Neural Networks*, 18(4), 1160-1171.
- Celep, H. (2012). *Model based adaptive PID controller with feedforward compensator for steam turbine speed control*: Texas A&M University-Kingsville.
- Chaloshitori, B. B., Isfahani, S. H., Kargar, A., & Abjadi, N. (2011). Power System Stabilizer (PSS) Design Using ANFIS Algorithm and Comparing the Results with conventional and fuzzy PSS. *Journal of Basic and Applied Scientific Research*, 1458-1469.
- Coman, S., & Boldisor, C. (2014). Adaptive PI controller design to control a mass-damper-spring process. *Bulletin of the Transilvania University of Brasov. Engineering Sciences. Series I*, 7(2), 69.
- Dash, A. R., Babu, B. C., Mohanty, K., & Dubey, R. (2011). *Analysis of PI and PR controllers for distributed power generation system under unbalanced grid faults*. Paper presented at the Power and Energy Systems (ICPS), 2011 International Conference on.
- Datta, M., Senjyu, T., Yona, A., Funabashi, T., & Kim, C.-H. (2011). A frequency-control approach by photovoltaic generator in a PV–diesel hybrid power system. *IEEE Transactions on Energy Conversion*, 26(2), 559-571.
- de Boer, P., & Raadschelders, J. (2007). Flow batteries. *Leonardo Energy*, 1-9.
- De Brabandere, K., Bolsens, B., Van den Keybus, J., Woyte, A., Driesen, J., & Belmans, R. (2007). A voltage and frequency droop control method for parallel inverters. *IEEE Transactions on power electronics*, 22(4), 1107-1115.
- De, D., & Ramanarayanan, V. (2010). Decentralized parallel operation of inverters sharing unbalanced and nonlinear loads. *IEEE Transactions on power electronics*, 25(12), 3015-3025.
- Delghavi, M. B., & Yazdani, A. (2009). *A control strategy for islanded operation of a distributed resource (DR) unit*. Paper presented at the Power & Energy Society General Meeting, 2009. PES'09. IEEE.
- Dhanalakshmi, R., & Palaniswami, S. (2011). *Application of multi stage fuzzy logic control for load frequency control of an isolated wind diesel hybrid power system*. Paper presented at the Green Technology and Environmental Conservation (GTEC 2011), 2011 International Conference on.
- Diaz, G., Gonzalez-Moran, C., Gomez-Aleixandre, J., & Diez, A. (2010). Scheduling of droop coefficients for frequency and voltage regulation in isolated microgrids. *IEEE Transactions on Power Systems*, 25(1), 489-496.

- Dou, C.-X., Liu, D.-L., Jia, X.-B., & Zhao, F. (2011). Management and control for smart microgrid based on hybrid control theory. *Electric Power Components and Systems*, 39(8), 813-832.
- Dreidy, M., Mokhlis, H., & Mekhilef, S. (2017). Inertia response and frequency control techniques for renewable energy sources: A review. *Renewable and Sustainable Energy Reviews*, 69, 144-155.
- Dulău, L. I., Abrudean, M., & Bică, D. (2016). Optimal Location of a Distributed Generator for Power Losses Improvement. *Procedia Technology*, 22, 734-739.
- Dursun, M., & Boz, A. F. (2015). The analysis of different techniques for speed control of permanent magnet synchronous motor. *Tehnicky Vjesnik-Technical Gazette*, 22(4), 947-952.
- Dydek, Z. T., Annaswamy, A. M., & Lavretsky, E. (2010). Adaptive control of quadrotor UAVs in the presence of actuator uncertainties. *AIAA Infotech@ Aerospace*, 20-22.
- Eciolaza, L., & Sugeno, M. (2012). *On-line design of lut controllers based on desired closed loop plant: Vertex placement principle*. Paper presented at the Fuzzy Systems (FUZZ-IEEE), 2012 IEEE International Conference on.
- Eid, B. M., Rahim, N. A., Selvaraj, J., & El Khateb, A. H. (2016). Control methods and objectives for electronically coupled distributed energy resources in microgrids: A review. *IEEE systems journal*, 10(2), 446-458.
- Ekka, S. (2014). *Automatic load frequency control of multi area power systems*.
- El Boubakri, A. (2013). *Analysis of the Performance of Droop Controlled Inverters in Mini-Grids*. Citeseer.
- Elbaz, M., & Feliachi, A. (2012). *Real time load frequency control for an isolated microgrid system*. Paper presented at the North American Power Symposium (NAPS), 2012.
- Ellis, A., Nelson, R., Von Engeln, E., Walling, R., McDowell, J., Casey, L., . . . Kirby, B. (2012). Reactive power interconnection requirements for PV and wind plants—recommendations to NERC. *Sandia National Laboratories, Albuquerque, New Mexico*, 87185.
- Entso-E, E. (2011). Deterministic Frequency Deviations Root Causes and Proposals for Potential Solutions. *Rep., Dec*.
- Eto, J., Lasseter, R., Schenkman, B., Stevens, J., Klapp, D., VolkommeRr, H., . . . Roy, J. (2009). *Overview of the CERTS microgrid laboratory test bed*. Paper presented at the Integration of Wide-Scale Renewable Resources Into the Power Delivery System, 2009 CIGRE/IEEE PES Joint Symposium.
- Farag, H. E., Abdelaziz, M. M. A., & El-Saadany, E. F. (2013). Voltage and reactive power impacts on successful operation of islanded microgrids. *IEEE Transactions on Power Systems*, 28(2), 1716-1727.
- Farrokhhabadi, M., Cañizares, C. A., & Bhattacharya, K. (2017). Frequency control in isolated/islanded microgrids through voltage regulation. *IEEE transactions on smart grid*, 8(3), 1185-1194.



- Federau, E., Blasius, E., & Janik, P. (2016). Classification of control features related to microgrid operation standardisation. *Przegląd Elektrotechniczny*, 92.
- Freitas, W., Vieira, J. C., Morelato, A., Da Silva, L. C., Da Costa, V. F., & Lemos, F. A. (2006). Comparative analysis between synchronous and induction machines for distributed generation applications. *IEEE Transactions on Power Systems*, 21(1), 301-311.
- Fuad, S. A. (2017). Consensus based distributed control in micro-grid clusters.
- Galassini, A., Costabeber, A., Gerada, C., Buticchi, G., & Barater, D. (2016). A modular speed-drooped system for high reliability integrated modular motor drives. *IEEE Transactions on Industry applications*, 52(4), 3124-3132.
- Gallestey, E., Al-Hokayem, P., Torrisi, M. G., & Paccagnan, M. D. (2015). Nonlinear Systems and Control. *Department of Information Technology and Electrical Engineering, Swiss Federal Institute of Technology*.
- Ganapathy, S., & Velusami, S. (2009). Decentralized load-frequency control of interconnected power systems with SMES units and governor dead band using Multi-objective Evolutionary Algorithm. *Journal of Electrical Engineering and Technology*, 4(4), 443-450.
- Gao, W., & Selmic, R. R. (2006). Neural network control of a class of nonlinear systems with actuator saturation. *IEEE Transactions on Neural Networks*, 17(1), 147-156.
- Ghadiri, M., Moeini, A., & Yassami, H. (2011). Impact of Islanding on Governor Signal of Distributed Resources. *Journal of Electromagnetic Analysis and Applications*, 2011.
- Glover, J. D., Sarma, M. S., & Overbye, T. (2012). *Power System Analysis & Design, SI Version*: Cengage Learning.
- Goyal, M., Ghosh, A., & Zare, F. (2013). *Power sharing control with frequency droop in a hybrid microgrid*. Paper presented at the IEEE Power and Energy Society General Meeting.
- Gözde, H., Taplamacıoğlu, M. C., Kocaarslan, İ., & Çam, E. (2008). Particle swarm optimization based load frequency control in a single area power system. *Electronics and Computer Science, Scientific Buletin*(8).
- Greacen, C. (2014). A Guidebook on Grid Interconnection and Islanded Operation of Mini-Grid Power Systems Up to 200 kW.
- Grillo, S., Massucco, S., Morini, A., Pitto, A., & Silvestro, F. (2010). Microturbine control modeling to investigate the effects of distributed generation in electric energy networks. *IEEE systems journal*, 4(3), 303-312.
- Guerrero, J. (2011). *Connecting renewable energy sources into the smartgrid*. Paper presented at the 2011 IEEE International Symposium on Industrial Electronics.
- Guerrero, J. M., De Vicuna, L. G., Matas, J., Castilla, M., & Miret, J. (2004). A wireless controller to enhance dynamic performance of parallel inverters in distributed generation systems. *IEEE Transactions on power electronics*, 19(5), 1205-1213.

- Guerrero, J. M., Matas, J., de Vicuna, L. G., Castilla, M., & Miret, J. (2007). Decentralized control for parallel operation of distributed generation inverters using resistive output impedance. *IEEE Transactions on industrial electronics*, 54(2), 994-1004.
- Guo, L. (2016). *Design and Performance Improvement of AC Machines Sharing a Common Stator*. Rensselaer Polytechnic Institute.
- Guo, Y., & Gawlik, W. (2014). A survey of control strategies applied in worldwide microgrid projects. *Tagungsband ComForEn, 2014*, 47.
- Gurkaynak, Y., & Khaligh, A. (2009). *Control and power management of a grid connected residential photovoltaic system with plug-in hybrid electric vehicle (PHEV) load*. Paper presented at the Applied Power Electronics Conference and Exposition, 2009. APEC 2009. Twenty-Fourth Annual IEEE.
- Hadjidemetriou, L., Kyriakides, E., & Blaabjerg, F. (2013). A new hybrid PLL for interconnecting renewable energy systems to the grid. *IEEE Transactions on Industry applications*, 49(6), 2709-2719.
- Han, H., Hou, X., Yang, J., Wu, J., Su, M., & Guerrero, J. M. (2016). Review of power sharing control strategies for islanding operation of AC microgrids. *IEEE transactions on smart grid*, 7(1), 200-215.
- Hasni, M., Touhami, O., Ibtouen, R., Fadel, M., & Caux, S. (2008). Synchronous machine parameter estimation by standstill frequency response tests. *JOURNAL OF ELECTRICAL ENGINEERING-BRATISLAVA-*, 59(2), 75.
- Hassanzahraee, M., & Bakhshai, A. (2012). *Adaptive transient power control strategy for parallel-connected inverters in an islanded microgrid*. Paper presented at the IECON 2012-38th Annual Conference on IEEE Industrial Electronics Society.
- Hatipoglu, K. (2013). *Dynamic voltage stability enhancement of a microgrid with different types of distributed energy resources*. Tennessee Technological University.
- Hatipoglu, K., Cakir, G., & Fidan, I. (2013). *Implementation of faults in a microgrid environment with MATLAB based GUI*. Paper presented at the Southeastcon, 2013 Proceedings of IEEE.
- Hausberg, F., Hecker, S., Pfeffer, P., Plöchl, M., & Rupp, M. (2014). Incorporation of Adaptive Grid-Based Look-Up Tables in Adaptive Feedforward Algorithms for Active Engine Mounts.
- He, J., & Li, Y. W. (2012). An enhanced microgrid load demand sharing strategy. *IEEE Transactions on power electronics*, 27(9), 3984-3995.
- He, J., Li, Y. W., Guerrero, J. M., Vasquez, J. C., & Blaabjerg, F. (2012). *An islanding microgrid reactive power sharing scheme enhanced by programmed virtual impedances*. Paper presented at the 2012 3rd IEEE International Symposium on Power Electronics for Distributed Generation Systems (PEDG).
- Hindman, R., Cao, C., & Hovakimyan, N. (2007). Designing a High Performance, Stable C1 Adaptive Output Feedback Controller.
- Horowitz, S. H., Phadke, A. G., & Renz, B. A. (2010). The future of power transmission. *IEEE Power and Energy Magazine*, 8(2), 34-40.

- Hou, X., Sun, Y., Yuan, W., Han, H., Zhong, C., & Guerrero, J. M. (2016). Conventional P- $\omega$ /QV droop control in highly resistive line of low-voltage converter-based ac microgrid. *Energies*, 9(11), 943.
- Ioannou, P. A., & Sun, J. (2012). *Robust adaptive control*: Courier Corporation.
- Jain, P., & Nigam, M. (2013). Design of a model reference adaptive controller using modified MIT rule for a second order system. *Advance in Electronic and Electric Engineering*, ISSN, 2231-1297.
- Jain, P., & Nigam, M. (2015). Comparative Analysis of MIT Rule and Differential Evolution on Magnetic Levitation System. *International Journal of Electronics and Electrical Engineering*, 3(2), 153-157.
- Jeddi, S. A., Abbasi, S. H., & Shabaninia, F. (2012). *Load frequency control of two area interconnected power system (Diesel Generator and Solar PV) with PI and FGSPi controller*. Paper presented at the Artificial Intelligence and Signal Processing (AISP), 2012 16th CSI International Symposium on.
- John, N., & Ramesh, K. (2013). Enhancement of load frequency control concerning high penetration of wind turbine using PSO-fuzzy technique. *International Journal of Computer Applications*, 69(14).
- Justo, J. J., Mwasilu, F., Lee, J., & Jung, J.-W. (2013). AC-microgrids versus DC-microgrids with distributed energy resources: A review. *Renewable and Sustainable Energy Reviews*, 24, 387-405.
- Kadri, R., Gaubert, J.-P., & Champenois, G. (2011). An improved maximum power point tracking for photovoltaic grid-connected inverter based on voltage-oriented control. *IEEE Transactions on industrial electronics*, 58(1), 66-75.
- Kaisinger, R. (2011). Electrical modeling of a thermal power station.
- Kazmi, S. A. A., Shahzad, M. K., Khan, A. Z., & Shin, D. R. (2017). Smart Distribution Networks: A Review of Modern Distribution Concepts from a Planning Perspective. *Energies*, 10(4), 501.
- Keshtkar, H., Solanki, J., & Solanki, S. K. (2012). *Application of PHEV in load frequency problem of a hybrid microgrid*. Paper presented at the North American Power Symposium (NAPS), 2012.
- Khodabakhshian, A., & Golbon, N. (2005). *Robust load frequency controller design for hydro power systems*. Paper presented at the Control Applications, 2005. CCA 2005. Proceedings of 2005 IEEE Conference on.
- Khorramabadi, S. S., & Bakhshai, A. (2015). Intelligent Control of Grid-Connected Microgrids: An Adaptive Critic-Based Approach. *IEEE Journal of Emerging and Selected Topics in Power Electronics*, 3(2), 493-504.
- Kim, J.-Y., Kim, H.-M., Kim, S.-K., Jeon, J.-H., & Choi, H.-K. (2011). Designing an energy storage system fuzzy PID controller for microgrid islanded operation. *Energies*, 4(9), 1443-1460.

- Kim, J., Guerrero, J. M., Rodriguez, P., Teodorescu, R., & Nam, K. (2011). Mode adaptive droop control with virtual output impedances for an inverter-based flexible AC microgrid. *Power Electronics, IEEE Transactions on*, 26(3), 689-701.
- Kiruthika, G. (2014). Vector control based PMSM drive using hybrid PI-FUZZY logic controller.
- Kumar, M., Kumar, P., Yadav, A., & Pal, N. (2016). *Fuzzy gain scheduled intelligent frequency control in an AC microgrid*. Paper presented at the Recent Advances in Information Technology (RAIT), 2016 3rd International Conference on.
- Kumar, R., Singla, S., & Chopra, V. (2015). Comparison among some well known control schemes with different tuning methods. *Journal of applied research and technology*, 13(3), 409-415.
- Kundur, P., Balu, N. J., & Lauby, M. G. (1994). *Power system stability and control* (Vol. 7): McGraw-hill New York.
- Laseter, R. H. (2011). Smart distribution: Coupled microgrids. *Proceedings of the IEEE*, 99(6), 1074-1082.
- Lee, C.-T., Chu, C.-C., & Cheng, P.-T. (2013). A new droop control method for the autonomous operation of distributed energy resource interface converters. *IEEE Transactions on power electronics*, 28(4), 1980-1993.
- Li, F., Li, R., & Zhou, F. (2015). *Microgrid technology and engineering application*: Elsevier.
- Lidula, N., & Rajapakse, A. (2011). Microgrids research: A review of experimental microgrids and test systems. *Renewable and Sustainable Energy Reviews*, 15(1), 186-202.
- Liu, J., Miura, Y., Bevrani, H., & Ise, T. Enhanced virtual synchronous generator control for parallel inverters in microgrids.
- Liu, S. (2014). *A Gain Scheduling Approach to The Load Frequency Control in Smart Grids*. Carleton University.
- Liu, S., Liu, P. X., & El Saddik, A. (2013). A Stochastic Security Game for Kalman Filtering in Networked Control Systems (NCSs) under Denial of Service (DoS) Attacks. *IFAC Proceedings Volumes*, 46(20), 106-111.
- Liu, S., Liu, P. X., & El Saddik, A. (2014). A stochastic game approach to the security issue of networked control systems under jamming attacks. *Journal of the Franklin Institute*, 351(9), 4570-4583.
- Liyanage, K. M., Manaz, M., Yokoyama, A., Ota, Y., Taniguchi, H., & Nakajima, T. (2011). *Impact of communication over a TCP/IP network on the performance of a coordinated control scheme to reduce power fluctuation due to distributed renewable energy generation*. Paper presented at the Industrial and Information Systems (ICIIS), 2011 6th IEEE International Conference on.
- Londero, R., Affonso, C., & Nunes, M. (2009). *Impact of distributed generation in steady state, voltage and transient stability—Real case*. Paper presented at the PowerTech, 2009 IEEE Bucharest.

- Lopes, J. P., Moreira, C., & Madureira, A. (2006). Defining control strategies for microgrids islanded operation. *IEEE Transactions on Power Systems*, 21(2), 916-924.
- Lu, X., Sun, K., Guerrero, J., & Huang, L. (2012). *SoC-based dynamic power sharing method with AC-bus voltage restoration for microgrid applications*. Paper presented at the IECON 2012-38th Annual Conference on IEEE Industrial Electronics Society.
- Madbouly, S. O., Soliman, H. F., Hasanien, H. M., & Badr, M. (2010). *Fuzzy logic control of brushless doubly fed induction generator*. Paper presented at the Power Electronics, Machines and Drives (PEMD 2010), 5th IET International Conference on.
- Mahela, O., & Ola, S. (2013). Modeling and Control of Grid Connected Photovoltaic System: A Review. *International Journal of Electrical and Electronics Engineering Research (IJEER)*, 3(1), 123-134.
- Mahzarnia, M., Sheikholeslami, A., & Adabi, J. (2013). A voltage stabilizer for a microgrid system with two types of distributed generation resources. *IJUM Engineering Journal*, 14(2).
- Majumder, R. (2013). Some aspects of stability in microgrids. *IEEE Transactions on Power Systems*, 28(3), 3243-3252.
- Majumder, R., Chaudhuri, B., Ghosh, A., Majumder, R., Ledwich, G., & Zare, F. (2010). Improvement of stability and load sharing in an autonomous microgrid using supplementary droop control loop. *IEEE Transactions on Power Systems*, 25(2), 796-808.
- Majumder, R., Ghosh, A., Ledwich, G., & Zare, F. (2009). Load sharing and power quality enhanced operation of a distributed microgrid. *IET Renewable Power Generation*, 3(2), 109-119.
- Majumder, R., Ghosh, A., Ledwich, G., & Zare, F. (2010). *Operation and control of hybrid microgrid with angle droop controller*. Paper presented at the TENCON 2010-2010 IEEE Region 10 Conference.
- Manaz, M. M., & Lu, C.-N. (2017). *Adaptive generation control for islanded AC microgrid frequency regulation*. Paper presented at the Future Energy Electronics Conference and ECCE Asia (IFEEC 2017-ECCE Asia), 2017 IEEE 3rd International.
- Marnay, C., & Bailey, O. C. (2004). The CERTS Microgrid and the Future of the Macrogrid. *Lawrence Berkeley National Laboratory*.
- Marzband, M. (2013). *Experimental validation of optimal real-time energy management system for microgrids*. PhD thesis, Departament d'Enginyeria Elèctrica, EU d'Enginyeria Tècnica Industrial de Barcelona, Universitat Politècnica de Catalunya.
- Marzband, M., Sumper, A., Gomis-Bellmunt, O., Pezzini, P., & Chindris, M. (2011). *Frequency control of isolated wind and diesel hybrid MicroGrid power system by using fuzzy logic controllers and PID controllers*. Paper presented at the Electrical Power Quality and Utilisation (EPQU), 2011 11th International Conference on.
- Mehrizi-Sani, A., & Iravani, R. (2010). Potential-function based control of a microgrid in islanded and grid-connected modes. *IEEE Transactions on Power Systems*, 25(4), 1883-1891.



- Meng, J., Wang, Y., Fu, C., & Wang, H. (2016). *Adaptive virtual inertia control of distributed generator for dynamic frequency support in microgrid*. Paper presented at the Energy Conversion Congress and Exposition (ECCE), 2016 IEEE.
- Micallef, A., Apap, M., Spiteri-Staines, C., & Guerrero, J. M. (2012). *Secondary control for reactive power sharing in droop-controlled islanded microgrids*. Paper presented at the Industrial Electronics (ISIE), 2012 IEEE International Symposium on.
- Mohamed, Y. A.-R. I. (2008). *New control algorithms for the distributed generation interface in grid-connected and micro-grid systems*. University of Waterloo.
- Mohamed, Y. A.-R. I., & El-Saadany, E. F. (2008). Adaptive decentralized droop controller to preserve power sharing stability of paralleled inverters in distributed generation microgrids. *IEEE Transactions on power electronics*, 23(6), 2806-2816.
- Mohammed, A. M. I. (2017). *Design of Adaptive Power System Stabilizer for Damping Power System Oscillations*. Sudan University of Science & Technology.
- Mondai, A., Ilindala, M. S., Renjit, A. A., & Khalsa, A. S. (2014). *Analysis of limiting bounds for stalling of natural gas genset in the CERTS microgrid test bed*. Paper presented at the Power Electronics, Drives and Energy Systems (PEDES), 2014 IEEE International Conference on.
- Mosaad, M. I., & Salem, F. (2014). LFC based adaptive PID controller using ANN and ANFIS techniques. *Journal of Electrical Systems and Information Technology*, 1(3), 212-222.
- Moussa, H., Shahin, A., Sharif, F., Martin, J.-P., & Pierfederici, S. (2015). *Optimal angle droop power sharing control for autonomous microgrid*. Paper presented at the Energy Conversion Congress and Exposition (ECCE), 2015 IEEE.
- Müller, N., & Isermann, R. (2004). On-line adaptation of grid-based look-up tables using a fast linear regression technique.
- Murty, P. (2011). *Operation and control in power systems*: BS Publications.
- Muse, J. A., & Calise, A. J. (2010). Adaptive control for systems with slow reference models. *AIAA Infotech@ Aerospace*.
- Nagrath, I. (2006). *Control systems engineering*: New Age International.
- Nguyen, K.-L., Won, D.-J., Ahn, S.-J., & Chung, I.-Y. (2012). Power sharing method for a grid connected microgrid with multiple distributed generators. *Journal of Electrical Engineering and Technology*, 7(4), 459-467.
- Nguyen, N., Huang, Q., & Thi-Mai-Phuong, D. (2016). An investigation of intelligent controllers based on fuzzy logic and artificial neural network for power system frequency maintenance. *Turkish Journal of Electrical Engineering & Computer Sciences*, 24(4), 2893-2909.
- Nguyen, T. D. (2016). *Adaptive and Optimal Control for Active Mass Dampers to Reduce Vibrations of Structures*. North Carolina Agricultural and Technical State University.
- Nisar, A., & Thomas, M. S. (2016). Comprehensive control for microgrid autonomous operation with demand response. *IEEE transactions on smart grid*.

- Ota, T., Mizuno, K., Yukita, K., Nakano, H., Goto, Y., & Ichiyanagi, K. (2007). *Study of load frequency control for a microgrid*. Paper presented at the Power Engineering Conference, 2007. AUPEC 2007. Australasian Universities.
- Pandey, S. K., Mohanty, S. R., & Kishor, N. (2013). A literature survey on load–frequency control for conventional and distribution generation power systems. *Renewable and Sustainable Energy Reviews*, 25, 318-334.
- Pankaj, K., Kumar, J. S., & Nema, R. (2011). Comparative analysis of MIT rule and Lyapunov rule in model reference adaptive control scheme. *Innovative Systems Design and Engineering*, 2(4), 154-162.
- Panora, R., Gehret, J. E., Furse, M. M., & Lasseter, R. H. (2014). Real-world performance of a CERTS microgrid in Manhattan. *IEEE Transactions on Sustainable Energy*, 5(4), 1356-1360.
- Paraskevadaki, E., Papathanassiou, S., & Papadopoulos, M. (2009). *Benefits from DG power factor regulation in LV networks*. Paper presented at the Electricity Distribution-Part 1, 2009. CIRED 2009. 20th International Conference and Exhibition on.
- Patrao, I., Figueres, E., Garcerá, G., & González-Medina, R. (2015). Microgrid architectures for low voltage distributed generation. *Renewable and Sustainable Energy Reviews*, 43, 415-424.
- Patterson, M. (2013). *Hybrid Microgrid Model based on Solar Photovoltaics with Batteries and Fuel Cells system for intermittent applications*. Arizona State University.
- Pawar, R., & Parvat, B. (2015). *Design and implementation of MRAC and modified MRAC technique for inverted pendulum*. Paper presented at the Pervasive Computing (ICPC), 2015 International Conference on.
- Peng, W., Yuan, J., Zhao, Y., Lin, M., Zhang, Q., Victor, D. G., & Mauzerall, D. L. (2017). Air quality and climate benefits of long-distance electricity transmission in China.
- Planas, E., Gil-de-Muro, A., Andreu, J., Kortabarria, I., & de Alegría, I. M. (2013). General aspects, hierarchical controls and droop methods in microgrids: A review. *Renewable and Sustainable Energy Reviews*, 17, 147-159.
- Pogaku, N., Prodanovic, M., & Green, T. C. (2007). Modeling, analysis and testing of autonomous operation of an inverter-based microgrid. *IEEE Transactions on power electronics*, 22(2), 613-625.
- Pota, H. R., Hossain, M., Mahmud, M., & Gadh, R. (2014). *Control for microgrids with inverter connected renewable energy resources*. Paper presented at the PES General Meeting| Conference & Exposition, 2014 IEEE.
- Prakash, R., & Anita, R. (2011). Design of Model Reference Adaptive Intelligent Controller using Neural Network for Nonlinear Systems. *International Review of Automatic Control*, 4(2), 153-161.
- Prakash, S., Sinha, S. K., Pandey, A. S., & Singh, B. (2009). Impact of slider gain on load frequency control using fuzzy logic controller. *ARNP J. Eng. Appl. Sci*, 4, 20-27.

- Prasanth, B. V., & Kumar, S. J. (2005). New control strategy for load frequency problem of a single area power system using fuzzy logic control. *J. Theor. Appl. Inf. Technol*, 253-260.
- Quamruzzaman, M., & Rahman, K. M. (2008). *Development of control strategy for load sharing in grid-connected PV power system*. Paper presented at the Electrical and Computer Engineering, 2008. ICECE 2008. International Conference on.
- Rahman, M. M. (2015). *Microgrid frequency control using multiple battery energy storage system (BESSs)*. Queensland University of Technology.
- Rebours, Y. G., Kirschen, D. S., Trotignon, M., & Rossignol, S. (2007). A survey of frequency and voltage control ancillary services—Part I: Technical features. *IEEE Transactions on Power Systems*, 22(1), 350-357.
- Renders, B., De Gussemé, K., Ryckaert, W. R., Stockman, K., Vandeveld, L., & Bollen, M. H. (2008). Distributed generation for mitigating voltage dips in low-voltage distribution grids. *IEEE Transactions on Power delivery*, 23(3), 1581-1588.
- Renjit, A. A. (2016). *Modeling, Analysis and Control of Mixed Source Microgrid*. The Ohio State University.
- Renjit, A. A., Illindala, M. S., & Klapp, D. A. (2014). Graphical and analytical methods for stalling analysis of engine generator sets. *IEEE Transactions on Industry applications*, 50(5), 2967-2975.
- Reza, M. (2006). *Stability analysis of transmission system with high penetration of distributed generation*: TU Delft, Delft University of Technology.
- Rostami, A., Abdi, H., Moradi, M., Olamaei, J., & Naderi, E. (2017). Islanding Detection based on ROCOV and ROCORP Parameters in the Presence of Synchronous DG Applying the Capacitor Connection Strategy. *Electric Power Components and Systems*, 45(3), 315-330.
- Ruzhekov, G., Slavov, T., & Puleva, T. (2011). *Modeling and implementation of hydro turbine power adaptive control based on gain scheduling technique*. Paper presented at the Intelligent System Application to Power Systems (ISAP), 2011 16th International Conference on.
- Sabahi, K., Nekoui, M., Teshnehlab, M., Aliyari, M., & Mansouri, M. (2007). *Load frequency control in interconnected power system using modified dynamic neural networks*. Paper presented at the Control & Automation, 2007. MED'07. Mediterranean Conference on.
- Sao, C. K., & Lehn, P. W. (2008). Control and power management of converter fed microgrids. *IEEE Transactions on Power Systems*, 23(3), 1088-1098.
- Sarabia, A. F. (2011). *Impact of distributed generation on distribution system*. Aalborg University.
- Schollhorn, D. (2012). *Micro grid control structures for better integration of renewable energy*. Paper presented at the Integration of Renewables into the Distribution Grid, CIRED 2012 Workshop.
- Selvakumar, K., Boopathi, C., & Harsha, M. S. (2016). Voltage Stability Assessment using Artificial Neural Networks. *Indian Journal of Science and Technology*, 9(38).



- Sengupta, R., & Dey, C. (2017). *Design and Performance Analysis of a Modified MRAC for Second-Order Integrating Processes*. Paper presented at the International Conference on Computational Intelligence, Communications, and Business Analytics.
- Shafiee, Q., Guerrero, J. M., & Vasquez, J. C. (2014). Distributed secondary control for islanded microgrids—A novel approach. *IEEE Transactions on power electronics*, 29(2), 1018-1031.
- Shah, N. N., & Kotwal, C. D. (2012). The State Space Modeling of Single, Two and Three ALFC of Power System Using Integral Control and Optimal LQR Control Method. *IOSR Journal of Engineering*, 2(3), 501-510.
- Shen, G., Zhu, X., Chen, M., & Xu, D. (2009). *A new current feedback PR control strategy for grid-connected VSI with an LCL filter*. Paper presented at the Applied Power Electronics Conference and Exposition, 2009. APEC 2009. Twenty-Fourth Annual IEEE.
- Shimada, T., Ueda, Y., & Kurokawa, K. (2008). *Look-ahead equalizing charge planning for grid-connected photovoltaic systems with battery storages*. Paper presented at the Photovoltaic Specialists Conference, 2008. PVSC'08. 33rd IEEE.
- Shokoochi, S., Sabori, F., & Bevrani, H. (2014). *Secondary voltage and frequency control in islanded microgrids: online ANN tuning approach*. Paper presented at the Smart Grid Conference (SGC), 2014.
- Soni, K. C., & Firdaus, F. B. (2015). MicroGrid during Grid-connected mode and Islanded mode—A review. *International Journal of Advance Engineering and Research Development*.
- Soultanis, N. L., Papathanasiou, S. A., & Hatziargyriou, N. D. (2007). A stability algorithm for the dynamic analysis of inverter dominated unbalanced LV microgrids. *IEEE Transactions on Power Systems*, 22(1), 294-304.
- Sparacino, A. R., Reed, G. F., Kerestes, R. J., Grainger, B. M., & Smith, Z. T. (2012). *Survey of battery energy storage systems and modeling techniques*. Paper presented at the 2012 IEEE Power and Energy Society General Meeting.
- Steenis, J. (2013). *Modeling and control for microgrids*.
- Stellet, J. (2011). Analysis and performance evaluation of model reference adaptive control.
- Su, L., Li, G., & Jin, Z. (2011). *Modeling, control and testing of a voltage-source-inverter-based microgrid*. Paper presented at the Electric Utility Deregulation and Restructuring and Power Technologies (DRPT), 2011 4th International Conference on.
- Swarnkar, P., Jain, S., & Nema, R. (2010). Effect of adaptation gain on system performance for model reference adaptive control scheme using MIT rule. *World Academy of science, engineering and technology*, 70, 621-626.
- Swarnkar, P., Jain, S., & Nema, R. (2011). Effect of adaptation gain in model reference adaptive controlled second order system. *Engineering, Technology & Applied Science Research*, 1(3), 70-75.

- Taher, S. A., Hematti, R., Abdolalipour, A., & Tabei, S. H. (2008). Optimal decentralized load frequency control using HPSO algorithms in deregulated power systems. *American Journal of Applied Sciences*, 5(9), 1167-1174.
- Taheri Ledari, H. (2017). *Robust adaptive nonlinear control of microgrid frequency and voltage in the presence of renewable energy sources*. École de technologie supérieure.
- Tan, W. (2011). *Load frequency control: Problems and solutions*. Paper presented at the Control Conference (CCC), 2011 30th Chinese.
- Ullah, N. R., Thiringer, T., & Karlsson, D. (2008). Temporary primary frequency control support by variable speed wind turbines—Potential and applications. *IEEE Transactions on Power Systems*, 23(2), 601-612.
- Usman, A., & Divakar, B. (2012). *Simulation study of load frequency control of single and two area systems*. Paper presented at the Global Humanitarian Technology Conference (GHTC), 2012 IEEE.
- Vandoorn, T. L., Renders, B., Meersman, B., Degroote, L., & Vandeveld, L. (2010). *Reactive power sharing in an islanded microgrid*. Paper presented at the Universities Power Engineering Conference (UPEC), 2010 45th International.
- Vargas-Martínez, A., Avila, L. I. M., Zhang, Y., Garza-Castañón, L. E., & Ortiz, E. R. C. (2013). Model-based fault-tolerant control to guarantee the performance of a hybrid wind-diesel power system in a microgrid configuration. *Procedia Computer Science*, 19, 712-719.
- Vargas-Martínez, A., & Garza-Castañón, L. (2011). Combining artificial intelligence and advanced techniques in fault-tolerant control. *Journal of applied research and technology*, 9(2), 202-226.
- Vargas-Martínez, A., Minchala Avila, L. I., Zhang, Y., Garza-Castañón, L. E., & Badihi, H. (2015). Hybrid adaptive fault-tolerant control algorithms for voltage and frequency regulation of an islanded microgrid. *International Transactions on Electrical Energy Systems*, 25(5), 827-844.
- Vasquez Quintero, J. C. (2009). Decentralized control techniques applied to electric power distributed generation in microgrids.
- Venkatachalam, J. (2013). *A Particle Swarm Optimization Algorithm For Automatic Generation Control Of Two Area Interconnected Power System*. Paper presented at the International Journal of Engineering Research and Technology.
- Venkataraman, G., & Marnay, C. (2008). A larger role for microgrids. *Power and Energy Magazine, IEEE*, 6(3), 78-82.
- Wang, K., & Crow, M. L. (2011). Power system voltage regulation via STATCOM internal nonlinear control. *IEEE Transactions on Power Systems*, 26(3), 1252-1262.
- Wilson, T. (2015). *Control and management of a microgrid and the use of Droop control*. Murdoch University.
- Wood, A. J., & Wollenberg, B. F. (2012). *Power generation, operation, and control*: John Wiley & Sons.

- Xu, Y. (2014). Adaptive Control for Power System Voltage and Frequency Regulation.
- Yadav, D. A., Gaira, K., AkankshaRawat, A. A., & Kumar, A. (2013). Speed Control of Separately Excited DC Motor Using Adaptive PID Controller. *International Journal of Research in Engineering & Applied Sciences*, 3(4).
- Yoo, D. K., & Wang, L. (2011). *A model predictive resonant controller for grid-connected voltage source converters*. Paper presented at the IECON 2011-37th Annual Conference on IEEE Industrial Electronics Society.
- Zamora, R., & Srivastava, A. K. (2010). Controls for microgrids with storage: Review, challenges, and research needs. *Renewable and Sustainable Energy Reviews*, 14(7), 2009-2018.
- Zhang, Y., Dong, L., & Gao, Z. (2009). *Load frequency control for multiple-area power systems*. Paper presented at the 2009 American Control Conference.
- Zhao-Xia, X., & Hong-Wei, F. (2012). Impacts of Pf & QV droop control on microgrids transient stability. *Physics Procedia*, 24, 276-282.
- Zhong, Q.-C. (2013). Robust droop controller for accurate proportional load sharing among inverters operated in parallel. *IEEE Transactions on industrial electronics*, 60(4), 1281-1290.
- Zhong, Q.-C., & Weiss, G. (2011). Synchronverters: Inverters that mimic synchronous generators. *IEEE Transactions on industrial electronics*, 58(4), 1259-1267.
- Zope, P. H., Bhangale, P. G., Sonare, P., & Suralkar, S. (2012). Design and Implementation of carrier based Sinusoidal PWM Inverter. *International Journal of advanced research in electrical, electronics and instrumentation engineering*, 1(4), 230-236.

The logo for UMP (University of Mumbai) is a large, stylized 'U' shape composed of several overlapping triangles in shades of blue, green, and yellow. The letters 'UMP' are printed in a bold, white, sans-serif font across the center of the 'U' shape.

UMP

## LIST OF PUBLICATION

1. "HIGH-PENETRATION, WITHOUT STORAGE, PV SOLAR-DIESEL GENERATOR IN ISOLATED SYSTEM", The 4th ICoGOIA 2015 International Conference, The International Conference on Global Optimization and its Applications , held in Pahang, Malaysia from 10 to 11 August 2015.
2. "Effects of Time Delay on the Performance of Harmonics Elimination in Active Power Filter", Research Journal of Applied Sciences, Engineering and Technology 11(7):770-779, 2015, Maxwell Science Organization.
3. Control Schemes For Shunt Active Filters To Mitigate Harmonics Using Triangular Carrier Current Controller", International Journal of Engineering Sciences & Research Technology, 4(8): 758-762, August, 2015.
4. Mahdi, M. M., & Ahmad, A. Z. (2016, October). Hybrid micro-grid control and active power sharing using MIT rule based on speed droop controller. In Automatic Control and Intelligent Systems (I2CACIS), IEEE International Conference on (pp. 113-118). IEEE.
5. "An analytical study of total harmonics reduction in APF using adaptive zero crossing detection techniques", International Journal of Engineering Sciences & Research Technology 5(11), November, 2016.
6. Mahdi, M. M., & Ahmad, A. Z. (2017, April). Load frequency control in microgrid using fuzzy logic table control. In Compatibility, Power Electronics and Power Engineering (CPE-POWERENG), 2017 11th IEEE International Conference on (pp. 318-323). IEEE.

## APPENDIX A

The proposed controllers in Chapter Three have been implemented and developed under MATLAB/ Simulink environments, the M-file programs used to evaluate the different cases are shown below:

### 1- Grid connected mode.

#### A- Conventional PI controller

```
function createobject1(Parent1, XData1, YData1)
%CREATEOBJECT1(PARENT1,XDATA1,YDATA1)
% PARENT1: subplot parent
% XDATA1: line xdata
% YDATA1: line ydata

% Create subplot
subplot1 = subplot(1,1,1,'Parent',Parent1,'YGrid','on','XGrid','on');
% Uncomment the following line to preserve the X-limits of the axes
% xlim(subplot1,[0 2]);
% Uncomment the following line to preserve the Y-limits of the axes
% ylim(subplot1,[49.7478444390389 50.0606830021357]);

% Create ylabel
ylabel('Freq (Hz)');

% Create xlabel
xlabel('Time');

% Create line
line(XData1,YData1,'Parent',subplot1,'Color',[0 0 1]);

%%%%%%%%%%%%%%%%%%%%%%%%%%%%%%%%%%%%%%%%%%%%%%%%%%%%%%%%%%%%%%%%%%%%%%%%%
```

#### B- MRAC using MIT rule based PI controller

```
function createobject1(Parent1, XData1, YData1, YData2)
%CREATEOBJECT1(PARENT1,XDATA1,YDATA1,YDATA2)
% PARENT1: subplot parent
% XDATA1: line xdata
% YDATA1: line ydata
% YDATA2: line ydata

% Create subplot
subplot1 = subplot(2,1,1,'Parent',Parent1,'YGrid','on','XGrid','on');
% Uncomment the following line to preserve the X-limits of the axes
% xlim(subplot1,[0 20]);
% Uncomment the following line to preserve the Y-limits of the axes
% ylim(subplot1,[-1 1]);
```

```

% Create ylabel
ylabel('Input 1');

% Create line
line(XData1,YData1,'Parent',subplot1,'Color',[0 0 1]);

% Create subplot
subplot2 = subplot(2,1,2,'Parent',Parent1,'YGrid','on','XGrid','on');
% Uncomment the following line to preserve the X-limits of the axes
% xlim(subplot2,[0 20]);
% Uncomment the following line to preserve the Y-limits of the axes
% ylim(subplot2,[-1 1]);

% Create ylabel
ylabel('Input 2');

% Create xlabel
xlabel('Time');

% Create line
line(XData1,YData2,'Parent',subplot2,'Color',[0 0 1]);

%%%%%%%%%%%%%%%%%%%%%%%%%%%%%%%%%%%%%%%%%%%%%%%%%%%%%%%%%%%%%%%%%%%%%%%%

```

### C- MRAC using MIT rule with ANN based PI controller

```

function createobject1(Parent1, XData1, YData1, YData2)
%CREATEOBJECT1 (PARENT1,XDATA1,YDATA1,YDATA2)
% PARENT1: subplot parent
% XDATA1: line xdata
% YDATA1: line ydata
% YDATA2: line ydata

% Create subplot
subplot1 = subplot(2,1,1,'Parent',Parent1,'YGrid','on','XGrid','on');
% Uncomment the following line to preserve the X-limits of the axes
% xlim(subplot1,[0 20]);
% Uncomment the following line to preserve the Y-limits of the axes
% ylim(subplot1,[-1 1]);

% Create ylabel
ylabel('Input 1');

% Create line
line(XData1,YData1,'Parent',subplot1,'Color',[0 0 1]);

% Create subplot
subplot2 = subplot(2,1,2,'Parent',Parent1,'YGrid','on','XGrid','on');
% Uncomment the following line to preserve the X-limits of the axes
% xlim(subplot2,[0 20]);
% Uncomment the following line to preserve the Y-limits of the axes
% ylim(subplot2,[-1 1]);

% Create ylabel
ylabel('Input 2');

```

```

% Create xlabel
xlabel('Time');

% Create line
line(XData1,YData2,'Parent',subplot2,'Color',[0 0 1]);

```

## 2- ISLANDED MODE

### D- Conventional PI controller

```

function createobject1(Parent1, XData1, YData1)
%CREATEOBJECT1(PARENT1,XDATA1,YDATA1)
% PARENT1: subplot parent
% XDATA1: line xdata
% YDATA1: line ydata

% Create subplot
subplot1 = subplot(1,1,1,'Parent',Parent1,'YGrid','on','XGrid','on');
% Uncomment the following line to preserve the X-limits of the axes
% xlim(subplot1,[0 0.19665]);
% Uncomment the following line to preserve the Y-limits of the axes
% ylim(subplot1,[0 50.0296622831867]);

% Create ylabel
ylabel('Input 1');

% Create xlabel
xlabel('Time');

% Create line
line(XData1,YData1,'Parent',subplot1,'Color',[0 0 1]);

%%%%%%%%%%%%%%%%%%%%%%%%%%%%%%%%%%%%%%%%%%%%%%%%%%%%%%%%%%%%%%%%%%%%%%%%

```

### E- FLTC

```

function createobject1(Parent1, xdata1, zdata1)
%CREATEOBJECT1(PARENT1,XDATA1,ZDATA1)
% PARENT1: axes parent
% XDATA1: surface xdata
% ZDATA1: surface zdata

% Create axes
axes1 = axes('Parent',Parent1,'YGrid','on','XGrid','on');
view(axes1,[-37.5 30]);
hold(axes1,'all');

% Create mesh

```

```

mesh(xdata1,xdata1,zdata1,'Parent',axes1,'Tag','LUTData');

% Create ylabel
ylabel('Column breakpoints');

% Create xlabel
xlabel('Row breakpoints');

% Create text
text('Parent',axes1,'Tag','LUTLabel','String','\leftarrow-1',...
     'Position',[1 -1 -12]);

% Create text
text('Parent',axes1,'Tag','LUTLabel','String','\leftarrow0',...
     'Position',[1 0 0]);

% Create text
text('Parent',axes1,'Tag','LUTLabel','String','\leftarrow1',...
     'Position',[1 1 14]);

% Create text
text('Parent',axes1,'String','Annotations denote column
breakpoints',...
     'Rotation',90,...
     'Position',[1.2 -1.2 -15]);

% Create title
title(['Table and breakpoints data for block: FLTC
Speed',sprintf('\n'),'Regulator2/Subsystem/Lookup',sprintf('\n'),'Table
(2-D)',sprintf('\n'),''],...
     'Interpreter','none');

```

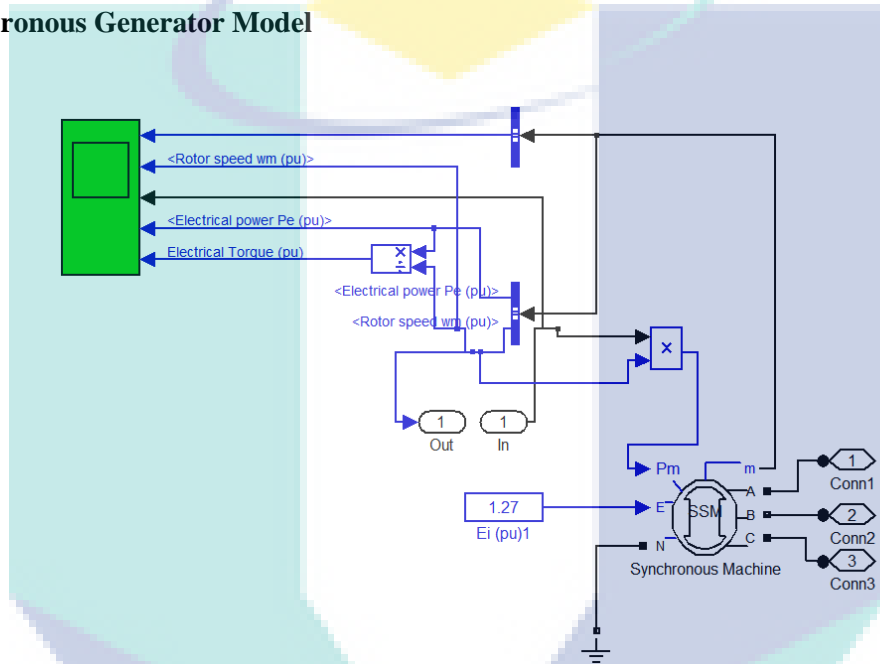


## APENDIX B

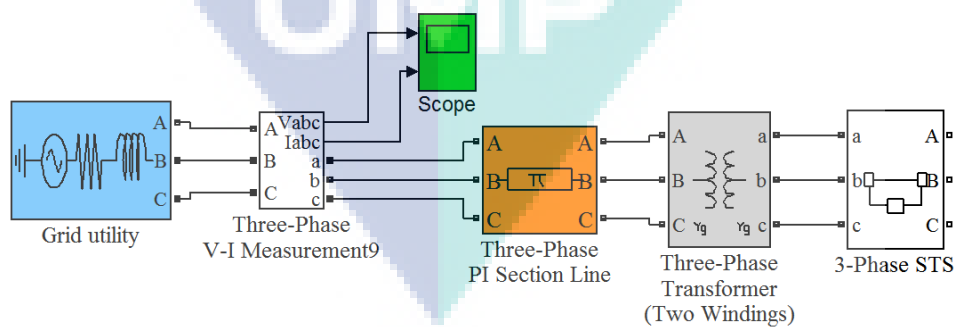
### Implemented Micro-grid in Simulink

The simulation results presented in this research were obtained with the help of Matlab. The models of the hybrid micro-grid in two modes operate are shown in figures below:

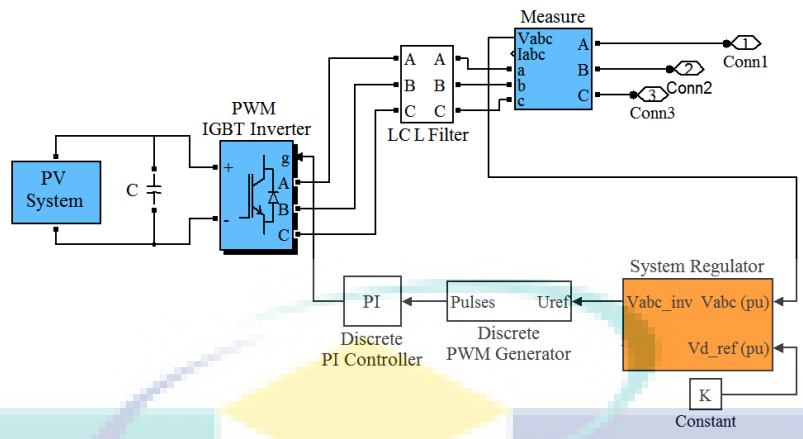
#### Synchronous Generator Model



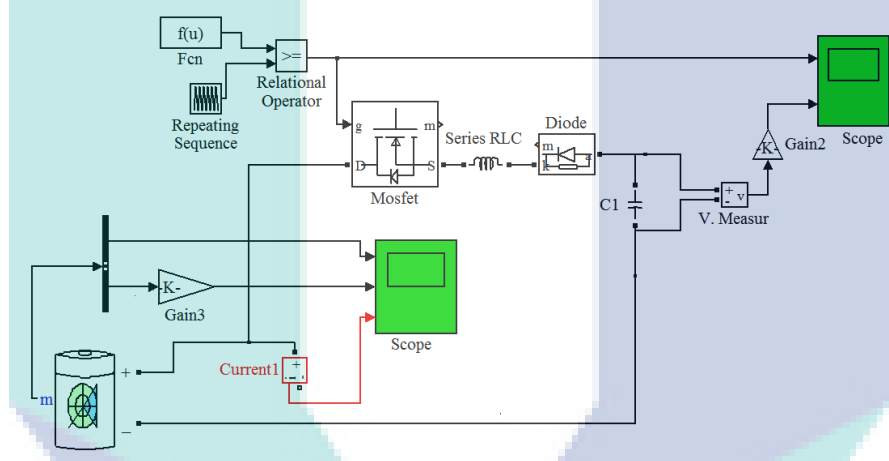
#### Grid Model



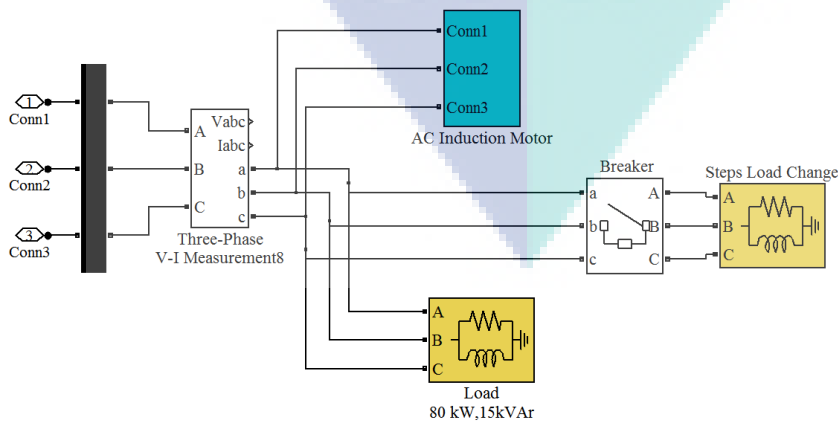
#### PV model



**Battery model with Bi-directional Converter**

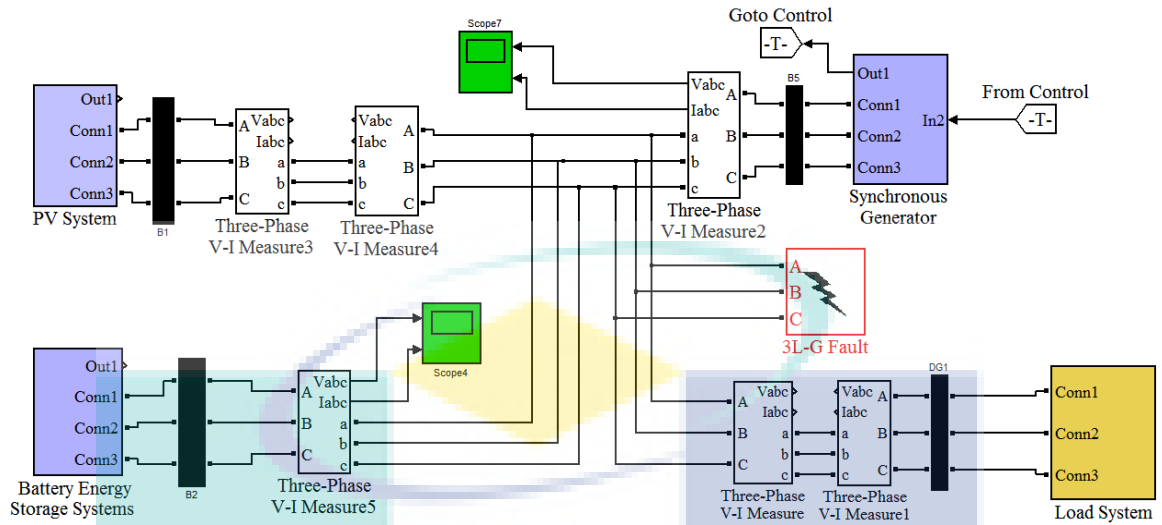


**Load system model**



**Micro-grid in Grid –Connected Mode**





### Speed Control in island mode

